Floristics and structure: object-based, hyperspectral remote sensing of native vegetation

Author:
Roff, Adam

Publication Date:
2015

DOI:
https://doi.org/10.26190/unsworks/2759

Floristics and Structure:

Object-Based, Hyperspectral Remote Sensing of Native Vegetation

Adam Roff

A thesis in fulfilment of the requirements for the degree of
Doctor of Philosophy

School of Biological, Earth and Environmental Sciences
Faculty of Science

March 2009

ORIGINALITY STATEMENT

'I hereby declare that this submission is my own work and to the best of my knowledge it contains no materials previously published or written by another person, or substantial proportions of material which have been accepted for the award of any other degree or diploma at UNSW or any other educational institution, except where due acknowledgement is made in the thesis. Any contribution made to the research by others, with whom I have worked at UNSW or elsewhere, is explicitly acknowledged in the thesis. I also declare that the intellectual content of this thesis is the product of my own work, except to the extent that assistance from others in the project's design and conception or in style, presentation and linguistic expression is acknowledged.'

Signed ………………………………………………...........

Date 18th of March, 2015

Abstract

An underlying premise of any segmentation method is that spectral similarity and thematic similarity are synonymous. This assumption holds true for image objects at an individual tree crown scale and they can be classified with a degree of accuracy. However, at coarser spatial scales, a large patch of vegetation can encompass a variety of thematic attributes. Mapping native vegetation using remote sensing suffers from an inability to make meaningful predictions through a change in scale.

I propose that heterogeneous vegetation needs to be analysed across multiple scales to categorise it as a vegetation community. A multi-scale, object-based, hierarchical approach was introduced to generalise floristic data collected at the plot scale to a vegetation community map using remote sensing. This framework uses the cover and abundance of classified tree crown objects to inform the classification of larger patches of vegetation. Community scale image objects can then be named using the same hierarchical framework used by ecologists in plant ecology.

Machine learning classification algorithms and patch scale segmentation algorithms were reviewed and benchmarked for this application. A crown delineation algorithm was formulated as well as a new way to combine lidar with optical imagery. The scope of this thesis was limited to three sensors: the HyMap hyperspectral airborne scanner, small footprint lidar, and the multi-spectral SPOT-5 satellite. To ensure that the results are relevant, the fieldwork for this thesis was based largely on operational standards. The result was a vegetation map classified on cover and abundance of dominant crown species. The extra resources required for individual tree crown surveys and the difficulty of analysis in highly diverse ecosystems are the main limitations.

Vegetation structure was assessed by quantifying forest fuel load using remote sensing. The correlation between field derived attributes and vegetation indices was stronger when narrow band hyperspectral vegetation indices were used. Small footprint lidar successfully penetrated the canopy and offered quantitative information about the structure of the understorey. However, the total fuel load assessed in the field was dominated by leaf litter component in wet forest, which was problematic to quantify with remote sensing.

Table of Contents

List of Figures

List of Tables

Acknowledgments

This thesis is dedicated to my parents and late grandparents who have been a source of great inspiration in my life. I would also like to dedicate it to the professional ecologists of NSW. This thesis was written to help bridge the gap between ecologists and remote sensing specialists.

I would like to gratefully acknowledge the herculean efforts of my supervisor, Associate Professor Geoff Taylor. Despite coming from a different field and being faced with the shortcomings of an eager but easily distracted student. He led by example with a peerless work ethic and a personal discipline, which I greatly admire but had difficulty replicating.

Our research group at the *University of New South Wales* (UNSW) fostered this research along with the *Cooperative Research Centre for Spatial Information* (CRCSI). Special thanks to my immediate team which included Michael Day and Anthea Mitchell. Also thank-you to Shawn Laffan, Geoff Horne, Tony Milne, Paul Adam, Ray Merton, Steve Bonser, Scott Mooney, Peter Woodgate, Graham Kernich, Clive Roberts, and Mike Ridout. Proof reading from Sam McGuiness was invaluable and I greatly appreciate the assistance of his 4 month old son Dominic and his partner Bianca.

Fieldwork was conducted with assistance from Christine Stone, Russel Turner and Murray Webster from Forests NSW, Chris Chafer from the Sydney Catchment Authority and John Hunter from the NSW National Parks and Wildlife Service. The Department of Environment and Conservation provided field data, SPOT-5 data and ancillary data courtesy of Dominic Sivertsen, Ron Avery, Mushtak Shaikh, Mick Dwyer and Geoff Horne. HyVista Corporation collaborated with our project and we encourage them to foster further research.

Scholarship funds were gratefully received from the Commonwealth Government's Australian Postgraduate Awards, the Cooperative Research Centre for Spatial Information, UNSW Graduate Research Centre and the UNSW School of Biological Earth and Environmental Science. Funding for the HyMap and the lidar was provided by the NSW Rural Fire Service under the Australian *National Disaster and Risk Management* program for research into assessing forest fuel loads. A special thanks to Duncan Sutherland from the NSW Rural Fire Service for making this research possible.

One of the community scale segmentation algorithms used in this thesis is *Size Constrained Region Merging* (Castilla, 2004). I gratefully acknowledge Guillermo Castilla for his permission for the use of his excellent algorithm.

Publications

Day et al, (2006) details the development of the imagery pre-processing techniques used in this thesis.

Day, M.B., Taylor, G.R., Roff, A.M, and Mitchell, A.L., (2006) Spectral discrimination of halophytic vegetation as an indicator of stressed arable land. *Journal of Spatial Science*. Vol 51, No. 2 pp 115-128.

Proceedings

Roff, A., Taylor, G., Turner, R., (2006) Hyperspectral and Lidar Remote Sensing of Forest Fuel Loads in Jilliby State Conservation Area. Proceedings of the *13th Australasian Remote Sensing and Photogrammetry Conference*, Canberra, 20th -24th November 2006.

Roff, A.M., Taylor, G.R., Sivertsen, D., Mitchell, A.L., and Day, M.B., (2008) Mapping native vegetation communities using SPOT 5: combining machine learning with an object-oriented approach. Proceedings of the *14th Australasian Remote Sensing and Photogrammetry Conference*, Darwin, 29th September – 3rd October, 2008.

Roff, A., Sivertsen, D., Taylor, G. Day, M. And Mitchell, A., (2008) Beyond land-cover mapping: Semi-automated delineation of vegetation pattern using segmentation, In *Digital Earth Summit on Geoinformatics 2008: Tools for Global Change Research*. Ehlers, Behncke, Gerstengarbe, Hillen, Koppers, Stroik, Wachter (Eds.)   Heidelberg, Germany.

Reports

The methods and results developed in this thesis were shared with government agencies as reports.

Roff, A., Goodwin, N. & Merton, R., (2005). *Assessing Fuel Loads using Remote Sensing*. Sydney: University of New South Wales.

Roff, A., Taylor, G., (2007) Modelling forest fuels with HyMap and ancillary data. In *Remote Sensing of Fuel Loads: Final Report*, Rural Fire Service, Sydney.

Roff, A.M., Taylor, G.R., (2008) Hyperspectral Remote Sensing of Vegetation. *Methodology manual, imaging spectrometry for natural resources management.* Taylor, G.R., Mitchell, A.L. (Eds.) Final report for CRCSI Project 4.4. Co-operative Research Centre for Spatial Information, Melbourne, Australia.

Chapter 1

Introduction

The aim of this thesis was to develop tools for the delineation and classification of native vegetation. The tools were created to interpolate physical vegetation measurements made in the field over a broader spatial scale. The scope of this thesis was limited to three sensors: the HyMap hyperspectral scanner, small footprint airborne lidar and the multi-spectral SPOT-5 satellite. The research aims to demonstrate the applicability of these data for their use in natural resource management. This research was focus primarily on using spectral information in an object-based approach.

Reliable identification of individual tree species has always been a goal of remote sensing. Information on the spatial distribution of tree species has potential uses in forest inventory, vegetation mapping and conservation management and is otherwise difficult to collect in the field. Much of the recent research in this area has focused on the automated delineation of tree crowns. There has been little discussion on what methods are best suited for differentiating species. Leckie et al. (2005b) reviewed a variety of automated crown delineation algorithms and found that most used spectral data and that very few studies examined the use of textural and structural information. Studies in temperate and tropical forests of the northern hemisphere have concluded that greater numbers of narrow spectral bands improve classification accuracy (Clark et al., 2005, Underwood et al., 2003). They also inferred that commonly used hyperspectral classification algorithms are not always the most suitable.

Hyperspectral data has shown considerable potential for differentiating native vegetation species by their spectral properties. Studies in temperate and tropical forests of the northern hemisphere have concluded that greater numbers of narrow spectral bands improve classification accuracy (Clark et al., 2005, Underwood et al., 2003). Australian studies into species classification have been less successful, with Eucalypt forests in particular being difficult characterise (Bunting and Lucas, 2006, Coops et al., 2004, Goodwin et al., 2005, Lucas et al., 2008). Eucalypt leaves generally hang vertically, making their canopies semi-transparent when viewed from above (Greaves and Spencer, 1993) increasing the soil component and shadow component in tree crown (Goodwin et al., 2005).

A series of crown scale remote sensing studies have been carried out at the Jilliby Catchment area in the past. Coops et al. (2004) attempted to differentiate species amongst eucalypt crowns and rainforest elements using 10 band CASI-2 data (1m spatial resolution). The study was limited by the small number of crowns surveyed but the results implied that the CASI-2 spectra of *Syncarpia glomurifia* and rainforest species could be easily confused with other species. They found that eucalypt species were best differentiated using CASI-2 bands centred on 720nm and 740nm and that *Eucalyptus* *panniculata*, Gray Ironbark, was relatively easy to differentiate. They warned that the results could be confounded by variation in tree health. A second study of the same CASI-2 data (Goodwin et al., 2005) was able to distinguish between *Syncarpia glomulifera*, mesic vegetation (primarily rainforest species) and an amalgamated group of eucalypt species, but was unable to differentiate between individual eucalypt species.

There is evidence in the literature that a greater spectral range can improve performance of crown species classification (Clark et al., 2004, Lucas et al., 2008). Unlike CASI-2 (405nm to 950nm) the HyMap hyperspectral scanner features bands in the short wave infrared where moisture content and various biochemicals have an effect on reflectance (450nm to 2500nm). I propose that HyMap data has a greater chance at differentiating tree species in tall, closed-canopy eucalypt forest than previously trialled sensors (CASI-2).

Chapter 2 provides some background to the field component of this research and features some definitions for forest ecology and remote sensing. It reviews how native forest is surveyed in NSW, including the assessment of vegetation type, and shows how forest fuel loads are quantified in the field with the use of visual assessments and destructive sampling.

One of the arguments established in Chapter 2 is that operational vegetation survey quadrat size is not large enough to survey the dominant species (trees), which conflicts with its stated role providing an effective representation of the floristic type. Hnatiuk et al. (2009) recommends that plot size vary with the height of the vegetation being sampled and that vegetation over twenty metres high be surveyed in 30m by 30m plots. Increasing the size of vegetation surveys for every stratum is not a practical solution for floristic surveys in Australia. An alternative is to survey vegetation at a variety of scales, or in a series of nested hierarchies.

Chapter 3 describes Jilliby and Coonabarabran study areas. It details the field survey data and the satellite and airborne remote sensing data used in this thesis. Following the conclusions of Chapter 2, a multi-scale nested survey design was applied in the field. Multiple operational approaches to surveying vegetation structure and floristics were employed in a nested hierarchy and encompassed by a tree crown survey. The scale of survey ranged from a 40m diameter circle for tree crowns to 1m squared, destructively sampled, leaf litter quadrats.

An underlying premise of any segmentation method is that spectral similarity and thematic similarity are synonymous. For image objects at an individual tree crown scale this assumption holds true, and they can be classified with a degree of accuracy. However, at coarser spatial scales, a large polygon can encompass a variety of thematic attributes. The main obstacles to the successful mapping vegetation using remotely sensed data has been a lack of spectral and spatial resolution and an inability to make meaningful predictions through a change in scale.

I propose that heterogeneous vegetation needs to be analysed across multiple scales to effectively categorise it as a vegetation community. Therefore, a multi-scale, object-based, hierarchical approach is introduced to generalise floristic data collected at the plot scale to a vegetation community map using remote sensing. This framework uses the cover and abundance of classified tree crown objects to inform the classification of larger patches of vegetation. Community scale image objects can then be named using the same hierarchical framework used by ecologists in plant ecology.

There are, however, a number of questions that need to be answered to accomplish this. What is an appropriate statistical approach to classify tree crowns based on image spectra? Can tree crowns be delineated automatically in complex native forest, particularly given the constraints of high spectral but low spatial resolution of hyperspectral scanners?

There are several segmentation algorithms in use that can be used to delineated patches of homogenous vegetation. Will the result be comparable with tradition air photo interpretation of vegetation patterns? Given that the segmentation parameters for these algorithms can be varied, how can they be selected to maximise performance, and using what imagery?

These questions are answered in a series of Chapters. Chapter 4 describes how spectral information from individual tree crowns can be classified to a species level. It uses HyMap hyperspectral scanner data and small footprint lidar to extract spectra and classifies these data with Machine Learning Algorithms (MLA). MLA are well suited to the analysis of hyperspectral data as they deal well with highly dimensional and highly correlated data. MLA have the advantage of allowing the investigation of the relative importance of input variables (spectral bands) in terms of their contribution to classification accuracy. Four algorithms are compared to select an appropriate classifier. Logistic Model Trees (LMT) were selected as the classifier in later chapters for their ability to automate the selection of relevant attributes (bands), how they deals with over-fitting, and their computational efficiency and performance.

To make crown scale analysis practical at a catchment scale Chapter 5 introduces the HyMap Crown Delineation Algorithm (HCDA), which automates the isolation of individual tree crowns in 3.5m HyMap data. The method applies spatial filters to accentuate the location of tree crowns based on the local maxima of sunlit crowns. A watershed algorithm that detects the local minima is then applied to separate individual crowns. This allows for the extraction of HyMap tree crown spectra for the entire study area.

Chapter 6 combines the series of steps in preceding chapters. The Size Constrained Region Merging (SCRM) algorithm was selected for patch scale segmentation (Castilla, 2004, Castilla et al., 2008, Hay et al., 2005). It is also an adaptive-filter/watershed based region-merging approach to segmentation. It effectively created homogenous patches of vegetation and was improved by the use of pre-processed hyperspectral data. The bands used in the segmentation were selected based on the feature reduction powers of the MLA. The HCDA from Chapter 5was used to delineate 330,000 crown objects. The spectral signature of each object was classified using LMT and their accuracy assessed with independent field data at each survey site. Vegetation patches were classified by dominant canopy species and used to create a vegetation community scale map.

Despite lower classification at a crown scale than seen in Chapter 4, I posit that a representative sample of large, classified dominant crowns may be sufficient for labelling vegetation types. Smaller tree crowns overlap at this spatial resolution but the HCDA produces image objects among smaller crowns that may be sufficient for a representative sample of sunlit vegetation. By using the ratio of dominant crowns in each patch there is some scope for error reduction through generalisation.

Vegetation community classification and forest fuels assessment are both concerned with quantifying vegetation structure. Many of the attributes sampled, such as understorey density and tree height, are shared. Vegetation structure is critical to the expression of vegetation type and its distribution. Structural characteristics also tend to be the most easily recognised features on air photos or on other remotely sensed images (Hnatiuk et al., 2009).

Research at the Jilliby Catchment area concludes in Chapter 7 with a comparison of the fuel load sampling methods employed at Jilliby. We examine the relationship between forest fuels assessed in the field and vegetation metrics derived from HyMap, lidar and satellite imagery. Forest fuel load was measured in the field at the Jilliby site using rapid visual assessments as well as labour intensive, destructive sampling.

Chapter 8 represents a shift away from catchment scale mapping to regional scale mapping. The multi-scale, object-based analysis approach developed in Chapter 6 is applied to SPOT-5 satellite data in New South Wales' central west. Chapter 8 begins by exploring some empirical discrepancy methods to quantify segmentation quality. It tests whether optimising segmentation parameters can allow replication of manually digitised vegetation patterns. Based on these results, and applying segmentation at multiple scales, this chapter demonstrates how homogenous patch scale objects may be classified based on crown size sub-objects in an operational environment.

Chapter 2

Operational vegetation survey in eastern Australia

The extensive land surface of the Australian continent and the sparse availability of biological surveys have seen remote sensing and spatial modelling become the basis for vegetation assessment (Ferrier and Guisan, 2006). Yet the focus of national and regional survey standards is on site assessment and local environmental planning at a property scale (Hnatiuk et al., 2009). There is a disparity between the geographic scale of vegetation surveys and the scale at which remote sensing and landform data were collected.

This chapter reviews the current operational survey methods used to collect information about native vegetation in the eastern states of Australia, with a particular emphasis on New South Wales (NSW). The existing approach for translating these data into vegetation maps are outlined. Issues with scale and remote sensing are introduced and I suggest a framework for a solution. I suggest a multi-scale, object-based, hierarchical approach to generalise floristic data collected at the plot scale to create a vegetation community map using hyperspectral remote sensing.

2.1 Forest ecology

From the early 20th century on, forest ecologists have studied stands of vegetation which they considered samples of a ‘plant community’ (Allen and Hoekstra, 1992, Watt, 1947). The stands are selected on the basis of uniformity and discreteness and should be discernible from surrounding vegetation (Ter Braak et al., 2004, van der Maarel, 2004). *Uniformity* means that the vegetation has the same appearance, i.e. the same height and the same plant species in a dominant position, and that the floristic composition does not vary. It is the degree of species *dissimilarity* over a geographical range that determines when species assemblages should be considered as separate communities and recorded as such (Benson, 2006).

The dominance of certain growth forms such as trees, shrubs and grasses allows plants to be grouped into formations. This grouping allows for large areas to be classified, such as a large area of mallee trees, or grasslands. An association is a plant community of definitive floristic composition, presenting a dominant growth form, and growing in uniform habitat conditions. The association is the fundamental unit of vegetation ecology (Westhoff and Van Der Maarel, 1978). The concept of using fidelity or ‘characteristic species’ to describe plant communities arose in and was pivotal in the seminal plant community classification methodologies developed in the 1930's (Braun-Blanquet et al., 1932).

Plant communities are also part of larger units. In the usual hierarchy the next higher unit above the community is the ecosystem, which in turn is part of a biome, a formation together with its fauna and environment. The plant community as defined above is a realistic concept only at a certain scale of observation (the scale at which it is possible to judge the relative uniformity and distinctness). This 'community scale' will vary with the structure of the community, from some meters squared for short grassland to several thousand metres squared in tall forest (van der Maarel, 2004).

Vegetation types rarely occur as single-species stands, but rather as assemblages of species that form a continuum in terms of composition, cover, abundance and height (McKenzie et al., 2008). Ecological theory suggests that similar environmental conditions should produce clumping of species into recognisable and predictable plant assemblages (McKenzie et al., 2008). Classification of vegetation is essentially a compromise between the desire to preserve these natural groupings as continuously varying entities and the need to subdivide them for more utilitarian purposes (Beadle and Costin, 1952).

2.2 The benefits and drawbacks of standardised vegetation assessment

There are many advantages to using standardised vegetation sampling methods; the methods are widely applied and incrementally improved, they are designed to allow for repeatable and comparable collection field data across a variety of landscapes, and they are designed to be used by a range of personnel, sometimes without localised botanical expertise. Perhaps most importantly, they are designed to answer questions that ecologists and natural resource managers pose, because they have been formulated by ecologists and natural resource managers. Spatial scientists are often criticised for applying their own sampling design, based around their own expertise, without answering practical questions posed by land managers. It is a case of answering what you can, rather than what is being asked.

Several publications are available to assist Australian vegetation scientists to survey, classify and map vegetation types to the association and sub-association level of detail. The Australian Soil and Land Survey Field (National Committee on Soil and Terrain, 2009) documents efforts towards an intra-Australian standardization of the description, characterization, naming and coding of vegetation site attributes. The Guidelines for Surveying Soil and Land Resources (McKenzie et al., 2008) is published by the Australia's national science agency and also promotes the development and implementation of consistent methods and standards for conducting soil and land resource surveys in Australia.

The problem with using standardised vegetation sampling methods is that they are not commonly designed to guide the classification of remote sensing data. The type of data collected in the field is very different to that collected by remote sensing instruments, partly because they are collected at different scales. For example, the understorey plays an important role in characterising vegetation structure. The density of shrubs is relatively simple to quantify in a field plot but that information is unlikely to be correlated with remotely sensed data, particularly if the understorey is obscured by a taller canopy. As a result, vegetation structure is not spatially modelled in an operational setting and is used exclusively in site assessments.

Australia contains over 20 000 vascular plant species and has patchy sampling and mapping of its vegetation in terms of quality and extent. Given the size of the country, it has a limited number of ecologists with the expertise to conduct research (Benson, 2006). A scattered collection of point data are not adequate for making natural resource management decisions. Classified remote sensing data are seen as an efficient tool for planning and biodiversity assessment at relatively large scales (Pressey and Nicholls, 1989) but can be too coarse in their thematic classification. They do not usually depict small patches of vegetation useful for property-scale site assessment

The lack of precision at this finer scale is because within any broad environmental classification, such as vegetation community, the distribution and structure of vegetation varies as a result of modification by humans or past natural disturbance e.g. (Prober et al., 1995). Consequently, coarse scale maps are of limited value for guiding property management decisions such as identifying the need for weed control, monitoring grazing regimes, and maintaining habitat (McElhinny, 2005). As a result, the requirement for fine scale mapping to assist with property-scale planning is increasing in Australia (Benson, 2008).

Presently, there is no consistent fine scale vegetation map for the New South Wales (NSW). Both regional and fine scale vegetation mapping remains patchy and there is no ongoing program to fill data gaps (Benson, 2006). Instead, natural resource managers in rely on property scale assessment to meet legislative requirements. While vegetation type and forest fuel load are routinely sampled using standardised field techniques, standards do not exist for spatially modelling these attributes across the landscape. There is a glaring disconnect between the routine collection of data at a plot scale and the creation of maps.

The NSW Rural Fire Service uses the Overall Fuel Hazard Guide (OFHG) (McCarthy et al., 1999) to quantify the volume of combustible material in the landscape. Fuel assessment is frequently used for planning hazard reduction burns and more recently, for predicting fire behaviour. The OFHG is typically used at a site scale for immediate and local management.

The NSW Department for Environment and Climate Change uses the Biometric tool (Gibbons et al., 2005) for property scale assessment of condition. Condition assessment is used to gauge the ‘naturalness’ of a particular stand of forest in comparison to pre-established benchmark values. It predicts the loss of biodiversity from proposed clearing (including thinning), gains in biodiversity from proposed offsets, and gains in biodiversity from management actions proposed for government incentives at the scale of the stand or patch.

Vegetation community classification and forest fuels assessment are both concerned with quantifying vegetation structure. Many of the attributes sampled, such as understorey density, are shared. Their commonalities have meant that all three methods are relevant for this thesis. A description of the fieldwork conducted for this thesis appears in Chapter 3.

2.3 Operational field methods for assessing native vegetation community type

Vegetation can be classified through structural or physiognomic attributes such as growth form, height of strata and canopy cover. Alternatively, vegetation can be classified through a floristic approach by describing variation in species composition across a region. The latter can involve analyses of patterns of dominant plant species or all plant species (Kent and Coker, 1992). Often elements of both structural and floristic approaches are used in vegetation classification (Benson, 2006). Growth form (trees, shrubs, vines etc.) is the core of the influential vegetation classification scheme of Beadle and Costin (1952). They are also a major component in the structural classifications of the widely used projected foliage cover and height class classification of Specht (1970) and the crown separation and height class classification of McDonald et al. (2009).

Structural characteristics describe the vertical and horizontal distribution of vegetation in space; its growth form, height, density and layering. It is recorded for growth forms of major plants, usually repeated for each major discernible layer. A set of schematic illustrations of vegetation structure from a selection of Australian vegetation types is presented in McDonald et al. (2009). These structural classifications have the advantage of requiring minimum knowledge of plant species taxonomy but they tend to classify vegetation into broad classes such as ‘tall open forest’ or ‘open shrubland’ and each class contains numerous floristic communities generally spread over large distributions. Structural characteristics also tend to be the most easily recognised features on air photos or on other remotely sensed images (Hnatiuk et al., 2009).

Vegetation classification at the highest level is based on the growth form and cover of the species forming the dominant stratum. The classes of vegetation at this level are called formation classes. Growth form is defined as: habit or general appearance of a plant. It is similar in definition to ‘life form’ (Hnatiuk et al., 2009). Floristic characteristics range from the names of dominant and characteristic plant species through to comprehensive species lists at the site.

Vegetation that has been identified in the field can then be classified through numerical classification of floristic plot data with the application of statistical procedures such as fidelity analysis, association measures, hierarchical divisive cluster analysis and ordination to extend linear regressions. In Australia, the non-agglomerative, flexible Unweighted Pair Group Arithmetic Averaging (UPGMA)

(Sokal and Rohalf, 1962) approach has gained favour (Benson, 2008). The algorithm examines the structure present in a pair wise distance matrix and then constructs a rooted tree (dendrogram) that has been used to visualise the relationship between samples and guide how species are clustered into communities e.g. (Keith and Bedward, 1999).

The convention for naming vegetation type generally uses floristic associations with species dominance and indicator species combined with the structural formation.

ASSOCIATION + STRUCTURAL FORMATION = VEGETATION NAME

E.g. *Eucalyptus populnea* tall woodland

Equation 1 The convention for naming vegetation type generally uses floristic associations with species dominance and indicator species combined with the structural formation.

Initially the most abundant or physically predominant species in the dominant stratum is selected. If another dominant stratum species is always present and conspicuous (a co-dominant species), it is also selected. In the absence of a second dominant stratum species, the most abundant or physically predominant species of the next most conspicuous stratum is selected. A third species is selected from any stratum, usually a lower stratum, as an indicator species (that is, a species, with known environmental preferences or of such abundance that it cannot be ignored), or to distinguish between associations (Hnatiuk et al., 2009).

More species names can be added to distinguish vegetation types that have similar structures and species dominants in the dominant stratum. The main problem in using the dominant species to qualify the structural formation is that dominance can vary spatially and, for example, in the case of two or more species occurring in varying amounts in essentially the same vegetation type, a variety of names is possible. Ideally, all species present in the sample site at the time of sampling should be recorded. However, the completeness of a species list will depend partly on the purpose of the survey, the season of sampling, the degree of disturbance and the botanical expertise of the sampler (Hnatiuk et al., 2009).

2.4 Operational field methods for assessing forest fuel loads

Fire models have been developed specific to Australian forests to help predict and understand fire behaviour and fire hazard. These require a variety of input data but generally use variables that describe the meteorological, topographic and fuel conditions (Adams and Simmons, 1999). They are designed to predict the way in which fuel will burn by applying mathematical relationships to describe different aspects of fire (Andrews and Queen, 2001a). The McArthur Forest Fire Danger Index (FFDI) (McArthur, 1967) is the most widely utilised forest fire behaviour model in eastern Australia. It was designed for general forecasting purposes and is based on the expected behaviour of fire in eucalypt forest. Spread rate is predicted as the product of meteorological variables and the fuel load (measured in tonnes per hectare). The overall fuel hazard can be combined with the current climatic conditions to calculate the probability of first attack success.

Experiments have revealed the FFDI can generally predict fire behaviour under moderate conditions but under very high to extreme conditions it may underestimate the rate of fire spread (Buckley, 1992). A major weakness of the model is that it does not take into account the spatial variability of fuel characteristics. By only using fuel load to characterise fuels the model neglects the importance of fuel structure. Indeed, the structure and quantity of surface fuel is of greater importance to wildfire behaviour than a measure of fuel load per unit area (Burrows, 2001).

(Luke and McArthur, 1978) established that independent crown fires do not occur in eucalyptus forests, as the amount of radiative heating from crowns is usually insufficient to maintain combustion in adjacent crowns. Crown fires in eucalypt forests are the result of pre-heating by convection from understorey fuels. The rate of spread of fire in Australian forests is dictated by surface and near surface fuel layer depths and the continuity and the height of the shrub layers. Forest fires in fuels with a developed shrub layer are likely to spread much faster, as are fires in litter fuels with a low shrub layer.

Chandler (1983) found that vertical gaps in the fuel layer 1.5 times the height of the flames can prevent crown fires developing, while a horizontal gap of 100m has the ability to ground a crown fire. Therefore, a fire of greater intensity is required to maintain a crown fire in areas where there is only low vegetation (Smith et al., 2004). In the right conditions, bark can act as a link between ground and crown fuels to produce crown fires (McCarthy et al., 1999). Bark can also defeat control in wildfire or even prescribed burn situations by producing spotting, burning embers that are transported by wind (McArthur, 1967).

Fuel refers to combustible organic material, both living and dead. The description of fuel properties is necessarily complex. To combat this, fuel classes are often described by grouping vegetation types with similar fire behaviour characteristics e.g. Van Wagner (1968). The vegetation species is not always relevant since the same species may present completely different fire propagation rates, for example, due to fuel load or changes in vertical continuity.

Fuel load is often divided into size classes in order to estimate the available fuel for burning (Papió and Trabaud, 1991). Not all fuel sizes are used to calculate fuel load. Usually only fine fuels (those less than 6mm in diameter) are used to calculate the fuel load. Fine fuels are used as these ignite and burn readily, whereas coarser fuels do not contribute as much to the flaming stages of combustion (Luke and McArthur, 1978). Coarse fuels are present as logs and thicker sticks in the litter layer and stems, trunks and limbs greater than 6mm in diameter of plants.

Fuels accumulate at different rates according to productivity, climate and plant species but fuel loads sufficient to be vulnerable to spotting can build up within 2-3 years after low intensity fires in most eucalypt forests and woodlands (Morrison, 2002, Raison et al., 1986, Tolhurst et al., 1992). The fuel properties of particular interest include: fuel load (weight per unit area), bulk density (weight per unit volume), fuel size (branch diameter), fuel moisture content, the spatial distribution of fuel (horizontal and vertical), the continuity of fuel, fuel height, and fuel type. Topography is an additional parameter of interest due to the interactions with forest fuel characteristics and fire behaviour.

Destructive sampling is considered to be the most accurate fuel load assessment technique at a particular sample point (Catchpole and Wheeler, 1992) and all other techniques are calibrated against it. Destructive sampling is simple, and can be used to determine the mass and fraction of selected parts of the fuel array, as well as other attributes such as density and proportion of dead fuel. Destructive sampling requires randomly laying sample frames over vegetation and litter fuel at ground level and removing all of the combustible vegetation material present. The resulting fuel sample is oven-dried and weighed to give a measure of fuel load in weight per unit area (t/ha). Destructive sampling of fuels is rarely used by fire managers due to the large commitment of resources required (Fernandes and Botelho, 2003). Standardised methods to rapidly assess fuel loads visually have been developed in response.

The Overall Fuel Hazard Guide (McCarthy et al., 1999) was originally developed by the Victorian Department of Natural Resources and Environment for south-eastern Australia. It simplifies the rapid assessment of understorey fuel loads by applying a visual scale for comparison. It has been adopted for operational use in NSW to ensure state-wide consistency in measuring fuel hazard levels.

Near-surface fuels, elevated fuels and bark hazard are ranked as low, moderate, high and very high and extreme according to well defined visual/physical descriptions. The rankings acknowledge fuel continuity (horizontal and vertical), height, amount (weight), and the proportion of dead material, thickness of the foliage and twigs, and flammability of the live foliage. Average equivalent fuel loads (in tonnes per hectare) can be devised for the various hazard levels for each fuel component.

Tables are used to convert the visually assessed surface fine fuel hazard rating score to fuel load in tonnes per hectare (Table 2.1) and combined with assessed levels of bark, elevated and surface fine fuel hazard to give an overall fuel hazard rating for a site (Table 2.2).

Table 2.1 The surface fine fuel hazard rating converts visually assessed scores to fuel load in tonnes per hectare.

Surface Fine Fuel Hazard Rating	Low	Moderate	High	Very high	Extreme
Litter-bed Height (mm)	< 1 5	15- 2 5	25- 3 5	35- 5 0	50 >
Equivalent Litter Load (t/ha)	< 4	4-8	8-12	12-20	20+

Source: The Overall Fuel Hazard Guide (McCarthy et al., 1999)

Table 2.2 Equivalent fuel loads (t/ha) for given hazard ratings.

FUEL	Low	Moderate	High	Very High	Extreme
Bark	0	0	2	5	7
Surface Fine	2	5	10	16	20
Elevated Fuels	0	0	2	6	10

Source: The Overall Fuel Hazard Guide (McCarthy et al., 1999)

The OFHG represents a significant change in the philosophy of assessing the fuel factors affecting fire behaviour. The FFDI only considers surface fine fuel loads (in t/ha) whereas the OFHG shifts the emphasis to a consideration the whole fuel complex, and particularly the bark and elevated fuels. Bark and elevated fuels are the fuel elements principally responsible for first attack failure and also for general suppression difficulty in Victorian forests, woodlands, deserts, heathlands and shrublands (McCarthy et al., 1999).

Current practices for collecting fuel load information in the field are problematic when applied to large and remote areas. Field sampling is costly, complex and time consuming. Fuel quantities are dynamic and consequently require periodic updating, but this is difficult to achieve due to the nature of data collection methods. Simply reproducing measurements of fuel loads taken in the field can be a challenging task (Chandler, 1983).

Brandis and Jacobson (2003) studied the relationship between fire history and fuel load and found that destructive sampling effectively reproduced fuel accumulation models. However, they found visual assessments, based on the Victorian OFHG, commonly underestimated fuel loads, especially the litter component. The study concluded that new methods to estimate fuel data regularly for large and remote areas were needed to improve fire risk assessment, fire behaviour prediction and fuel management plans (Brandis and Jacobson, 2003).

The CSIRO's Forestry and Forest Products division is currently working towards replacing fuel load with a numerical index, or hazard score, which should give more reliable predictions for fire spread. This technique places even more emphasis on quantifying the whole fuel complex by combining a hazard rating for each of the different fuel layers i.e. bark, elevated, near-surface and surface fuels layers (Gould, 2003).

There is a clear management advantage to having an understanding of fuel continuity across the landscape. The provision of data for spatial simulation models is critical in active fire fighting and aids prescriptive burning. Maps of fuel loads are not available in most Australian environments. Fire history mapping and assessment of fuel reduction efficiency is haphazard at best. Current management practice is to estimate fuel loads at the landscape level based on expert experience in the local environment. This subjective approach, coupled with relatively poor fire history records outside major conservation reserves, has the potential to lead to non-strategic fuel mitigation strategies

2.5 Operational field methods for assessing the condition of native vegetation

The concept of vegetation *condition* or ‘quality’ has arisen in Australia with the need to set conservation priorities at local and regional scales. Species richness and species diversity have been used as a measure of (Sarkar and Margules, 2002, Smith et al., 2002a). This is problematic because it is not possible to sample all species at all levels in a hierarchy and because it ranks communities with high richness (Margules and Pressey, 2000), such as tropical rainforests, above those with inherently low richness, such as woodlands and dry forests (McElhinny, 2005). Studies into groups of species or ‘indicator species’ have concluded that they are not representative of biodiversity as a whole (Margules et al., 2002).

Noss (1999) suggested that vegetation condition encompasses vegetation structure, composition and function and numerous surrogates have been suggested (Gibbons et al., 2005, McElhinny, 2005, Parkes et al., 2003, Tongway, 1995). The theory is that ecosystems with a variety of structural components are likely to have a variety of resources. These resources will provide for a corresponding variety of species (McElhinny, 2005). Consequently, there is often a positive correlation between elements of biodiversity and measures of the variety and complexity of structural components within an ecosystem e.g. McElhinny (2005). Depending on specific objectives, different combinations of these surrogates can be combined into indices of vegetation *condition* (McElhinny, 2005).

Methods for assessing condition in rangelands, arid and semiarid ecosystems are routine (Dyksterhuis, 1949, Ludwig et al., 2007, Reeves et al., 2001). However, the concepts of ecological condition or quality of native vegetation or 'habitat' in more mesic and temperate systems are still relatively vague and poorly defined (Gibbons et al., 2006). Recent approaches such as 'Habitat Hectares' (Parkes et al., 2003) and the ‘Biometric Tool’ (Gibbons et al., 2005) provide rapidly obtained indices of native vegetation condition by using comparisons to reference condition states, or 'benchmarks', to provide managers of native vegetation with simple measures of vegetation ‘quality’ or *condition*.

A variety of methods have since been proposed including Watson et al. (2001) Habitat Complexity Score, the Site Condition Score component of Habitat Hectares Index of (Parkes et al., 2003) the Vegetation Condition Score of the Biodiversity Benefits Index (Oliver and Parkes, 2003), the Vegetation Condition Score component of the Biometric assessment tool (Gibbons et al., 2005) and the Stand Scale Index of Structural Complexity (McElhinny, 2005).

Table 2.3 A comparison of condition attribute weighting. The metrics common to all three condition assessment methods include measures of compositional diversity, the amount of regeneration; percent cover at various scales, and the occurrence of large trees.

Stand Structural Complexity (McElhinny, 2005)	
Condition Attribute	**Weight (%)**
Perennial species richness (native)	7.7
Lifeform richness (native)	7.7
Vegetation cover >0.5m	7.7
Vegetation cover <0.5m	7.7
Stand basal area of live trees	7.7
Number of regenerating overstorey stems	7.7
Litter dry weight	7.7
Total log length	7.7
Total large log length	7.7
Quadratic mean diameter	7.7
Number of live stems > 40cm dbh	7.7
Number of hollow bearing trees	7.7
Number of dead trees	7.7
Total	100

Site Condition Score (Parkes et al., 2003)	
Condition Attribute	**Weight (%)**
Richness of native species within lifeforms assessed concurrently with cover of native understorey lifeforms	33
Tree (canopy) cover	6.7
Presence of adequate regeneration in woody perennial native species	13
Lack of weed cover	20
Litter cover	6.7
Total log length assessed concurrently with Large logs	6.7
Number of large trees	13
Total	100

Vegetation Condition Score (Gibbons et al., 2005)	
Condition Attribute	**Weigh t (%)**
Native plant species richness	20
Native foliage cover (grasses)	5
Native foliage cover (shrubs)	5
Native foliage cover (other)	10
Native mid-storey foliage cover	5
Native overstorey foliage cover	5
Proportion of overstorey species occurring as regeneration	10
Lack of exotic plant foliage cover	5
Total length of fallen logs	5
Number of trees with hollows	30
Total	100

Source: Adapted from McElhinny (2005).

A single index is useful as it facilitates comparisons between stands (Koop et al., 1995, Newsome and Catling, 1979, Watson et al., 2001) and provides a summary value with which to seek correlations with remote sensing data (Table 2.3). This index also provides a means of ranking stands in terms of their potential contribution to biodiversity (Parkes et al., 2003, Van Den Meersschaut and Vandekerkhove, 1998). Indices that are related to vegetation structure are seeing increased use as policy instruments for mitigating development, guiding investment decisions, and in biodiversity banking (Gibbons et al., 2005, Parkes et al., 2003). They provide a summary variable for a larger pool of structural attributes.

The Vegetation Condition Score component of the Biometric tool of Gibbons et al. (2005) was designed for the to assess the impacts (positive and negative) of management activities on terrestrial biodiversity (Table 2.3). Condition assessments scores are derived using the Biometric tool to predict the loss of biodiversity from proposed clearing (including thinning), gains in biodiversity from proposed offsets, and gains in biodiversity from management actions proposed for government incentives at the scale of the stand or patch.

The Vegetation Condition Score attributes (Gibbons et al., 2005) detailed in Table 2.3 are compared to benchmark ranges as part of the *Biometric* process. Vegetation with relatively little evidence of modification generally has minimal timber harvesting (few stumps, coppicing, cut logs), firewood collection, and exotic weed cover, grazing and trampling by introduced herbivores or over abundant herbivores, soil disturbance and canopy dieback. There will be no evidence of recent fire or flood, or high frequency burning, and there will be positive evidence of recruitment of native species. The benchmarks allow interpreters to rank vegetation communities according to the relative evidence of alteration, disturbance or modification by humans since European settlement. A list of benchmark values have been published (Gibbons et al., 2005) based on broad vegetation classes from Keith (1994).

McElhinny (2005) criticised Parkes et al. (2003) and Gibbons et al. (2005) for misapplying the concept of benchmarking, by characterising attributes in terms of a benchmark range or average level. This approach ignores the processes that underpin variation at the stand level, such as the increased development of some attributes at particular successional (seral) stages, and the fact that condition attributes can respond differently to disturbance agents.

Successional stages of vegetation range from the time of disturbance, through recovery, maturing, senescence and to disturbance again. In some cases there will be progressive replacement of the dominant and other species with new species. This problem is common to all benchmark based methods that are based on sampling at a single point in time.

A temporal scale is important for effective decision making in most contexts. Site assessment can provide relevant information for a proposed development but ignores successional stages of vegetation over time. Mapping condition across the landscape is still useful as it can provide spatial arrangement of sites in good condition and sites in bad condition. It can help target management actions towards areas affected by disease or over grazing, or help target restoration projects. However, the final objective of condition research should be to classify vegetation condition both spatially and temporally.

2.6 Scaling issues for field survey

The problem faced in the conversion of information collected in the field for spatial models using remote sensing is largely one of scale. Many challenging aspects of natural resource survey have resulted from unavoidable mismatches between scales of measurement, estimation and prediction.

Measurement is the vegetation survey (forest type), estimation is the process of providing a numerical value for the measured vegetation type (e.g. mean, median, environmental layer, altitude) and prediction is modelling the type across the landscape based on environmental layers (vegetation map).

Field measurements are necessarily restricted to finite areas at sparsely distributed locations. Manipulations of grain and extent enable us to translate information between scales. Grain is the finest level of spatial resolution in an observation set or model (McKenzie et al., 2008). *Extent* is the areal expanse over which observations with a particular grain is run. Course scales can be reached by increasing the grain and, usually, the extent of the observation set and usually involves some form of averaging. For example, moving from a community to a formation. Making the observation set more fine grained is not as easy (McKenzie et al., 2008).

Various aspects of land resource survey require movement within the scale hierarchy. For example, estimating average values for vegetation type from a limited number of field observations. Or relating field data to remotely sensed imagery where the support for the former is often several orders of magnitude smaller than for the later. All of these involve movement within the scale hierarchy, and the steps involve some form of downscaling or upscaling. Scaling literally means to reduce or increase in size. Upscaling is a popular term that refers to transferring information from a given scale to a coarser scale it involves moving up the hierarchy either through enlarging extent, or coarsening grain, or both. Downscaling is the opposite process (Bloschl and Sivapalan, 1995).

Some forms of upscaling are trivial. For example, it is straightforward to compute the NDVI for a single stand of trees. It is less clear how to calculate a regional mean for NDVI across an area that features scattered trees, grasses and soils. It will often be the extremes of the distribution that determine behaviour at the coarser scale.

Allen and Hoekstra (1992) recognised that, at various scales of perception, any phenomenon will appear simpler at some scale than it will at others. They suggest that robust prediction requires consideration of at least three levels of organisation in a hierarchy. The level in question (e.g. vegetation association) the level below (individual plants) and the level above (formation or broad floristic unit made up of associations). This line of reasoning suggests that predictive relationships developed at one level are unlikely to be useful for prediction at a level more than one removed.

As an example, the collection of individual plants at a survey site may inform or be characteristic of the association. However, multiple associations are combined to create a formation. Knowing the formation will not be helpful in predicting the vegetation at the survey site. The mismatch in scale between the measurement and process constrains the utility of prediction (McKenzie and Ryan, 1999).

The spacing and area of the field surveys determines whether coherent patterns can be detected. If the gaps between surveys are too large, the variation in type appears random. If the gaps between surveys are small enough but the extent over which the surveys have been made is too limited then it will not capture the true nature of the variation. Ideally, vegetation properties should be observed at dimensions that match the scale of the relevant process (McKenzie et al., 2008).

McCauley (2006) advises that homogenous patches of vegetation should be sampled in the field to improve condition modelling performance. Unfortunately, native vegetation rarely occurs in homogenous stands. Instead it occurs in heterogeneous patches nested in a mosaic (Forman, 1995). Ideally, the sampling of vegetation should take place at dimensions that match the scale of the relevant process. Since resource limitations and floristic heterogeneity make it impractical to survey large areas I would argue that the landscape needs to be treated as a nested hierarchy.

2.6.1 Plot size

A survey site is a small area of land considered representative of the landform, vegetation and other land features. The Australian Soil and Land Survey Field Handbook (National Committee on Soil and Terrain, 2009) recommends vegetation be surveyed in a square site of 0.04 ha (i.e. 20m by 20m) when sampling floristics.

However, the optimal area will vary greatly for different associations relative to the apparent complexity of composition and structure of the community. The scale at which vegetation community is expressed will vary with the structure of the community, from some meters squared for short grassland to several thousand metres squared in tall forest (van der Maarel, 2004). The complexity of the pattern or process is clearly important. If the underlying pattern is highly complex than many samples are required. If the same community exists over a wide area without a break then fewer samples are needed.

A plot size of 0.04 ha (20m by 20 m) is the most frequently used (Benson and Ashby, 2000, Keith and Bedward, 1999, Keith and Benson, 1988, Sivertsen and Metcalfe, 1995). The exceptions are usually smaller plot sizes used in grassland or heathland surveys (Benson, 1994, Keith, 1994), or larger plots sizes used in open woody communities where the overstorey is the main focus (Binns, 1997, Helman, 1983, Jurskis et al., 1995, Portners et al., 1997).

Species area curves are traditionally used to determine the most efficient plot size for a given vegetation type. The aim is to capture the majority of the species on site (alpha diversity) and the number of plots needed to capture the full range of species occurring across the extent of the vegetation type (beta diversity) (Kent and Coker, 1992, Mueller-Dombois and Ellenberg, 1974).

A species-area curve plots the number of species found in an association on the y-axis coordinate with the area of the stand which is plotted on the x-axis. When several association individuals of various sizes have been examined, the species-area points define a characteristic curve. This curve rises rapidly from the intersection of the y and x (Rice and Kelting, 1955). The point on the curve at which the curve flattens strongly and tends to become asymptote with the x axis (on which area is plotted) is taken to indicate the minimal area. At that point, increasing the area of the plot no longer increases the variety of plants found. This led to the concept of minimal area, ‘the smallest area which can contain an adequate representation of an association' (Braun-Blanquet et al., 1932).

For an effective representation of the floristic type a site survey should be large enough to survey the dominant species, the structure should be homogenous enough to be characteristic, and it should contain characteristic species for the association, i.e. those of high fidelity (Rice and Kelting, 1955).

Vegetation surveys are most commonly 20m by 20m. This survey size is not large enough for a representative survey of tall trees, so it follows that it cannot provide an effective representation of the floristic type. Hnatiuk et al. (2009) recommends that plot size vary with the height of the vegetation being sampled. That is, vegetation over twenty metres high be surveyed in 30m by 30m plots, vegetation under twenty metres high a 20m by 20m plot is adequate, and for vegetation <1 m high a 5m by 5m plot will suffice. In a larger plot, a larger number of tree species from the upper stratum are able to be identified, which increases the probability that diagnostic species for the association will be encountered.

Increasing the size of vegetation surveys for every stratum is not a practical solution for floristic surveys in Australia. An alternative is to survey vegetation at a variety of scales, or in a series of nested hierarchies. Nested hierarchies involve levels which consist of, and contain, lower levels (O'Neill et al., 1996). Following Hnatiuk et al. (2009), I propose that plot size could vary with the height of the stratum being sampled.

2.6.2 Multi-scale survey

Soil survey and mapping already has standards for sampling at multiple scales in Australia. Landforms are observed as a mosaic in a nested hierarchy (National Committee on Soil and Terrain, 2009). A landform mosaic is treated as if the tiles are of two distinct sizes, the larger ones being themselves mosaics of the smaller ones.

The larger tiles, 600 m across, are called landform patterns. About 40 types of land form pattern are defined. They include, for example, flood plain, dunefield and hills. Relief and stream occurrence describe landform patterns. The smaller tiles, which form mosaics within landform patterns, are 40 m across. These are called landform elements. Among more than 80 defined types of landform element are included, for example, cliff, footslope and valley flat. Slope and position are key attributes for landform elements.

2.7 Prediction of operational survey attributes using remote sensing

Natural resource managers have not always enjoyed good advice when selecting remote sensing products and services, and are wary of spatial analysis that does not meet their needs. Mapping the attributes of canopy species across the landscape is a complex task. In any one stand of trees there are countless combinations of species, disturbance, structure, shadow, and other attributes that confound analysis. This makes it difficult to consistently generalise vegetation classes across a landscape using remote sensing, especially with pixel-based classification. As a result there has been a tendency to rely on expert opinion and manual interpretation of remotely sensed imagery.

There are three broad approaches to mapping vegetation communities using remote sensing. The first is a manual process driven by visual interpretation of aerial photo patterns. The second uses spatial models to predict the distribution of vegetation. It uses numerical relationships between site-based data and independent environmental variables such as landform, climate and remote sensing. The third combines these approaches in a hybrid system to incorporate the advantages of quantitative analysis with expert qualitative knowledge.

2.7.1 Visual interpretation

Visual interpretation of remotely sensed data allows operators to intuitively delineate and attribute complex patterns by using expert knowledge. The landscape patterns are then correlation with sample data, and extrapolated based on similar geology, topographic position, floristic attributes and structural formation (Bell and Driscoll, 2006, Ismay et al., 2004, Neldner et al., 2005, Sivertsen and Metcalfe, 1995). The argument has been that variables such as texture, spatial relationships and diffuse boundaries, cannot be incorporated into a digital analysis (Emery et al., 2001). Stereo imagery is widely used for the tree height and structural attributes it adds to the cognitive process.

However, drawing a line between communities is an exercise in judgement, not one always following a clear demarcation in the vegetation, particularly where there is a gradual transition from one vegetation community to another (Kitchener and Harris, 2005). Visual interpretation of remote sensing data can be resource intensive and difficult to implement consistently over large areas (Asner and Warner, 2003, Gellie, 2005). A significant amount of field observation is required to both confirm and revise the initial air photo interpretation. The work is constrained by limitations on how rapidly a human interpreter could physically review and interpret air photographs and by the restricted access to largely inaccessible terrain (MacMillan et al., 2007). Automated routines can be readily replicated across wide areas but they are generally less accurate than visual interpretation (Culvenor, 2002)

2.7.2 Spatial modelling of environmental layers

Spatial modelling using environmental layers aims to utilise the landform variables and remote sensing attributes used to aid visual interpretation and combine these using quantitative analysis. Floristic surveys are used to estimate a numerical value that represents a given vegetation type (e.g. mean, median, environmental layer, altitude). The use of quantitative field sampling and remotely sensed data allows for explicit multivariate analysis, which may detect patterns that escape recognition by traditional intuitive methods. Modelling vegetation reduces the role of non-repeatable intuitive classification and mapping decisions (Keith and Bedward, 1999). One of the advantages of using environmental layers as a basis is that the pre-European distribution of native vegetation in Australia can be modelled determined based on remnant vegetation. This has important biodiversity implications for setting reserve targets and conservation priorities.

Generalised dissimilarity modelling (GDM) has been a popular approach to modelling using environmental variables in Australia (Ferrier and Guisan, 2006, Overton et al., 2009). GDM studies the spatial turnover of community composition (beta diversity) between pairs of sites as a function of environmental differences between sites. Regression approaches are thought to be most appropriate if the density of survey sites within a region is high relative to the spatial distribution of classes within the region (Ferrier et al., 2007).

A greater variety of modelling approaches feature in the literature internationally. Generalised dissimilarity modelling (GDM), generalised linear models (GLM), generalised additive models (GAM) (Dobrowski et al., 2008, Overton et al., 2009), multivariate adaptive regression splines (MARS) (Leathwick et al., 2006, Leathwick et al., 2005), artificial neural networks (ANN) (Filippi and Jensen, 2006, Joy and Death, 2004) random forests (RF) (Cutler et al., 2007), classification tree analysis (CART) (Accad and Neil, 2006, Chastain Jr et al., 2008, Vogiatzakis and Griffiths, 2006) and Canonical Correspondence Analysis (CCA) (Dirnböck et al., 2003) have all seen use in recent studies.

Consensus or ensemble approaches to classification combine the results of some of these models to increase the overall accuracy (Elith et al., 2006, Marmion et al., 2009). Marmion et al. (2009) modelled the distribution of 28 threatened plant species in pine and spruce dominated forests in Finland. The probability outputs of eight single-modelling techniques were combined to provide an ensemble of predictions. Generalised linear models (GLM), generalised additive models (GAM), multivariate adaptive regression splines (MARS), artificial neural networks (ANN), general boosting method (GBM), random forests (RF), classification tree analysis (CART) and mixture discriminant analysis (MDA) were the models used. The results of single models performed between RF (0.813) and CTA (0.697). Combining the results by weighted average showed the highest predictive performance (0.85).

2.7.3 Hybrid modelling

Keith and Bedward (1999) developed a hybrid decision tree / expert rule based approach to mapping vegetation. They interpolate the distributions of floristic classes from point samples using relationships between the classes and environmental and remote structural variables that were available as spatial data layers. This provides a framework for incorporating non-formal expert knowledge into the map by offering a choice between multiple significant variables at each node, facilitating exploration of alternative tree structures. This kind of knowledge is difficult to build into statistical models, which traditionally rely upon quantitative sample data (Austin, 1987). Tozer (2003) used the same decision tree / expert rule based approach and described vegetation communities, extant and pre-European. Point scale assessment gave overall accuracy as 50% but an accuracy assessment based on validation points buffered to 500m yielded improved performance (95%).

In another example, Gellie (2005) modelled the distribution of vegetation groups in support of expert decision vegetation mapping. Generalised additive modelling (GAMS) (Austin and Belbin, 1982, Yee and Mitchell, 1991) was used to test some of the assumptions held by the mapping experts about the distributions of vegetation groups within a regional landscape setting. McCauley (2006) mapped an area in the Hunter Valley using SPOT 5 imagery as well as environmental layers. They found that the seasonal variation and the low dynamic range of SPOT 5 hampered discrimination of vegetation types.

2.7.4 Scale and remote sensing

Strahler et al. (1986) developed a framework to distinguish between the scene, which is real and exists on the ground, and the image, which is drawn from the scene. Scene models may be discrete, in which the scene model consists of discrete elements with boundaries (e.g. tree crowns), or continuous, in which matter and energy flows are taken to be continuous and there are no clear or sharp boundaries in the scene (e.g. elevation). In the discrete case, there are two possibilities for models. For high spatial resolution the resolution cells of the image are smaller than the elements (e.g. tree crowns), and thus the elements may be individually resolved. For coarse resolution imagery the cells are larger than the elements and so the elements cannot be resolved (see Figure 2.1).

When the vegetation is considered as part of a hierarchical scene model (Woodcock and Harward, 1992), the scale and square representation implied by pixels do not fit this model (Fisher, 1997) . Ideally, we hope to map patches of natural vegetation that have relatively homogenous spectral and physical values. Such a patch will hardly ever be square, so pixels will only sporadically match a natural scale level (Addink et al., 2007). For pixel-based studies confusion matrix evaluation can be problematic since at coarse resolution a pixel element may include several vegetation types (Xie et al., 2008).

Cracknell (1998) addresses various issues with the fact that a pixel or the related instantaneous geometric field-of-view (IGFOV) on the ground often larger than we would like it to be. IGFOV is the area sampled on the ground by one pixel element taking into account the altitude and geometry of the sensor (Joseph, 2005). It raises some important issues for this study such as how resampling can leads to further complications in understanding the origin of the signal. The general conclusion is that it is important to realise that what contributes to producing the digital number (pixel value) where there is resampling, compression, mixed pixels and when the objects of study are smaller than the IGFOV.

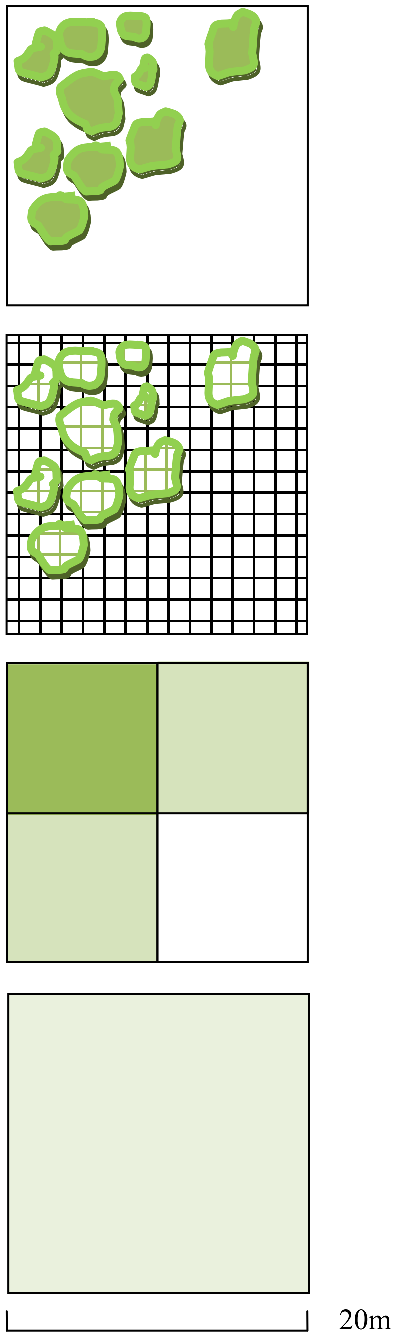

The distribution of tree crowns within a 20m by 20m plot is not uniform when assessing native vegetation.

An image with a 1m IGFOV will divide a plot into 400 pixels. For high spatial resolution the resolution cells of the image are smaller than the elements (e.g. tree crowns), and thus the elements may be individually resolved.

For coarse resolution imagery the cells are larger than the elements (tree crowns) and so individual the elements cannot be resolved. This SPOT 5 pixel (10m by 10m) can however detect variation of cover within a plot.

The mean of tree cover within a plot may not be representative of the actual distribution of trees. Clearings and shadow in particular can heavily weight the mean because of their extreme values.

Figure 2.1 Tree cover and IGFOV in the remote sensing of tree cover.

The possibility of identifying individual tree crowns in very high spatial and spectral resolution imagery raises questions regarding the best scale to map stand-scale vegetation parameters. Careful consideration of the spatial scale of mapping is important because, as stated in the Modifiable Area Unit Problem (MAUP) (Openshaw, 1984) , the choice for the spatial unit affects the outcome of the analysis, implicating the existence of an optimal unit for quantitative analysis (Nijland et al., 2009).

The common pixel-based approach to analysing remote-sensing imagery is a specific case of the MAUP, because pixels represent artificial sampling units ignoring the spatial patterns on the earth surface (Fisher, 1997, Marceau and Hay, 1999). The minimum pixel size is influenced by the spatial structure of the investigated objects. The use of image-based segmentation makes it possible to optimize both the shape and size of the prediction units.

The spatial resolution of hyperspectral sensors has developed to a point that it is possible to derive quantitative data in heterogeneous vegetation (Addink et al., 2007, De Jong et al., 2003). HyMap airborne sensor (Hyvista, 2009) is capable of collecting hyperspectral imagery with a 3.5 m ground resolution. At this resolution, individual tree crowns can often be identified, depending on their size and spacing. The benefits of fine resolution images are obvious: spatially continuous information of vegetation characteristics can be derived directly at hill-slope, forest-stand or even smaller scales (Nijland et al., 2009).

2.7.5 Hyperspectral remote sensing of vegetation

The focus of hyperspectral remote sensing of vegetation in recent years has been on detection and identification of plant health (Schmidtlein and Sassin, 2004) and on monitoring invasive species (Asner et al., 2008a, Noujdina and Ustin, 2008, Underwood et al., 2003). Biochemical applications include the retrieval of moisture content (Cheng et al., 2008, Cheng et al., 2006) and isolating elements such as carbon (Grace et al., 2007), nitrogen (Martin et al., 2008, Smith et al., 2002b, Townsend et al., 2003) and potentially phosphorus (Mutangao and Kumar, 2007). The pigment and photosynthetic system of vegetation is of increasing interest, which will allow coupling models from molecules to leaf, plant and canopy scales (Schaepman et al., 2009). Less research has been performed on mapping vegetation species (Jia et al., 2006, Kokaly et al., 2003, Okin et al., 2001).

Im and Jensen (2008) reviewed research devoted to documenting robust relationships between in situ vegetation measurements and remote sensing-derived measurements to predict or monitor vegetation biophysical and biochemical characteristics (Beeri et al., 2007, Hu et al., 2004, Johnson et al., 1994, Perry and Davenport, 2007, Wu et al., 2008, Asner, 1998). Many studies have focused on remote sensing of leaf area index (Hu et al., 2004, Spanner et al., 1990) and biomass (Calva and Palmeirim, 2004, Catchpole and Wheeler, 1992, De Jong et al., 2003, Fazakas et al., 1999, Foodya et al., 2003, Popescu et al., 2003, Steininger, 2000, Turner, 2006) as well as chlorophyll (Datt, 1999c, Datt, 1999a, Gitelson and Merzlyak, 1994, Hu et al., 2004, Wu et al., 2008).

Generalised assessments of vegetation structure and composition can be made over closed canopies with lidar (Clark et al., 2004, Coops et al., 2007, Koukoulas and Blackburn, 2005, Mutlu et al., 2008, Turner, 2006). Sparse and clumped canopies are currently the greater challenge (Duthoit et al., 2008, Kotz et al., 2004, Sluiter et al., 2004). Many hyperspectral imaging studies use spectral mixture analysis to addresses the issues with sparse vegetation conditions (Asner et al., 2008b, Elmore et al., 2000, Garcia and Ustin, 2001, Okin et al., 2001, Roberts et al., 1997).

Malenovsky et al. (2007) looked at canopy composition at various levels of detail with three pixel-based approaches: radiative transfer, spectral mixture analysis, and data fusion. The use of hyperspectral data have allowed for spectral separability in heterogeneous vegetation by using radiative transfer models (Kotz et al., 2004) and contextual approaches (Sluiter et al., 2004) (Schaepman et al., 2007). Species have been separated from complex surroundings using a combination of lidar and spectral mixture analysis (Asner et al., 2008b) and unique biochemical species composition (Asner et al., 2008a).

Schaepman et al. (2009) notes that bridging spatial and spectral scaling gaps has always been a predominant topic in remote sensing (Chen et al., 1999, Marceau and Hay, 1999, Wessman, 1992). The jump from leaf to canopy to community has remained underexplored in hyperspectral research but is now receiving increased attention (Lewis and Disney, 2007, Roberts et al., 2004).

2.7.6 Object-based vegetation mapping

As we have seen, there are problems associated with sub-pixel variability, particularly for coarse resolution sensors (Figure 2.1). The salt-and-pepper effect of pixel-based classifiers is a particular issue when attempting to delineate tree crowns due to shadows, understorey and local heterogeneity (Kelly et al., 2008).

Object-based classification methods have been shown to significantly increase classification accuracy relative to pixel-based method in part due to their ability to handle within-object variability (Liu et al., 2007). An object-based approach was successful in delineating coniferous, deciduous, and mixed forest stand boundaries using either small-footprint lidar data or high resolution hyperspectral data (van Aardt and Wynne, 2004). Object-based methods have aided in mapping shrub encroachment and its intensity by segmenting the image at varying scales, identifying individual shrubs at finer scales, and then using that data to determine shrub density at coarser scales (Laliberte et al., 2004).

Hierarchy theory is a dialect of general systems theory. It has emerged as part of a movement toward a general science of complexity. In it, different levels of a system consist of subsystems or super systems of each other. New characteristics emerge that can't be deduced from the qualities of the subsystems (Allen and Hoekstra, 1992). I propose that heterogeneous vegetation needs to be analysed across multiple scales to be able to effectively categorise it as a vegetation community. Individual tree crown delineation and classification alone will not describe a community. Nor is it possible to delineate a patch of vegetation and decipher the component species based on the average spectral response.

Roberts et al. (2004) is a poignant example of a multi-scale approach. They quantified leaf, branch and stand scale variation in spectral reflectance for dominant species with a handheld spectrometer. They found that discrimination of plant species varied with wavelength and scale. However, contrary to expectations, plant species were most distinct at the branch scale and least distinct at the stand scale. At the stand scale (20m by 20m), broadleaf and conifer species were spectrally distinct, as were most conifer age classes. Intermediate separability occurred at the leaf scale.

In this thesis I introduce a multi-scale, object-based, hierarchical approach to generalise spectral information collected at the crown or branch scale, where plant species are likely the most distinct, and use it to classify vegetation communities at the patch scale.

2.8 Conclusion

This chapter introduced the operational approaches to surveying floristics and structure in New South Wales. They were formulated to collect information at the stand or property scale where individual natural resource decisions are made.

Floristic surveys have been designed using species area curves to determine floristic diversity and define characteristic species. The size of the plots is not well suited to analysis of over-storey species, nor for finding correlations with environmental and remote sensing variables. Condition and fuel load surveys are better suited to the scale at which the process occurs in the environment. The mismatch in scale between the measurement and process constrains the utility of prediction. Appropriate matching of scales of measurement, analysis and prediction is a major and largely unsolved problem for natural resource scientists (McKenzie, 2008).

Existing vegetation maps can be efficient tools for planning and biodiversity assessment at relatively large scales (Pressey and Nicholls, 1989). However, they are often too coarse in their thematic classification and usually do not depict small patches of vegetation useful for property-scale site assessment (Benson, 2008). Ideally, vegetation maps would include small patches of vegetation, have fine thematic classification, and be spatially extensive.

I propose that operational vegetation survey and classification should be at multiple scales. The scale of analysis should match the scale of the relevant growth form (grass, shrub, and tree) and the relevant hierarchy (individual plant, association and formation). This will support the extrapolation of vegetation surveys using spatial modelling without making assumptions about changes in scale. Chapter 3 details the nested survey design undertaken for this thesis.

Chapter 3

The Jilliby and Coonabarabran study areas

This chapter introduces the Jilliby and Coonabarabran study areas. It details the field survey data, the satellite data and the airborne sensor data used in this thesis. The basis of the approach is a series of nested sample plots that enable a thorough floristic and structural survey of the vegetation site at multiple scales. The survey of individual tree crowns gives a spatial dimension to species information within a plot. Multi-scale survey methods have been used to inform multi-scale, object-based analysis of remotely sensed data to create maps of vegetation type and structure.

The Jilliby catchment area is located on the central coast of New South Wales, Australia. The study area is described as well as the dominant tree species. The methods used for stratification and survey are detailed.

The Coonabarabran study area is located in central western New South Wales, Australia. The Coonabarabran work represents a shift away from catchment scale mapping towards operational and regional applications. Traditional survey methods have been used to inform multi-scale, object-based analysis of remotely sensed data.

The remote sensing data collected and acquired for this thesis is also described. It provides details of an airborne hyperspectral scanner, an airborne laser scanner and the SPOT 5 satellite and describes the steps taken in calibrating and pre-processing the hyperspectral data.

3.1 The Jilliby study area

The Jilliby study area is centred over Dooralong Valley and the Jilliby State Conservation Area (33^0 9’ 22’’S, 151^0 21’ 00’’E) on the central coast of New South Wales, Australia (see Figure 3.1). The study area incorporates 12,800 ha of state forest, national park and rural lands and includes the southern tip of the Watagan mountain range. The site is approximately 100 kilometres north of Sydney within Wyong Council Shire. The site is arranged as an 8km x 16km rectangle with the longer boundary angled north (Map North, MGA94). Figure 3.1 shows the study area in relation to the Wyong subregion of the Sydney Basin Bioregion (IBRA, 2009).

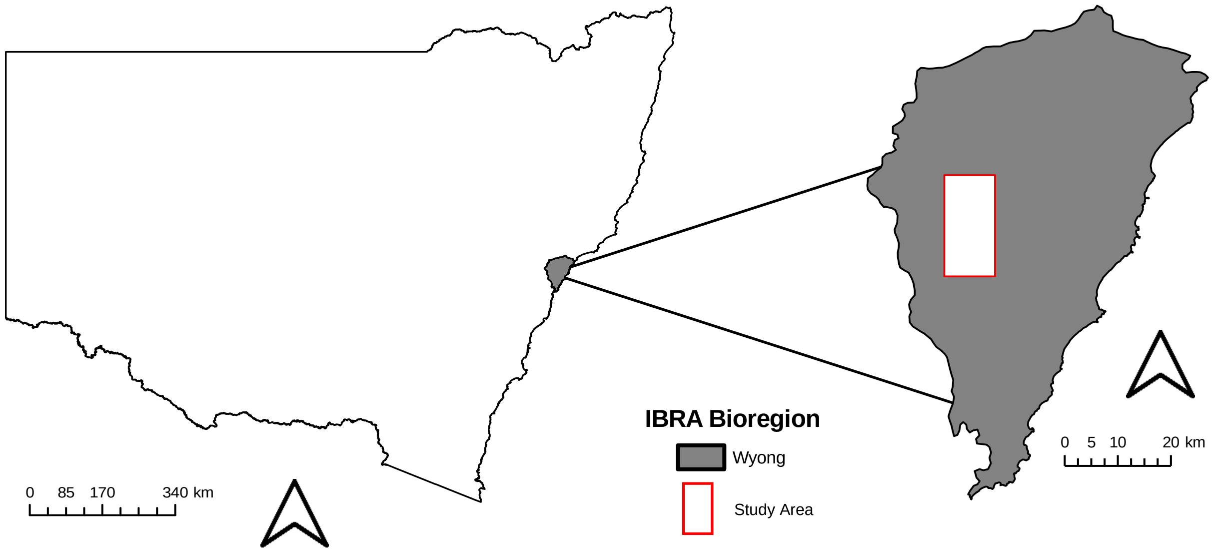

Figure 3.1 The Jilliby Study Area is in the Wyong IBRA subregion, New South Wales, Australia.

The topography is characterised by a central valley surrounded by flat ridgelines, numerous sandstone cliffs, steep slopes and deeply fissured gullies (see Figure 3.2). Ground elevation ranges from 11m above sea level in Jilliby valley to 435m on the mountain plateau. Slopes range from 0 to 90^0 with a mean of 17^0 across the study area (Turner, 2007).

The Jilliby site has a wide array of vegetation communities, which are relatively complex in terms of floristics and structure when compared to vegetation communities common within the Sydney Sedimentary Basin (McCauley, 2006). The distribution of mesic forest and rainforest species is strongly linked to topography and to a lesser extent by wildfire, disease, weed invasion, and past harvesting practices. Parts of the site were harvested early last century and there has been continuous but sporadic logging from the 1970's to the present. Much of the forested area was recently converted from commercial native forest into a State Conservation Area.

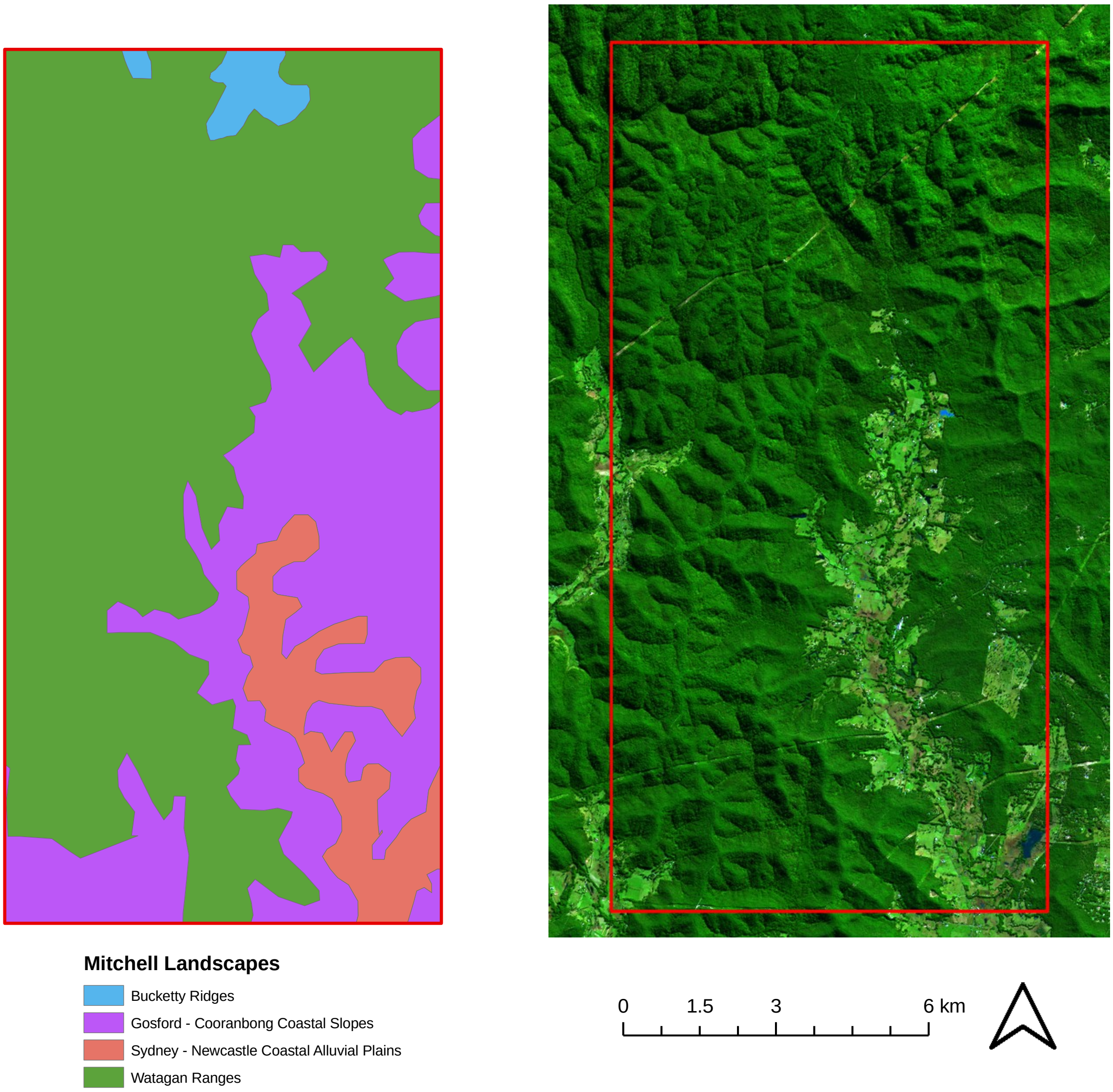

Figure 3.2 A location map of the Jilliby study area showing the Mitchell Landscape ecosystem types (left) (EcoLogicalAustralia, 2008) and a SPOT 5 image (right) from 2005.

The Mitchell Landscapes identified in Figure 3.2 are based on an ecosystem classification (Mitchell, 2002) and later updated (EcoLogicalAustralia, 2008). Mitchell landscapes are driven by geologic, geomorphic and pedologic factors. The majority of the study area falls within the Watagan Ranges landscape. These ranges are steeply dissected with small areas of plateau on Triassic lithic sandstone, shale, tuff and claystone. Woodlands dominate the slopes with pockets of rainforest in the creeks. The Bucketty Ridges are undulating ridges on horizontal Triassic quartz sandstone and shale feature drier more open forest.

The geology of the area is dominated by Hawkesbury and Narrabeen group sandstones. The bedrock is comprised of horizontally bedded Triassic quartz sandstone and shale. The frequent terracing across the mountain range is the result of differential weathering of layers. Consequently, sandstone boulders and outcrops are common. The soils are generally well-drained, acidic sandy loams with low to moderate fertility (NPWS, 2010).

The prevailing climate of the region is temperate maritime with a high summer and low winter rainfall (average annual rainfall is 1266.3mm). Maximum monthly temperature varies between a mean of 15.8^{0}C in the winter months to 21.9^{0}C in summer. The range of temperatures recorded at the site varies between 0.0^{0}C to 42.9^{0}C. Table 3.1 summarises some of the climactic variation experienced at Peats Ridge, the nearest operational weather station to the Jilliby site. Figure 3.3 shows the variation in average rainfall illustrating the low winter rainfall.

Table 3.1 Climate averages near Jilliby for the years 1981-2008 (BOM, 2008).

Maximum Monthly Temperature (C^{0})	**Minimum Monthly Temperature (C^{0})**	**Temperatures Recorded (C^{0})**	**Mean Annual Rainfall (mm)**	**Minimum Monthly Rainfall (mm)**	**Maximum Monthly Rainfall (mm)**
15.8 - 21.9	6 - 16.2	0.0 - 42.9	1266.3	842.9	2186.0
PEATS RIDGE (WARATAH ROAD) - Site number: 061351 - Location: 33.31°S, 151.24°E - Elevation: 280 m					

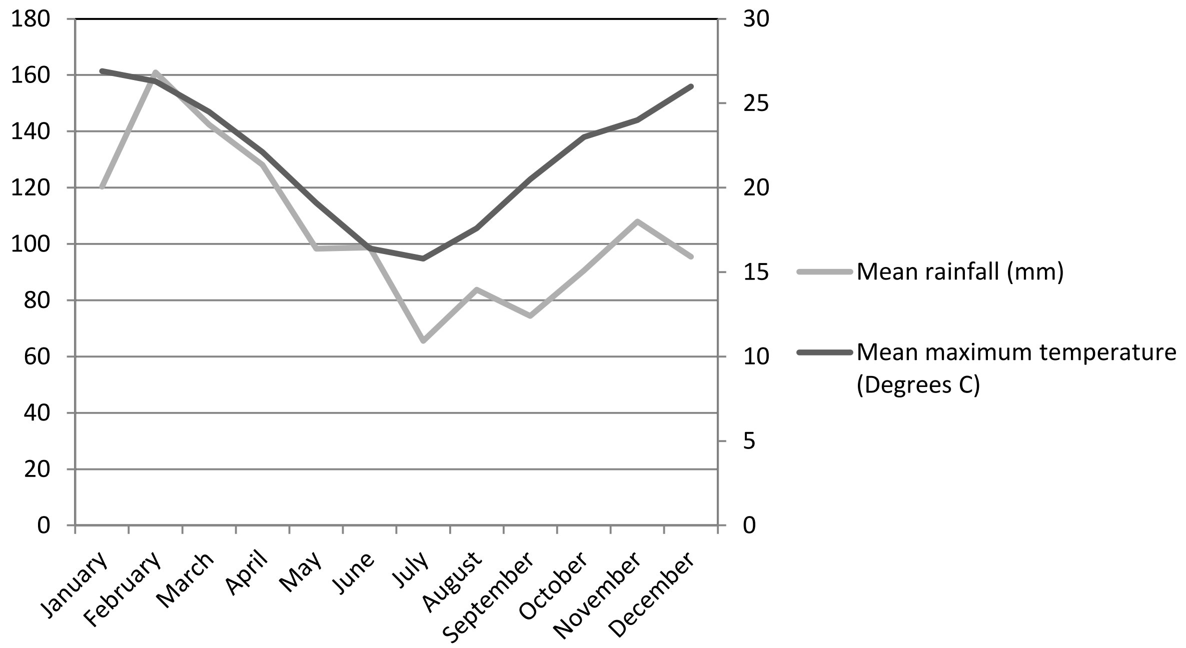

Figure 3.3 Mean rainfall and mean maximum temperature for the Jilliby site between 1981 and 2008 (BOM, 2008).

In general, dry eucalypt forests occupy ridges and westerly slopes, while moist eucalypt forests and rainforest predominate in more sheltered southerly aspects and gully systems (Turner, 2007). The most common tree species are Blackbutt (*Eucalyptus pilularis*), Spotted Gum (*Corymbia maculata*), Sydney Blue Gum (*Eucalyptus* saligna), Round-leaved Gum (*Eucalyptus deanei*), Forest Oak (*Allocasuarina torulosa*), Turpentine (*Syncarpia glomulifera*), Rough-barked Apple (*Angophora floribunda*), Smooth-barked Apple (*Angophora costata*), Grey Ironbark (*Eucalyptus paniculata*), Sydney Peppermint (*Eucalyptus piperita*), White Mahogany (*Eucalyptus acmenioides*), Red Mahogany (*Eucalyptus Resinifera*), and Blue-leaved Stringybark (*Eucalyptus agglomerata*), along with various Wattle (*Acacia sp.*) and rainforest species. Dry ridge tops and north-west facing slopes are dominated by xeric understorey species such as Coastal Banksia (*Banksia serrata*), Native Holly (*Oxylobium ilicifolium*), Prickly Moses (*Acacia ulicifolia*), Narrow leaved Geebung (*Persoonia linearis*), Bladey grass (*Imperata cylindrical*) and Kangaroo grass (*Themeda australis*). Moist south-east slopes and gullies contain mesic understorey species such as Bracken fern (*Pteridium esculentum*), Tree fern (*Dicksonia sp.),* Brush Turpentine (*Rhomdammnia trinervia*), and Native grape (*Cissus antarctica*).

Prescribed burning in this area is normally undertaken in April through to September. The statutory wildfire season occurs between 1st October and 31st March but this may be extended if weather conditions lead to increased fire danger outside of this period (NPWS, 2006). Fire regimes are nominally managed to maintain floristic and structural diversity with low frequency, low intensity burns. Table 3.2 gives the benchmark fire regime values from the Jilliby State Conservation Area Fire Management Plan (NPWS, 2006).

Table 3.2 Jilliby State Conservation Area draft fire management strategy biodiversity thresholds.

Vegetation Communities and Biodiversity Thresholds	
Shrubby Dry Sclerophyll Forest	Avoid successive fires at intervals < 7 years Avoid fire exclusion for a period of > 30 years
Wet Sclerophyll Forest	Avoid successive fires at intervals < 25 years Avoid successive fires at intervals > 60 years Avoid fire exclusion for a period of > 200 years
Semi-mesic grassy forest	Avoid successive fires at intervals < 10 years Avoid successive fires at intervals > 50 years
Rainforest	Avoid any fire occurrence (limited recovery ability exists)

Source: Jilliby State Conservation Area Fire Management Plan (NPWS, 2006).

The native vegetation of the Jilliby catchment area was mapped by Bell and Driscoll (2006). Vegetation pattern was delineated manually with the aid of stereo air photos and the map was published at a scale of 1:25,000. Vegetation classes were derived using expert knowledge rather than cluster analysis of field samples used by other such as Keith and Bedward (1999). Full floristic data were collected at 60 field plots and rapid assessment data were collected at almost 1000 locations. Polygons devised from visual interpretation of the aerial photography (API) were attributed based on expert knowledge and the interpolation of field data. The resulting API map is an improvement on existing vegetation maps of the area (Bell and Driscoll, 2006). It contains a ground sampling density of 1 point per 12 hectares and provides a useful independent data set for floristic patterns and vegetation type.

3.1.1 Stratification

Effective stratification is essential to adequately sample the full range of biotic and environmental variation (Thackway et al., 2007). A number of tools can be used to assess the adequacy of sampling in geographic and environmental space (Ferrier et al., 2007, Neldner et al., 2005). Strategies include use of ecological gradients, random and representative sampling, stratified random sampling, and gradient-oriented transect sampling (Thackway et al., 2007).

The operational survey standards in New South Wales (Sivertsen, 2009) dictate that where complex patterns are observed in environmental sampling units, approximately 200 sampling plots will be required for a 1:100,000 map sheet. However, for the same area where the environmental sampling units exhibit broad patterns 100 - 200 sample plots are adequate. The surveys are also required to sample ecotones and disturbed vegetation in addition to undisturbed vegetation.

For the Jilliby study site there were enough resources for 130 surveys, a greater density than that required by the standard. Surveys were restricted to the area within 200m of an access trail, a slope of no more than 25 degrees, and no closer than 20m to a clearing or road to avoid edge effects. Since the purpose of the study was to assess the attributes of forest communities the survey sites were restricted to woody vegetation.

The location of survey plots were selected using random-stratified sampling. The study site was partitioned into four classes based on an unsupervised ISODATA classification of 2005 SPOT 5 imagery (10m) and a digital elevation model (25m). ISODATA is an unsupervised classification method that calculates class means that are evenly distributed in the data space then iteratively clusters the remaining pixels using minimum distance techniques (Tou and Gonzales, 1974).

The results of the ISODATA classification were partitioned into four broad classes. Subsequently, 30 field plots were randomly located in each of the four strata. Candidate sampling locations were further reduced by selecting strata areas with a minimum size limit of 50 pixels (0.5 hectares) in an effort to sample homogenous vegetation. Several sites were added opportunistically in the field across all four strata as some of the random plots were inaccessible. Every practical effort was made to sample at the randomly selected location but there were numerous insurmountable obstacles due to the varied terrain.

The four ISODATA classes represented the spectral response and height above sea level (see Figure 3.4). The charts illustrate the broad trend to greater height and biomass increasing in order of class. Class 4 was dominated by tall closed Blackbutt forest which is common in the high areas. Class 1 was dominated by dry and open Spotted Gum and open Blackbutt forest that is common in the low areas. Class 2 and 3 were less definitive but were more likely to be gully rainforest species, Turpentine forest and Blackbutt forest in the mid altitude areas. The limited radiometric and spectral resolution of

SPOT 5 multispectral data limits its use in the separation of vegetation communities. However, it provides an effective indication of canopy cover. Topography is seen as a major driver in the variation of vegetation type at the Jilliby site (Bell and Driscoll, 2006). The relatively high density of field surveys in the Jilliby study site mitigates the chance of omitting rarer communities. However, the limited discriminating power of the stratification resulted in survey sites that were not always within homogenous patches.

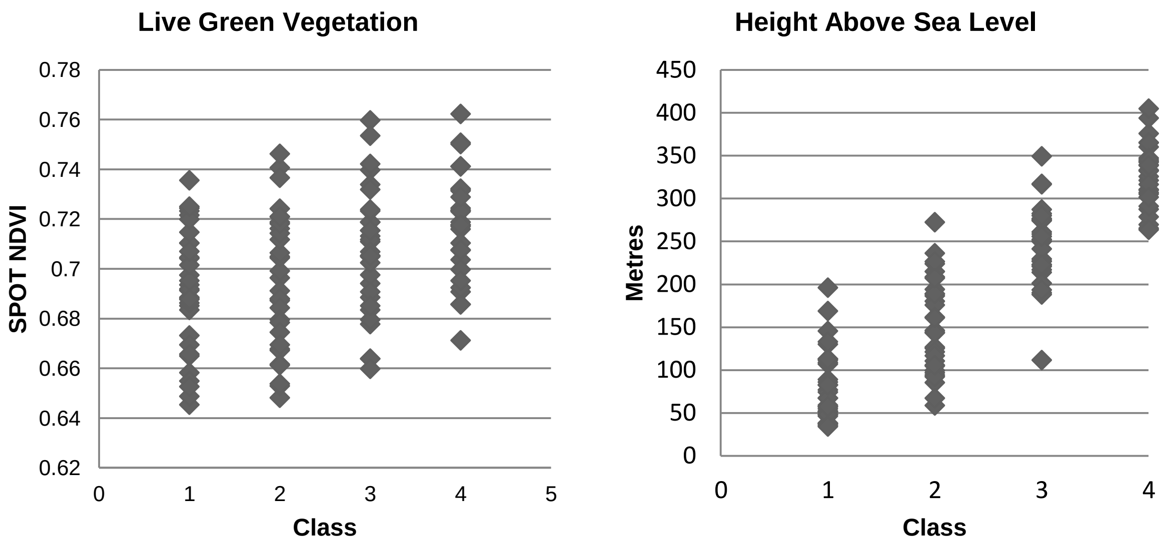

Figure 3.4 Spectral response from SPOT 5 and height above sea level and were used to stratify the Jilliby site into four classes.

3.1.2 Survey sites

In Chapter 2, I argued that the size of vegetation survey plots is not well suited to analysis of over-storey species, nor is it suited to finding correlations with environmental and remote sensing variables. I proposed that operational floristic vegetation surveys in Australia should be conducted at multiple scales to match the scale of the relevant growth form. That is, vegetation over twenty metres high be surveyed in 30m by 30m plots, vegetation under twenty metres high a 20m by 20m plot is adequate, and for vegetation <1 m high a 5m by 5m plot will suffice.

The survey design used in the Jilliby study area provides an example of how floristic survey can be conducted at multiple scales. Each plot was circular in shape and 40m in diameter, which is over 3 times the area of the operational standard. A larger number of species from the dominant stratum are able to be identified which increases the probability that diagnostic species for the association will be encountered. In addition, individual tree crowns were identified and their location was recorded. This allows for dominant species to be modelled across the landscape at the scale they are observed in the field. Structural attributes were surveyed at the Jilliby study area in a series of nested sub-plots with different sizes specific to each growth form. The shrub layer was assessed in 5m sub-plots and grasses and litter was assessed in sub-plots measuring 1m by 2m.

The centre of survey sites was recorded in the field using a Trimble differential GPS (see Table 3.3). The mean error was 0.73m after post-processing. At the centre of each plot a heavy duty iron star picket was hammered into the ground and numbered. This allowed multiple groups of researchers to visit each of the numbered sites in a repeatable fashion. The plot boundary was measured using tape and marked with spray paint at the 20m point in four directions. Digital photographs were taken to capture the four cardinal directions (magnetic).

Table 3.3 Precision and error of plot centres as measured by differential GPS.

DGPS Precision	Mean	Standard Error	Median	Mode	Standard Deviation	Range	Min	Max	Count
	0.73 m	0.03	0.7 m	0.6 m	0.29	1.6 m	0.3 m	1.9 m	130

Fieldwork at the Jilliby catchment study site was conducted in collaboration with other researchers in April, May and June of 2006. A rapid species list was compiled including dominant species lists and cover scores for multiple strata. These data were collected for this thesis and for use in other research related to Bell Miner associated dieback (Stone et al., 2008). The dominant tree species were surveyed specifically for this thesis. The condition measures were collected as part of the general floristic description with additional metrics collected specifically for this thesis.

Fuel load data were collected by volunteer and professional staff as part of a multi-sensor remote sensing project to assess fuel loads. The sampling included the collection of leaf litter and combustible material for drying and weighing (destructive sampling), a visual assessment of fuel load (OFHG), and the measurement of structural variables related to fire behaviour (VESTA).

3.1.3 Floristics and crown scale classification

The floristic attributes of each plot were described in a species list by NPWS staff. The intention was to maximise the number of plots without leaving out relevant floristic data. The main focus was on the dominant canopy species, the shrub layer and the dominant vascular ground cover species. The full range of groundcover species was not described.

The plant species were categorised into a particular stratum. A stratum is an easily seen layer of foliage and branches of a measurable height (see Figure 3.5). Following Hnatiuk et al. (2009) strata are named as follows: Dominant or upper stratum, mid-stratum and ground stratum. The tallest stratum will usually be the dominant stratum but tree crowns emerging above the canopy (emergents) are an exception. The tallest plants in some vegetation are so sparse that they no longer form the dominant or most significant layer (less than 5% cover). For example, a few tall Eucalyptus trees may rise above a closed rainforest canopy, or widely scattered eucalypts.

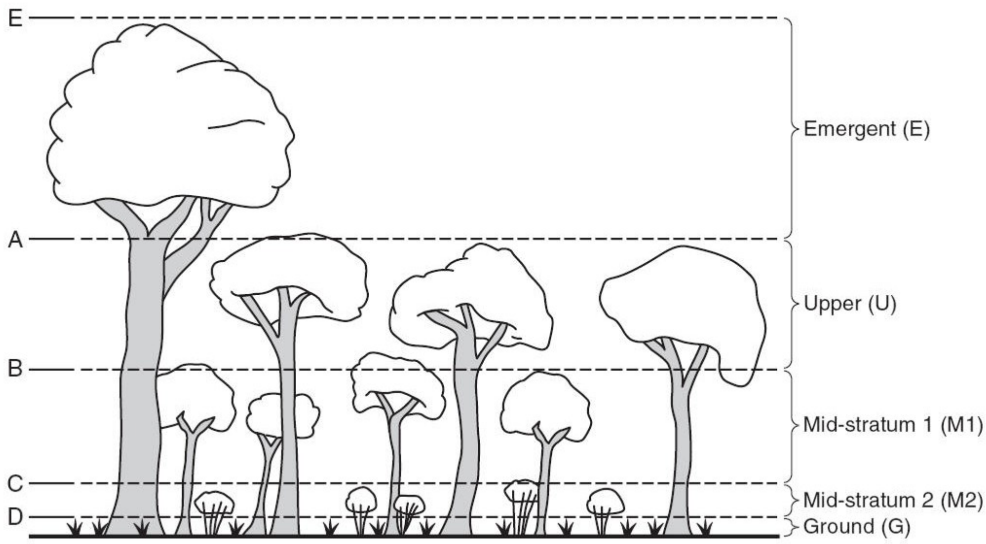

Figure 3.5 The plant species were categorised into a particular stratum based on foliage height.
Source: Hnatiuk et al.*, 2009.*

The mid-stratum, if present, is between the dominant stratum and the lowest or ground stratum. There was no mandatory height limit on the ground layer, but it is usually less than 2m tall. At times subdivisions of the three main strata were recorded. The average height of each stratum was measured at each site with a Haglöf Vertex III Ultrasonic Hypsometer.

The structure of the vegetation was at Jilliby was tied to community type and past disturbance. At one extreme the Spotted Gum (*Corymbia maculata*) open dry forest dominated by had no mid-stratum and a grassy ground cover. At the other, rainforest sites featured emergent Sydney Blue Gum (*Eucalyptus saligna*) with a mid stratum of juvenile tree species and tall, shade tolerant rainforest species. The ground stratum was often composed of ferns, vines and shrubs.

Crown cover was estimated for each stratum regardless of species. Crown cover was defined as the percentage of the total area of a sample site that is covered by a vertical projection of the crown, taken from Hnatiuk et al. (2009).

The rapid estimate of crown cover was supplemented with upward looking photography using a wide angle lens. Exposure was set to create a silhouette of the mid-stratum and upper stratum from the centre point of the circular plot. This is a measure of the *Projected Foliage Cover* (FPC), the proportion of ground that would be shaded if sunshine came from directly overhead (Carnahan, 1981). FPC is It has been generally accepted as the measure of foliage quantity in Australia (Walker, 1981) and is used in the Specht (1970) vegetation classification system. The photographs were converted to binary images and the amount of foliage was converted taken as a measure of FPC.

Tree species were identified and the location of the largest trees that intersected each plot was recorded. Up to ten trees per plot were selected in decreasing order of the diameter of the tree stem at breast height (DBH).

The largest tree crowns in the upper stratum were identified to a species level and spatially located within the plot by recording a bearing and a distance from the centre. The bearing was recorded using a compass. The distance from the plot centre to the base of each tree was measured with a Leica laser rangefinder. Where the laser beam was obscured by vegetation the distance from the plot centre was estimated with reference to the measured plot centre or one of the four plot boundary markers labelled with spray paint and measured with tape. The maximum distance of any recorded crown from a measured location was 10m. Field sketches were also made to avoid confusion when aligning field and image data, noting clearings as well as crowns and dead trees.

Estimated ranges were always calibrated with the laser rangefinder and this level of precision was found to be adequate for reliably locating the trunks of large crowns. This follows Clark et al. (2004) who located crown centroids through visual adjustment of trunk points. They used a lidar canopy height model to select canopy-emergent trees as they were 'easy to locate unequivocally'. Clark et al.'s measurements were later used in individual tree crown discrimination studies (Clark et al., 2005). They selected 212 emergent trees with large, exposed crowns that provided a large sample of pixels that were less influenced by spectral shadowing or scattering by neighbouring trees. They also found that large emergent trees were easy to locate in orthorectified hyperspectral imagery.

The diameter at breast height (DBH) was estimated for each surveyed tree. Each tree was put into one of 5 classes according to the estimated diameter. The recorded DBH values can only be used as indicative and they were not subject to quantitative analysis in this thesis. The health of the dominant canopy was also described based on the shape of the crowns, the presence of dead or dying tree limbs and the presence of epicormic shoots (Stone et al., 2008).

Figure 3.6 shows tree stem locations displayed as point data, labelled by species code, with each point size scaled to the DBH estimates. The vector data were subsequently overlayed on the imagery to assist with individual tree crown recognition and identification. At the conclusion of the fieldwork campaign 889 tree trunks had been identified and their location recorded.

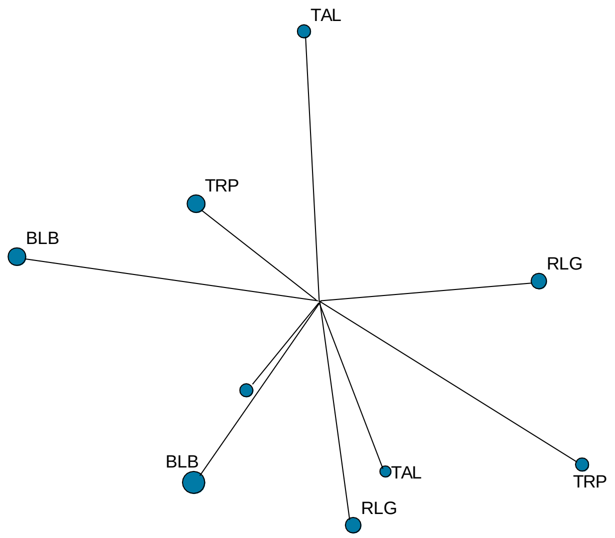

Figure 3.6 Tree stems were surveyed with a bearing from a differential GPS survey point and labelled by species.

3.1.4 Fuel load assessment

There were two major field campaigns to assess fuel loads at the Jilliby catchment site in June of 2006. The simpler of the two followed the *Overall Fuel Hazard Guide* (McCarthy et al., 1999). Three levels of fuel (ground, elevated, bark/canopy) were estimated by measuring litter depth and comparing elevated and bark fuels with illustrated examples from the fuel hazard guide booklet (McCarthy et al., 1999). Estimated fuel loads for the strata at each site are then summed to compute an estimated total available fuel load in tonnes per hectare (t/ha).

The second and more elaborate method was derived from a prototype of the CSIRO's *Project Vesta Field Guide* (Gould et al., 2007). The Vesta field guide was developed to provide a systematic method for assessing fuel hazard and predicting potential fire behaviour in dry eucalypt forest. It is based on the effects of fuel age and understorey vegetation structure on fire behaviour. The guide provides tables to predict the potential rate of spread of a bushfire burning in dry eucalypt forest under summer conditions, and can also be used to predict flame height and maximum spotting distance.

The Vesta fuel attributes were collected in *four* nested 5m radius sub-plots in each of the 130 main plots (see Figure 3.7). The nested sub-plots were in the cardinal directions (magnetic) and located with a measure of rope attached to the central picket. The Vesta method estimated fuel hazard and percentage cover for surface, near surface, elevated and intermediate canopy and over-storey canopy layers. Surface layers are comprised of dry particulate matter on the forest floor (i.e., humus, twigs, leaves and bark). Near-surface fuels include live and dead fuels just above the ground surface, including grasses, sedges and rushes, low shrubs and fine twiggy material, and bark not lying directly on the ground. Elevated fuels are comprised of shrub, heath, bracken, tall grasses and suspended flammable material, with foliage generally less than 8m tall (Turner, 2007).

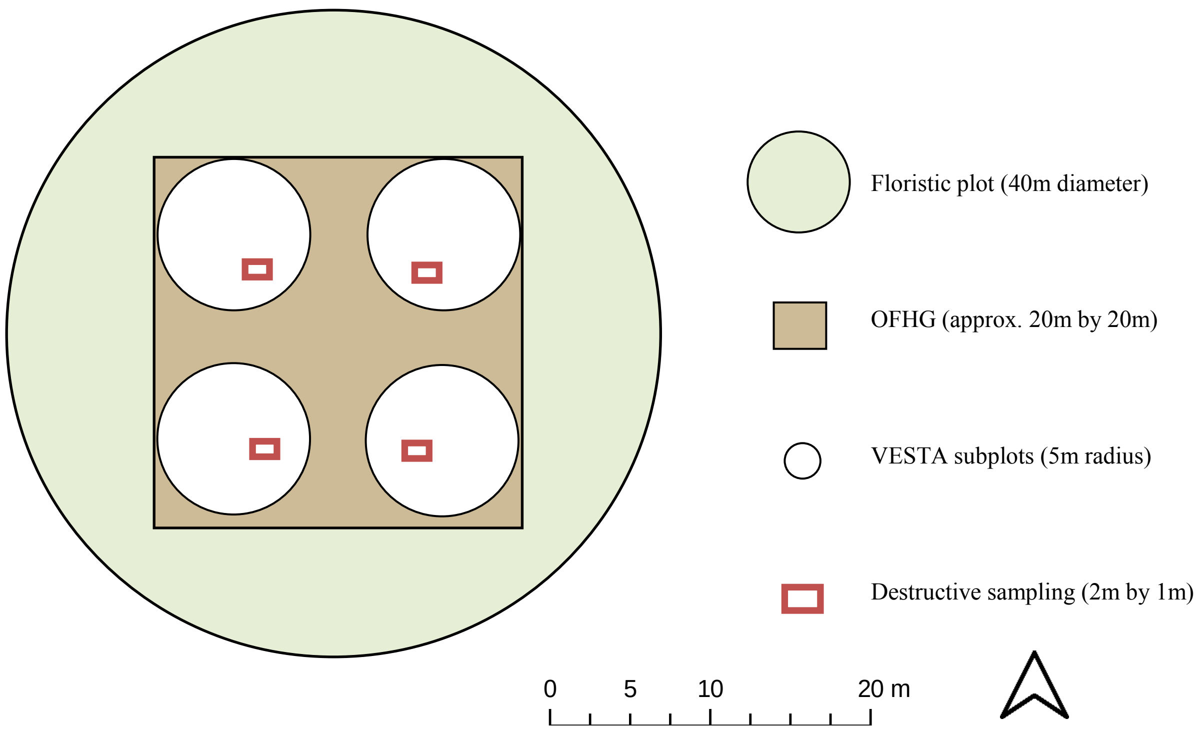

Figure 3.7 Forest fuel attributes were sampled in a series of multi-scale nested plots. The OFHG quadrats (20m by 20m) were placed inside floristic plots (40m diameter). Each OFHG quadrat was further divided into four nested (5m radius) sub-plots for Vesta sampling. Half of the plots (65) were subject to destructive sampling (2m by 1m).

The development of the Vesta fuel scoring prototype aims to improve the ability of fire fighters to predict fire behaviour but, to some extent, has made remote sensing of fuel properties more difficult. Fuel scores are no longer linked directly to the biomass of fuels. Instead, they are tied to their arrangement both horizontally and vertically. For example, a thick understorey of dead woody material would add substantially to the overall biomass and understorey structure as assessed by remote sensing. However, any twigs over a 6mm in diameter are not considered, as they would not add to the available fuel in a fire event.

Unfortunately, the Vesta prototype presented a series of attributes without any way to combine them into a single numerical score. For the purposes of this project I developed a multiplicative formula (see Equation 3.1) to produce a single numerical score. It combines the fuel hazard and percent cover scores from each stratum into a single numerical score for correlating with remotely sensed variables. In the remainder of this thesis, when Vesta fuel hazard scores are referred to, I am referring to fuel hazard scores multiplied by percent cover scores in four separate strata. These scores were then added together to represent an overall fuel hazard.

$$\sum_{\text{strata}}^{n} \text{Fuel Hazard} \times \text{Percent Cover}$$

Equation 2Multiplicative fuel hazard score derived from Vesta attributes.

Half of the 130 plots were also subject to destructive sampling. Destructive sampling involves the physical removal of litter and available fuel and is an expensive and time consuming process. Between 4 and 8 samples were taken in each plot (in 2m by 1m subplots) and oven dried and weighed. Destructive sampling was conducted after all of our other measurements so as not to disturb the sites.

3.1.5 Field survey summary

A summary of all variables recorded in the field campaign, their units of measurement and the method of observation or measurement are summarised in Table 3.4.

Table 3.4 Jilliby survey site data

Data Collected	**Units**	**Methods**
Plot boundary	Metres	A length of rope was stretched from the central picket to mark foliage at 20m in the four cardinal directions
Plot centre	Metres	Location determined using a Trimble differential GPS unit with sub-meter accuracy
Tag	Alpha Numeric	Each plot centre was marked with a star picket and tagged with a unique identifier
Strata	Class	The plant species were categorised into a particular stratum following Hnatiuk et al. (2009)
Strata height	Metres	The average height of each stratum was measured at each site with a Haglöf Vertex III Ultrasonic Hypsometer.
Cover Score	Percentage	Crown cover was estimated as the percentage of the total area of a sample site that is covered by a vertical projection of the crown (see Hnatiuk et al., 2009).
Dominant species	List	The dominant species recorded in three strata was recorded by a botanist
Rapid species list	List	A rapid list of all species in the plot was recorded by a botanist (the rapid list did not include all groundcover species)
Large crowns identified	List	The largest tree crowns in the upper stratum were identified to a species level by a botanist and given a unique identifier
Distance of large crowns from plot centre	Metres	The distance from the plot centre to the base of each tree was measured with a Leica laser rangefinder. Where the laser beam was obscured by vegetation the distance from the plot centre was estimated with reference to the measured plot boundary that was marked with spray paint
Bearing of large crowns from plot centre	Degrees	The bearing to each large crown was recorded using compass and magnetic north as 0 degrees
Diameter at breast height	Five classes	The diameter at breast height (DBH) of the surveyed crowns was estimated after the observer had calibrated themselves using a measuring tape. Each crown was put into a 5 classes according to an estimate of diameter
Overall fuel hazard	Tonnes per hectare	Fuel load estimates for the strata (ground, elevated, bark/canopy) at each site are based on illustrated examples. They are summed to calculate an estimated total available fuel load in tonnes per hectare (t/ha) (see McCarthy, 1999)
Fuel hazard and percentage	Metres and percentage	Fuel hazard and percentage cover was estimated for surface, near surface, elevated and intermediate canopy and over-storey canopy layers. Estimates are based on physical measurements such as the height, the number of times debris cross a tape on the ground or the number of branches that touch a vertically aligned pole (see Gould et al., 2008)

Destructive sampling	Kilogram per Metres^2	Physical removal of litter and available fuel at between 4 and 8 samples in ever second plot (in 2m by 1m subplots). The collected material was oven dried and weighed
Exotic species	Presence or absence	Derived from species list
Time since fire	Years	Estimated based on fire scars
Timber harvest	Presence or absence	Evidence of harvesting was based on presence of log dumps, stumps and stand age and location
Tree development	Five classes	Five classes from sapling to over-mature based on the shape of tree crowns, the presence of dead or dying tree limbs and the presence of epicormic shoots
Digital Photographs	JPG	Four photos of the cardinal directions at each site as well as upward looking canopy photos from the plot centre, photos of leaf litter, and photos of each of the 2m by 1m sub-plots used for destructive sampling.

3.2 The Coonabarabran study area

The Coonabarabran study site is in the central west of NSW, Australia. The centre of the study area (31^{0}12"0'S, 149^0 5" 30'E) is approximately 500 kilometres north-west of Sydney. The area is a mix of National Park reserve, native forest, and farmland. The Coonabarabran 1: 100, 000 map sheet was the subject of intensive floristic sampling a year before this research project began. Unfortunately, the project was cancelled before the vegetation mapping in the area was finished (Ismay et al., 2004). Out of 903 full floristic plots sampled in the region only 293 were included in the completed mapping. Creating a relatively automated way of spatially modelling the unmapped vegetation communities in the region would represent an important contribution. The Coonabarabran site represents an opportunity to apply the multi-scale, object-based analysis methods developed at the Jilliby site to satellite imagery. Figure 3.8 illustrates the location of the site in NSW in relation to the Brigalow Belt South IBRA Bioregion.

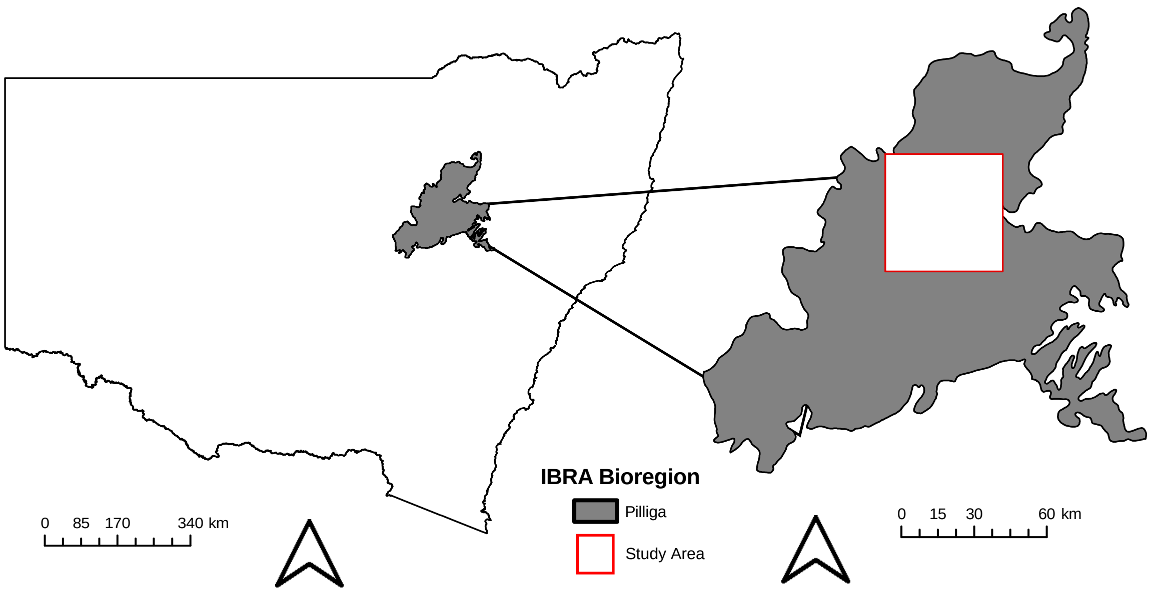

Figure 3.8 The Coonabarabran study area is in the Pilliga IBRA subregion, New South Wales, Australia.

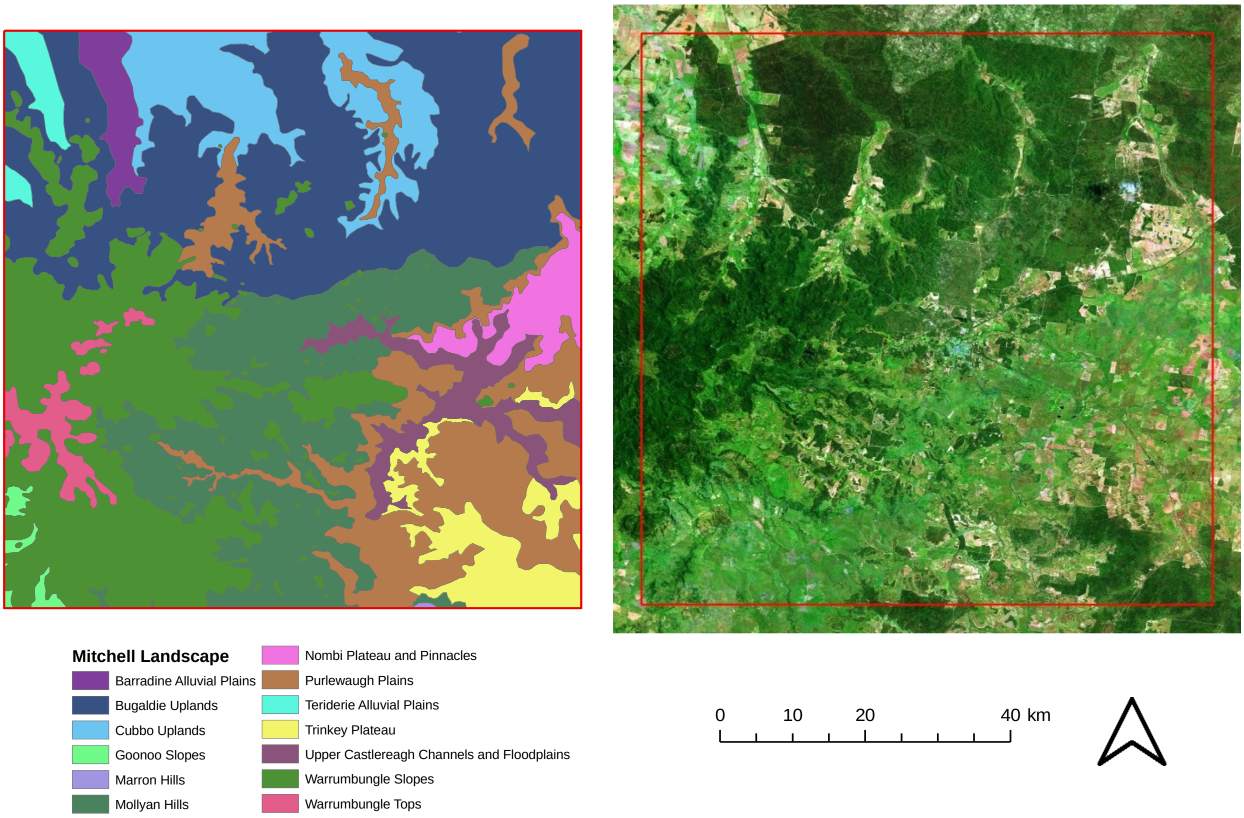

Figure 3.9 A location map of the Coonabarabran study area showing the Mitchell Landscape ecosystem types (left) (EcoLogicalAustralia, 2008) and a SPOT 5 image (right) from 2005.

The Warrumbungle National Park features the remains of a large eroded shield volcano, creating some distinctive volcanic landforms (Figure 3.9). The combination of the arid western plains, moist eastern slopes and elevation above the surrounding plains, bestows the Warrumbungle's with greater floristic diversity (DECC, 2008). Wattles and open woodlands dominate the drier western slopes while the more sheltered southern and eastern aspects feature tall to very tall open forest, with pockets of rainforest species in the gullies.

The bedrock is comprised of horizontally bedded Jurassic and Triassic quartz sandstone and shale, with limited areas of conglomerate and basalts. The most obvious formations are Pilliga Sandstone, which dominates the northern area and runs centrally to the south, and basalt in and around the Warrumbungle National Park. Soils vary greatly across topography, as do micro-climate and aspect. Thus, it is necessary to differentiate areas of hill tops and plateau from slopes and valley floors in both sandstone and basalt areas as all of these factors affect the distribution of vegetation (DECC, 2008).

Table 3.5 summarises some of the climactic variation experienced at Coonabarabran (Namoi Street), the nearest operational weather station to the centre of the Coonabarabran site. Coonabarabran is in the eastern subhumid region of Australia, with no dry season and a hot summer, with small patches to the east falling within the temperate zone (average annual rainfall is 747.4mm). The maximum monthly temperature varies between a mean of 14.8^{0}C in the winter months to 31.7^{0}C in summer. The range of temperatures experienced at the site is extreme, varying between minus 9.0 to plus 42.9 ^{0}C (Namoi Street). Figure 3.10 shows the variation in average rainfall illustrating the low winter rainfall and the relatively dry conditions with respect to the Jilliby site.

Table 3.5 Climate averages at Coonabarabran for the years 1879-2008 (BOM, 2008).

Mean Maximum Temperature (C^0)	Mean Minimum Temperature (C^0)	Range of Temperatures Recorded (C^0)	Mean Annual Rainfall (mm)	Minimum Average Monthly Rainfall (mm)	Maximum Average Monthly Rainfall (mm)
14.8 - 31.7	0.0 -15.0	-9.0 - 42.6	747.4	49	90.4
COONABARABRAN (NAMOI STREET), Site number: 064008, Location: 31.27 °S, 149.27 °E, Elevation: 505 m					

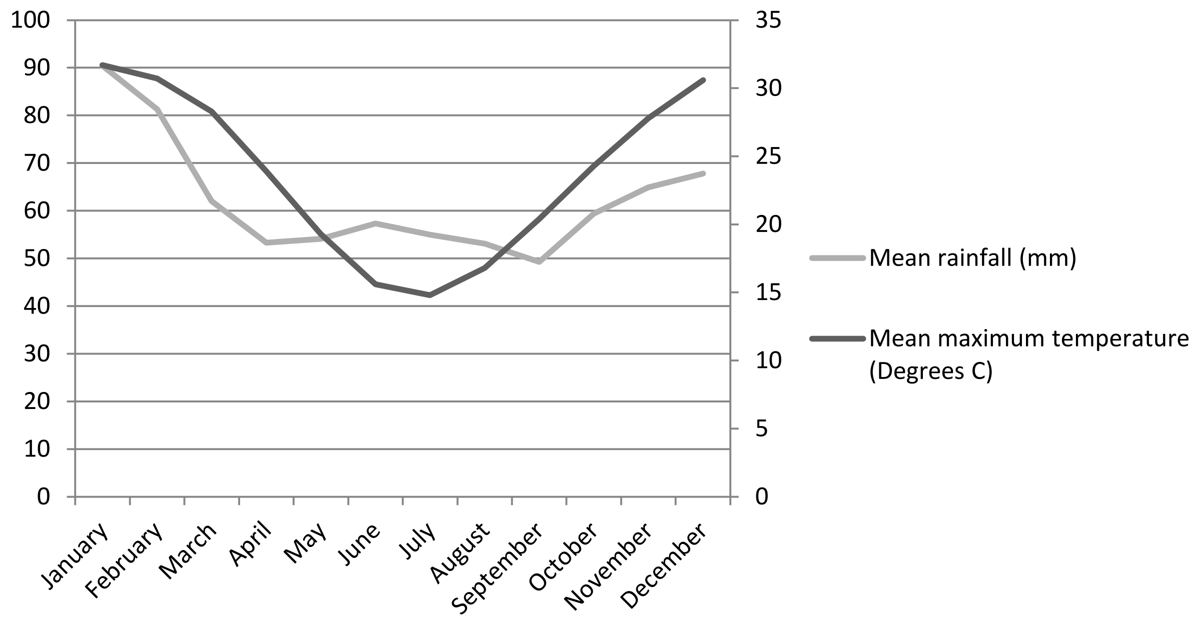

Figure 3.10 Mean rainfall and mean maximum temperature for the Coonabarabran site between 1981 and 2008 (BOM, 2008).

The sandstone areas of the study area support various forests and woodlands. The tall open woodlands and open forest in the north are dominated by a mixture of pilliga box (*Eucalyptus pilligaensis*), black cypress pine (*Callitris endlicheri*), white cypress pine (*Callitris glaucophylla*), narrow-leaved Ironbark (*Eucalyptus crebra*), white box (*Eucalyptus Albens*) dirty gum (*Eucalyptus chloroclada*), kurrajong (*Brachychiton populneus*) and white bloodwood (Corymbia trachyphloia subsp. Amphistomatica). River red gums (Eucalyptus camaldulensis), yellow box (*Eucalyptus melliodora*), and Blakely's red gum (*Eucalyptus blakelyi*) are also relatively common in open forest. The Warrumbungles host rough-barked apple (*Angophora floribunda*) and river red gums (*Eucalyptus camaldulensis*), with woodlands of white gums (*Eucalyptus rossii*) and narrow-leafed ironbark (*Eucalyptus crebra*).

3.2.1 Native Vegetation Mapping Program (NVMP) floristic plot data

The Native Vegetation Mapping Program (NVMP) was initiated in 2000 to provide consistent, fine scale vegetation mapping of much of the state. It was curtailed in 2004 when there was a switch of emphasis to property scale planning. Most of the work carried out for the NVMP, including species lists and descriptions from thousands of plots, has not been published (Benson, 2006).

The Coonabarabran study site, and its surrounds, was the subject of intensive floristic sampling (Ismay et al., 2004). The NVMP program aimed to provide an 'independent, high quality, spatial information of the extant native vegetation accurate at a regional scale, and to contribute towards the building of a standard state-wide coverage' (Ismay et al., 2004).

The Coonabarabran 1:100 000 map sheet was the only completed vegetation map from the six map sheets subject to floristic surveys (Figure 3.11). This layer serves as a reference point for the expected spatial distribution of species and provides a benchmark on how human interpreters define vegetation patterns at the 1: 100 000 scale. Out of 903 full floristic plots sampled in the region only 293 have been utilised in spatial modelling.

The following extract describes the methodology of the vegetation mapping program conducted at Coonabarabran and the surrounding map sheets (see Figure 3.12). It is used with permission. The description is taken from Ismay et al. (2004).

> *Vegetation patterns were recognised and delineated spatially using air photo interpretation (1:50,000 scale). Satellite imagery was used to geo-reference the API. A consistent provisional vegetation code was assigned to each unique vegetation pattern. Comprehensive floristic data were collected for 547 plots using a random stratified sampling procedure. Field surveys were conducted between May 2003 and July 2004, during which time drought conditions varied across the study area. Data were supplemented by 372 existing plots from previous surveys. The study area was stratified on geology, elevation, slope and aspect to inform the survey design. A proportional sampling regime was applied to the stratification and plots randomly located within stratification units independent of land tenure. An additional mask layer was applied to distinguish between 'woody' and 'non-woody' vegetation to target survey effort toward wooded communities.*
>
> *Plot data were classified into 44 woody floristic groups using PATN (Belbin, 1989). Additional analysis techniques included fidelity, homogeneity, nearest neighbour and indicator species analysis. Floristic groups are defined using structural dominance, diagnostic/indicator species and character species data. The provisional vegetation pattern codes from aerial photo interpretation were interrogated with respect to floristic groups to produce the map units. A generalised, additive model was used to investigate patterns in ironbark/redgum/pine assemblages in the south of the study area, where direct relationships between spatial and floristic data were unclear.*
>
> *A total of 24 woody map units were developed to represent woody assemblages and three map units spatially depict non-woody areas, non-native areas and*

regenerating vegetation (at time of mapping). These map units are described with respect to structure, floristic composition and landform unit on the accompanying five maps. Mapping of the non-woody environment was limited to recognising 'candidate' native non-woody vegetation.

Figure 3.11 The Coonabarabran map sheet was one of six that was sampled with full floristic and structural descriptions for the Native Vegetation Mapping Program.
Source: Ismay et al. (2004)

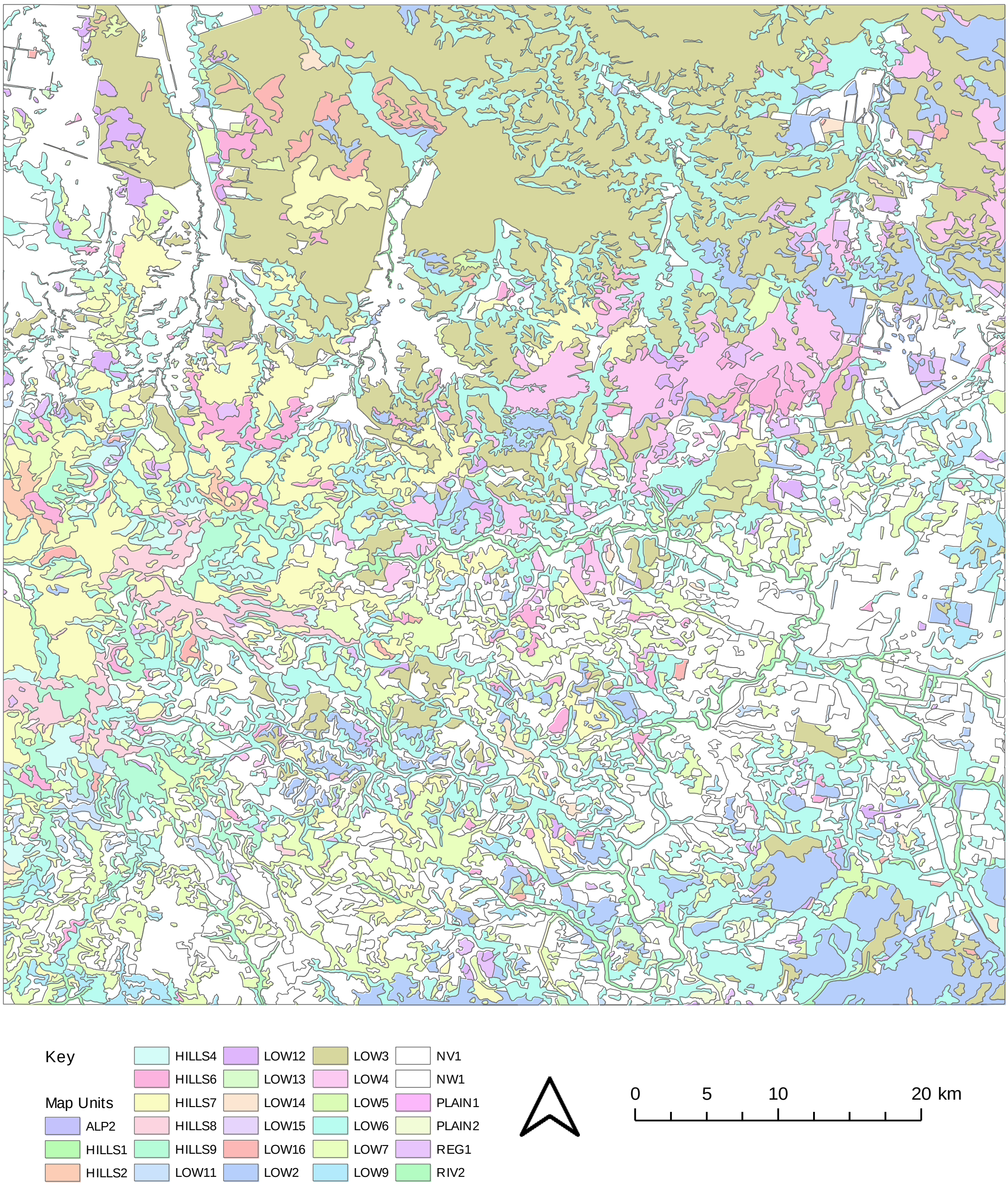

Figure 3.12 Coonabarabran Vegetation Map sheet (1:100 000) from the 2004 Native Vegetation Mapping Program. Source: Ismay et al. (2004)

The field survey recorded 1797 species from 151 families. Exotic species represented 20% of taxa (358 species). For a complete list of taxa and a summary of significant species (including threatened species) see Ismay *et al.*, (2004). Table 3.6 details the floristic groups derived from field sampling. Floristic groups were further generalised into *Map Units* to create the final map layer.

Table 3.6 Floristic groups derived from field sampling, environmental stratification, topographic position and vegetation structure (Ismay et al., 2004). Floristic groups were further generalised into final map units.

Unit	n	Group Title	Structure	Total
LOW9	2	*Brachychiton populneus subsp. populneus (Callitris glaucophylla and/or Eucalyptus albens)*	Tall Open Woodlands to Woodlands	7
LOW6	3	*Angophora floribunda Eucalyptus camaldulensis chloroclada intergrades (Eucalyptus chloroclada and/or other intergrades and/or Callitris glaucophylla) grassy*	Tall Open Woodlands to Open Forests on sandstone	10
LOW3	2	*Eucalyptus pilligaensis (Callitris endlicheri and/or Eucalyptus albens)*	Tall Open Woodlands to Open Forests	4
HILLS1	1	*Notelaea microcarpa var. microcarpa Geijera parviflora (Alphitonia excelsa and/or Callitris glaucophylla)*	Mid-high Open Woodlands to Woodlands	11
LOW6	7	*Eucalyptus blakelyi (Angophora floribunda and/or Eucalyptus melliodora) grassy*	Very Tall Open Woodlands to Forests	15
LOW6	6	*Angophora floribunda grassy*	Tall Open Woodlands to Open Forests	22
HILLS7	18	*Angophora floribunda with Olearia elliptica subsp. elliptica Cassinia quinquefaria (Callitris endlicheri and/or mixed eucalypts) shrubby Tall*	Open Woodlands to Forests	25
HILLS8	2	*Eucalyptus bridgesiana Angophora floribunda grassy*	Very Tall Open Forests on Tertiary Basalts	2
HILLS8	3	*Eucalyptus nortonii Eucalyptus macrorhyncha with Olearia elliptica subsp. elliptica Cassinia quinquefaria (Angophora floribunda) shrubby Tall*	Woodlands to Open Forests on Tertiary Basalts	3
HILLS9	15	*Eucalyptus macrorhyncha Angophora floribunda (mixed eucalypts) shrubby*	Tall Open Woodlands to Forests	20
HILLS8	7	*Eucalyptus volcanica Eucalyptus macrorhyncha Tall*	Open Woodlands to Forests on Tertiary Basalts	7
HILLS6	14	*Eucalyptus albens (Olearia elliptica subsp. elliptica and/or Notelaea microcarpa var microcarpa and/or Dodonaea viscosa) shrubby*	Tall Open Woodlands to Open Forests	39
HILLS6	3	*Eucalyptus albens Callitris endlicheri with Cassinia arcuata and/or Acacia decora shrubby*	Tall Open Woodlands to Open Forests	9
HILLS4	9	*Eucalyptus dealbata northern complex with Olearia elliptica subsp. elliptica and/or Callitris endlicheri shrubby*	Mid-high Open Woodlands to Open Forests	19
LOW3	13	*Callitris glaucophylla (Eucalyptus crebra)*	Tall Open Woodlands to Open Forests on sandstone	21
LOW12	2	*Callitris glaucophylla*	Tall Open Woodlands to Open Forests on variable substrate	15
LOW7	7	*Callitris glaucophylla Eucalyptus albens grassy*	Tall Open Woodlands to Open Forests	14
PLAIN1	8	*Allocasuarina luehmannii Eucalyptus crebra Callitris glaucophylla*	Tall Open Woodlands to Woodlands	15
PLAIN2	1	*Eucalyptus microcarpa (Callitris glaucophylla) grassy*	Tall Open Woodlands to Open Forests	12
LOW6	24	*Angophora floribunda (Callitris endlicheri and/or Eucalyptus blakelyi)*	Very Tall Open Woodlands to Open Forests on sandstone	43
LOW2	36	*Mixed shrubby complex with Callitris endlicheri and/or Eucalyptus crebra and/or Eucalyptus macrorhyncha*	Tall Open Woodlands to Open Forests on Pilliga Sandstone	88
LOW3	74	*Corymbia trachyphloia subsp. amphistomatica Callitris endlicheri (Eucalyptus crebra) northern complex shrubby*	Tall Open Woodlands to Open Forests on Pilliga Sandstone	113
LOW4	12	*Corymbia trachyphloia subsp. amphistomatica Eucalyptus rossii northern complex shrubby*	Tall Woodlands to Open Forests on Pilliga Sandstone	14
LOW14	1	*Callitris endlicheri with Eucalyptus crebra and/or Eucalyptus macrorhyncha (mixed eucalypts)*	Tall Open Woodlands to Forests on sandstone	52
RIV2	7	*Casuarina cunninghamiana subsp. cunninghamiana (Angophora floribunda and/or Callistemon sieberi)*	Very Tall Open Woodlands to Forests	23
LOW11 LOW6	5	*Eucalyptus melliodora grassy*	Tall Open Woodlands to Open Forests	25

LOW11 LOW6	2	*Eucalyptus conica (Eucalyptus melliodora and/or Callitris glaucophylla) grassy*	Tall Open Woodlands to Forests	8
LOW7	9	*Eucalyptus albens grassy*	Tall Open Woodlands to Open forests	66

The Coonabarabran study area was visited along with several other sites with similar vegetation. Several of the NVMP plots were within the area of acquisition of the HyMap data and were visited and documented with digital photos. This helped to establish familiarity with the physical expression of the mapped floristic communities. The local variance and heterogeneity within several plots was assessed in a qualitative measure of how suitable each site was as a training sample for remote sensing data.

3.3 Remote Sensing data

HyMap hyperspectral scanner data, SPOT-5 and Landsat satellite data and Airborne laser scanner data were acquired or collected for the Jilliby study site. Remote sensing data were restricted to SPOT 5 and HyMap data at the Coonabarabran site.

3.3.1 HyMap hyperspectral scanner data

The HyMap hyperspectral scanner is manufactured by an Australian company, the Hyvista Corporation (Hyvista, 2009). Hyvista owns and operates the instrument in Australia. For the Jilliby and Coonabarabran acquisitions it was configured to collect 128 contiguous spectral bands across the reflective solar wavelength region of 450 - 2500 nm (except in the atmospheric water vapour bands). The sampling interval is 13–17 nm recorded by 4 separate spectrographic modules. Each module provides 32 spectral channels giving a total of 128 spectral measurements for each image pixel (Cocks et al., 1998). HyMap's detector array has 512 elements, so the swath width is 512 pixels wide.

The signal received by a remote sensor above a tree is a complicated combination of the interactions between photons and atmosphere, canopy and background. Although we have limited control over canopy characteristics, we can still extract useful information from canopy reflectance by developing methods that reduce atmospheric and background effects (Huang et al., 2004).

Spectral and radiometric calibration of the HyMap sensor was accomplished prior to the survey by the imagery provider. In-flight recorded DN (digital numbers) were corrected for dark current/electronic offsets and converted to radiance using laboratory radiometric calibration information and inflight measurements of the on-board calibration lamp. This information was used to allow the conversion of the raw DN counts to radiance values in $\mu W/cm^2$ nm sr. The data were rescaled to preserve dynamic range, especially in the SWIR range. This rescaling involves multiplying bands 1 – 62 by 1000 and bands 63 – 126 by 4000. The wavelength and bandwidth information in nanometres (nm) is imbedded in the imagery metadata. Image data were recorded with a radiometric resolution of 15-bits per pixel with co-registered bands and stored in 16-bit BIL format (Müller et al., 2001).

Atmospheric correction is an essential pre-processing step to remove artefacts in the reflectance spectrum related to aerosol properties, atmospheric absorptions and scattering, water vapour and other atmospheric constituents (Sanders et al., 2001). HyVista uses the HyCorr program for converting radiance HyMap images to apparent surface reflectance. The Hycorr program is essentially the ATREM (Atmosphere Removal Program) model Centre for the Study of Earth from the Space (CSES), 1992. Gao and Goetz (1990) modified the algorithm to accept data collected by the HYMAP instrument.

HyCorr offers two levels of processing: the simpler level is essentially compatible with ATREM 3 processing and the more advanced level consisting of an ATREM pass followed by an Effort polishing pass to remove systematic ATREM errors (Boardman, 1998). Effort processing was used and the reflectance product was provided as a BIL short-integer image and was scaled by 10,000 (reflectance*10000). Wavelength is displayed as micrometres (μm).

Huang et al. (2004) found that vegetation spectra extracted from HyMap data corrected with Hycorr to be acceptable for tree crown studies and that atmospheric effects, such as the atmospheric water vapour absorption, were largely removed. They found the typical mean reflectance spectrum of a eucalypt tree was similar to that of the whole fresh leaf spectrum for most of the wavelengths.

HyVista uses proprietary software for geocorrecting hyperspectral images collected by the HyMap airborne hyperspectral scanner. The software uses HyMap sensor position and orientation data collected at the same time as the image to calculate the position of each pixel in the image. The software uses this position information to map input image pixel values onto a geo-referenced grid of output image pixels.

The HyMap system is mounted on a Zeiss SM2000 gyro-stabilised platform that provides 5 degrees of pitch and roll correction and 8 degrees of yaw correction. High quality DGPS integrated with a Boeing CMIGITS II GPS/INS inertial monitoring unit was used to provide sensor pointing data to precisely geocode the raw data. Geometric correction factors are provided to convert the data to map coordinates and provide map-based products. All geocoded products are in the UTM projection and WGS84 datum.

HyMap has achieved high performance in relation to signal-to-noise ratio (SNR), band to band registration, calibration and geometric accuracy in past missions (Cocks et al., 1998, Kruse et al., 2000). Spectral calibration accuracy is typically better than 0.5nm, band-band registration is within 1/10th of a pixel, and the signal to noise ratio can be as high as 1000:1 in some bands with adequate calibration (Cocks et al., 1998).

3.3.2 Jilliby HyMap acquisition and pre-processing

For the Jilliby HyMap acquisition the sensor was flown in a twin-prop fixed-wing aircraft at an average altitude of 1900m near simultaneously with the field campaigns. At this altitude the HyMap sensor produces imagery with a spatial resolution of 3.5m. Six swaths were flown in map north and map south directions, with an average overlap between swaths of approximately ten percent. Imagery was acquired in clear conditions with light winds at (and around) solar noon on April 11, 2006. The sun was at an azimuth close to zero and an elevation of 48.75^0.

Seven reflectance bands were visibly affected by sensor noise or water absorption and were subsequently excluded from analysis. Improper calibration can lead to reduced signal quality, variable spectral resolution and shifts in band centre wavelengths in any part of the spectrum. These factors can limit consistent detection of subtle absorption features (Gao et al., 2004). The bands removed were in the strong water absorption features at 1404, 1419, 1434 and 1953nm. The bands affected by sensor noise (band 1, 124 and 125) were at 456, 2479 and 2494nm respectively.

A brightness gradient was observed that spanned the cross-track dimension of the image, which is commonly associated with variation in sensor view-angle (Kennedy et al., 1997). As most vegetation canopies show a backward scattering characteristic the backlit side of the scanned image receives less reflected energy than the forlit side. Following Schlerf et al. (2005) we applied a generally applicable method of correction to minimize the brightness gradient and preserve the low-amplitude spectral features necessary for species discrimination. Along-track mean values were calculated and were used to show the mean variation in the cross-track direction (Exelis, 2008). A polynomial function, with an order of 4, was fit to the means and used to remove the variation. A mosaic of the corrected swaths was created and clipped to the study area.

The preliminary cross-track illumination correction was biasing the corrections of some swaths because of the linear feature of bright grasslands and exposed soils in the central valley. To counter this effect each swath was classified and the cross-track illumination corrections recalculated so that only pixels of closed canopy woody vegetation were used. The classes were based on a conservative band threshold of band 12 (626.2nm) in the visible red range. While the sun azimuth was near perpendicular to the flight line direction, the sun elevation was fairly low due to the autumn acquisition date. This led to significant shadow forming to the south of individual crowns and on the southern aspects of ridges and gullies. The corrected data showed almost no variation with change in across-track position. However, cross track correction compensated for view-angle effects only, not for sun-angle effects that would vary between images acquired at slightly different times (Kennedy et al., 1997).

3.3.3 Jilliby Lidar acquisition and pre-processing

Small-footprint lidar data were acquired on May 18 and 19, 2006, using an ALS50 Airborne Laser Scanner (Leica, 2009). It was mounted in a fixed-wing aircraft operated by Fugro Spatial Solutions (Fugro, 2009). The system was configured for a pulse rate of 83,000 pulses per second, with a mean footprint size of 60cm, a maximum 20 degree scan angle, a mean swath width 500m and a mean point density of 2 pulses/m. Up to 3 returns for each outbound 1084nm NIR laser pulse were recorded as well as return signal intensity values (Turner, 2007). Raw lidar point data were supplied as comma-delimited text files, each representing a 2km x 2km area. The data provider operated synchronised GPS base stations and supplied the point data with geometrically registration.

All lidar data for the Jilliby site was pre-processed (Turner, 2007) to create a 1m resolution canopy height model and a 1m resolution DEM. To improve modelling performance the 2km by 2km point cloud tiles were separated into ground or non-ground (vegetation) and filtered (thinned). The processed data contained x, y and z coordinates, intensity value, layer type and time (only, first, intermediate or last return) (Turner, 2007).

The thinned point cloud data were converted into 1 m pixel resolution raster surfaces using linear triangulation surface modelling. Only ground points were used to construct the DEM, while all points were used to build the *Canopy Elevation Model* (CEM). The CEM represents tree height over varying terrain. The DEM was then subtracted from the CEM to produce a *Canopy Height Model* (CHM) (Turner, 2007). The *Canopy Height Model* (CHM) is the product most commonly referred to in this thesis and it represents the first return which is nominally the absolute tree height (i.e. the tree height regardless of variations in topography). A *Canopy Height Model* (CHM) proved ideal for the reliable identification and manual delineation of large tree crowns. The lidar data were acquired three weeks after HyMap was flown.

3.3.4 Co-registration of lidar and HyMap

The HyMap data were supplied with geometric corrections based on differential GPS, integrated inertial monitoring, and a Digital Elevation Model (DEM). Despite this the spatial error was over 50m in some locations, largely due to the low flight altitude and the complex topography. The DEM available at the time was based on coarse resolution (~90m) Shuttle Radar Topographic Mission (SRTM) data (van Zyl, 2001). To improve the spatial accuracy of the data, and to provide consistent comparisons between data sets, the HyMap data needed to be spatially aligned to an orthorectified base layer, or co-registered.

The advantages of using lidar for co-registration are numerous. The image objects will have attributes from both sensors. For example, tree height data and structural attributes can be derived from lidar, and spectral attributes such as foliar chemistry can be derived from hyperspectral data. A highly accurate DEM can be used and individual tree crowns can be used as tie points in both image sets (Clark et al., 2004). However, the warping of optical data are non-linear and varies over topography and with aircraft pitch and yaw. Crown scale studies that hope to use both data sets simultaneously require that tree crowns must overlap. Manually selecting enough ground control points to assure that every crown would overlap is not practical.

To co-register the HyMap and lidar data an existing tool was used in an innovative way. The ENVI automatic image co-registration tool (Exelis, 2008) was used to automatically select ground control points. The co-registration tool uses an area-based matching algorithm to obtain tie points. It compares the greyscale values of patches of two or more images and tries to find conjugate image locations based on similarity in the greyscale patterns. The results of area-based matching largely depend upon the quality of the approximate relationship between the base image and the warp image (Exelis, 2008).

A single band of HyMap data were pre-processed to emulate the lidar Canopy Height Model (CHM). Once the tie points and geometry corrections were calculated they could be applied to all 125 bands. A histogram stretched and saturation stretched band 12 (621.2nm) was used as the warp image to highlight crowns for matching. The CHM was resampled to 3.5 m (nearest neighbour) to match the spatial resolution of HyMap for co-registration. This had the advantage of smoothing the sometimes noisy lidar data, and the HyMap bands can be processed at their native resolution.

The default number of automatically selected Ground Control Points (GCPs) is set to 25 in ENVI. By forcing the algorithm to automatically select over 10,000 tie points, I was able to generate thousands of low error tie points, which were used to warp the HyMap data to fit the lidar data. The GCP list was sorted by root mean squared error (RMSE) and any spurious tie points with an RMSW over 10.0 were deleted. Manually selecting several additional GCPs at the very corners of the warp band prevented any cropping. For the Jilliby data over 10,000 GCPs were generated with an average RMSE of less than 3.0. The accuracy of the method was sufficient in most cases to co-register individual tree crowns (see Figure 3.13). Nearest neighbour resampling was used to co-register the HyMap to the lidar.

The co-registration algorithm is area based and relies on a moving window. The number of tie points needed, the moving window size, and the RMS threshold, is determined by the size of the image and its spatial resolution. For very high resolution images (images with resolution around 1 m), the moving window size needs to be set to a larger area (for example, 17 x 17 or higher) in order to achieve robust matching results (Exelis, 2008). The settings would therefore need to be modified according to the configuration and altitude of the instrument in other applications.

Each co-registered image, or each swath, was approximately 1800m wide. Illumination effects and geometric errors were greatest at the edge of each swath. By planning the flight to include an overlap between swaths some of these errors were mitigated. The six swaths collected over the Jilliby site were combined in a mosaic with approximately ten percent overlap. Manually drawn cutlines were used to include the least distorted portions of each swath without feathering, thereby minimising edge effects between swaths.

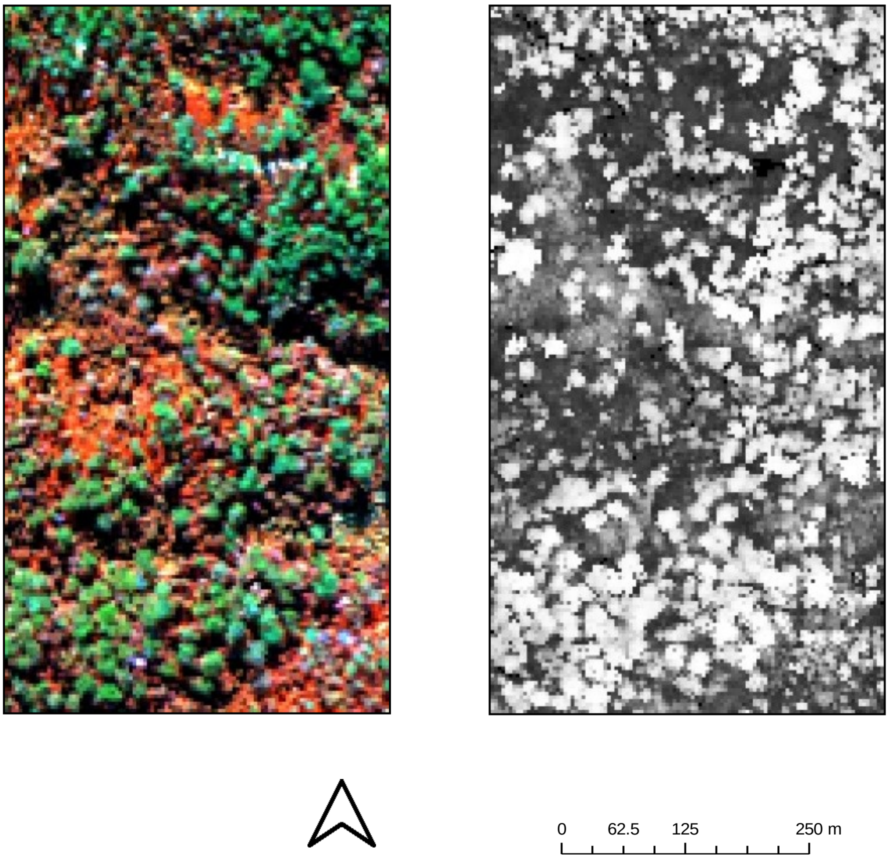

Figure 3.13 The co-registration of HyMap (left) and Lidar data (right) used several thousand automatically generated GCPs.

3.3.5 Coonabararan HyMap acquisition and pre-processing

HyMap data were acquired at the Coonabarabran site with similar operational specifications to the Jilliby site. It was flown in a twin-prop fixed-wing aircraft at an average altitude of 1700m at (and around) solar noon on August 4, 2005. At this altitude the HyMap sensor produces imagery with a spatial resolution of 3.1m. A single swath with a length of 22km was acquired for the Coonabarabran site. The over-flight was on a NNE heading and was selected to encompass as much variation in vegetation type as possible. Almost 20 floristic plots collected by Ismay et al. (2004) were included within the swath and public road access was maximised.

The HyMap and SPOT-5 data for the Coonabarabran site were co-registered. Several ground control points were selected manually and the area-based matching algorithm was used to automatically obtain additional co-registration points. The SPOT-5 2.5m panchromatic image was used as the base after it was resampled to 3.5m using the cubic convolution resampling method. Band 12 (621.2nm) of the HyMap data were used to automatically create co-registration ground control points.

3.3.6 SPOT-5 satellite data

Multispectral SPOT-5 satellite imagery is available as a statewide coverage acquired in an 18 month period beginning in 2005. The coverage was acquired from late October 2004 to August 2005 and consisted of 336 scenes extending over more than 800,000 sq km. Radiometric calibration is achieved with a simple gain and offset calculation for each band to convert raw digital numbers to radiance. The imagery was geocoded to the best available control, which included aerial orthophotos, GPS points and topographic datasets. The spatial accuracy ranges from 1.25-3.75m. Source scene accuracy and gain and offset data were available in individual scene metadata records (Peters et al., 2006).

Although the spatial resolution of SPOT-5 is superior to the pre-existing Landsat TM and ETM+ coverage, its use is problematic. The low spectral and radiometric resolution of SPOT-5 and the greater mismatch between scenes has hampered digital mapping of vegetation (McCauley, 2006). The 'between class' spectral variation is more likely to be obscured by 'within-class' variance with the use of low spectral and radiometric resolution satellite data.

The spatial resolution is 10m in the Green, Red and Near Infra-Red (NIR) bands (b1, b2 and b3 respectively), and 20m in the Short Wave Infra-Red (SWIR) band (b4). The panchromatic band is acquired as two separate 5m bands resampled to generate a 2.5m composite product. Table 3.7 and Table 3.8 provide detail on the launch and sensor characteristics.

Table 3.7 SPOT-5 Satellite Launch Characteristics.

Spot-5 satellite launch characteristics	
Launch date	May 3, 2002
Equator crossing time	10:30 AM (descending node)
Revisit time	2-3 days, depending on latitude
Swath width	60 km x 60 km to 80 km at nadir
Metric accuracy	< 50m horizontal position accuracy (CE90%)
Digitization	8 bits

Source: [SPOT Image]

Table 3.8   SPOT-5 Satellite Sensor Characteristics.

SPOT-5 Satellite Sensor Characteristics		
Nadir resolution (m)	Pan	2.5
	MS	10
	SWI	20
Image bands (nm)	Pan	480-710
	Green	500-590
	Red	610-680
	Near IR	780-890
	Shortwave IR	1,580-1,750

Source: SPOT Image

3.4 Conclusion

This chapter introduced the Jilliby catchment area, the Coonabarabran study site and the remote sensing data collected for my thesis. The criticisms of operational floristic sampling raised in Chapter 2 were addressed by conducting fieldwork at multiple nested scales. The sampling design is a combination of methods in operational use and those introduced to quantify variables at multiple scales.

Forest fuel loads were comprehensively assessed at multiple scales with an aim to investigate the spatial expression of fuels. Condition attributes were sampled with particular emphasis on the over-storey species, as this stratum is visible to remote sensing instruments.

The use of hyperspectral HyMap data in an object-based approach should yield improvements in modelling performance over other studies. My exploration of the data collected begins in Chapter 4 with a study of the relationship between the field data and HyMap hyperspectral data at the crown scale.

This chapter also introduced the Coonabarabran site. It demonstrated how the availability of unpublished floristic plot data makes it an ideal study area to trial new techniques to increase the efficiency of vegetation mapping. Chapter 8 usesSPOT-5 remote sensing data in multi-scale, object-based modelling of vegetation type.

Chapter 4

Classifying tree crowns using HyMap hyperspectral imagery

The aim of the research described in this chapter was to determine whether manually delineated tree crowns can be classified using their mean spectral signature. The spatial resolution of HyMap has largely restricted its use in crown studies in the past but its broad spectral range should be beneficial for differentiating species. Machine Learning Algorithms (MLAs) were used for their ability to classify highly dimensional and highly correlated data. Four MLAs are compared to assess their relative performance. Each of the methods have a different approach for selecting the relative importance of input variables (spectral bands) in terms of their contribution to classification.

4.1 Classification of tree crowns with hyperspectral data

The spectral response of individual tree crowns in closed forest is a combination of shaded leaves, sunlit leaves, bark, and understorey plants and exposed soil. Goodwin et al. (2005) reviewed numerous studies and examined the optimal approach for extracting crown spectra from image pixels for classification purposes. Variations include using the whole crown, a single pixel representing the local maxima, the mean sunlit spectra and the mean sunlit and shaded spectra combined.

Leckie et al. (2003a) concluded that either the whole tree or the sunlit tree sampling methods were the most suitable methods to derive consistent and representative spectral response for crown modelling. Lucas et al. (2008) examined open eucalypt forest and found that when mean sunlit spectra were used, an increase in overall accuracy of around ten percent was achieved, compared to the use of single pixels associated with local maxima. Goodwin et al. (2005) found that separating sunlit and shaded aspects of tree crowns did not increase the overall classification accuracy in their work at the Jilliby site.

Huang et al. (2004) found that the spatial resolution of HYMAP data (about 3 m), was adequate to identify individual trees as most of the trees occupy several pixels on the image. However, in closed forest the spatial resolution of HyMap imagery (3.5m) was too coarse to reliably identify crown scale objects at the Jilliby site without a secondary source of high spatial resolution data.

Fortunately, lidar with a mean footprint size of 60cm was acquired near simultaneously with HyMap. A Canopy Height Model (CHM) derived from a mosaic of Lidar tiles proved ideal for the reliable identification and manual delineation of large tree crowns. For this chapter I used manual on-screen digitisation to extract HyMap pixels from the crown of each tree sampled, incorporating sunlit and shaded portions.

A vegetation map derived from image classification is considered accurate if it provides a true representation of the region it portrays (Foody, 2002, Weber, 2006). A widely accepted practice is to use finer resolution satellite data to assess coarser resolution products (Cihlar et al., 2003) , although the high-resolution data are themselves subject to interpretation and possible errors (DeFries et al., 1995). One of the problems caused by the pixel-based confusion matrix evaluation is that a pixel at a coarse resolution may include several vegetation types (Xie et al., 2008). Ideally, independent field samples are available to test classification accuracy.

The Maximum Likelihood (ML) classifier has been one of the most widely used supervised classification for satellite images in the past (Sohn and Rebello, 2002, Xu et al., 2005). However, since ML classification assumes that the statistics for each class in each band are normally distributed to calculate the probability that a given pixel belongs to a specific it is less applicable in complex areas (Xie et al., 2008).

4.2 Machine learning

Four MLAs were selected for use in the analysis of the HyMap data. Classification and Regression Trees (CART), Neural Networks (MP), Logistic Model Trees (LMT) and Linear Discriminant Analysis (LDA). Machine learning refers to induction algorithms that analyse information, recognise patterns, and improve prediction accuracy through automated and repeated learning from training data (Malerba et al., 2001). The approach used at the Jilliby site was to use Machine learning algorithms (MLAs) to sift through large spectral databases automatically, seeking regularities or patterns (Witten and Frank, 2005).

MLAs are ideal for classifying oversampled hyperspectral data as they allow for the investigation of the relative importance of input variables in terms of their contribution to classification accuracy (Foody and Arora, 1997). They readily accommodate both categorical and continuous ancillary data (Lawrence and Wright, 2001) and their non-parametric nature deals well with multi-modal, noisy and missing data (Hastie et al., 2001). There is now a large body of research that demonstrates the abilities of machine learning techniques, particularly the use of classification trees and artificial neural networks, to deal effectively with tasks involving highly dimensional and highly correlated data (Gahegan, 2003). Lastly, they are flexible and can be adapted to improve performance for particular problems by allowing users to make use of what is already know about the target (Lees and Ritman, 1991).

A general flaw of machine learning algorithms is that they are potentially subject to over-fitting if not carefully applied. Over-fitting can occur when a learning algorithm adjusts to very specific random features of the training data that have no causal relation to the target function. The performance on the training examples increases while the performance on unseen data becomes worse (Tetko et al., 1995). In addition, the performance of classifiers in general deteriorates when the dimensionality of these data increases but the training sample size remains fixed. In the remote sensing literature this has been referred to as the Hughes Effect (Foody and Arora, 1997, Hughes, 1968, Pal and Mather, 2003). Since we are faced with a relatively small sample size (n = 242) and a large number of bands (b = 118) both of these issues needed to be addressed.

The Hughes Effect is addressed by each of the four MLAs in a unique way. Each algorithm is capable of selecting a subset of bands for classification, improving the ratio of bands to classes. To address over-fitting, cross validation is used. Cross-validation (or jack-knifing) assesses how the results of a statistical analysis will generalize to an independent data set. Ten folds were used to calculate classification accuracy scores for the machine learning algorithms. The results were averaged to produce a single value (Witten and Frank, 2005). This maximises the use of the training data in the validation without lessening the number of training samples.

4.3 Machine Learning Algorithms

CART are non-parametric regression technique, that 'grow' a decision tree based on a binary decisions that recursively splits the data until groups are either homogeneous or contain not less observations than a user-defined threshold. CART were selected as they represent information in a way that is intuitive and easy to visualize and has shown recent success in classification using hyperspectral data (Andrew and Ustin, 2006, Andrew and Ustin, 2008).

Decision trees have been found to outperform traditional remote sensing classifiers (Brodley and Friedl, 1997, Hansen et al., 1996). CARTs are structurally explicit, allowing for clear interpretation of the links between the dependent variable of class membership and the independent variables of remote sensing and/or ancillary data (see Figure 4.5) (Lawrence and Wright, 2001). A confidence factor of 0.1 was used to induce severe pruning, simplifying the tree without greatly lowering the classification accuracy.

Neural networks consist of several layers of nodes (neurons) that are in connection with each other. In the input layer, the predictor variables are inserted; the output layer delivers one or more predictive values for the response variable. In between there is a hidden layer and the network is trained using an iterative method to adjust the weights of the connections between the units. Neural networks have shown to be accurate and robust classifiers of vegetation in remote sensing (Filippi and Jensen, 2006, Pu, 2009, Weng and Hu, 2008). A Multilayer Perceptron (MP) was implemented here for its ability to deal with high dimensionality and because outperformed CART with real world data in benchmarks (Maier and Dandy, 2000).

Neural networks "learn" by iteratively considering each training observation and then multiplying the explanatory variables by a set of weights (Franklin et al., 2003). The utility of artificial neural network models in this case lies in the fact that can be used to infer a function from observations. The complexity of the spectral responses of each species makes the design of such a function by hand impractical. MP results should be robust despite large number of highly correlated bands and without knowing which bands or thresholds are important for differentiating species.

MP solves problems stochastically, which means it won't give the same answer if you run it multiple times, but it allows for approximate solutions for complex problems. The main disadvantage is that it is it is a ‘black-box’ method, in which the weights are not interpretable. In this implementation one hidden layer was used as well as backpropagation.

Linear Discriminant Analysis (LDA) was included because it has been used frequently in species classification (Bunting and Lucas, 2006, Clark et al., 2005, Pu, 2009, van Aardt and Wynne, 2007, Wang and Sousa, 2009, Xu and Gong, 2007). Its purpose is to find the linear combination of features which maximizes the ratio of between-class variance to within-class variance. This is particularly relevant given the small variations we expect between species and the large variation within species.

It also features useful data reduction tools available for use in band selection. A forward step-wise Linear Discriminant Analysis classification using Wilks’ Lambda was applied in this case. Step-wise methods select input bands and models based on statistical merit. However, there is a risk is that these methods may choose predictors that have no practical significance. Thus, removing noise bands was important.

Logistic Model Trees (LMT) combine the transparency of CART, the performance of MP and the inbuilt parameter (band) selection of LDA. It uses a supervised training algorithm that combines logistic regression and decision tree learning. A step-wise fitting process constructs the logistic regression models and can select relevant attributes (bands) in the data in a natural way. It builds the logistic regression models at the leaves by incrementally refining those constructed at higher levels in the tree (Landwehr et al., 2005). The LogitBoost algorithm is used to produce a logistic regression model at every node in the tree and then the node split using CART (C4.5). It uses cross-validation to find a number of boosting iterations (Friedman et al., 2000) so that it doesn't overfit the training data.

4.4 Methods

4.4.1 Individual tree crown identification

Tree species were identified and the location of the largest trees that intersected each plot was recorded. Up to ten trees per plot were selected in decreasing order of the diameter of the tree stem at breast height (DBH).

As discussed in Chapter 3, the largest tree crowns in the upper stratum were identified to a species level and spatially located within the plot by recording a bearing and a distance from the centre. The distance from the plot centre to the base of each tree was measured with a Leica laser rangefinder. Where the laser beam was obscured by vegetation the distance from the plot centre was estimated with reference to the measured plot centre, or one of the four plot boundary markers labelled with spray paint and measured with tape.

Estimated ranges were always calibrated with the laser rangefinder and this level of precision was found to be reliably locate the trunks of large crowns. Clark et al. (2004) geo-located tree trunks relative to the closest grid marker using a tape measure and compass (in a 50-100m grid). They used a lidar canopy height model to select canopy-emergent trees as they were 'easy to locate unequivocally'. Clark et al.'s measurements were later used in individual tree crown discrimination studies (Clark et al., 2005). The authors selected 212 emergent trees with large, exposed crowns that provided a large sample of pixels that were less influenced by spectral shadowing or scattering by neighbouring trees. They found that large, emergent trees were easy to locate in orthorectified hyperspectral imagery.

4.4.2 Manual tree crown delineation

In this study, tree crowns were manually delineated by the author using on screen digitisation (Figure 4.1). A single HyMap band (band 12) and lidar data were overlayed with nominal tree stem locations and lidar. A single greyscale image was used to minimise bias that may have been apparent were colour observable.

A conservative approach was taken to ensure that each crown in the imagery was correctly attributed to the stem surveyed in the field. Only the largest of the surveyed trees were used. At the conclusion of the fieldwork, 889 tree stems were identified. For this chapter, a subset of 242 of the largest tree crowns was selected so as to be clearly identifiable in both image sources and not obscured by overlapping tree crowns or shadow. The manual delineation of tree crowns follows Clark et al. (2004) who located crown centroids through visual adjustment of trunk points.

Objects were buffered by less than a pixel to help smooth artefacts of hand drawn boundaries. Only pixels within the crown were delineated to avoid edge effects. Pixels belonging to individual trees deviate from assumptions of pixel independence and normality of distribution in multispectral space (Nagendra, 2001). The average of multiple pixels was used to create a *crown-object* and these data were used in the analysis.

A spectral library was created using the hand drawn vector outlines of tree crowns and all available bands of the HyMap reflectance data. Seven reflectance bands were visibly affected by noise and excluded from the analysis. The bands removed were in the strong water absorption features at 1404, 1419, 1434 and 1953 nm and sensor noise at bands 1, 124 and 125 (456, 2479 and 2494 nm).

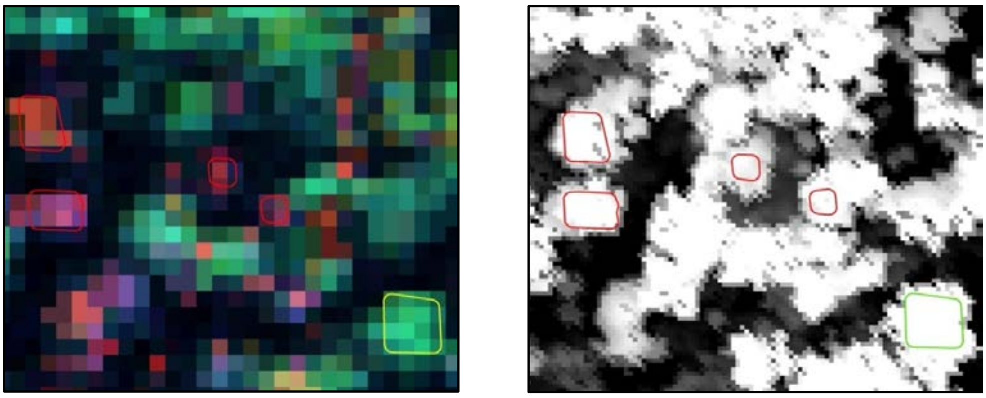

Figure 4.1 Individual tree crowns were delineated manually (left) using 3.5m resolution HyMap data and the 1m resolution lidar Canopy Height Model (right).

4.5 Results

4.5.1 Differential GPS

The Trimble differential GPS system was used to locate the centre of each plot with sub-metre accuracy (Table 4.1). The mean error was 0.73m. Differential GPS for plot centres made it possible to locate large tree crowns.

Table 4.1 Precision and error of plot centres as measured by differential GPS.

DGPS Precision	Mean	Standard Error	Median	Mode	Standard Deviation	Range	Min	Max	Count
	0.73 m	0.03	0.7 m	0.6 m	0.29	1.6 m	0.3 m	1.9 m	130

4.5.2 Crown scale samples

Eucalyptus pilularis (Blackbutt) is the most common over-storey species in the study area, and had the highest frequency in sampling. We found *Syncarpia glomulifera* (Turpentine) to be ubiquitous; its presence is recorded in every sample plot. It is generally restricted to the mid-storey stratum, which makes it harder to isolate on the imagery, but it is relatively spectrally distinct. *Eucalyptus saligna* (Sydney Blue Gum), *Eucalyptus deanei* (Round-leaved Gum), *Eucalyptus microcorys* (Tallowood), and *Eucalyptus acmenioides* (White Mahogany) were sampled as very tall emergent trees, while *Eucalyptus propinqua* (Grey Gum) and *Eucalyptus agglomerata* (Blue Leaved Stringybark) were sampled as individual crowns in stands of trees of similar heights.

Several other species common to the study area were sampled in the field but were not suitable for crown extraction. *Allocasuarina torulosa* (Forest Oak) and *Allocasuarina costata* (Smooth-barked Apple) were both common but were frequently obscured in the mid-storey. Crowns of *Eucalyptus* *umbra* (Broad Leaved White Mahogany) were easy to extract but were not sampled in sufficient number to be included in the analysis. *Corymbia maculata* (Spotted Gum) and *Eucalyptus paniculata* (Grey Ironbark) were both common on the foothills. The similar heights of individual trees in stands of open forest made crown delineation difficult. *Eucalyptus paniculata* had been shown to be spectrally distinct in previous studies (Coops *et al*., 2004). Table 4.2 summarises the species selected from the field survey. The mean spectral response was extracted from 242 large, emergent crowns from the 889 trunks recorded in the field. Abbreviations of the common name of tree species are given as three letter codes.

Table 4.2 The tree species selected for the manual delineation of crowns and the attributes of each sample group.

Name	Code	Common Name	Number Sampled	Avg. DBH (cm)
Eucalyptus pilularis	BLB	Blackbutt	81	65
Eucalyptus acmenioides	WMG	White Mahogany	25	80
Syncarpia glomulifera	TRP	Turpentine	49	63
Eucalyptus saligna	BLG	Sydney Blue Gum	26	65
Eucalyptus propinqua	GRG	Grey Gum	27	54
Eucalyptus deanei	RLG	Round-leaved Gum	8	99
Eucalyptus microcorys	TAL	Tallowood	9	61
Eucalyptus agglomerata	BLS	Blue Leaved Stringybark	17	51

4.5.3 Crown scale spectral reflectance

When individual pixels of vegetation spectra were extracted they can be distorted by shadow or other effects. As an average of multiple pixels, a crown-object is less sensitive to noise. The low reflectance in the visible spectrum is largely a result of absorption from chlorophyll and other pigments. The high reflectance in the near infrared (NIR) can be attributed to the multiple scattering in the leaf structure (Asner, 1998, Knipling, 1970). For each species, the and standard deviation of reflectance was calculated for all crown objects (Figure 4.2). Spectra were pre-processed with EFFORT polishing.

The arrangement and density of leaves and foliage will govern the crown scattering environment and the degree to which leaf biochemical properties are accentuated at pixel or crown scales (Clark et al., 2005). *Eucalyptus propinqua* (GRG) had relatively low NIR reflectance as it occurred in more open forest with lower crown density. *Syncarpia glomulifera* (TRP) had lower reflectance overall as it was primarily sampled as a mid-storey species and it foliar structure is more complex. By contrast *Syncarpia glomulifera* (TRP) had the highest reflectance in the SWIR due to its low leaf moisture content.

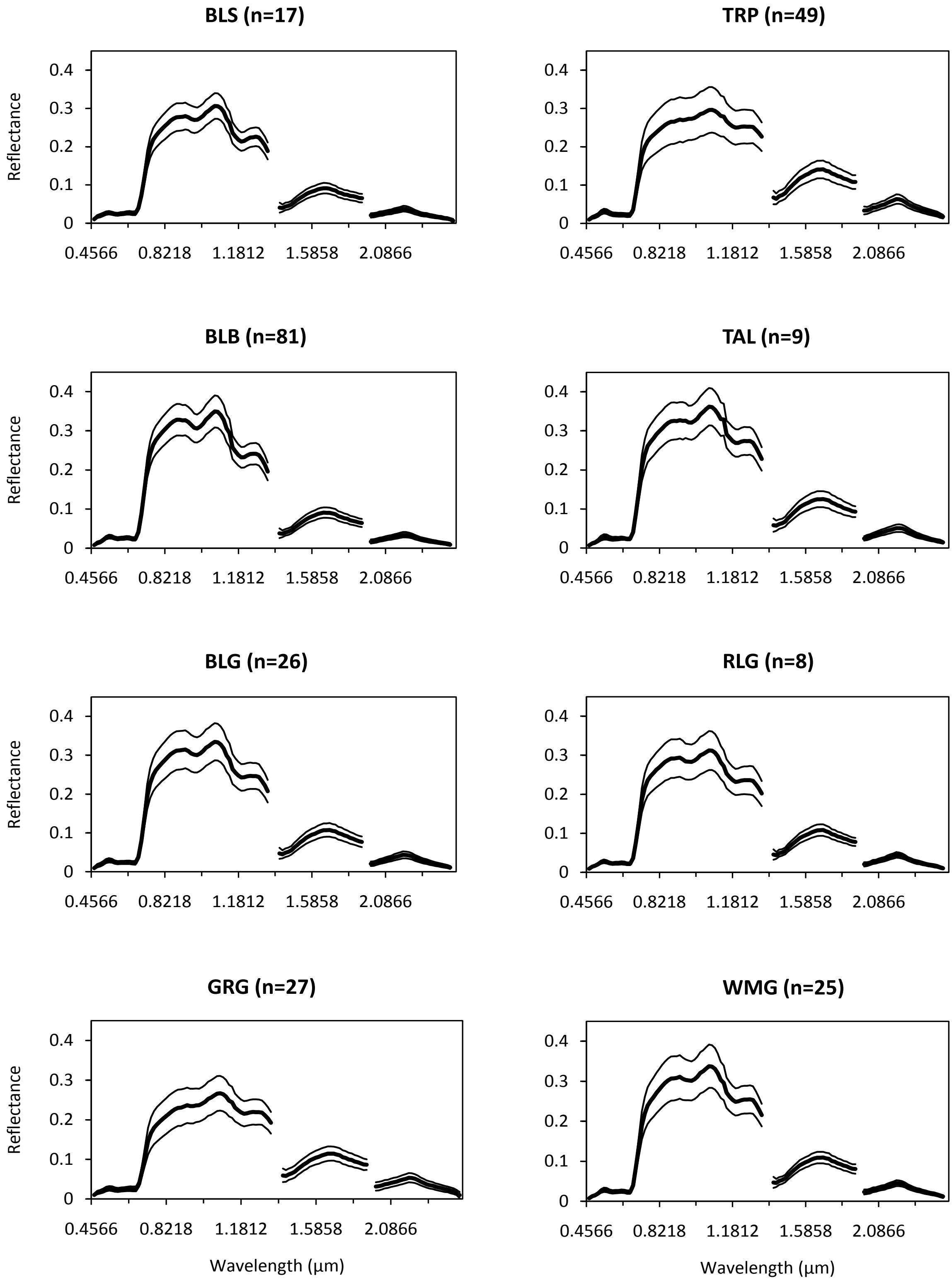

Figure 4.2 The mean (bold line) and standard deviation (thin line) of reflectance was calculated for all crown objects of each species. Reflectance values have been scaled.

4.5.4 Classification accuracy

The overall classification accuracies for the algorithms employed are presented in Table 4.3 and differ between algorithms by as much as 24%. All 118 noise free bands were supplied to each algorithm.

Table 4.3 Crown-object species classification accuracy with a Kappa statistic.

Algorithm	Acronym	Correctly Classified	Kappa	Bands used	Cross Validation
Pruned J48 Decision Tree	J48	62.4%	0.53	118	Yes
Multilayer Perceptron	MP	83.0%	0.79	118	Yes
Logistic Model Trees	LMT	83.90%	0.8	118	Yes
Linear Discriminant Analysis	LDA	86.4%	0.83	16	Yes

The pruned decision tree algorithm (J48) classified 62.4% of the crowns as the correct species (Figure 4.3). A confidence factor of 0.1 was used to induce severe pruning, without greatly lowering the classification accuracy. Overall accuracy for J48 was 62.4% with a Kappa of 0.53. Bands labelled as wavelength (nm) and threshold given as scaled reflectance . As a result of this pruning, the classifier selected nine bands that best differentiate species to use in the classification and regression tree.

The neural network (MP) correctly classified 83% of crown-objects with one hidden layer. Linear Discriminant Analysis (LDA) used Wilks' Lambda to optimise band selection in a step-wise fashion to pre-select 16 bands for analysis. Results are reported as the mean result for 10 iterations using cross-validation. LDA classified 86.4% of species correctly, demonstrating the Hugh's Effect (performance deteriorates with more bands if the training sample size remains fixed).

Cohen's kappa coefficient is included for each algorithm as a statistical measure of reliability. The measure is preferred to a simple percent agreement calculation as it takes into account the agreement occurring by chance.

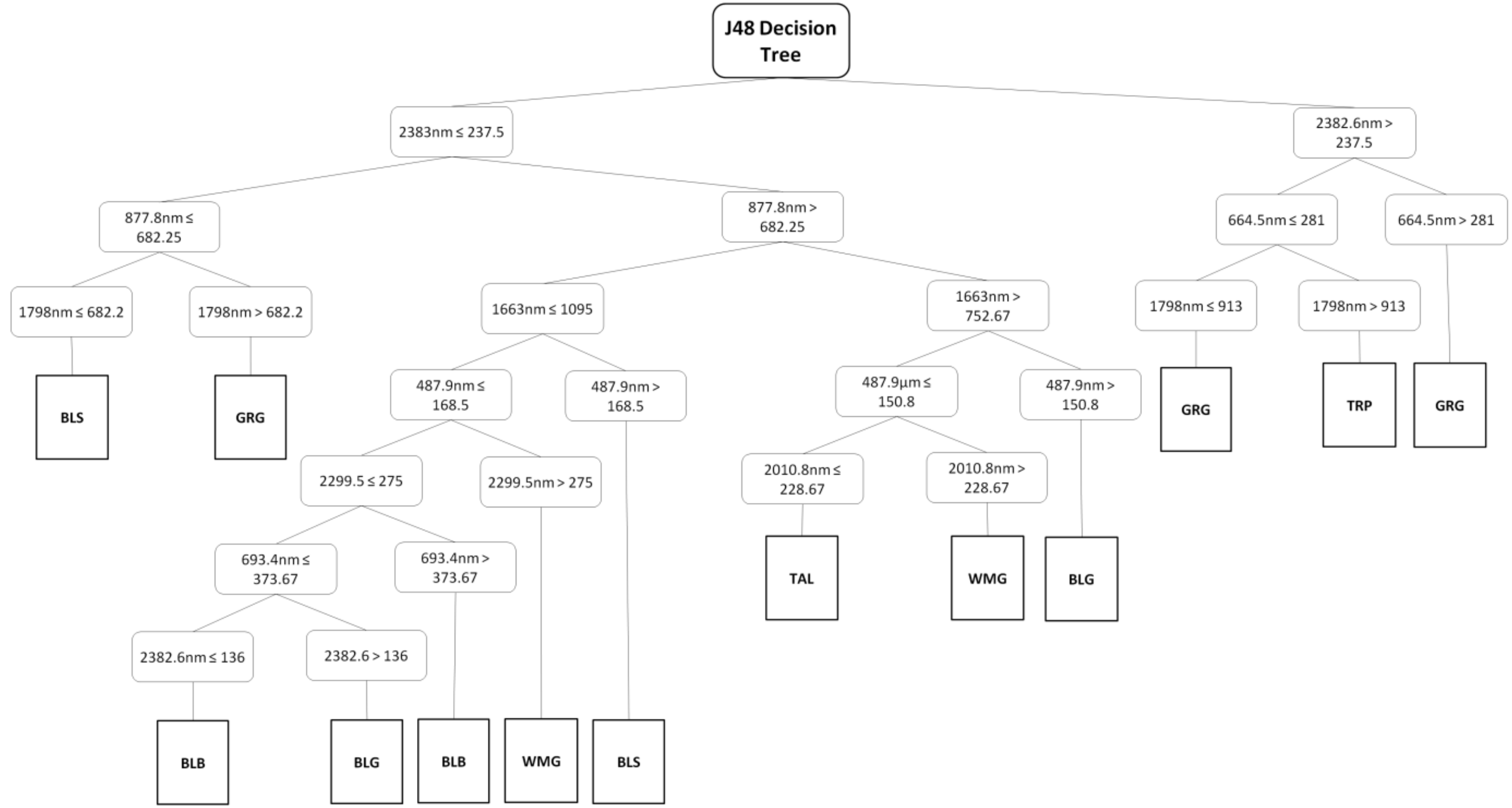

Figure 4.3 Decision tree generated by the pruned J48 algorithm.

One of the advantages of machine learning algorithms, and one of the main reasons their use is argued for here, is that they are designed to discover structural patterns within these data. They evaluate what the most important attributes are and determine how they relate to a numeric outcome. For example, decision trees give a graphical representation of which bands are the most important and what thresholds are applied. They allow for a clear interpretation of the links between the dependent variable of class membership and the independent variables of remote sensing and/or ancillary data (Lawrence and Wright, 2001).

The bands selected by CART in the visible part of the spectrum coincided with leaf pigments (*chlorophyll a* at ~480nm). This region is characterized by strong absorption by carotenoids and chlorophylls (Jensen, 2005). Only a single band was selected in the NIR, which may indicate that leaf structure was either; not detected, or not significant in the differentiation of species. Water present in the spongy mesophyll of a plant absorbs much of the energy in the mid-infrared spectral region. Hence, as the water content of vegetation increases, the reflectance generally decreases in the mid-infrared regions (Jensen, 2005).

In the SWIR, the reflectance of leaves increases when liquid water content decreases (Hoffer, 1978). The bands differentiating *Syncarpia glomulifera* for from the eucalypts were 2382 nm (SWIR), 664 nm (NIR) and 1798 nm (SWIR). Grey Gum and *Syncarpia glomulifera* both had characteristically low SWIR reflectance.

LMT similarly created a classification tree but had a linear logistic regression at each node. It selected 56 bands in total and selected a custom set for each class, or species. At every node in the tree it creates a logistic regression model and then the node split using CART (C4.5). An example of a logistic regression model for BLS is the following linear equation (Equation 3). It illustrates the bands used and their relative power for discriminating BLS from other species.

$$BLS = 18.97 + [0.5027] * 0.17 + [0.6499] * 0.04 + [0.7225] * -0.02 + [1.7259] * -0.01 + [2.2647] * -0.02 + [2.2995] * -0.07 + [2.4314] * -0.03$$

Equation 3 Example of a logistic regression tree produced by LMT.

LDA and LMT both contain a step-wise feature that can select relevant attributes (bands). It was an effective data reduction tool for HyMap data and both models were able to select the bands that contributed the most to differentiating vegetation species. The bands selected to be used in each model are illustrated in Figure 4.4 and Figure 4.5. In both cases bands were primarily selected from the visible, red edge, and SWIR.

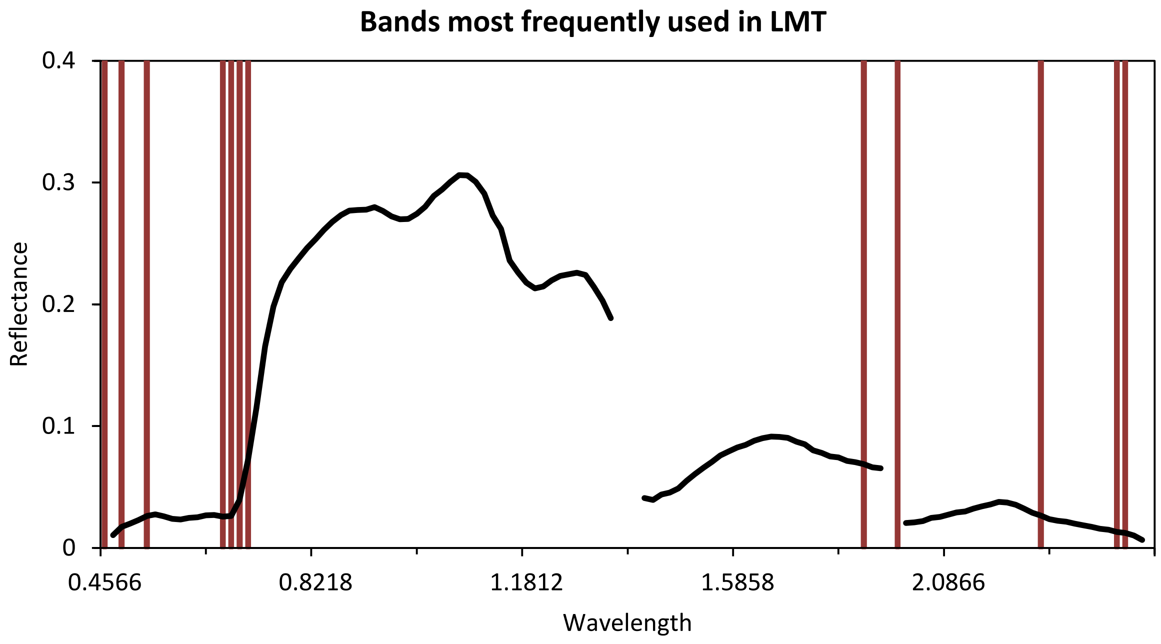

Figure 4.4 The bands used three or more times in LMT for all species.

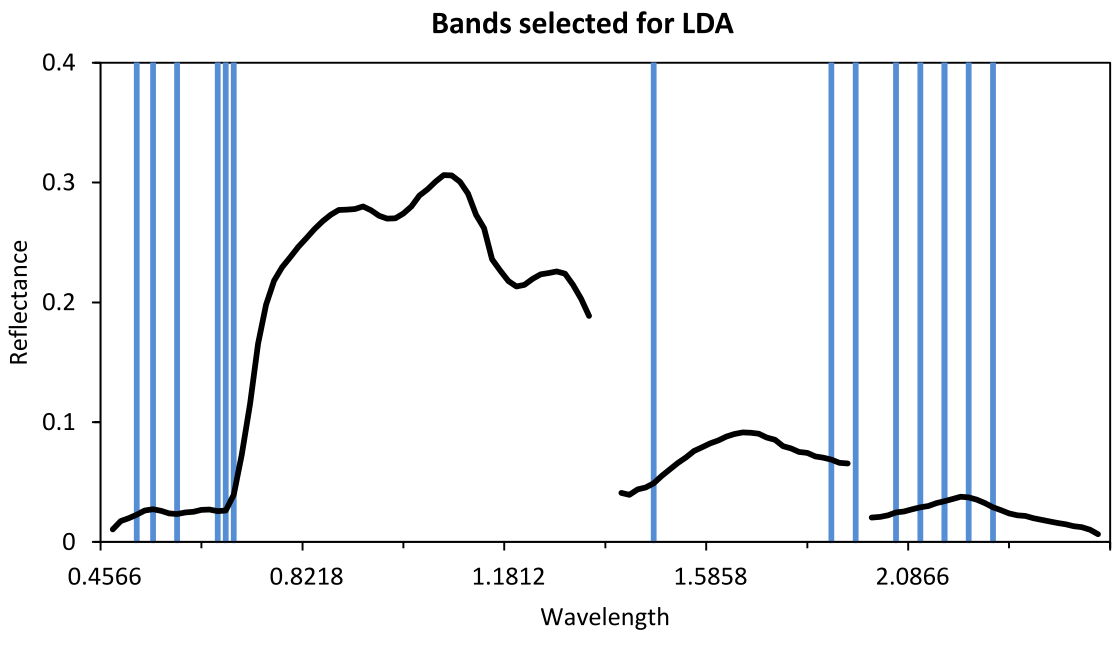

Figure 4.5 The bands selected step-wise for all species by LDA.

Wilks' Lambda is the measure used in this case to determine a variable's potential for discriminating between groups. The value is generated for each band as part of the LDA model output. In Figure 4.6, the higher the Wilks' Lambda value (bold line), the better the variable is at discriminating between groups, or species. It is plotted against the average of all the sampled *Eucalytus agglomerata* spectra (thin line). For comparison both are scaled to values between 0 and 1. Note the peaks in Wilks'

Lambda are associated with chlorophyll absorption in the visible spectrum, the relative importance of the red edge, and in particular the uniform high power of the SWIR bands.

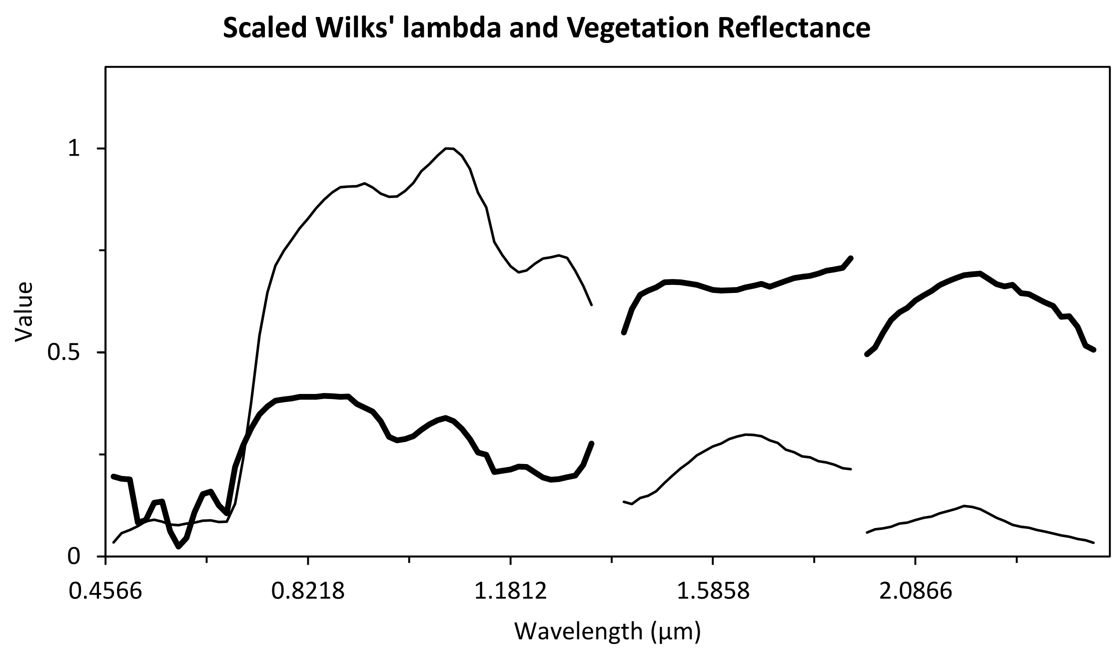

Figure 4.6 Wilks' Lambda (bold line) and the average of all the sampled Eucalytus agglomerata *(BLS) spectra (thin line). Both are scaled to values between 0 and 1.*

Stone et al. (2001) looked at red coloration at the Jilliby site and found that insect-damaged mature leaves and healthy young expanding leaves of some species was caused by the presence of anthocyanin pigmentation. For the mature leaves, the level of red coloration was significantly correlated with insect herbivory and leaf necrosis. Significant correlations were also found between the level of red pigmentation and the following spectral features: maximum reflectance in the visible at the green peak (550 nm); the wavelength position and maximum slope of the red edge (690–740 nm), both of which were selected by LDA and LMT.

The maximum reflectance at 750 nm in the near-infrared portion of the electromagnetic spectrum was also an indicator but much of the NIR was ignored by the algorithms. Using spectral sensitivity analysis Barry et al. (2011) found that, wavelengths between 679 and 695 nm were most sensitive to the presence of necrosis in young *Eucalyptus globulus* but that 706 to 726 nm was the least sensitive. These studies raise concern that vegetation canopy condition could hamper species discrimination and may contribute to the power of SWIR.

The LDA results are displayed in a confusion matrix in Table 4.4 as an example of how classification accuracy varied with each species. The matrix gives a breakdown of each species with user and producer accuracy results. The most difficult species to differentiate was *Eucalyptus deanei* (RLG) which was frequently misinterpreted as *Eucalyptus propinqua* (GRG) or *Eucalyptus saligna* (BLG).

This is to be expected because of the small sample size of *Eucalyptus deanei* (RLG) and the similarities the species shares with *Eucalyptus saligna* (BLG). Both have white or light grey smooth trunks, dark green leaves and similarly shaped fruit, are found in wet forests in slopes and gullies (Harden, 1991) and are relatively difficult to differentiate in the field. By contrast, *Eucalyptus microcorys* (TAL) and *Syncarpia glomulifera* (TRP) were classified correctly more frequently.

Table 4.4 Confusion matrix for the most successful classifier, step-wise Linear Discriminant Analysis with Wilks' Lambda. The classifier selected 16 optimal bands for use with the classifier (Kappa = 0.83).

Species	Field	BLB	BLG	BLS	GRG	RLG	TAL	TRP	WMG	Total	Users
Model	BLB	76	4	1	-	-	-	-	-	81	93.80%
Results	BLG	1	16	1	2	4	-	-	2	26	61.50%
	BLS	-	-	17	-	-	-	-	-	17	100%
	GRG	-	-	-	21	3	-	-	3	27	77.80%
	RLG	-	3	-	1	4	-	-	-	8	50.00%
	TAL	-	-	-	1	-	8	-	-	9	88.90%
	TRP	-	1	-	2	1	-	45	-	49	100%
	WMH	-	1	-	2	-	-	-	22	25	88.00%
	Total	77	25	19	29	12	8	45	27	242	
Producers		98.70%	64.00%	89.50%	72.40%	33.30%	100%	100%	81.40%		86.36

Note: for acronyms of species see Table 4.2.

4.6 Discussion

This chapter compared a variety of classification algorithms. Spectral information from tree crowns surveyed in the field was used as training data. As discussed, it is assumed that the algorithm will reach a state where it will be able to predict the species of unknown crowns (Witten and Frank, 2005) generalising what was learned from the known samples across the landscape.

Although there are examples in the literature of crown scale analysis of HyMap data (Lucas et al., 2008) most of the crown scale research referenced in this chapter uses very fine spatial resolution data (1m or less) for delineating and classifying tree crowns. Most have used CASI-2 data (Bunting and Lucas, 2006, Coops et al., 2004, Goodwin et al., 2005, Lucas et al., 2008, Wang and Sousa, 2009) or high resolution air photograph (Leckie et al., 2003a). O'Neill et al. (1996) recommend, as a practical rule of thumb, that the spatial resolution should be two to three times smaller than the objects of interest.

Mapping individual trees using high spatial resolution data poses problems not encountered when mapping associations or habitat patches. Pixels covering different components of a tree, such as bark and leaf, can be extremely variable in intensities. This makes the spectral signature of a species of tree difficult to define (Cracknell, 1998, Nagendra, 2001).

The relatively low spatial resolution of HyMap limits the number of pixels that represent a single tree crown. Pixels belonging to individual trees deviate from assumptions of pixel independence and normality of distribution in multispectral space There are numerous assumptions built into conventional classifiers (e.g. independence), as they were developed for the analysis of low resolution satellite imagery (Crane et al., 1972). Pixels belonging to individual trees deviate from assumptions of pixel independence and normality of distribution in multispectral space (Nagendra, 2001). Non-parametric machine learning algorithms and hyperspectral data were employed to mitigate these effects. Alternately, individual tree crowns rather than pixels are used as objects for classification, through prior (manual or automated) delineation of tree crowns (Nagendra, 2001), which is another advantage of the object-based approach pursued here.

The majority of the bands selected by the LMT, LDA and CART algorithms came from the short wave infrared (SWIR) wavelengths and visible wavelengths. SWIR bands were unavailable in previous crown scale studies (Coops et al., 2004, Goodwin et al., 2005). The results here confirm previous vegetation spectra studies at the leaf scale (Datt, 1999b, Datt, 1999a), and other studies using HyMap (Lucas et al., 2008), that demonstrated the value of the SWIR wavelengths for species classification.

MLA approaches also allow for the use of expert knowledge to select bands allowing a machine learning to suggest or explore new relationships. The stepwise linear regression (LMT) method evaluated in this study exhausts all possible combinations of predictor variables in searching for the one that minimizes the impact of multi-collinearity without losing a significant portion of the explanatory power of a data set (Miller, 1990)

Manual delineation of tree crowns is a natural first step in any crown scale study, regardless of the spatial resolution of the imagery. It helps establish a relationship between the imagery and the field data, which allows for the extraction of spectra of individual tree crowns. However, it is not practical for the classification of tree crowns across the landscape.

Crown scale delineation must be automated for practical conservation applications at a landscape scale. In this study, a high spatial resolution lidar data set was available, but very high spatial resolution optical data would also be applicable. For automated crown delineation to be successful at the Jilliby site, one or both of the following practical limitations need to be overcome: either multiple sources of high spatial resolution data need to be co-registered with the HyMap data, or a technique must be created for crown delineation with coarse spatial resolution data.

Co-registering the lidar and the HyMap data were the ideal solution. It allowed for the automated extraction of crowns using the lidar Canopy Height Model and improved the spatial location accuracy of the HyMap data. The lidar data also contains tree height and other useful structural attributes.

Sources of error include spatial miss-registration, selecting the wrong crown species in the field, selecting the wrong crowns in the imagery and uncertainty due to the atmospheric effects, radiometric effects, and Bidirectional Reflectance Distribution Function (BRDF) effects. Spatial errors were minimised with the use of a lidar CHM. Atmospheric effects were corrected for using HyCorr and illumination variance addressed with cross track correction. The risk with over-fitting is that the classification models developed in this chapter will not generalise across the landscape. The best available method for testing how robust the models are is to test them using independent field plots for verification. This is the approach taken in Chapter 6.

Stand and community type delineation and classification is the obvious successor to crown scale classification, but it is less developed in the literature. The countless combinations of species diversity, structure, and other attributes in a stand of mixed species makes consistent generalisation of vegetation units across a landscape difficult. The combination of structural attributes from lidar, spectral and textural attributes from hyperspectral imagery and the machine learning algorithms introduced here, provide a promising approach for future research.

4.7 Conclusions

This chapter aimed to differentiate large tree at a species level in tall, closed canopy eucalypt forest using HyMap data. The HyMap hyperspectral scanner (128 bands, 4567-2944nm) is not routinely used for crown scale studies as its relatively coarse spatial resolution (2-8m) limits the analysis to large crowns. However, the high spectral resolution of HyMap, particularly the bands in the SWIR, proved to be important for differentiating several species. Combining lidar and HyMap allowed individual tree crowns to be identified given location information recorded in the field.

Results showed that machine learning algorithms revealed structural patterns in data by selecting the bands most useful for discriminating target species and weighting their importance. The machine learning algorithms included in the comparison (J48, MP, and LMT) performed nearly as well (64-84%) as the more commonly applied LDA (86%). LMT was selected as the classifier in later chapters for its ability to automate the selection of relevant attributes (bands), how it deals with over-fitting, and its computational efficiency and performance. LMT was competitive in this comparison with 84% overall accuracy.

The results show that the spatial resolution of HyMap was adequate for classification of some of the species in closed, tall eucalypt forest. However, a high spatial resolution dataset in essential for locating training samples and delineating tree crowns. The small number of training samples and high dimensionality of these data may have had an effect on the results of the classification. Cross validation was used to mitigate this but additional independent samples are desirable.

Crown scale mapping using HyMap is not practical for conservation applications at a landscape scale, without automated crown scale delineation.

Chapter 5

Individual tree crown delineation with hyperspectral data

Chapter 4 established that hyperspectral data can be used to differentiate tree crown species within tall, closed canopy eucalypt forest. However, the method used requires image objects. This is not practical using HyMap without automating the delineation of tree crowns.

This chapter presents the HyMap Crown Delineation Algorithm (HCDA) which aims to automate the isolation of individual tree crowns in native forest using HyMap data. The ultimate aim of the research is to create an accurate community scale map using multi-scale image objects. The HCDA is based on existing pattern recognition concepts but represents the first time HyMap has been used to segment individual tree crowns. The method applies spatial filters to accentuate the location of tree crowns based on the local maximum of sunlit crowns. A watershed algorithm that detects the local minima is then applied to separate individual crowns. The HCDA can be used to make crown objects, which can be classified using the machine learning approaches described in Chapter 4. Chapter 6 will demonstrate using both procedures in combination.

5.1 Background

In the field of computer vision, segmentation refers to the process of partitioning a digital image by simplifying its representation into something that is more meaningful, thus enabling clearer analysis. In remote sensing, image segmentation is typically used to locate objects and boundaries in images. Asner et al. (2002) found that visual interpretation of remote sensing is resource intensive and difficult to implement consistently. Automated routines can be readily replicated across wide areas but they are generally less accurate (Culvenor, 2002). The recognition of single trees is one of the most important tasks to undertake when deriving forest information from high spatial resolution remote sensing data (Hirschmugl et al., 2007).

Using tree crown species identified in the field to guide the classification of tree crowns at a catchment scale is a relatively new approach to dealing with the problem of scale. The aim is to emulate the way ecologists classify vegetation type in the field by recording dominant species. The ultimate goal of this research is to create a nested hierarchy of polygons where crown scale objects are contained within community scale objects. This would give the community polygons a quantifiable degree of certainty not previously seen in vegetation mapping and allow for new measures of ecological diversity across the landscape. Even a representative sample of large trees characteristic of each community would be a significant improvement over existing operational techniques.

5.2 Existing crown scale delineation algorithms

A variety of automated pattern recognition methods are used to isolate individual trees from high spatial resolution optical data. Their success depends on the spatial resolution of image data in comparison with the size of the tree to be detected. Most approaches use data with an IGFOV smaller than the average crown width (Culvenor, 2002, Leckie et al., 2005a, Pouliot et al., 2002, Read et al., 2003, Leckie et al., 2003b).

Photographic imagery has been used for the estimation of crown diameter and density (Falkowski et al., 2006, Jennings et al., 1999, Larsen and Rudemo, 1998). Videography has been used to analyse individual crowns in transects (Culvenor, 2002) and airborne lidar has been used in crown delineation (Falkowski et al., 2006, Leckie et al., 2003a, Popescu et al., 2003, Turner, 2006, Heurich, 2008) and the measurement of structural variables. Bunting and Lucas (2006) reviewed crown delineation algorithms and identified two broad approaches, detecting crown centroids and boundaries, following valleys (also referred to as contouring).

Crown centroid detection involves the identification of local intensity maximum (bright points at the peak of the crown) and mapping of crown boundaries by expanding to local minima (Pouliot et al., 2002, Wulder et al., 2000). Culvenor (2002) developed the *Tree Identification and Delineation Algorithm* (TIDA) which is based on spectral maximum, but takes the spectral minima into consideration. The delineation uses a top-down approach that begins at the centroid and finishes either at the minima boundaries or at user-defined threshold, both in terms of distance and spectral signature.

Boundary (valley) following or contouring methods use similarities in data values as a delimiter between an object (e.g., a tree crown) and the background (Bunting and Lucas, 2006). The *Individual Tree Crown* (ITC) *Suite* (Gougeon and Leckie, 2003, Leckie et al., 2005a) is an example of this approach. ITC is based on following valleys of shade between tree crowns after spatial filtering and resampling. The authors have optimised their approach for the use of image data with 50cm spatial resolution. Small indentations were identified and used to separate crown groups while a 'jump-factor' was used to remove small ridges in the surface, thereby ensuring a more precise separation (Gougeon, 1995, Leckie et al., 2005a). The authors suggest that the ITC suite is designed for delineation of Canadian forests, and that very large crowns of tropical forests may be analysed better at 1m spatial resolution. Table 5.1 summarises some of the methods previously explored in the literature.

Table 5.1 A selection of tree crown delineation research.

Research topic	Authors
Crown delineation and pattern detection	(Bai et al., 2005)
Multi-scale approach for the automatic delineation of individual tree crowns	(Brandtberg and Walter, 1998, Leckie et al., 2003a, Leckie et al., 2003b)
Automated tree crown detection and delineation	(Brandtberg and Walter, 1998, Culvenor, 2002, Pouliot et al., 2002, Pouliot et al., 2005, Wang et al., 2004, Leckie et al., 2003b)
Segmentation and classification of individual tree crowns	(Bunting and Lucas, 2006, Erikson, 2004, Leckie et al., 2003a)
Tree detection with local maximum methods	(Perko, 2004, Wulder et al., 2000, Wulder et al., 2004)
Canopy shadow in IKONOS satellite observations	(Asner and Warner, 2003)
Crown-following approach to the automatic delineation of individual tree crowns	(Gougeon, 1995)
Lidar and multispectral imagery for individual tree crown analysis	(Heurich, 2008, Leckie et al., 2003a)
Retrieving individual tree crown data with lidar	(Coops et al., 2007, Falkowski et al., 2006, Hyyppä et al., 2004, Popescu et al., 2003, Turner, 2006)
Remote sensing for retrieval of forest stand attributes	(Hyyppä et al., 2000, Leckie, 1990)
Classification of tree crowns	(Clark et al., 2005, Goodwin et al., 2005, Gougeon, 1995, Haara and Haarala, 2002)

Existing crown scale research shows a strong bias toward forests with low species diversity and relatively regular geometric crown shapes (Culvenor, 2002, Falkowski et al., 2006, Larsen and Rudemo, 1998, Leckie et al., 2005a, Popescu et al., 2003, Pouliot et al., 2002). The methods are often developed for the identification of conifer trees near the nadir of images as they fulfil the assumption that crowns are of similar size and have only one bright point located close to their centre (Bunting and Lucas, 2006).

The Jilliby site's diverse range of tree species, growth stages and canopy cover provides a challenging environment for tree crown delineation. Other authors have noted that crowns in native forest do not always have clear boundaries, are not symmetrical and vary in size and shadows and overlaps are common (Leckie et al., 2005a). Perhaps unsurprisingly, the crown delineation methods reviewed in Table 5.1 did not perform well on the Jilliby dataset.

Chapter 4 concluded the spectral resolution of HyMap data were sufficient to differentiate the tall eucalypt species, but a new algorithm is required for delineating tree crowns with HyMap. The spatial resolution of HyMap at the Jilliby site (GIFOV 3.5m) was adequate for the manual delineation of large tree crowns but a high degree of uncertainty was introduced when delineating smaller crowns. A finer spatial resolution reference data set that is co-registered with the HyMap is required.

Comparing the results of a segmentation algorithm to manually delineated crowns is an established method for accuracy assessment Pouliot et al. (2002) . It is commonly performed at an individual tree level using reference data consisting of tree locations visually interpreted from the imagery

(Brandtberg and Walter, 1998, Gougeon, 1995, Niemann et al., 1998, Pollock, 1998, Walsworth and King, 1998) .

5.3 Introducing the HyMap Crown Delineation Algorithm (HCDA)

Two of the more commonly used algorithms for automated analysis of canopies are local maximum filtering and local minima value finding. Local maximum filtering isolates the bright spot at the peak of each crown and relies on the assumption that the area surrounding the brightest local value can be associated with the location of a single tree crown (Culvenor, 2002, Wulder et al., 2000). Local minima value finding is used to detect the separation between crowns, with the assumption that the darker image values are created by shadows between crowns (Gougeon, 1995, Leckie et al., 2003a, Pouliot et al., 2002). Automated crown detection algorithms using a combination of local maximum filtering and local minima value finding have been developed (Leckie et al., 2005a, Pouliot et al., 2002) but have not been applied to HyMap data.

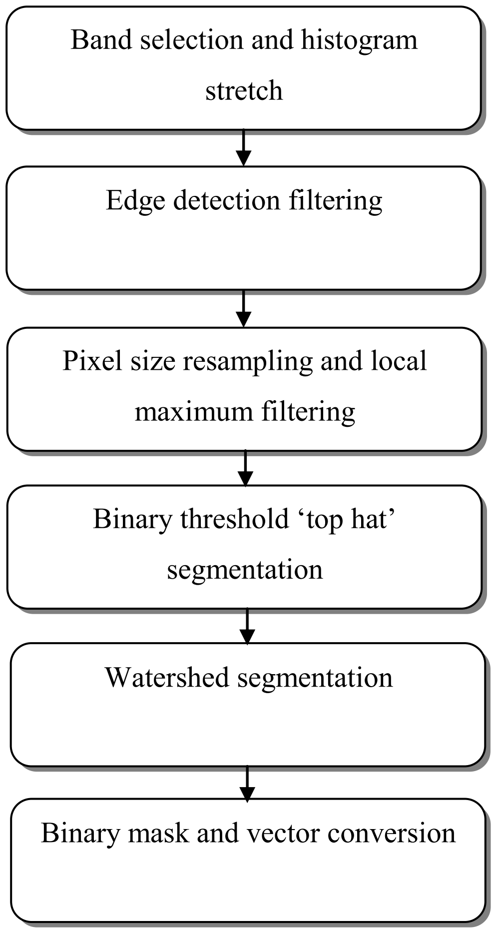

Figure 5.1 Flow chart of the HyMap crown delineation algorithm.

The automated crown detection algorithm described here uses a combination of local maximum filtering and local minima value finding. It relies on a combination of histogram-based segmentation, edge detection, binary threshold segmentation, focal statistics and watershed delineation to isolate crowns from the matrix of shadow, cleared areas and the understorey. There are several processing steps illustrated in Figure 5.1.

The automated crown detection algorithm presented here was designed using existing pattern recognition concepts for high spatial resolution remote sensing data. The algorithm is based on spatial analysis of the brightness patterns in the image (visible reflectance or digital number). The specific kernel size for the filters employed in this method, and the thresholds used, will depend on the spatial resolution of the input data set and the size of the tree crowns. Thus, it cannot be presented as a truly automated approach. However, in a graphical user interface the threshold at each step could be adjusted iteratively to get the best result for the specific dataset.

Note that the output of the HCDA is a binary image of tree crowns. This is applied as a mask to the original reflectance data for use in object-based classification. Histogram equalisation and the filters described below are not applied to reflectance data used in classification. The spectral and geometric quality of the data were not altered because the filters are not applied to reflectance data used in classification.

5.3.1 Band selection and histogram stretch

Band 12 (0.6212 μm) was selected as the basis for the HCDA. Many of the bands available from HyMap are useful for classification but much of the data were redundant for crown delineation. Band 12 was selected as it is in the visible wavelengths (RED) so the method has potential for application to other sensors. The dark woody signature was also stable across multiple swaths of imagery. Once the crown objects are delineated using band 12, the raw reflectance from all 125 available bands can be extracted for each object for use in classification classification.

The Jilliby Catchment study site is dominated by woody vegetation. It features a grassy central valley, shadow in the gullies, and clearings connected by highly reflective roads. Most of the scene is forested, so the DN histogram shows most variation in low digital numbers (see Figure 5.2).

A 2% equalisation stretch was applied to band 12. This adjusted the 8-bit greyscale image represents the range of woody vegetation in the image and improved the contrast. Changing the data range of an input file helps maximise the contrast between sunlit crown peaks and the surrounding matrix of shadow, clearings and understorey. For the remainder of this thesis this process is referred to as a histogram stretch or histogram equalisation. To automate contrast stretching, the modal, maximum, and minimum brightness values of the image are calculated per scene.

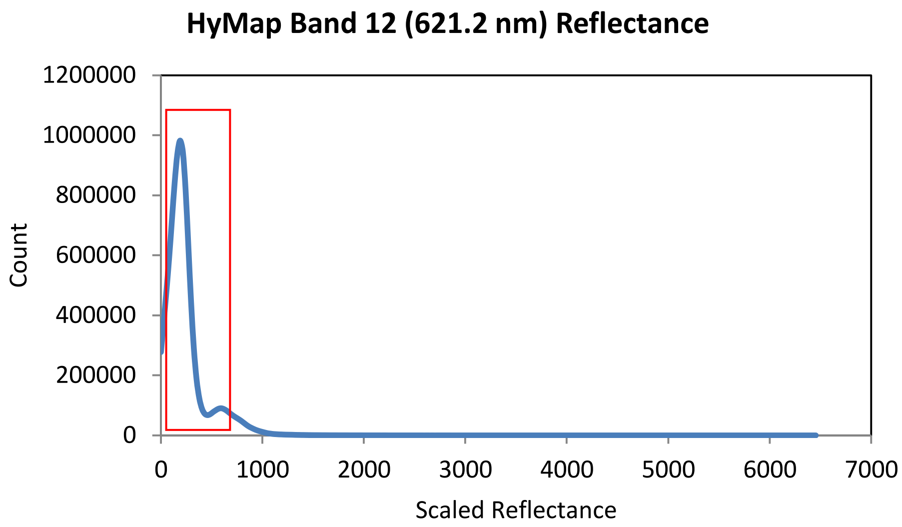

Figure 5.2 A histogram of reflectance illustrates the low dynamic range. For segmentation, the pixel values of interest lie between 20 and 819.

5.3.2 Edge detection filtering

Edge detection and sharpening filters help determine the boundaries of a region (i.e. the size and shape of tree crowns). Region boundaries and edges are closely related since there is often a sharp change in intensity at region boundaries. Spatial filters work by producing output images where brightness value at a given pixel is a function of some weighted average of the brightness of the surrounding pixels. The moving window kernel size and the weighted value can be altered to produce a variety of effects. The high pass filter and a Sobel edge detection filters were used to isolate the brightest part at the peak of each crown.

High pass filters are commonly used in pattern recognition for image smoothing and sharpening. A moving window high pass filter with a 7 x 7 kernel was used to isolate the local maxima and suppress noise. The Sobel edge detection filter was used in effect to 'buffer' the local maxima by accentuating their edges. The brighter and larger the tree crown, the larger the resulting buffered area. This helped differentiate tree crown diameters without the use of variable size moving windows. Kernel size for the Sobel filter cannot be altered and is set to 3 x 3. 'Adding back' the original high pass filtered image to the Sobel filtered image ensures that the edges are accentuated without the loss of the spatial location associated with tree crowns. The result is a model of where tree crowns are likely to appear based on the location of bright peaks in the imagery (Figure 5.3).

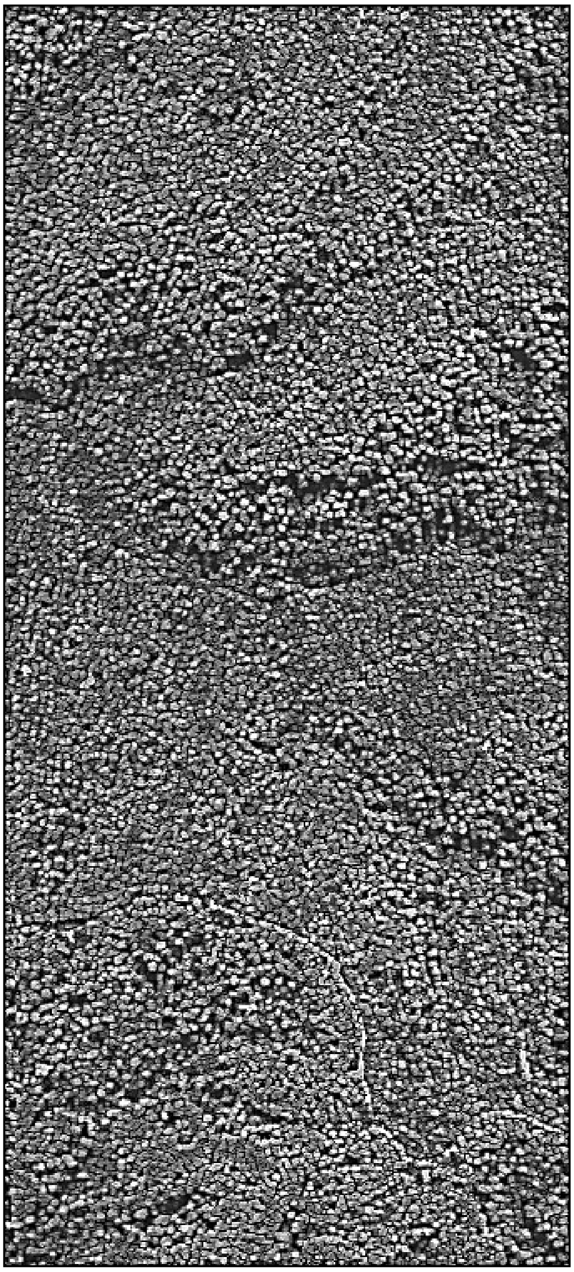

Figure 5.3 Histogram stretched HyMap data (Band 12) (left). A moving window filters buffers the local maxima that represent tree crowns (right).

5.3.3 Image resampling and focal statistics

Tree crowns are not uniformly visible across the landscape in 3.5m spatial resolution data. Large isolated crowns are clearly visible, but stands of smaller crowns tend to merge. In addition, the watershed algorithm (see Section 5.3.5) cannot operate effectively on crowns smaller than 2 x 2 pixels. To correct for these ambiguities the image is resized to 1m spatial resolution using cubic convolution resampling.

Cubic convolution uses the weighted average calculated from the 16 nearest input cell centres and their values. The new value for the output cell is a weighted average of these 16 values, adjusted to account for their distance from the centre of the output cell. This interpolation method results in a smoother-looking surface than nearest neighbour. It has a tendency to sharpen the edges of the data more than bilinear interpolation, since more cells are involved in the calculation of the output value. Both of these effects are desirable when trying to using feature recognition to define crown boundaries. It can be thought of as a surface, like a DEM, that can be smoothed as it is a continuous surface. Nearest neighbour resampling was used for HyMap reflectance data before extracting spectral information.

A moving window analysis of local maximum with a circular kernel (radius 3m or 3 pixels) can be optionally applied in to remove noise from the resampled image and to round the edges of the filtered local maxima. This was applied to the Jilliby HyMap data.

5.3.4 Binary thresholding or 'top hat' segmentation

A 3-dimensional (3D) representation of the filtered image is displayed in Figure 5.4. The height of these 3D objects is determined by the brightness of the local maxima, which is in turn determined by sensor geometry, sun-angle and crown size. A lidar derived canopy height model for the same area is provided for comparison. In a lidar *Canopy Height Model* (CHM) height of the 3D objects in the lidar image is a quantitative measure of tree height that is independent of illumination conditions. Despite the different way the information is derived, there are similarities in the size and location of large and small tree crowns.

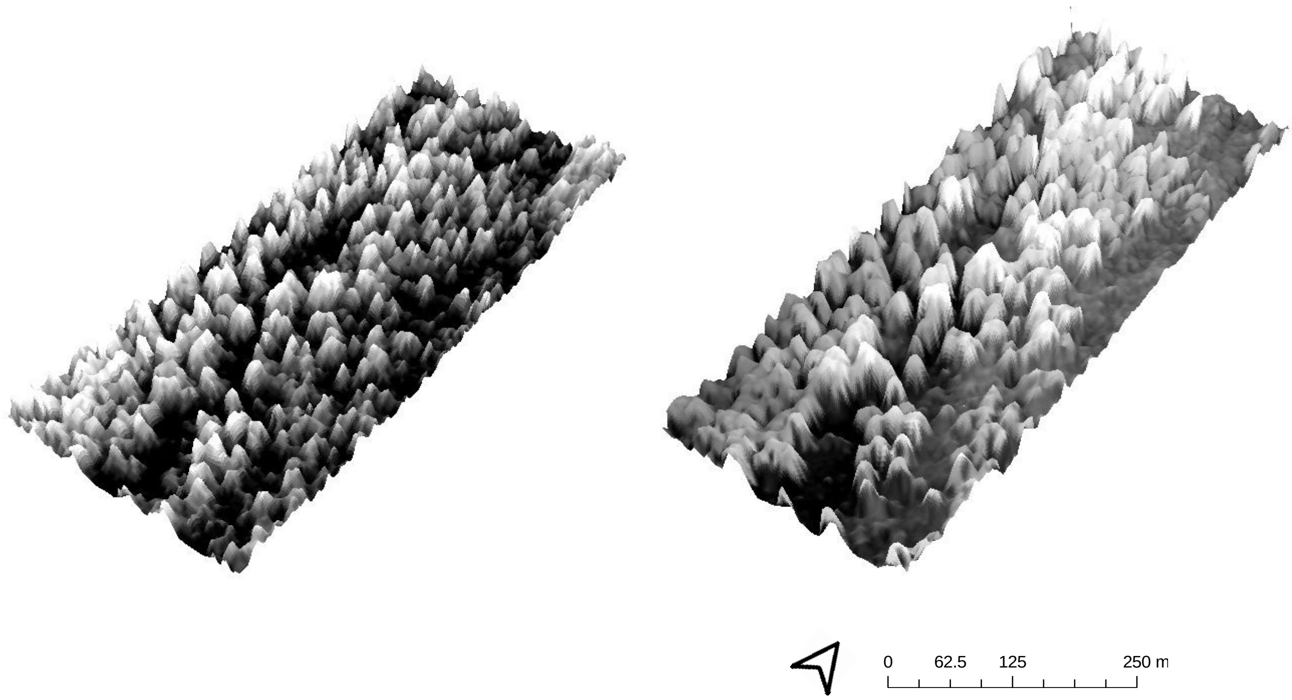

Figure 5.4 3D crown-objects derived from a greyscale HyMap image (left) and a lidar derived canopy height model (right).

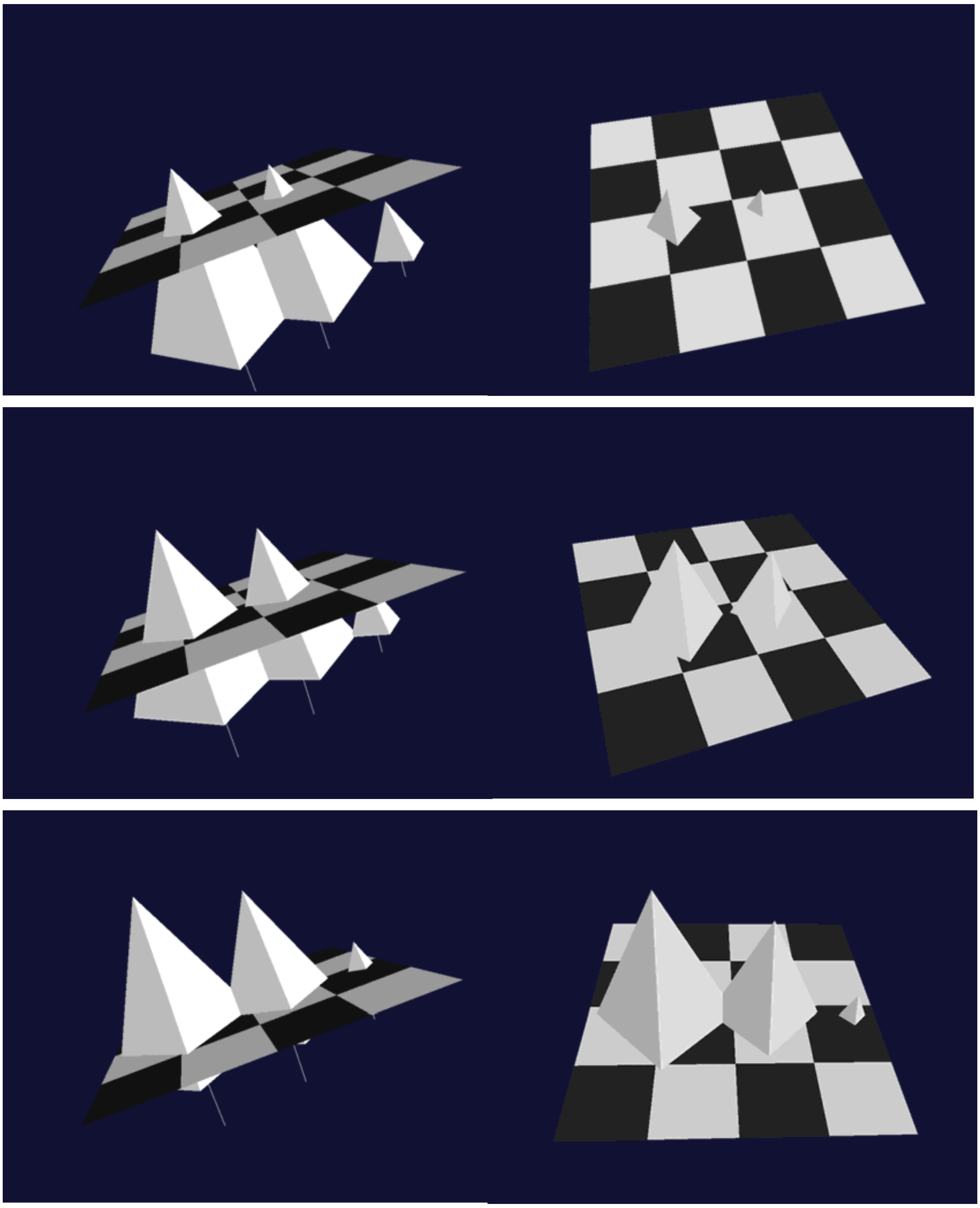

Figure 5.5 A threshold at the peak of a simulated canopy (top) isolates the largest crowns but ignores small crowns. A compromise between crown size and separation (centre) ignores small crowns and a low threshold (bottom) captures all of the crowns but merges large crowns together.

To isolate each local maximum the 3-dimensional representation of the HyMap data needs to be 'sliced' using 'top hat' segmentation. The aim is to choose a threshold that effectively separates the larger crowns but also includes smaller or dimly lit crowns. To help visualise this problem Figure 5.5 provides three images that represent 'slicing' a 3D representation of the filtered image at the peak of the crowns (top) at the middle (centre), and at the base (bottom). The chequered plane represents a user defined threshold. Setting the threshold too high will only get the tips of the largest and brightest crowns (top). If the threshold is applied at too low a level (bottom), discontinuities are bridged between crowns, and two or more crowns are merged together. A threshold in the middle presents a compromise between crown size and separation (centre) but some small crowns are still excluded.

The transition from missing out on too many crowns and merging too many crowns together is too variable to be iteratively selected across a scene consistently. HCDA therefore combines a conservative binary threshold that captures the most crowns with a watershed algorithm.

5.3.5 Watershed segmentation

The watershed segmentation algorithm used is a function in the IDL library. It considers the gradient magnitude of an image as a topographic surface. Pixels having the highest gradient magnitude intensities correspond to watershed lines which represents the region boundaries. Put simply, it turns the 3D filtered greyscale image upside down and, treating each crown as a sink-hole, and simulates 'filling them each with water'.

The 'water' placed on any pixel enclosed by a common watershed line flows downhill to a common local intensity minima. When applied to the filtered greyscale image of tree crowns (Figure 5.3) the simulation fills each crown tip with water, and a line is drawn around the base of each crown.

In summary, HCDA combines a conservative binary threshold that captures the most crowns with a watershed algorithm. The base threshold image represents applying a threshold at the base of each tree (local maxima filtering). This effectively separates crowns from shadow, but merges too many crowns. To combat this, the layer is combined with the watershed results (local minima) using a binary mask (Figure 5.6). The result is a series of crown scale objects that are individually coded and that can be easily converted into a vector-based polygon feature of tree crowns. The source code for applying the watershed algorithm in IDL is available in the Appendix.

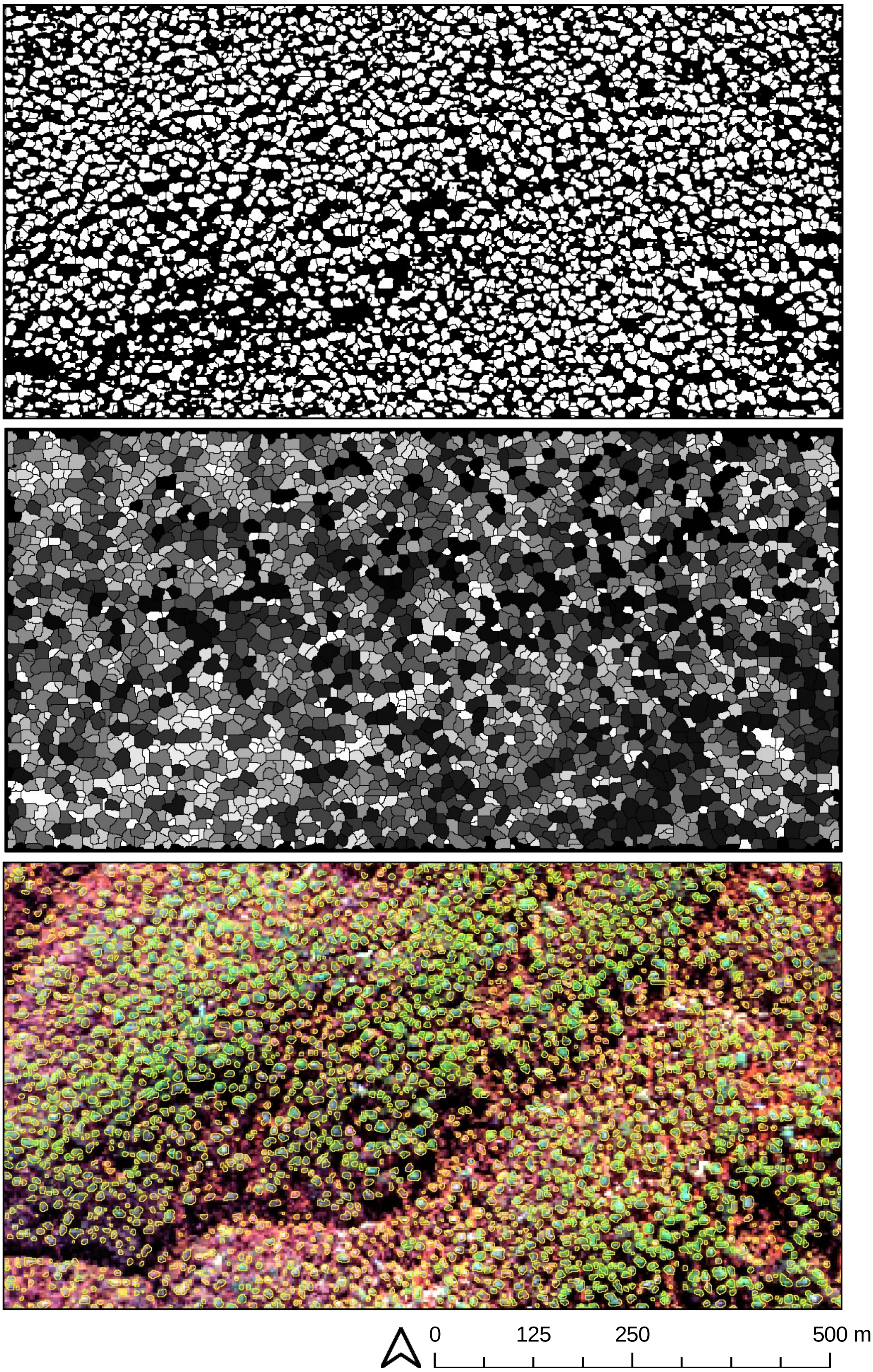

Figure 5.6 Combining the base threshold of the filtered greyscale image (top) and a watershed algorithm (middle) creates crown objects (bottom).

To create a map, crown-objects in clearings or on roads need to be removed using a mask. To create a mask Band 12 was thresholded to remove clearing (dn = 255) (clearing) and shadow (dn = 0). The results are visually satisfying and capture the variation in tree crown volume without being affected by the mesic understorey or dark shadows. Figure 5.7 represents 3D tree crowns derived from greyscale HyMap data with a histogram stretched 3-band HyMap composite overlaid. The mesic understorey appears rusty or orange, blackbutt trees appear green and Sydney bluegums appear light blue or grey.

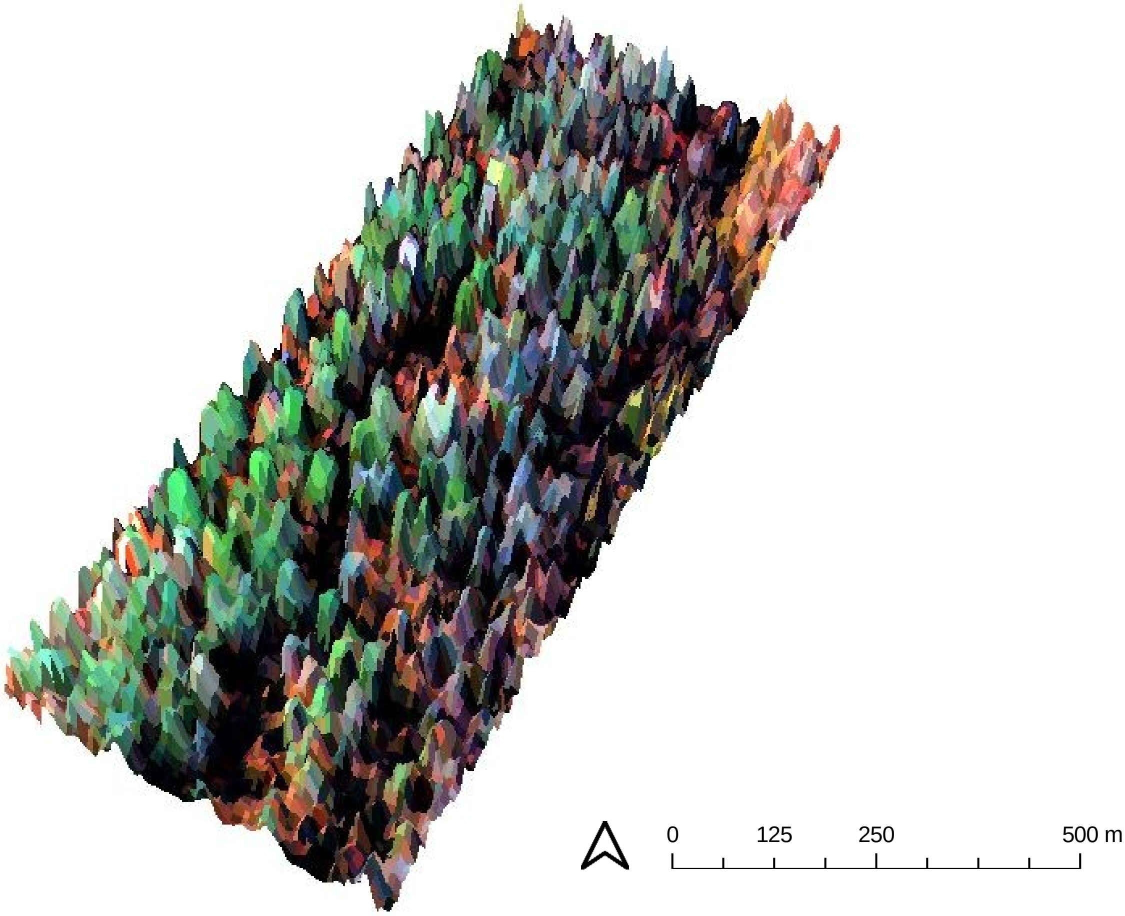

Figure 5.7 Tree crowns derived from greyscale HyMap data with a histogram stretched 3-band HyMap composite overlaid.

5.4 Accuracy assessment of the HyMap Crown Delineation Algorithm

The HCDA delineate individual large crowns across the study area. However, uncertainty exists as to whether the algorithm will divide the imagery into too many objects (where large crowns could be separated into numerous branches) or too few objects (where small crowns are grouped into a patch) (Figure 5.8).

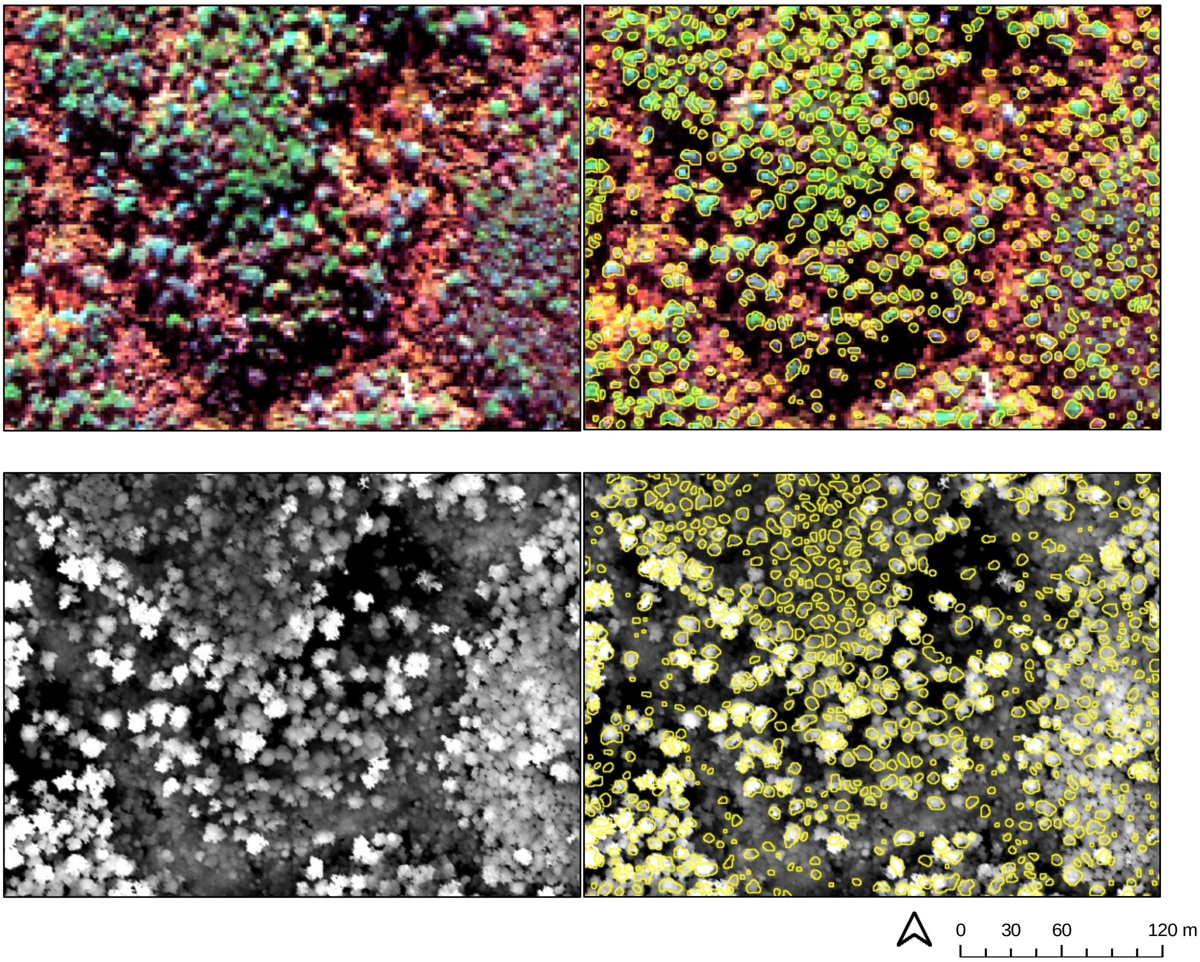

Figure 5.8 Crown objects created with the HCDA overlaid on HyMap (top) and lidar data (bottom).

To provide a measure of accuracy a group of tree crowns were delineated manually with on-screen digitisation. The reference lidar data were used to locate a representative sample of large emergent crowns in a matrix of small homogenous crowns. 161 segmentation reference crowns were manually delineated in a without reference to HDCA results or the site data. The extent of the segmentation reference set was used to select the intersecting HDCA crown-objects from the study wide data set. A comparison of the number of crown-objects created, their relative area and perimeter was then made (see Figure 5.9). These are global segmentation quality statistics.

To provide local segmentation quality statistics several metrics were calculated. The proportion of the area of manual crown-objects that overlap HDCA crown-objects was calculated, as well as the proportion of HDCA area to manual crown-object area (both of which are topological accuracy metrics). Finally, the distance between HDCA crown-object centroid and the nearest manual crown-object centroid was calculated (geometric accuracy metric). For more detail on assessing segmentation quality and a definition of terms please refer to Chapter 9.

5.5 Results

Detailed view comparing manually delineated crown-objects (hollow black) and HDCA crown-objects (solid green). The centroid of each HDCA crown-object (point) is also displayed.

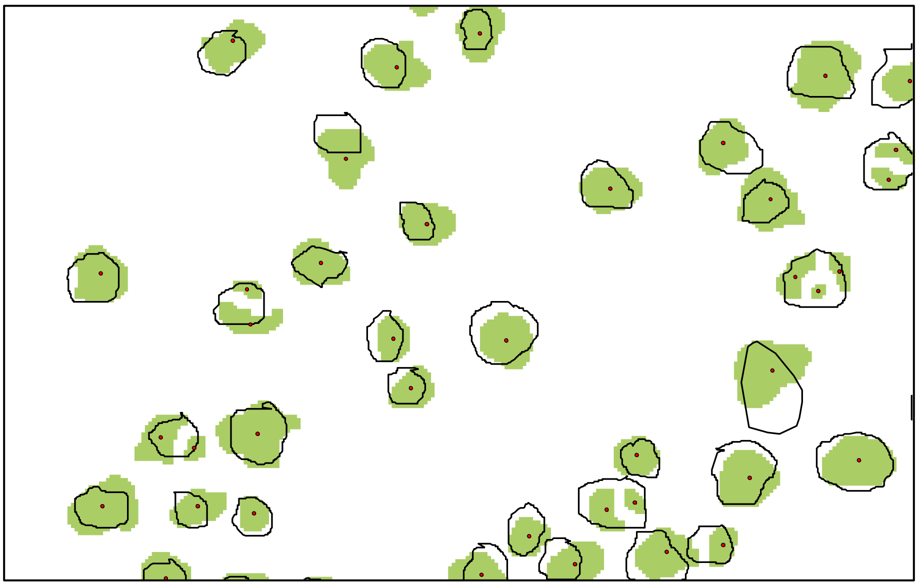

Figure 5.9 Accuracy assessment incorporated 'polygon in polygon' statistics and average distance between centres of gravity.

The HyMap Crown Delineation Algorithm over-segmented crowns when compared to manual segmentation (194 HDCA vs. 161 manual). This was due to some crowns being split into two or three large branches. The maximum size of the crowns was very similar (ratio of 0.94), as was the mean areas (ratio of 0.87) (Table 5.2). The mean distance between centroids of manually derived and HDCA crowns were only 3.62m which is approximately a single pixel (Table 5.3).

Table 5.2 Global statistics of HyMap Crown Delineation Algorithm accuracy assessment for 161 manually delineated crown-objects.

Global Stats	Manual Area	HDCA Area	Ratio	Manual Perimeter	HDCA Perimeter	Perimeter Ratio
Count	161	194	1.20	161	194	1.20
Minimum (m^2)	33	14	0.42	25	16	0.63
Maximum (m^2)	332	313	0.94	77	92	1.19
Sum (m^2)	22348	23316	1.04	7896	9636	1.22
Mean (m^2)	139	120	0.87	49	50	1.01
Standard Deviation	62	67	1.07	11	16	1.47

Table 5.3 HyMap Crown Delineation Algorithm accuracy measures for 161 manually delineated crown-objects.

	Area of manual crown-objects that overlap HDCA crown-objects	Proportion of HDCA area to manual crown-object area	Distance between HDCA crown-object centroid and the nearest manual crown-object centroid
Count:	194	1.20	194
Minimum	0	0.00	0.23 m
Maximum	248.53 m^2	0.75	13.97 m
Mean	78.38 m^2	0.56	3.63 m
Total	15205.70 m^2	0.68	703.47 m

Sources of error include over-segmentation (splitting a crown into multiple objects), under-segmentation (including multiple crowns in a single crown-object), spatial error (miss-registration between lidar and HyMap), and user error (errors in manual digitisation). The quantitative assessment of segmentation was performed in an area of the Jilliby site that features a mesic understory and large emergent crowns. The HCDA would not be as successful in the open, dry forest to the east of the site where background reflectance is higher and crowns are smaller, with less dense foliage.

5.6 Conclusions

A spatial resolution of 3.5m is barely adequate for precise crown scale delineation. The HDCA was used to delineate individual tree crowns by using a filtering and watershed approach. The HCDA was able to replicate tree crowns identified with the visual interpretation of lidar/HyMap data. The HCDA over-segmented crowns when compared to manual segmentation (194 HDCA vs. 161 manual). The mean distance between centroids of manually derived and the crowns that were delineated by the HDCA crowns were only 3.62m, which is approximately a single pixel.

Culvenor (2002) notes that individual tree crown delineation from remotely sensed imagery is not a realistic expectation — even for human interpreters — in structurally complex forests. The spatial resolution was a clear limitation for delineating small crowns. Tree delineation results derived from HCDA in complex forest types are still useful. A representative sample of crowns, even as a stand or crown component, may prove to be adequate for precise classification of vegetation type when averaged. The ultimate aim of the research is to create an accurate community scale map.

Chapter 6

Multi-scale, object-based classification of vegetation communities using hyperspectral imagery

Chapter 4 established that the mean spectral response extracted from tree crown objects could be classified using Machine Learning Algorithms (MLAs). Chapter 5 introduced the HyMap Crown Delineation Algorithm (HDCA), a new method for automatically delineating tree crowns using HyMap data. HDCA is based on local maxima filtering and local minima watershed segmentation. The combination of MLAs and HDCA provides an opportunity to map tree crown species across the landscape. However, maps used operationally for the management of native vegetation are provided at the community scale. Therefore, a method is required to cluster individual tree crown objects into meaningful community type objects.

The countless combinations of species diversity, structure, and other attributes in a stand of mixed species makes consistent generalisation of vegetation units across a landscape difficult. The spectral response of a vegetation type polygon will not be consistent across the landscape but delineating transitions between vegetation types is achievable. The difference between open dry forest and tall moist forest, for example, can be discerned based on structure, spectral response or landscape position. Classification of vegetation communities with multi-scale, object-based hyperspectral data is not well developed in the literature.

A variety of segmentation algorithms are capable of community scale segmentation of vegetation extent. An existing community delineation algorithm, Size Constrained Region Merging (SCRM) (Castilla, 2004), was chosen to produce community scale polygons for the Jilliby site. The aim of this chapter is to combine crown scale segmentation (HCDA) and community scale segmentation (SCRM) to create a multi-scale object-based classification of vegetation type.

6.1 Background

There are several categories of forest type mapping that use satellite or aerial remote sensing data. Landcover mapping is frequently at the regional or continental scale and predicts the distribution of broad classes such as woody vegetation and water (Jung et al., 2006). Statistical models of vegetation type incorporate ancillary spatial layers and survey data as well as remotely sensed data and can predict vegetation type at regional scales (Elith et al., 2006, Elith et al., 2008, Ferrier and Guisan, 2006, Ferrier et al., 2007). Fine scale classification of vegetation attributes like community type are usually restricted to small areas (Johansen et al., 2007, Kokaly et al., 2003, Laliberte et al., 2004), as are studies relying on hyperspectral imagery (Okin et al., 2001, Underwood et al., 2003).

Operational vegetation mapping at a fine scale is most commonly a product of visual interpretation of stereo imagery (Bell and Driscoll, 2006, Benson, 1994, Gellie, 2005, Keith and Bedward, 1999). Aerial photographic interpretation is time-consuming, particularly if high spatial or temporal detail is required, (Gellie, 2005, Leckie et al., 2005a) and not always repeatable. Visually interpretation of vegetation relies on recognising discrete patches of vegetation based on structure, condition and type. The argument traditionally has been that variables such as texture, spatial relationships and diffuse boundaries, cannot be incorporated into a digital analysis (Emery et al., 2001).

Image segmentation, referred to here as segmentation, is the process of partitioning a digital image into multiple segments or patches. Segmentation algorithms can be used for a range of image processing tasks such as edge detection and feature extraction. Working with image objects instead of pixels is widely recognised as beneficial (Burnett and Blaschke, 2003, Hay et al., 2003, Laliberte et al., 2004) and allows for the use of textural and semantic information in classification.

In ecological studies, image segmentation is especially appropriate (Laliberte et al., 2007) landscapes consist of mosaics of discrete patches. Segmentation at multiple scales can offer insights into ecological processes (Burnett and Blaschke, 2003, Hay et al., 2002, Laliberte et al., 2007). Delineating vegetation patterns with segmentation has the potential to increase the efficiency of a mapping at a regional scale by making it faster and more repeatable.

6.1.1 Vegetation patch scale segmentation

This thesis features three commercially available segmentation algorithms for patch and community scale segmentation: Definiens Developer 7, the ENVI 4.5 Feature Extraction Module, and Size Constrained Region Merging (Table 6.1). Definiens Developer uses a region-growing algorithm that is limited by heterogeneity, Size Constrained Region Merging uses a spatial filter to create blobs and then aggregates them based on similarity, and ENVI Feature Extraction Module uses an edge detection process followed by region-merging.

Table 6.1 An overview of the segmentation software and the technology behind the algorithms.

Segmentation Software	*Definiens Developer 7*	*Size Constrained Region Merging* (SCRM)	ENVI *Feature Extraction Module*
Provider	Definiens	ITT Visual Solutions	Exelis
Reference	(Baatz and Schäpe, 2000)	(Castilla, 2004)	(Exelis, 2008)
Method	Fractal net evolution approach, globally uniform region growing.	Adaptive filter, watershed, aggregated by dissimilarity.	Edge detection, Lambda-Schedule region merging.
Size Limit	No.	Yes. (2 megapixel images for freeware)	No.

Adjusting the scale parameter can lead to 'over-segmentation' or 'under-segmentation' (Delves et al., 1992). Over-segmentation occurs where the algorithm generates too many objects. An extreme case is where every tree crown has been delineated, or even every pixel. The visual clutter created renders the results impracticable for use as a management tool or for deriving broad vegetation classes. Under-segmentation occurs when too few objects are generated. The extreme case of under-segmentation is where multiple vegetation classes are combined into one super-object that has no practical meaning for natural resource management.

6.1.2 Size Constrained Region Merging (SCRM)

Size Constrained Region Merging (SCRM) was developed by Castilla (2004) and has been tested and refined with the aid of others (Castilla, 2004, Castilla et al., 2008, Hay et al., 2005). It is an adaptive-filter/watershed based region-merging approach to segmentation and the source code is written in IDL.

In order to use SCRM, four parameters must be specified: (a) the desired mean size of output polygons, (b) the minimum size required for polygons, or minimum mapping unit, (c) the maximum allowed size, and (d) the minimum distance between vertices in the vector layer, or minimum vertex interval (MVI). MVI is an indication of the positional accuracy of boundaries and is internally used to define the working IGFOV, that is, spatial resolution (Castilla et al., 2008). The larger the specified minimum mapping unit, and maximum allowed size, the more objects can be fused and the larger the objects grow.

SCRM uses the radiometric distance between region centroids (mean value of inner pixels) to merge regions (Castilla, 2004). The SCRM application first filters the input image with Gradient Inverse Weighed Edge Preserving Smoothing (GIWEPS) (Castilla, 2004). The process is similar to anisotropic filtering or any adaptive filter. The result is equivalent to applying a median filter iteratively several times. Eventually patches appear as like regions merge. The output is an almost piecewise constant image, from which the gradient magnitude is computed. The resulting regions are aggregated iteratively by increasing dissimilarity until they all exceed the size of the minimum mapping unit (Castilla et al., 2008). The labelled image containing the final partition is then converted into a vector layer.

6.1.3 Definiens Developer 7

The multi-resolution segmentation algorithm in *Definiens Developer 7* uses a 'fractal net evolution approach'. The functionality of the FNEA-algorithm is described in detail by Baatz and Schäpe (2000) and Benz et al. (2004). The process is analogous to merging nearby objects that contribute the least to heterogeneity. It uses local mutual best-fit heuristics to find the least heterogeneous merge following the gradient of the best-fit. The algorithm can be applied with pure spectral heterogeneity or with a mix of spectral and form heterogeneity Shi et al. (2005).

Definiens' multi-resolution segmentation is a bottom up region-merging technique starting with one-pixel objects. In numerous subsequent steps, smaller image objects are merged into bigger ones. Through this pair-wise clustering process, the underlying optimization procedure minimizes the heterogeneity of the objects weighted by size of the objects. In each step, the pair of adjacent image objects which results in the smallest growth of the defined heterogeneity is merged. If the smallest growth exceeds the threshold defined by the scale parameter, the process stops (Benz et al., 2004).

The algorithm is novel because it includes the shape of the object in its measurement of heterogeneity. The dissimilarity between adjacent objects is measured as a linear combination of radiometric heterogeneity (expressed by the mean of the variance in each band of pixels within the segment) and form heterogeneity (expressed by the ratio between the actual edge length of a segment, and the edge of a square with the same number of pixels as the segment) (Benz et al., 2004). It allows the user to skew the segmentation in favour of regions with smooth edges and a more or less compact form. The larger the scale parameter, the more objects are allowed to grow, creating larger segments.

The software allows the user to classify image objects at a fine scale and run the segmentation again on a specific class, making it useful for multiple types of data. Castilla (2004) reviewed the ecological grounding from numerous segmentation algorithms and argued that, although multi-resolution segmentation produces aesthetically pleasing results, it has no grounding in ecology. I would argue that with the addition of textural variables and enhancing the spectral between-class variations I am adding a missing component in the ecological grounding of the algorithm.

6.1.4 ENVI Feature Extraction Module

ENVI's Feature Extraction Module first applies a simple edge-based segmentation algorithm that only requires one input parameter (scale level). By suppressing weak edges to different levels, the algorithm can yield multi-scale segmentation results from finer to coarser segmentation. Applied by itself it does not perform well at coarse scales. However, it is designed to generate fine scale objects for the second, more important step of region merging.

The region merging routine employs the Full Lambda-Schedule algorithm created by Robinson et al. (2002). The algorithm iteratively merges adjacent segments based on a combination of spectral and spatial information. Merging proceeds for a pair of adjacent regions if the merging cost is less than a defined threshold lambda value.

Redding et al. (1999) argue that segmentation is in effect a compressed description of the image, and that an unavoidable consequence of compression is the introduction of some error. High quality segmentation is therefore one which has a very efficient description given the associated error. Redding et al. (1999) suggests viewing segmentation as a compromise between the shape of a boundary and the fitting error in the region enclosed by the boundary.

The compromise between fitting error and shape can be presented in a rigorous mathematical framework by expressing the segmentation problem with variational methods using the Mumford-Shah functional (Mumford and Shah, 1985). David Mumford is a Fields Medallist in algebraic geometry and, together with Shah, provided a unifying framework for image segmentation.

The Mumford-Shah functional does not depend on any a priori knowledge of the statistics of the image and has the properties of compactness of the set of approximate solutions, convergence of minimizing sequences of solutions, and smoothness of the locally optimal solutions. The simplified form of the Mumford-Shah functional expresses the segmentation as one of minimizing problem.

$$E(u, K) = \int_{\Omega \setminus K} \|u - g\|^2 dx\, dy + \lambda l(K)$$

Where;
Ω is the domain of the image
K is a set of boundaries with total length l(K)
g is a scalar or vector-valued function of the channels of the image on the domain Ω
u is a piecewise constant approximating scalar or vector-valued function for the image which is constant over each region
λ is the regularization parameter for the boundaries.

If λ is small, then a lot of boundaries are allowed and a fine segmentation results. As λ increases, coarser and coarser segmentations result. The channels g can be derived from texture features so that the method is completely general and can be used to segment textured regions. The channels of the image are simply the pixel intensities in the simplest case of grey level segmentation (Redding et al., 1999).

The contribution of Redding et al. (1999) is the Full Lambda Schedule. Instead of the regions being merged by scanning arbitrarily through the list of regions and selecting the best possible merge from the neighbours of each region at the current λ value, it considers all pairs of neighbouring regions in the image (the full λ-schedule) and chooses the smallest value to merge.

The original motivation for development of the algorithm was the segmentation of synthetic aperture radar (SAR) imagery into homogeneous regions for near real time target detection in military analyst support software. It was designed to reduce the labour intensive process of picking out objects of interest over broad areas. The algorithm has computational complexity of the order of the Fast Fourier Transform, the benchmark for very fast algorithms.

6.2 Multi-scale vegetation mapping

SCRM was selected to perform patch scale segmentation in this chapter. SCRM aims to transform aerial or satellite imagery into a polygon vector layer that resembles the work of a human interpreter who has been given the task of partitioning the image into a specific number of relatively homogeneous polygons without a priori knowledge of the scene (Castilla et al., 2008).

Castilla (2004) recommends that the polygon layer be used as an initial template in the task of an interpreter, who needs to aggregate (and/or correct) pre-delineated regions. In a multi-scale approach to SCRM the patch scale objects can be given attributes based on the classification of individual tree crowns (sub objects), not just similarity between mean object values. The result is that small community scale objects are merged into large community scale objects based on type, maintaining the continuity of manually drawn patterns.

The names of the vegetation units used in the existing Jilliby mapping are based on previous regional classifications (NPWS, 2000) as well as several new variants from (Bell and Driscoll, 2006). They are derived directly from the field data and from a hierarchical classification structure. The crown species are similar in each of the vegetation types in some cases they are only differentiated by the order of dominance or crown cover (see Table 6.2).

Table 6.2 An extract of vegetation classes at three scales derived from field data for the Jilliby State Conservation area. Community types frequently share the same dominant crown species (in a different order of dominance) making them hard to differentiate.

Community	Type	Crown species	Common name
Coastal Wet Gully Forest	Coastal Wet Gully Forest	*Syncarpia glomulifera* *Eucalyptus saligna* *Eucalyptus deanei Eucalyptus acmenioides*	Turpentine Sydney Blue Gum Round-leaved Gum White Mahogany
	Coastal Warm Temperate - Subtropical Rainforest	*Eucalyptus saligna* *Eucalyptus deanei* *Eucalyptus acmenioides* *Syncarpia glomulifera* *Eucalyptus pilularis*	Sydney Blue Gum Round-leaved Gum White Mahogany Turpentine Blackbutt
Coastal Narrabeen Moist Forest	Coastal Narrabeen Bluegum Ridge Forest	*Eucalyptus saligna* *Eucalyptus deanei* *Syncarpia glomulifera* *Eucalyptus acmenioides*	Sydney Blue Gum Round-leaved Gum Turpentine White Mahogany
	Coastal Narrabeen Mahogany - Bluegum Forest	*Eucalyptus umbra* *Syncarpia glomulifera* *Eucalyptus deanei* *Allocasuarina torulosa* *Angophra floribunda* *Eucalyptus acmenioides* *Eucalyptus saligna*	Broad Leaf White Mahogany Turpentine Round-leaved Gum Turpentine Rough Barked Apple White Mahogany Sydney Blue Gum

Source : Bell and Driscoll (2006)

An underlying premise of any segmentation method is that spectral similarity and thematic similarity are synonymous. At an individual tree crown scale this assumption holds true, and image objects can be classified with a degree of accuracy. However, at coarser spatial scales, a large polygon can encompass a variety of thematic attributes.

The spectral value of a large polygon containing a particular forest type may have a significantly different mean spectral value to its neighbour, of the same forest type, for a number of reasons. For example, the extent of canopy cover can vary exposing highly reflective soils. Or the spectral response can be altered by topography. A sheltered gully will produce shadow that can bias the mean value of community scale polygons, making them difficult to classify accurately.

This study features a multi-scale approach to vegetation classification. Crown delineation allows for classification that is based on spectrally and thematically homogenous sub-objects. Higher level objects emulate boundaries between vegetation communities. Community polygons can be labelled based on the proportion of classified sub-objects, or tree crowns. Pixels that represent shadow or exposed soil can be ignored in the classification. The hierarchical structure used to derive vegetation community names (Table 6.2) is emulated in classification of multi-scale remote sensing data (Figure 6.1).

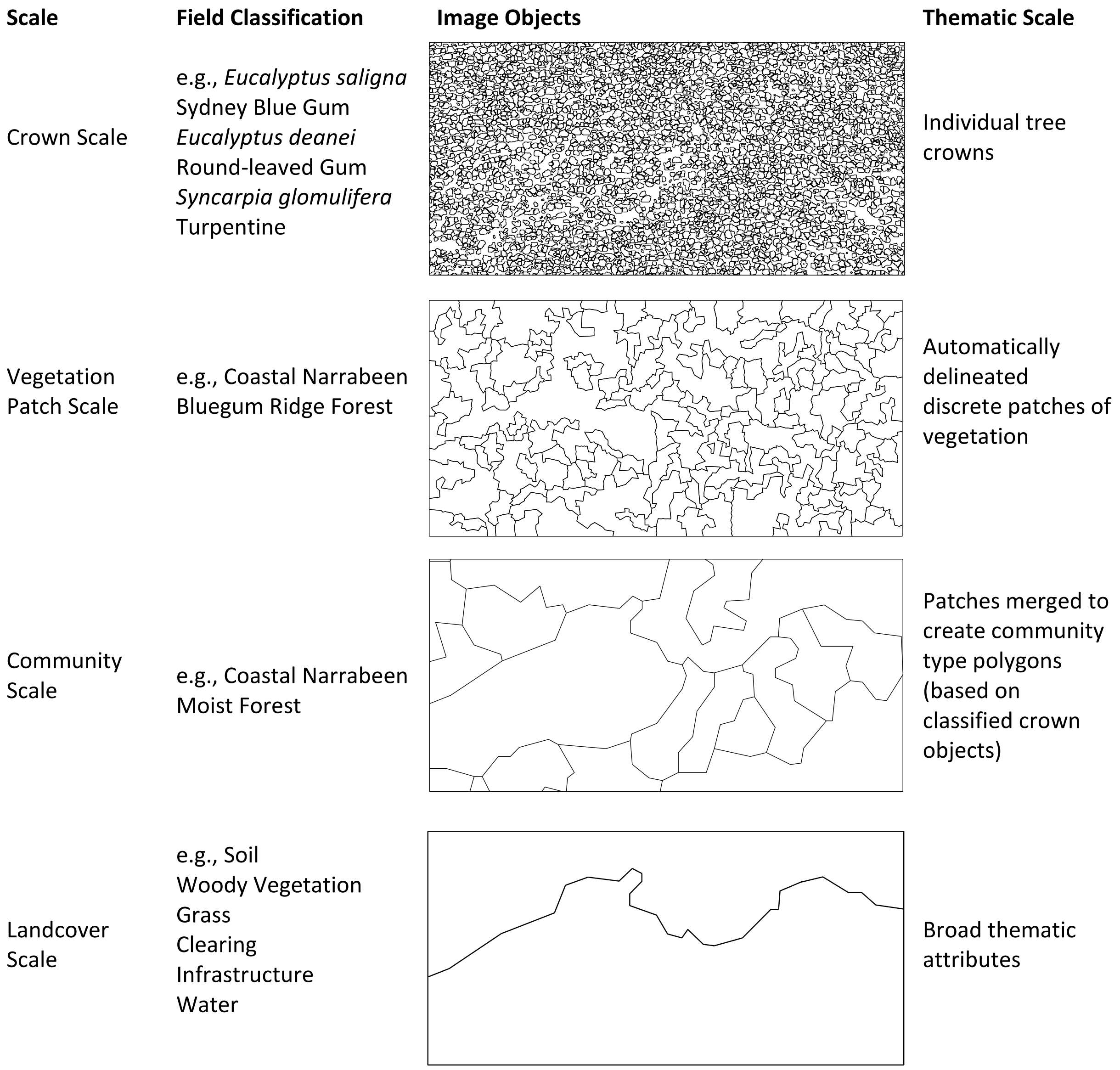

Figure 6.1 From the crown scale to the community scale: the hierarchical classification of field data with examples and the corresponding image object scale.

6.2.1 Crowns scale classification

Chapter 3 described how 889 tree stems were identified in the field. The further each crown is from the surveyed centre of the plot, and the smaller the crown, the less confidence there is in the crown location recorded in the field. Only large crowns that could be positively identified with a high degree of confidence were used as training and test data.

The Jilliby study site is approximately 8 km by 16 km or almost 128,000,000 square metres. The HyMap crown delineation algorithm generated over 330,000 objects with their own unique spectra. The spectral values for all 118 noise free bands were extracted for every crown object across the study site. The spectral response of the crowns isolated using HDCA differed subtly from the spectra from manually delineated crowns due to changes in the shape of the training areas. Therefore, selection of training crowns needed to be repeated. 309 automatically delineated tree crowns were selected because they could be labelled with a species with a high degree of confidence based on site survey data and lidar CHM. Manual crowns were delineated without reference to HDCA results.

Again, a conservative approach was taken to ensure that each crown in the imagery was correctly attributed to the stem surveyed in the field. This cannot be automated because a survey in the field locates the stem of the tree, not necessarily the centre of the crown. Clark et al. (2004) also located crown centroids through visual adjustment of trunk points using a lidar canopy height model. Enough variation was sampled to include 12 separate species in the analysis, 10 of which are of the eucalyptus genera. Table 6.3 provides the acronyms that are used to denote each species for the remainder of the chapter.

Table 6.3 The tree species of the crowns selected from the automatically delineated crowns and the attributes of each sample group. Total number of tree crowns sampled was 309. Abbreviations of the common name of tree species are given as three letter codes.

Name	**Code**	**Common Name**	**No. Sampled**
Eucalyptus pilularis	BLB	Blackbutt	86
Eucalyptus acmenioides	WMG	White Mahogany	31
Syncarpia glomulifera	TRP	Turpentine	35
Eucalyptus saligna	BLG	Sydney Blue Gum	36
Eucalyptus punctata	GRG	Grey Gum	16
Eucalyptus deanei	RLG	Round-leaved Gum	29
Eucalyptus microcorys	TAL	Tallowood	15
Eucalyptus agglomerata	BLS	Blue Leaved Stringybark	12
Corymbia maculata	SPG	Spotted Gum	17
Eucalyptus sparsifolia	NLS	Narrow Leaved Stringybark	5
Eucalyptus paniculata	IRB	Grey Iron Bark	12
Eucalyptus umbra	BWM	Broad Leaved White Mahogany	15
Total			**309**

Tree spectral signatures were classified using Logistic Model Trees (Witten and Frank, 2005) (LMT). LMT was used in preference to LDA because it improved computational efficiency without a corresponding decrease in performance. The crown scale statistics were calculated using 10-fold cross validation to maximise the number of crowns used in training. Twelve separate species were included in the analysis. The results of the model based on training data were stored as a rule base and run on the spectra of all crown objects.

All crowns intersecting the study site were delineated and classified. Up to four dominant species were independently recorded by an ecologist in the field (Chapter 3). These are compared for each field site to see if the dominant species predicted from the crowns scale modelling matched the dominant species recorded by the ecologist.

6.2.2 Vegetation community scale classification

The over-segmented community scale objects derived using Size Constrained Region (SCRM) merging could then be classified based on dominant crown species, area/abundance scores or any one of a variety of ecological classification regimes based on dominant canopy species (Figure 6.2).

For each patch scale polygon the frequency of classified crown scale objects determined the vegetation type. The objects were then labelled using names from the existing classification scheme (Bell and Driscoll, 2006). Crown scale objects with unique 'crownID' are given a common 'scrmID' for each community polygon. The frequency of each tree species recorded is calculated and populates new fields at the community type scale where 'scrmID' is the join field.

crownID	crownAREA	Tree	scrmID
6575	9	WMG	20365
7010	125	BLB	20365
7224	33	WMG	20365
7225	175	WMG	20365
7261	34	BLB	20365
7310	9	WMG	20365
7402	18	BLB	20365
7564	128	BLB	20365
7565	42	BLB	20365
7650	78	BLB	20365
7709	225	WMG	20365
7825	128	BLB	20365
7967	152	BLB	20365
8025	71	BLB	20365
8026	62	BLB	20365
8523	90	BLB	20365
8524	128	WMG	20365
8550	78	TAL	20365
8578	23	BLB	20365
8796	34	BLB	20365
9856	37	BLB	20365
10114	66	BLB	20365
10424	15	BLB	20365
10774	66	BLB	20365

scrmID	Frequency	Tree
20365	17	BLB
20365	1	TAL
20365	6	WMG

Figure 6.2 An example of the spatial join of crown scale objects and community scale objects.

The results at a plot scale are based on LMT of the mean spectral response of each of 309 tree crowns that were located inside and outside the plots. The three dominant tree crowns were calculated based on frequency (raw count) and the proportionate area of each species was also calculated. Tree crowns that overlapped the edge of each plot were included. Dominant tree crowns were categorised independently (Stone et al., 2008). Dominant species were listed in emergent, over-storey and upper-mid storey strata.

6.2.3 Image pre-processing

The use of reflectance data without any pre-processing for segmentation can lead to the creation of image objects with artefacts sensor geometry, sun angle and topography. This is particularly relevant in the highly variable topography of the Jilliby Catchment area. Dark objects are generated in hill shade and gullies; light objects are created on brightly lit ridges, with analogous patches adding noise in between. The patterns delineated by SCRM using reflectance data had more in common with a hill shade image of a digital elevation model than it did with vegetation type.

Therefore, pre-processing was applied to remove artefacts and correct for topographic effects. HyMap's spectral bands are powerful for classification but much of the data were redundant for community scale segmentation. A data reduction algorithm was applied.

The Linear discriminant analysis (LDA) algorithm (used in Section 4.5.4) ranked the contribution of each of the 118 available noise-free bands to the classification of species type. 16 bands were selected in a step-wise fashion, most of which are in the Short Wave Infrared (SWIR). Each band was pre-processed Figure 6.3 by only taking the DNs that represented woody vegetation and saturation stretched (see Section 5.3.1).

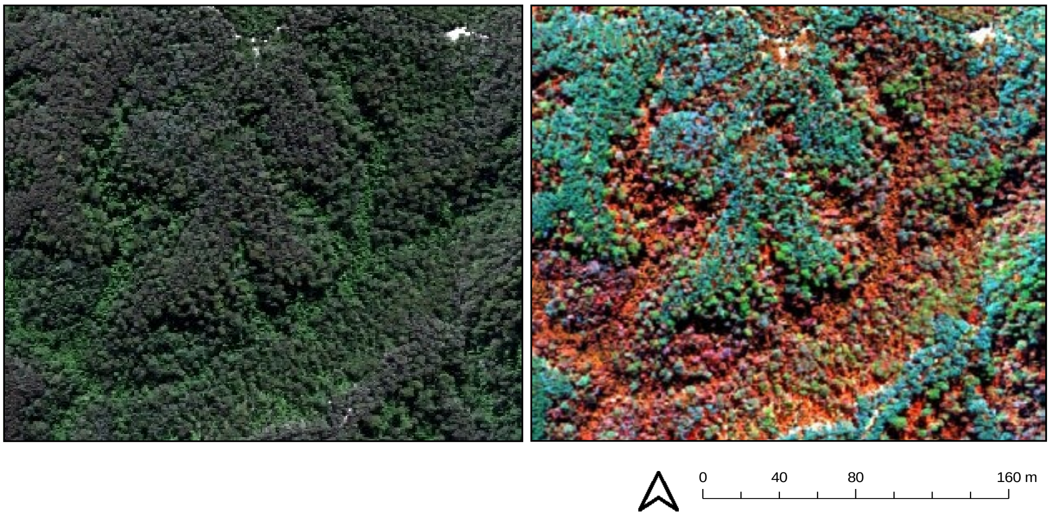

Figure 6.3 Pre-processing aims to enhance between class variance of vegetation using hyperspectral data. Unmodified imagery (left) and a histogram, saturation stretch of LDA selected bands(right).

6.3 Results

6.3.1 Image pre-processing and patch scale objects

After pre-processing the spatial patterns visible in the processed imagery were consistent with the existing community mapping based on visual interpretation. The spectral response of an image object is more likely to be representative of the target material if the object boundary is the same size or smaller than the target (Nagendra, 2001). So, over-segmentation (partitioning of the data into smaller units than required) at the patch scale increases the chance the image object will be a homogenous sample of a single thematic unit (vegetation patch). Castilla (2004) similarly recommends that the polygon layer be used as an initial template in the task of an interpreter, who needs to aggregate and correct.

6.3.2 Crown scale classification

Classification accuracy is lower than the results presented in Chapter 4 which used different samples of crowns. There is also a greater variety of tree species in the modelling and infrequently sampled species were used.

Eucalyptus paniculata (IRB) and *Eucalyptus sparsifolia* (NLS) were mistaken for other species. This is due to the difficulty discriminating different eucalypt species and the lower average tree height, which leads to occlusion and shadow effects. Of the 309 tree crowns available for classification (Table 6.4) 62% were correctly classified. Table 6.5 gives accuracy per class (species).

Table 6.4 Crown scale classification statistics using LMT

Classification Measure	**Count**	**Value**
Correctly Classified Instances	192	0.62
Incorrectly Classified Instances	117	0.38
Kappa statistic		0.56
Total Number of Instances		309

Table 6.5 Detailed crown scale classification statistics from LMT by class

Class	TP	FP
BLB	0.86	0.80
BLG	0.53	0.56
BWM	0.60	0.47
BLS	0.92	0.79
GRG	0.27	0.29
IRB	0.00	0.00
NLS	0.00	0.00
RLG	0.28	0.38
SPG	0.67	0.55
TAL	0.27	0.50
TRP	0.86	0.81
WMG	0.68	0.53

The True Positive (TP) rate is the proportion of examples which were classified as class x, among all examples which truly have class x, i.e. how much part of the class was captured (Table 6.5). The False Positive (FP) rate is the proportion of examples which were classified as class x, but belong to a different class. The confusion matrix illustrates errors of commission and omission (Table 6.6).

Table 6.6 A confusion matrix of twelve crown species based on LMT.

a	b	c	d	e	f	g	h	i	j	k	l	classified	as	
74	4	1	0	0	0	0	2	2	0	0	3	a	=	**BLB**
6	19	0	1	2	1	1	3	1	0	0	2	b	=	**BLG**
2	0	9	0	1	0	0	0	1	0	0	2	c	=	**BWM**
0	0	0	11	0	0	0	0	1	0	0	0	d	=	**BLS**
0	1	2	0	4	2	0	2	4	0	0	0	e	=	**GRG**
1	1	2	1	0	0	0	2	0	0	1	4	f	=	**IRB**
0	0	3	1	0	0	0	0	0	0	1	0	g	=	**NLS**
4	5	1	0	2	1	0	8	1	0	2	5	h	=	**RLG**
1	1	0	0	3	0	1	0	12	0	0	0	i	=	**SPG**
3	0	0	0	1	1	0	2	0	4	3	1	j	=	**TAL**
0	0	0	0	1	0	0	1	0	1	30	2	k	=	**TRP**
2	3	1	0	0	0	0	1	0	3	0	21	l	=	**WMG**

6.3.3 Multi-scale vegetation map of dominant crown species

Figure 6.4 shows a subset of the distribution of tree crowns species delineated with the HCDA and modelled using LMT. In this example the distribution of modelled tree species follows field observations. Blackbutt (BLB) crowns are present on the dry ridge tops. Sydney Bluegums (BLG) appears as large emergent trees on the slopes and amongst White Mahogany in the mesic flats.

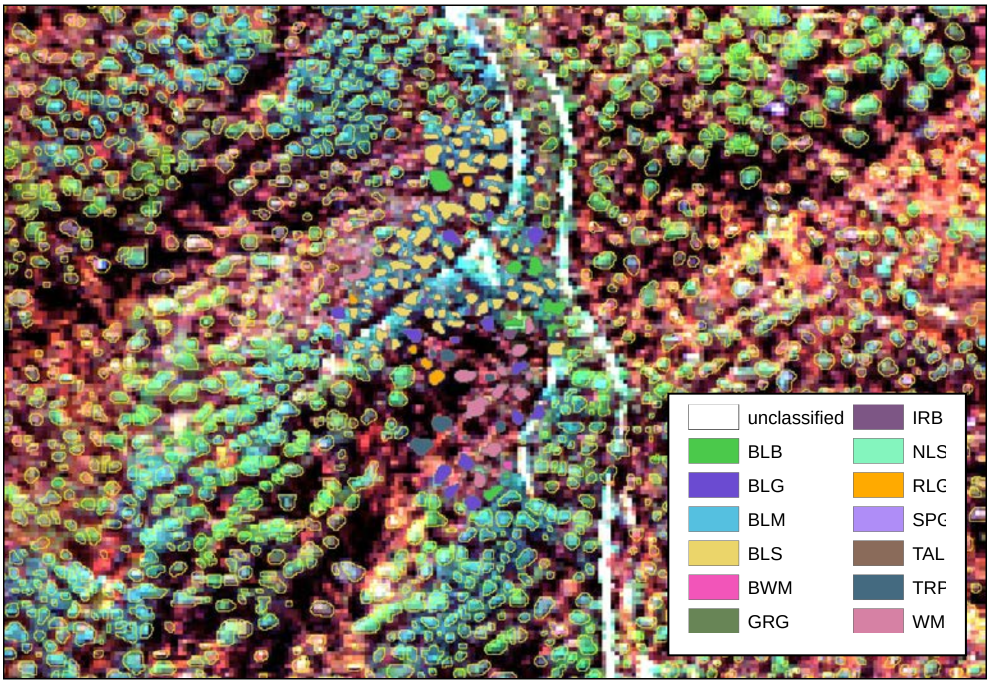

Figure 6.4 A subset of the distribution of crowns species modelled in the Jilliby Catchment area.

The SCRM 'community type' polygons were intentionally over-segmented to account for variation at the fine scale. They were then combined based on the dominant species. This multi-scale data structure allows for interpretation at the familiar community scale, and if more information is needed the user can switch to finer scale for local applications (Figure 6.5).

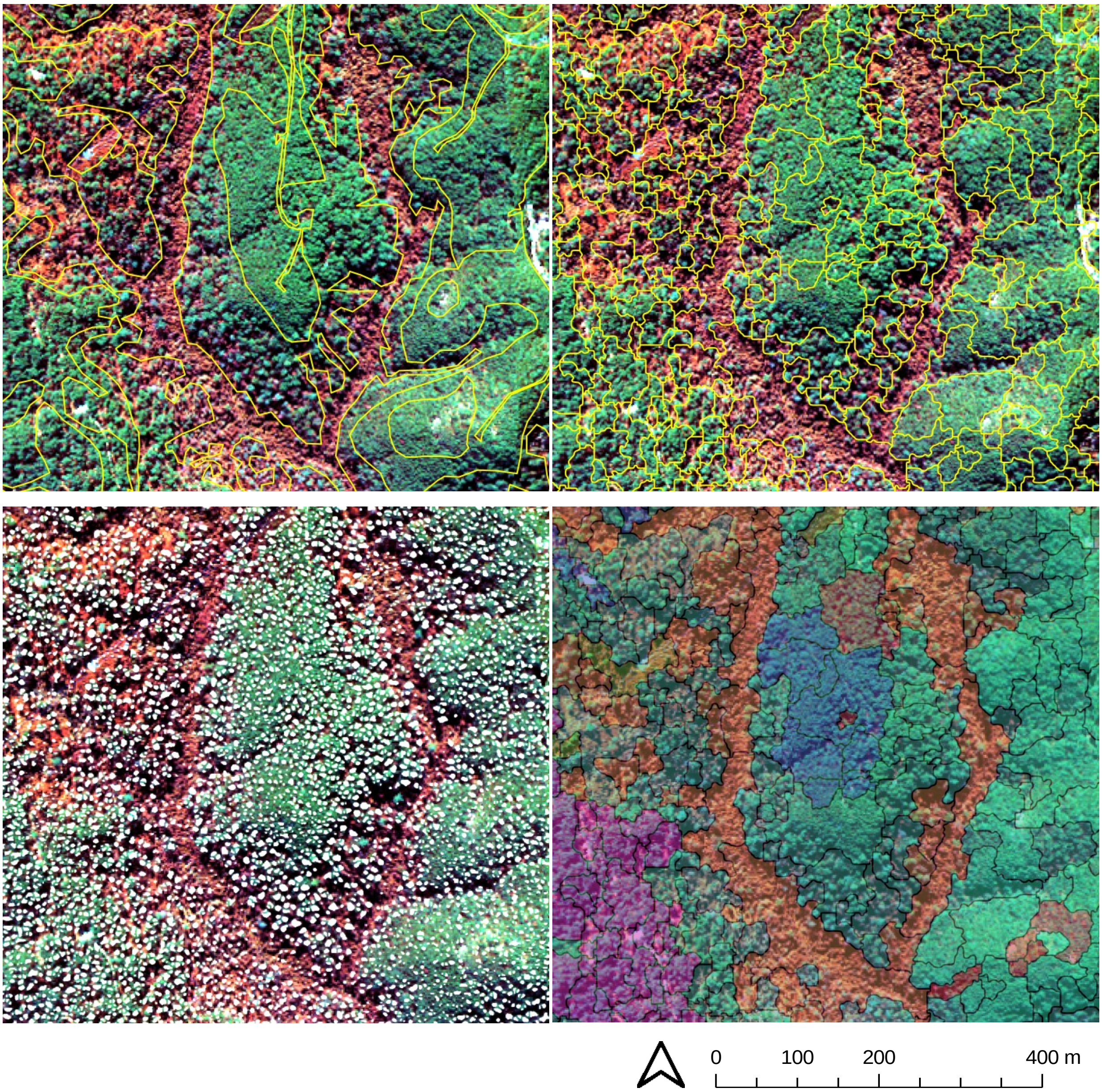

Figure 6.5 Manual air photo interpretation of type (top left) and a patch scale segmentation (SCRM) of vegetation patterns (top right). Tree crowns (bottom left) are classified and species dominance used to classify SCRM patch polygons (bottom right) to create a map of vegetation community.

6.3.4 Plot scale accuracy assessment

Tree crowns delineated using HCDA that intersected with the 20m radius boundary were analysed at 129 plots. Not all sites had three dominant species so the percentage of crowns classified correctly is given (see Table 6.7). Up to four dominant species were recorded independently by an ecologist in the field.

Table 6.7 Plot scale accuracy assessment of crown species in all 20m plots.

Modelling at 20m	Most dominant species modelled as most dominant	Most dominant modelled as present	One of the three most abundant species present	Number of trees crowns modelled
Field assessment of dominant species	47%	63%	87%	0 - 12

One site from each class in the stratification has been represented graphically in Figure 6.6 to Figure 6.9 . The examples from Class 4 and Class 1 show the crown modelling correctly identifying species presence/absence but not predicting the order of dominance. The examples from Class 2 and Class 3 correctly identify crown species presence/absence and predict the order of dominance.

Plot number 4023	
Dominant crown species	Eucalyptus pilularis
	Eucalyptus saligna
Modelled crown species	Eucalyptus saligna
	Eucalyptus pilularis
Presence/absence	present
Order of dominance	no
Presence of species in community polygon in the field	yes
Number of crowns	5

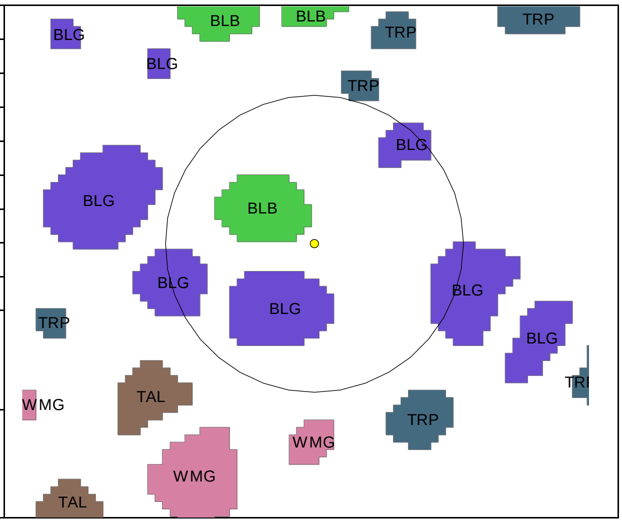

Figure 6.6 Plot number 4023 provides an example from Class 4 of the modelling correctly identifying species presence/absence but not predicting the order of dominance.

Plot Number 3008	
Dominant crown species	Eucalyptus acmenoides
	Syncarpia glomulifera
Modelled crown species	Eucalyptus acmenoides
	Syncarpia glomulifera
	Eucalyptus saligna
Presence/absence	present
Order of dominance	yes
Presence of species in community polygon in the field	yes
Number of crowns	7

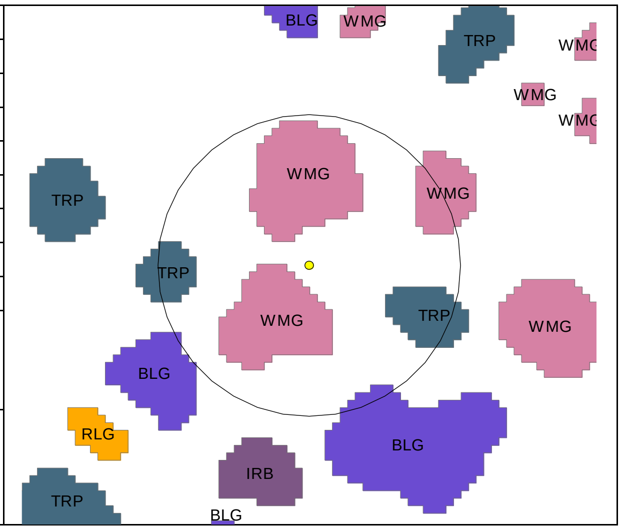

Figure 6.7 Plot number 3008 provides an example in Class 3 of the modelling correctly identifying crown species presence/absence and predicting the order of dominance but included species on the edge of the plot.

Plot Number 2002	
Dominant crown species	Eucalyptus pilularis
	Corymbia maculata
Modelled crown species	Eucalyptus pilularis
	Corymbia maculata
	Eucalyptus microcorys
Presence/absence	present
Order of dominance	yes
Presence of species in community polygon in the field	yes
Number of crowns	8

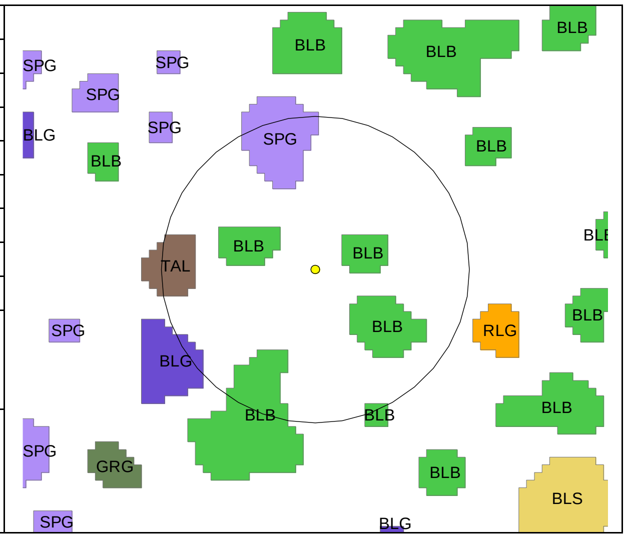

Figure 6.8 Plot number 2002 provides an example in Class 2 of the modelling correctly identifying crown species presence/absence and predicting the order of dominance.

Plot Number 1007	
Dominant crown species	Eucalyptus pilularis
	Eucalyptus punctata
	Eucalyptus deanei
Modelled crown species	Eucalyptus punctata
	Eucalyptus deanei
	Eucalyptus pilularis
Presence/absence	present
Order of dominance	no
Presence of species in community polygon in the field	yes
Number of crowns	7

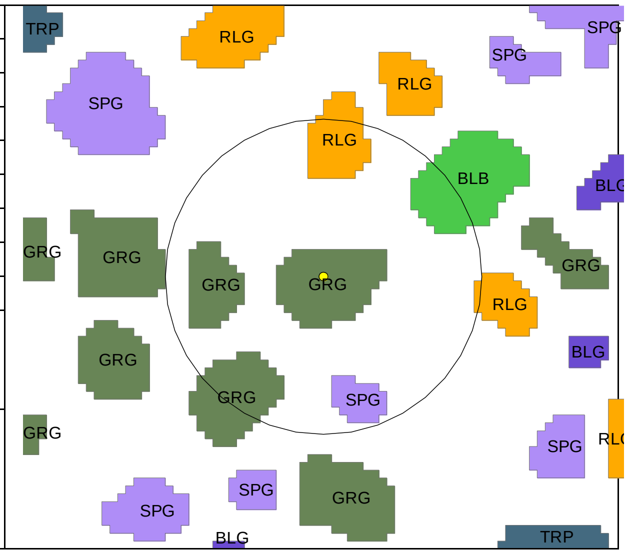

Figure 6.9 Plot number 1007 provides another example in Class 1 of the modelling correctly identifying species presence/absence but not predicting the order of dominance.

6.4 Discussion

For community scale vegetation mapping, a representative sample of large, classified dominant crowns was sufficient for labelling vegetation types. For stands of smaller trees, the crowns overlap at this spatial resolution. However, an algorithm that produces image objects among smaller crowns generated a representative sample of sunlit vegetation. Each object supports spectral extraction, and classification, even if some crowns were not delineated. To increase the geometric accuracy of tree delineation for small tree crowns required higher resolution imagery.

Other products such as vegetation indices, tree height from the lidar canopy height model, and DEM derivatives could also be extracted to improve classification if required. Other studies (Johansen et al., 2007) have shown that texture can be a useful predictor.

As demonstrated in Chapter 4, classification accuracy was over 85% when the eight species with large sample groups were examined. Classification accuracy in Chapter 6 was 62% at a crown scale with twelve unique species using cross validation. The independent validation data set available for this research was a list of dominant species described for each plot, which is typical of the data available to vegetation managers in NSW. At the plot scale the most dominant species was recorded as present 63% of the time. One of the three most abundant species present 87% of the time.

6.5 Conclusion

This chapter demonstrated how a multi-scale, object-based approach can be used for mapping native vegetation with hyperspectral data. An existing community delineation algorithm (SCRM) (Castilla, 2004) was used to produce community scale polygons for the Jilliby site in ENVI. SCRM can be enhanced with the use of high spectral resolution data and pre-processing to create vegetation patch scale polygons. The HyMap Crown Delineation Algorithm (HCDA) introduced in Chapter 5 was applied to the entire study area and a machine learning algorithm was used to classify dominant canopy species (see Chapter 4). It is an appealing approach because there were no assumptions about the consistency of spectral response between different scales. The scale of the sampling (tree crown) equals the scale of the map (crown objects).

Unfortunately, the approach is burdened by the need to survey tree crowns precisely, which is unlikely to gain wide usage at operational scales. The method can also be confounded by complex vegetation structure and composition. The HCDA and the field survey were limited to emergent crowns and as such cannot represent the floristic diversity found in native forest.

Chapter 7

Assessing fuel loads with remote sensing

Chapter 6 dealt with the multi-scale classification of vegetation type using HyMap data. Vegetation structure is critical to the expression of vegetation type and its distribution. The convention for naming vegetation type generally uses floristic associations with species dominance and indicator species combined with the structural formation. So using remote sensing to quantifying structural attributes of vegetation can provide the precursor for mapping type.

The aim of this chapter was to evaluate the operational approaches to surveying vegetation structure, in the form of fuel loads, and determine if the results are correlated with remote sensing variables. Remote sensing data included vegetation indices calculated from HyMap and satellite imagery and lidar variables derived from a canopy height model.

The surface and near surface fuel layer depths and the arrangement of the shrub layer are important for fire hazard assessment in Australia. Since more than one approach to field survey is currently under consideration, both the OFHG and the Vesta methods are used in the study so that its finding may be beneficial for either standard. Due to the potential difficulties of isolating the structure of forest in a particular strata multiple sensors are utilised. The results may also be useful to guide selection of survey methods best suited for future remote sensing studies of fuel loads.

7.1 Background

Imprecise use of certain terms regarding forest fuels often causes confusion and misunderstanding. It is worthwhile to briefly review the main ones (Arroyo et al., 2008). Fuels are defined in terms of the physical characteristics of the live and dead biomass that contribute to the spread, intensity and severity of wildland fire (Andrews and Queen, 2001b) .

Maps of surface fuel characteristics are more common in the conifer and deciduous tree forests of the northern hemisphere. The advantage of working with conifer and deciduous tree species is that surface fuel models can be determined based on overall vegetation structure. For example, Anderson (1982) characterised fuel models for the United States (US) into grasses, brush, timber, and slash. Grass dominated sites are easy to detect with remote sensing and, in the US, ground fires spread much more slowly than surface and crown fires (Mutlu et al., 2008). Closed canopy stands of short-needle or long-needle conifers and hardwoods, or timber, have a relatively predictable litter load and can host crown fires that feed on live and dead foliage (Scott et al., 2001).

Similarly, the main criterion of classification in the European context system is the type and height of the propagation element (grass, shrubs or ground litter). Fuel types are therefore described according to the spatial distribution of these three major groups. Fire behaviour can be modelled by simply taking into account fuel height and density (Riaño et al., 2002) leading to relatively high classification accuracies.

Unfortunately, each fuel type classification is only applicable for similar geographic locations and cannot be used for other environments. Moreover, when foreign systems have been adopted for different locations the results have been poor (Fogarty et al., 1998) for example, discuss the problems of adopting the Canadian system for New Zealand.

Fire models specific to Australian forests have been developed to help predict and understand fire behaviour and fire hazard. They require a variety of input data but generally use meteorological, topographic and fuel conditions as variables (Adams and Simmons, 1999). They are designed to predict the way in which fuel will burn by applying mathematical relationships to describe different aspects of fire (Andrews and Queen, 2001b).

In mild weather conditions, fire behaviour can be predicted to some degree according to the type and structure of the vegetation, the level of moisture in the fuel, the arrangement of the fuel and the terrain. For example, fire burns more readily up a slope, and is less likely to burn in deep, generally moister gully areas (Bushfires, 2002).

The rate of spread of fire in Australian forests is dictated more by surface and near surface fuel layer depths and the continuity and the height of the shrub layers. Fires are likely to spread much faster in forest with a developed shrub layer and fires in litter fuels are likely to spread much faster in areas with a low shrub layer. Previous research has found that the structure and quantity of surface fuel is of greater importance to wildfire behaviour than a measure of fuel load per unit area (Burrows, 2001).

Cheney (1994) established that independent crown fires do not occur in eucalypt forests as the amount of radiative heating from crowns is usually insufficient to maintain combustion in adjacent crowns. Crown fires in eucalypt forests are the result of pre-heating by convection from under-storey fuels. Vertical gaps in the fuel layer can prevent crown fires developing, while horizontal gaps have the ability to ground a crown fire (Chandler, 1983). Isolated, field-based fuel load sampling cannot quantify these variables across the landscape. A major weakness of the models currently in operational use (see Chapter 3) is that they do not take into account the spatial variability of fuel structure.

7.2 Remote sensing of fuel loads

There is a clear management advantage to having an understanding of fuel continuity across the landscape. Current practice is to estimate fuel loads at the landscape level based on expert experience in the local environment. This subjective approach, coupled with relatively poor fire history records outside major conservation reserves, has the potential to lead to non-strategic fuel mitigation strategies (Chafer et al., 2004).

Field sampling is costly, complex and time consuming. Fuel quantities are dynamic and consequently require periodic updating, but this is difficult to achieve due to the nature of data collection methods. New methods to regularly estimate fuel data for large and remote areas are needed to improve fire risk assessment, fire behaviour prediction and fuel management plans.

(Keane et al., 2001) suggested that remote sensing data with a high degree of accuracy may not be essential for fuel assessment, supporting the case for medium resolution satellites. Absolute measurements of fuel quantities are unnecessary as qualitative estimates are more common in the field, for example the (OFHG) (McCarthy et al., 1999) uses a descriptive scale (low, moderate, high, and extreme).

In Australia, the predominance of eucalypt forests makes variation in fuel characteristics more difficult to map. The challenge for remote sensing is to quantify the variation in the structure of an under-storey that can fluctuate independently to changes in canopy structure. An accurate map of tree height, shrub height and grassland parameters that are used in fuel models for US forests will not be a necessarily be transferable. As discussed, the rate of spread of fire in Australian forests is dictated more by surface and near surface fuel layer depths and the continuity and the arrangement of the shrub layer. There is little research in Australia on remote sensing of forest fuel properties, with the notable exception of Brandis and Jacobson (2003) and Chafer et al. (2004). For a summary of national and international studies see Table 7.1.

Remote sensing has the potential to reduce uncertainty when assessing fuel loads and improve our ability to assess spatially and temporally varying fuel characteristics (Chafer et al., 2004). The advantages of remote sensing include: a potential reduction in the need for expensive fieldwork, the assessment of inaccessible areas, the measurement of fuel characteristics at the landscape scale, and the provision of contemporaneous spatial data for active fire fighting.

Table 7.1 Advantages and disadvantages of various remote sensing data for assessing fuel loads.

Sensor	Methodological approach	Advantages	Disadvantages	Reference
Landsat, SPOT, ASTER	Supervised classification of multi-temporal imagery, ancillary data and texture	Broad spatial coverage; availability	Do not allow to see underneath the canopy; limited spatial resolution	(Chuvieco and Congalton, 1989, Chuvieco and Salas, 1996, Francesetti et al., 2006, Guang-xiong et al., 2007, Riano et al., 2003, Van Wagtendonk and Root, 2003, Lasaponara and Lanorte, 2007b, Brandis and Jacobson, 2003, Chafer et al., 2004)
QuickBird, IKONOS	Object-based classification; maximum likelihood classification	Detailed information; adequate for wild urban interface	Mostly limited small to small scale studies; limited spectral resolution	(Arroyo et al., 2008, Giakoumakis et al., 2002, Gitas et al., 2006, Lasaponara and Lanorte, 2007a)
AVIRIS, Hyperion, DAIS7915, HyMap	Spectral mixture analysis; supervised classifications	Can assess fuel features; biophysical components mapping	Spectral resolution; ability to model sub-pixel abundance; greater range of vegetation indices; limited to small scale studies	(Jia et al., 2006, Keramitsoglou et al., 2008, Kotz et al., 2004, Roberts et al., 2003, Thenkabail et al., 2004)
Lidar (airborne small footprint)	Regression analysis; tree segmentation; vertical profiles	Direct height measurement; penetrates canopy	Complicated data processing; lidar specifications inconsistent between acquisitions	(Morsdorf et al., 2004, Riano et al., 2003, Skowronski et al., 2007)
RADAR	Semi-empirical algorithms over SAR imagery	Broad spatial coverage; penetrates the canopy	Uncertainty in the estimation greater than 5 m (satellites) or 1 m (airborne). Insensitive to high biomass levels; not operative on steep slopes	(Saatchi et al., 2007)
Combined methods	ASTER modelling; Lidar + multispectral; Lidar + hyperspectral	Integration of information; broad scale and canopy penetrating	Complicated data processing; expensive	(Falkowski et al., 2006, Mutlu et al., 2008, Poulos et al., 2007, Riano et al., 2003, Varga and Asner, 2008, Lefsky et al., 2002)

Source: Adapted from (Arroyo et al., 2008)

7.2.1 Multi-spectral Medium Spatial Resolution Satellites

Landsat-TM and SPOT-HRV have been widely used to estimate percent canopy cover, canopy height, tree biomass, and tree volume using empirical approaches (De Wulf et al., 1990, Oza et al., 1996, Spanner et al., 1990). Both sensors have seen widespread operational use due to their cost effective coverage, established image processing techniques, and their extensive historical archive. Indices, such as spectral vegetation index, simple ratio, and normalised difference vegetation index (NDVI), obtained from satellite data have been shown to be useful predictors of leaf area index (LAI), biomass, and productivity in grasslands and forests (Jakubauskas, 1996, Paruelo and Lauenroth, 1998, Steininger, 2000, Tieszen et al., 1997). However, recent international studies highlight the need to recalibrate remotely sensed indices for each vegetation type (Calva and Palmeirim, 2004, Foodya et al., 2003, Riaño et al., 2002).

Chafer et al. (2004) used SPOT2 satellite imagery before and after fire to examine the severity and intensity of the Christmas 2001 wildfires in the greater Sydney Basin. In the process they introduced a relatively simple method for estimating fuel load biomass using a combination of the satellite image and rapid field assessment using the OFHG. Chafer et al. (2004) extracted the mean Normalised Difference Vegetation Index (NDVI) for each site and correlations were extrapolated across the landscape using an exponential regression model. Subsequent field validation of the model indicted an overall accuracy of 79% for the six classes developed subjectively for the fuel model. While this would appear to be an acceptable degree of accuracy for the purpose of fuel load assessment for fire management planning, more research is required to determine how transferable this method is to other regions.

In arid and semiarid environments, the use of vegetation indices such as NDVI is rarely effective. Vegetation indices are likely to underestimate live biomass in deserts and are insensitive to non-photosynthetic vegetation (Okin et al., 2001) . Todd and Hoffer (1998) found that NDVI is affected by soil colour and is therefore not always comparable across a homogenous scene. Medium spatial resolution multi-spectral satellite remote sensing relies on superficial observations of reflectance from the canopy, and therefore, it is difficult to identify the understory component of forest fuels. Additionally, reflectance is not directly related to vegetation height, which is a critical variable to discriminate fuel types (Riaño et al., 2002). Since canopy closure is so limiting (Asner, 1998, Spanner et al., 1990) and litter lacks distinguishable spectral properties (Brandis and Jacobson, 2003).

7.2.2 Hyperspectral sensors

Active areas of relevant research into the use of hyperspectral sensors include vegetation structure and dynamics (Miller et al., 1991, Ustin and Trabucco, 2000) and canopy species identification (Bunting and Lucas, 2006). Hyperspectral remote sensing systems can analyse biophysical and chemical information that's directly related to the quality of wildfire fuels, including fuel type, fuel moisture, green live biomass and fuel condition (Roberts et al., 2003) . Roberts & Dennison (2003) used a variation of spectral mixture analysis to map dominant vegetation types with hyperspectral data. A vegetation map produced with this method can be reclassified to standard fuel models such as those presented by (Anderson, 1982), providing species specific fuels information otherwise inaccessible through remote sensing alone.

Roberts et al. (1997) pioneered the spectral characterization of fuel condition (relative proportion of live to dead or senescent fuel) using a temporal sequence of airborne hyperspectral data. Jia et al. (2006) implemented spectral mixture analysis techniques for mapping three major forest components.

Hyperspectral data have also been employed for other fire-related applications, such as mapping fire temperature and land cover in wildland fires (Dennison et al., 2006).

While hyperspectral data has the advantage of being able to contribute to the classification of vegetation species, this is not always relevant; since the same species may present completely different fire propagation rates if, for example, their fuel load or vertical continuity changes (Anderson, 1982).

7.2.3 Lidar

Gould et al. (2007) burnt a series of test plots and varied the stand structure and fuel load of native Australian vegetation between plots. The results suggest a linear correlation may exist between stand height and surface fine fuel load, and between stand height and litter-bed height. The number of samples was too small for a conclusive result but the findings indicate that mature tree stand height may be used as a predictor of the surface fine fuel hazard. This may allow for the use of lidar canopy height models for the prediction of expected surface fine fuel hazard levels over large areas.

Airborne lidar systems have been used for estimating critical parameters for fire behaviour, which have produced better results than aerial photography, airborne hyperspectral sensors (e.g. AVIRIS), and airborne profiling radar (Hyyppä et al., 2000, Hyyppä et al., 2004, Lefsky et al., 2002, Riano et al., 2003, Saatchi et al., 2007).

Lidar remote sensing can provide detailed information about the forest canopy and ground surface Lefsky et al. (2002) that can be useful for mapping fuel hazard. For example, Riano et al. (2003) compared lidar to traditional aerial photography and fieldwork and found that airborne scanning laser systems provide better spatial coverage and could improve the temporal resolution for the update of fuel maps. Morsdorf et al. (2004) has used individual tree crown dimensions derived from lidar for forest fire risk assessment and Mutlu et al. (2008) combined airborne lidar data with multi-spectral satellite data for mapping fuels.

Fine spectral resolution can be more important than high spatial resolution for characterising forest structure in some cases (Thenkabail et al., 2004). Narrow band indices can detect the presence and relative abundance of pigments, water, cellulose and carbon as expressed in the solar-reflected optical spectrum (400 nm to 2500 nm).

The integration or fusion of lidar and optical data has the potential to complement deficiencies of the alternate technology as well as improve the accuracy, and increase the number of applications possible for forest characterisation (Lefsky et al., 2002, Mutlu et al., 2008, Riano et al., 2003). For example, integrating lidar data with delineated tree crown maps (derived from multispectral imagery) can increase the level of accuracy by removing falsely identified tree crowns or identifying the surface canopy types (shrubs, young forest, grassland, etc.).

7.3 Methods

This study quantified forest fuel load and fuel hazard in the field and compares it with remotely sensed variables. Isolating the structure of forest in a particular strata presents difficulties with remote sensing due to occlusion under the canopy. However, this is necessary for assessing fire hazard in Australia as surface fuel and the arrangement of the shrub layer are the main drivers. To quantify the usefulness of a remote sensing approach for the Jilliby area multiple sensors were employed. Data from HyMap, lidar and satellite data from SPOT 5 and Landsat TM were quantitatively compared to field data. Since more than one approach to field survey is currently under consideration, both the OFHG and the Vesta were used in the study so that its finding may be beneficial for either standard. The aim is to provide a guide to which survey methods are best suited for mapping forest fuel using remote sensing and which remote sensing platform would provide the best data to implement these methods.

7.3.1 Fieldwork

Chapter 3 described the sampling design and the comprehensive range of field measurements that were collected at the Jilliby site. In summary, three approaches were taken in the assessment of fire hazard in the field. The first was a rapid visual assessment using the Overall Fuel Hazard Guide (OFHG) (McCarthy et al., 1999) that is used operationally in eastern Australia. The second was an early prototype of the CSIRO's Project Vesta field guide methodology (Vesta), which has since been published by Gould et al. (2007).

Data from the various field-based methods were compared through cross tabulation. The visual scoring methods were based on ordered categories, not continuous variables, and were converted to numeric values for comparison. *Spearman's ρ* was chosen to measure the association between rank orders and test for significant relationships. Spearman's ρ can be used for quantitative variables as well as variables with ordered categories and does not assume normal distribution. Two outliers were removed (Site 1016 and Site 3003) due to their extreme field values.

The OFHG gives a fuel hazard class to each vertical height strata of the fuel layers based on visual assessment and the use of reference photographs from the guide. A table is used to convert these classes (e.g. VH (very high)) to values (e.g. 6 t/ha).

The Vesta method quantifies elevated fuels that comprise of shrubs, heath, bracken, tall grasses, tall sedges and suspended material. The hazard level assigned depends on fuel amount (weight), height, horizontal and vertical continuity, proportion of dead material, thickness of the foliage and twigs, and flammability of the live foliage. Elevated fuels are considered within 2 m of the forest floor and are generally less than 8 m tall.

Destructive fuel loads were sampled at 64 sites in nested 1m by 2m quadrat (see Figure 3.7). Destructive sampling requires the physical removal of fuel samples from the field which are subsequently dried and weighed. Either 8 or 4 quadrats were performed at each site. Fuel collected included all the elevated fuel from inside the 1m by 2m quadrat. All senesced or dead material <6mm in diameter and all green or live material <3mm in diameter was collected, oven dried and weighed. Destructive sampling is considered to be the most accurate fuel load assessment technique at a particular sample point (Bradstock et al., 2002) and all other techniques are calibrated against it.

Upward looking photos were taken at each site and converted to black and white binary images as a coarse measure of canopy cover. Projected Foliage Cover is the proportion of ground that would be shaded if sunshine came from directly overhead (Carnahan, 1981). It has been generally accepted as the measure of foliage quantity in Australia (Walker, 1981) and is used in Specht (1970) vegetation classification system.

7.3.2 Remote sensing

Several remote sensing approaches were used in a data mining exercise to test for correlations with field data. Lidar volume metrics were calculated at multiple heights with an aim of determining the horizontal and vertical arrangement of fuel. Crown image object metrics and moving window texture analysis were trialled to isolate textural contribution to the relationship between fuel load scores and imagery. Digital elevation model derivatives were trialled to examine if there was a relationship between topographic position and fuel load. Each of the variables generated were placed in a database and cross tabulated against field attributes using non-parametric correlation. Results of the vegetation indices and lidar variables are presented here.

OFHG and Vesta metrics were compared to a vegetation indices at 127 sites. Five narrow band vegetation indices selected based on a review of the literature, including NDVI, were calculated using HyMap data (Table 7.2). To create a spatial model of the results, a non-linear (power) function was applied to the Atmospherically Resistant Vegetation Index (ARVI).

Following Chafer et al. (2004) broad band NDVI was calculated using SPOT 5 and Landsat TM data for the area within each plot. Broad band NDVI (Landsat TM 5 data, 2005-08-11) was extracted from each 20m quadrat OFHG plot and a non-linear function was fitted (power). Absolute fuel quantities are unnecessary and qualitative estimates are more common in the field. The OFHG (McCarthy et al., 1999) uses a descriptive scale (low, moderate, high, and extreme). In some cases, remote sensing data with a high degree of accuracy may not be essential. In some cases, the results were then divided into 5 broad classes.

Table 7.2 Vegetation Indices that were applied to the HyMap hyperspectral data

Name and reference	Acronym	Description
Normalized Difference Vegetation Index (Rouse et al., 1973)	NDVI	One of the oldest, most well known, and most frequently used VIs. The combination of its normalized difference formulation and use of the highest absorption and reflectance regions of chlorophyll make it robust over a wide range of conditions. It can, however, saturate in dense vegetation conditions when LAI becomes high.
Simple Ratio Index (Birth and McVey, 1968)	SRI	The SR is the ratio of the highest reflectance; absorption bands of chlorophyll makes it both easy to understand and effective over a wide range of conditions. As with the NDVI, it can saturate in dense vegetation when LAI becomes very high.
Enhanced Vegetation Index (Huete et al., 2002)	EVI	Developed to improve the NDVI by optimizing the vegetation signal in LAI regions by using the blue reflectance to correct for soil background signals and reduce atmospheric influences, including aerosol scattering. This VI is therefore most useful in high LAI regions, where the NDVI may saturate.
Atmospherically Resistant Vegetation Index (Kaufman and Tanre, 1992)	ARVI	An enhancement to the NDVI that is relatively resistant to atmospheric factors (for example, aerosol). It uses the reflectance in blue to correct the red reflectance for atmospheric scattering. It is most useful in regions of high atmospheric aerosol content, including tropical regions contaminated by soot from slash-and-burn agriculture.
Red Edge Normalized Difference Vegetation (Sims and Gamon, 2002) (Gitelson et al., 1996)	RENDI	This VI differs from the NDVI by using bands along the red edge, instead of the main absorption and reflectance peaks. The NDVI 705 capitalizes on the sensitivity of the vegetation red edge to small changes in canopy foliage content, gap fraction, and senescence.

The correlation between lidar metrics and surface fuel load was examined following McCarthy (2004). Turner (2007) differenced first return and ground strikes to create a CHM. This layer was used to find maximum canopy height, leaf litter height and mid-storey density at each plot.

7.4 Results

The Jilliby Catchment area has historically been managed for commercial native forestry. Evidence of this can be seen in condition attributes collected at Jilliby. Table 7.3 provides a summary of 'time since fire' and 'evidence of logging' at recorded at each plot. Almost 90% of plots had visible evidence of logging. Only a small proportion (17%) of the plots had been exposed to recent fire.

Table 7.3 Binary condition attributes sampled at a plot scale at Jilliby with a count of those recorded and the proportion of plots affected.

Condition attribute	Sampled	Proportion of Plots effected
Evidence of fire	96	0.74
No evidence of fire	11	0.09
Recent fire	22	0.17
Stumps	113	0.88
No evidence of logging	7	0.05
Recent logging	9	0.07
Old logging	34	0.26

Table 7.4 summarises some of the condition attributes that were not assessed directly with remote sensing instruments. The high number of hollows is further evidence of forestry management with the conservation of over-mature trees as potential habitat. The occurrence of large dead trees that had been ringbarked, or died due to declining canopy condition, could be readily observed lidar.

While rare, the most commonly encountered exotic species was *Lantana camara*. A percent cover score was calculated at each site the species was present. While it is a native species, *Cissus hypoglauca* vine was abundant in many areas, particularly those subject to die back, and covered much of the lower mid-storey and the upper mid-storey in gullies. Fallen logs were ubiquitous as a result of past management and the nature of tall, closed forest.

Table 7.4 Condition attributes from the Vegetation Condition Score component of Biometric with mean values.

Condition attribute	Hollows (count)	Exotic percent cover	Fallen logs (m)	Lantana percent cover	Cissus percent cover
Mean	1.85	0.03	40.3	0.09	0.12
Range	6	0.6	200	1	1
Minimum	0	0	0	0	0
Maximum	6	0.6	200	1	1
Sum	231	4.11	5037	11	15
Count	125	125	125	125	125

Estimates of canopy cover and stand height were made in the field at each plot based on measured tree heights. The linear correlations in Figure 7.2 demonstrate how even simply measured field based variables can be difficult to quantify using remote sensing.

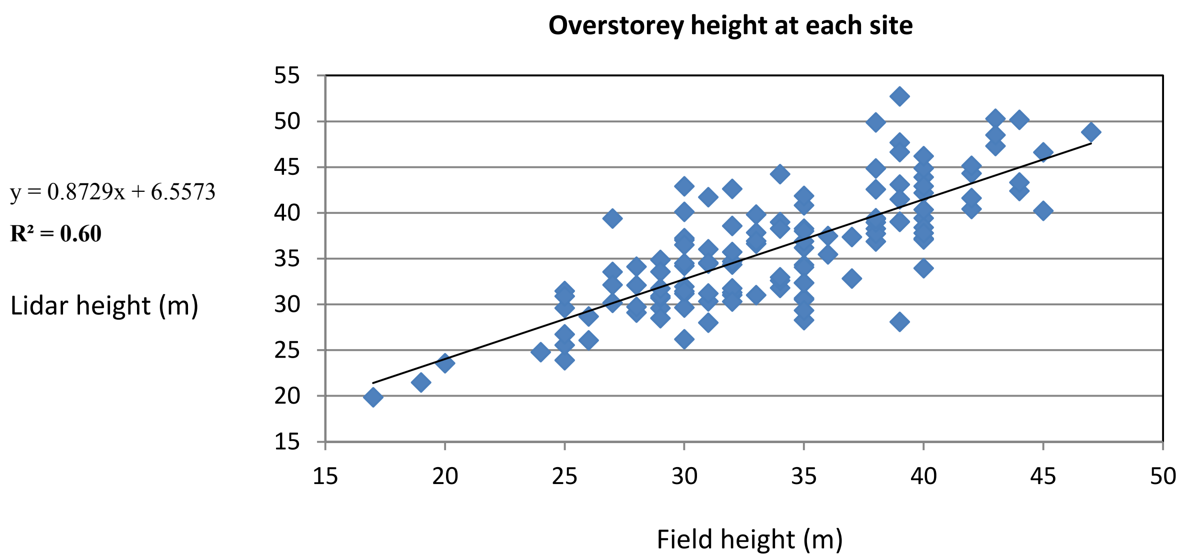

Figure 7.1 Over-storey height measured with a vertex in the field and a field estimate of lower mid-storey percent cover.

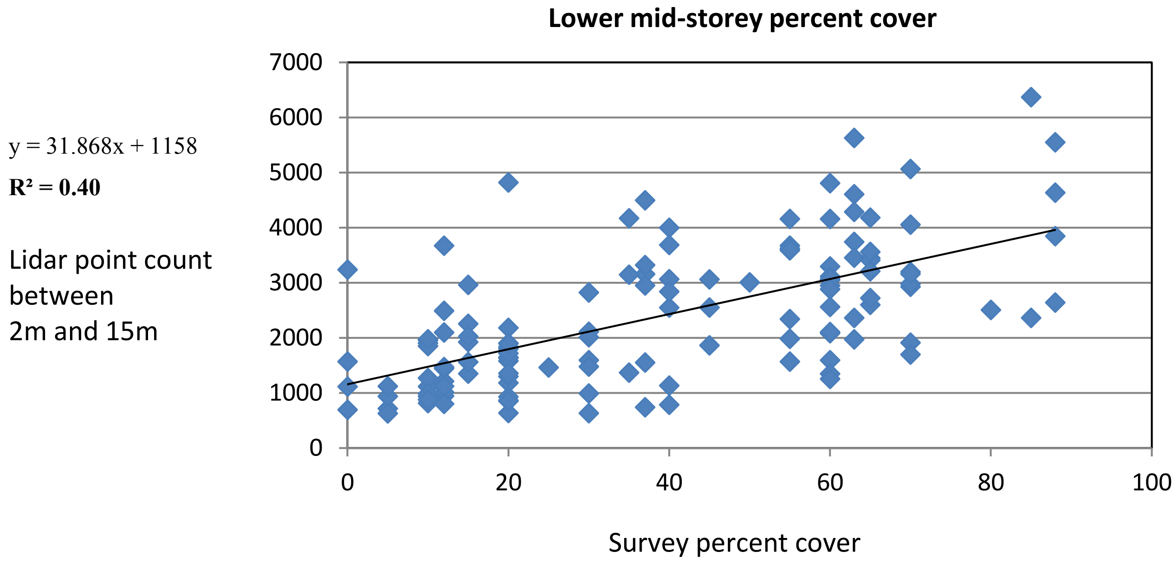

Figure 7.2 Correlation between estimate of mid-storey percent cover and lidar returns registered between 2m and 15m.

7.4.1 Field Results

Details of two plots illustrated below (

Table 7.5) provide an example of how the visual assessment successfully categorises variation in the understorey and can be effective at differentiating sites. However, the black and white reference photographs show a similar amount of shadow cast by the canopy, despite the fuel load being dramatically different. This demonstrates how the over-storey canopy can potentially vary independently of fuel load. Site 3010 featured very high surface fuel loads (litter) but moderate elevated fuel (easy to walk through) and bark hazard that did not add to the overall fuel hazard. By contrast Site 4028 featured very high elevated fuel (difficult to walk through) as well as high surface and bark hazard. Note that in both cases the canopy is closed, obscuring the variation in fuel hazard in the understorey.

Site 3010	Surface	Elevated	Bark	Total
OFHG Class	Very High	Moderate	Moderate	10 t/ha
Fuel Load (t/ha)	10	0	0	

Site 4028	Surface	Elevated	Bark	Total
OFHG Class	High	Very High	High	18 t/ha
Fuel Load (t/ha)	10	6	2	

Table 7.5 Overall Fuel Hazard Guide results with reference photographs.

Table 7.6 demonstrates how the *Vesta* scoring system would rank each of these sites. Note that many of the features of the *Overall Fuel Hazard Guide* are replicated but the result is different. The leaf litter measured was similar between the *Vesta* and *OFHG* scores but the average percent cover score (PCS) gave Site 3010 (with the lowest elevated fuels) a higher *Vesta* total. The closed canopy and high near surface fuels weighted the PCS score.

Site 3010	Height (m)	PCS	FHS	Bark	Litter (mm)	PCS Average	FHS Average	Vesta score
Surface	0.0137	3.50	2.00	1	13.75	12.75	8.00	102
Near Surface	0.1125	3.00	3.00					
Elevated	2.75	1.00	1.00					
Intermediate	15.00	1.75	1.00					
Over-storey	25.00	3.00	1.00					

Site 4028	Height (m)	PCS	FHS	Bark	Litter (mm)	PCS Average	FHS Average	Vesta score
Surface	0.013	1.75	2.00	1.25	13	9.25	9.25	86
Near Surface	0.10	1.75	1.75					
Elevated	4.00	4.00	4.00					
Intermediate	3.50	0.25	0.25					
Over-storey	27.50	1.50	1.25					

Table 7.6 Vesta *score distributes scores relatively evenly from each stratification class, indicating that it may be better suited for use with remote sensing variables.*

7.4.2 Comparing the sampling regimes

Only a very weak correlation exists between the *OFHG* scores and the *Vesta* multiplicative score (r=0.259) (Table 7.7). This is not unexpected as the scores are designed to measure different variables. However, surface hazard (Surface) from the *OFHG* score and the surface profile depth (SPDpth) from the *Vesta* score only showed a weak (but significant) correlation for variables that were measured using very similar techniques. The measurement of elevated fuels was more consistent between methods. The elevated fuel hazard score (EFHS) and the elevated fuels as measured by *OFHG* had a correlation coefficient of r=0.62.

Table 7.7 Nonparametric Correlations (Spearman's ρ) between the four OFHG variables and 14 visual Vesta variables measured at 129 plots (statistics for each pair of variables are based on all the cases with valid data for that pair).

Fuel Type	Spearman's ρ		Surface	Elevated	Bark	Total
Score	Vesta	Correlation Coefficient	.210*	.210*	0.143	.259**
		Sig. (2-tailed)	0.017	0.017	0.107	0.003
Surface	Depth	Correlation Coefficient	.308**	-0.089	.180*	.188*
		Sig. (2-tailed)	0	0.318	0.041	0.033
	Percent Cover	Correlation Coefficient	0.154	-.183*	0.111	0.034
		Sig. (2-tailed)	0.082	0.037	0.211	0.705
	Fuel Hazard	Correlation Coefficient	.284**	-0.064	0.117	0.169
		Sig. (2-tailed)	0.001	0.47	0.188	0.056
Near Surface	Height	Correlation Coefficient	-0.04	0.122	-0.133	-0.039
		Sig. (2-tailed)	0.656	0.17	0.132	0.659
	Percent Cover	Correlation Coefficient	0.051	0.088	-0.058	0.072
		Sig. (2-tailed)	0.563	0.32	0.517	0.42
	Fuel Hazard	Correlation Coefficient	0.094	0.115	0.006	0.124
		Sig. (2-tailed)	0.29	0.195	0.943	0.16
Elevated	Height	Correlation Coefficient	0.132	.459**	0.114	.309**
		Sig. (2-tailed)	0.136	0	0.198	0
	Percent Cover	Correlation Coefficient	.220*	.652**	0.141	.458**
		Sig. (2-tailed)	0.012	0	0.111	0
	Fuel Hazard	Correlation Coefficient	0.141	.612**	0.142	.366**
		Sig. (2-tailed)	0.112	0	0.108	0
Intermediate	Height	Correlation Coefficient	.314**	-0.016	0.151	.260**
		Sig. (2-tailed)	0	0.859	0.088	0.003
	Percent Cover	Correlation Coefficient	0.169	-0.155	0.168	0.09
		Sig. (2-tailed)	0.055	0.08	0.058	0.309
	Fuel Hazard	Correlation Coefficient	0.01	-0.143	0.166	-0.016
		Sig. (2-tailed)	0.907	0.107	0.061	0.853
Over-storey	Height	Correlation Coefficient	0.147	0.126	.189*	.199*
		Sig. (2-tailed)	0.097	0.156	0.032	0.023
	Percent Cover	Correlation Coefficient	0.144	-.306**	0.015	-0.034
		Sig. (2-tailed)	0.103	0	0.864	0.705
	Fuel Hazard	Correlation Coefficient	-0.051	-0.077	.284**	-0.031
		Sig. (2-tailed)	0.563	0.386	0.001	0.729
**. Correlation is significant at the 0.01 level (2-tailed). *. Correlation is significant at the 0.05 level (2-tailed).						

Table 7.8 demonstrates how the *OFHG* and *Vesta* methods vary in relation to destructive sampling results. In addition to the methods already introduced, upward looking canopy photos from each plot were converted to black and white 2-bit images and the proportion of dark material was calculated. This is a coarse estimate of foliage projected cover. Site 2034 exhibits a low destructive mean weight with corresponding low scores using the other methods.

Site 2034	Destructive weight	Destructive Standard Deviation	Number of Samples	Canopy Photo	*OFHG*	*Vesta*
	11.8	7.3	8	0.60	12	38

Site 3001	Destructive weight	Destructive Standard Deviation	Number of Samples	Canopy Photo	*OFHG*	*Vesta*
	26.2	16.2	8	0.78	28	123

Site 1025	Destructive weight	Destructive Standard Deviation	Number of Samples	Canopy Photo	*OFHG*	*Vesta*
	18.2	8.2	8	0.40	8	110

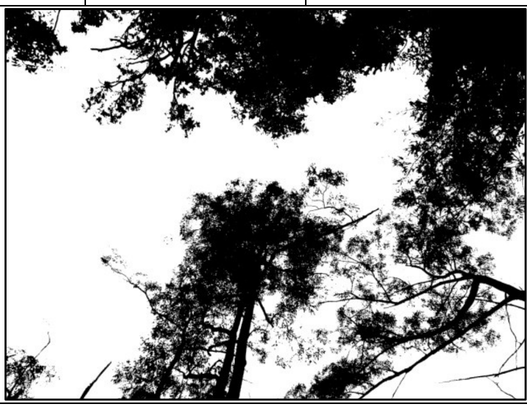

Table 7.8 A comparison of destructive sampling results, the Overall Fuel Hazard Guide, the Vesta method and upward look canopy photographs at three plots.

The result is presented in a comparison of three plots in Figure 7.3 and is representative of the problems faced at the Jilliby site. The impacts of forest condition, canopy health and weed invasion can have a profound effect on remotely sensed variables and those collected in the field. Site 1025 has high cover of exotic species and low canopy cover due to damaged by Bell Miner associated dieback. The histograms give a course indication of the range and mean values recorded. Visual assessment has overestimated the fuel load measured by weighing dried samples (destructive).

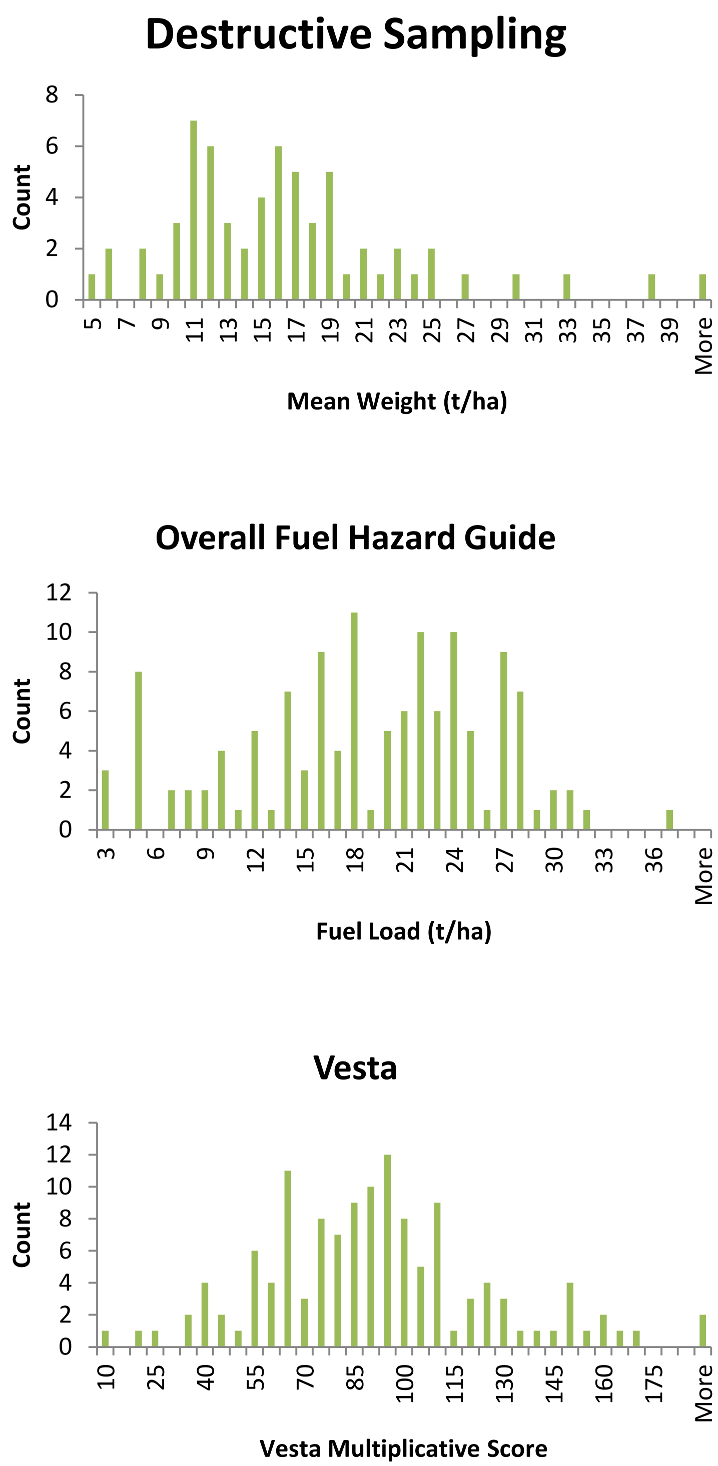

Figure 7.3 Histograms of results of destructive sampling, the Overall Fuel Hazard Guide and Vesta score.

Site 3001 exhibits a relatively high destructive sampling mean weight with corresponding high visual score components. Site 1025 confounds predictions by featuring a relatively high destructive fuel load, a very low OFHG score, a high Vesta score and a low upward looking canopy photo score.

The destructive sampling results were presented as mean weight per unit area in tonnes per hectare for each plot (n=64). The Spearman's ρ correlation coefficients indicated that the surface fuel measurements from the OFHG were weakly correlated with the destructive sampling results but that the total score did not have a statistically significant relationship (Table 7.9). The Vesta score performed better with a correlation coefficient of r=0.508 and with similar relationships in each of the surface profile measurements; Surface Profile Depth (SPDepth), Surface Profile Percent Cover (SPPCS) and Surface Profile Fuel Hazard Score (SPFHS).

Table 7.9 Spearman's ρ correlations coefficients for destructive sampling of available fuel weights, the visual assessments and key remote sensing variables from 64 plots.

Spearman's ρ		Fuel Load Mean
Surface	Correlation Coefficient	.331**
	Sig. (2-tailed)	.008
	N	64
Elevated	Correlation Coefficient	.100
	Sig. (2-tailed)	.434
	N	64
Bark	Correlation Coefficient	.095
	Sig. (2-tailed)	.455
	N	64
Total	Correlation Coefficient	.231
	Sig. (2-tailed)	.067
	N	64
Vesta	Correlation Coefficient	.508**
	Sig. (2-tailed)	.000
	N	64
Surface Depth	Correlation Coefficient	.561**
	Sig. (2-tailed)	.000
	N	64
Surface Percent Cover	Correlation Coefficient	.350**
	Sig. (2-tailed)	.005
	N	64
Surface Fuel Hazard	Correlation Coefficient	.529**
	Sig. (2-tailed)	.000
	N	64
**. Correlation is significant at the 0.01 level (2-tailed). *. Correlation is significant at the 0.05 level (2-tailed).		

After a poor relationship between destructive sampling and the OFHG sampling had been established, further independent resampling was carried out at 33 plots. A two related samples test, the Wilcoxon test (Table 7.10). The Wilcoxon signed-rank test is a non-parametric statistical hypothesis test for the case of two related samples or repeated measurements on a single sample (Wilcoxon, 1945). The test indicates that the sampling results between recorders were only moderately correlated, despite receiving the same training.

Table 7.10 The Wilcoxon signed-rank test comparing the original Overall Fuel Hazard Guide sampling conducted by the Rural Fire Service and additional sampling by the author at identical plot locations.

Test Statistics[b]	
	UNSW OFHG - RFS OFHG
Z	-0.589056832
Asymp. Sig. (2-tailed)	0.55582315

[a]. Based on positive ranks.
[b]. Wilcoxon Signed Ranks Test

Ranks				
		N	Mean Rank	Sum of Ranks
UNSW *OFHG* - RFS *OFHG*	Negative Ranks	18[a]	15.44444	278
	Positive Ranks	13[b]	16.76923	218
	Ties	2[c]		
	Total	33		

[a]. UNSW *OFHG* < RFS *OFHG*
[b]. UNSW *OFHG* > RFS *OFHG*
[c]. UNSW *OFHG* = RFS *OFHG*

7.4.3 The Overall Fuel Hazard Guide

The independent OFHG sampling showed a weak relationship with the VESTA variables collected by Rural Fire Service staff. The elevated fuels are consistent between samplers (indicating the consistency of their estimation) but the surface fuel loads varied substantially between samplers. Rural Fire Service staff did not record continuous integers when assessing surface fuel load, instead assigning one of four classes. The surface fuel load is the major component of the total fuel load at the Jilliby site. Simply reproducing measurements of fuel loads in the field proved to be a challenging task as discovered in other research (Chandler, 1983).

Unfortunately, when all sites are considered, the dynamic range of the OFHG values (the ratio between the smallest and largest possible values) is very small for forest with such complex structure. Elevated fuels add little to the overall fuel hazard as calculated (see Figure 7.5). Any variation in fuel hazard is therefore largely due to the amount of surface fuel, which is largely composed of leaf litter. In more than half of all cases where elevated fuels and bark hazard added to the overall fuel total, they only added the lowest amount, two tonnes per hectare, further lowering the intrinsic range of the fuel measurements (see Figure 7.4). There are four categories in surface fuels, three categories of elevated fuels and three categories of bark hazard at 130 sites in the Jilliby Catchment study area. This offers low dynamic range as a basis for comparison with the continuous variables generated from remote sensing.

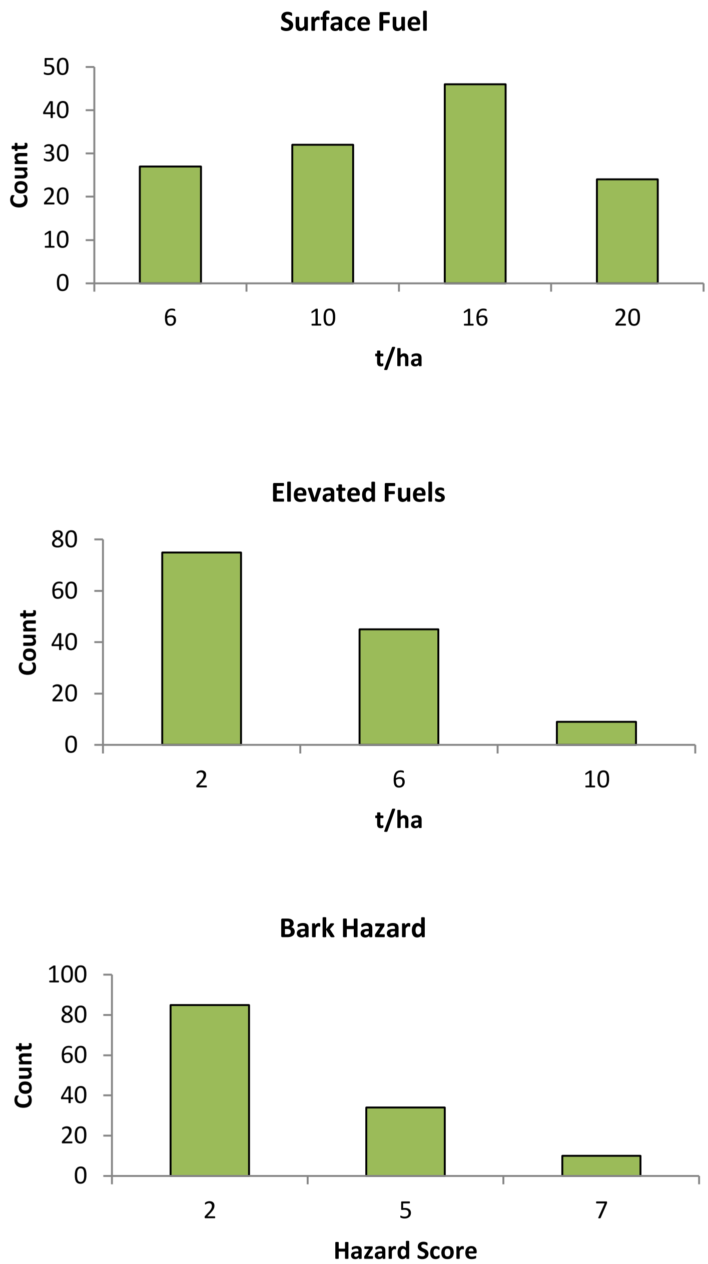

Figure 7.4 Histograms of the results of Overall Fuel Hazard Guide sampling at 130 sites.

These results indicate that any variation in fuel hazard is largely due to the amount of surface fuel, which is largely composed of leaf litter. If leaf litter at the Jilliby site does not offer any distinguishable spectral properties, as seen in other studies (Brandis and Jacobson, 2003), then OFHG may be difficult to quantify with optical remote sensing. Similarly, lidar ground returns cannot differentiate between leaf litter and the ground surface. The Vesta sampling regime has a larger number of structural components representing elevated fuels, and is therefore likely to be better suited to analysis with remote sensing.

Figure 7.5 The surface fuel component clearly dominates the total available fuel load as measured by the Overall Fuel Hazard Guide at the Jilliby Catchment study area.

7.4.4 Vesta prototype

Figure 7.6 demonstrates how the Vesta scoring system would rank each of these sites. Note that many of the features of the Overall Fuel Hazard guide are replicated but the result is different. The leaf litter measured was similar between the Vesta and OFHG scores but the average percent cover score (PCS) gave Site 3010 (with the lowest elevated fuels) a higher Vesta total. The closed canopy and high near surface fuels weighted the PCS score.

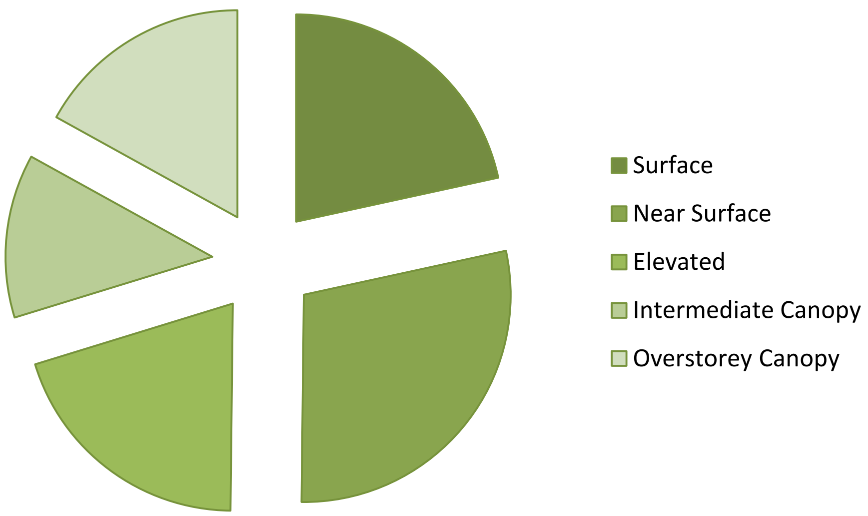

Figure 7.6 No single fuel component clearly dominates the total available fuel hazard score as measured by the Vesta prototype scoring system at the Jilliby Catchment study area.

7.4.5 Remote Sensing Results

There was no relationship between the NDVI values and the field data (see Figure 7.7). Landsat NDVI rose rapidly with the increase in fuel load measured and approached saturation asymptotically as a result of the high aboveground biomass encountered in the field. No relationship was observed between lidar derived maximum height and the OFHG survey data.

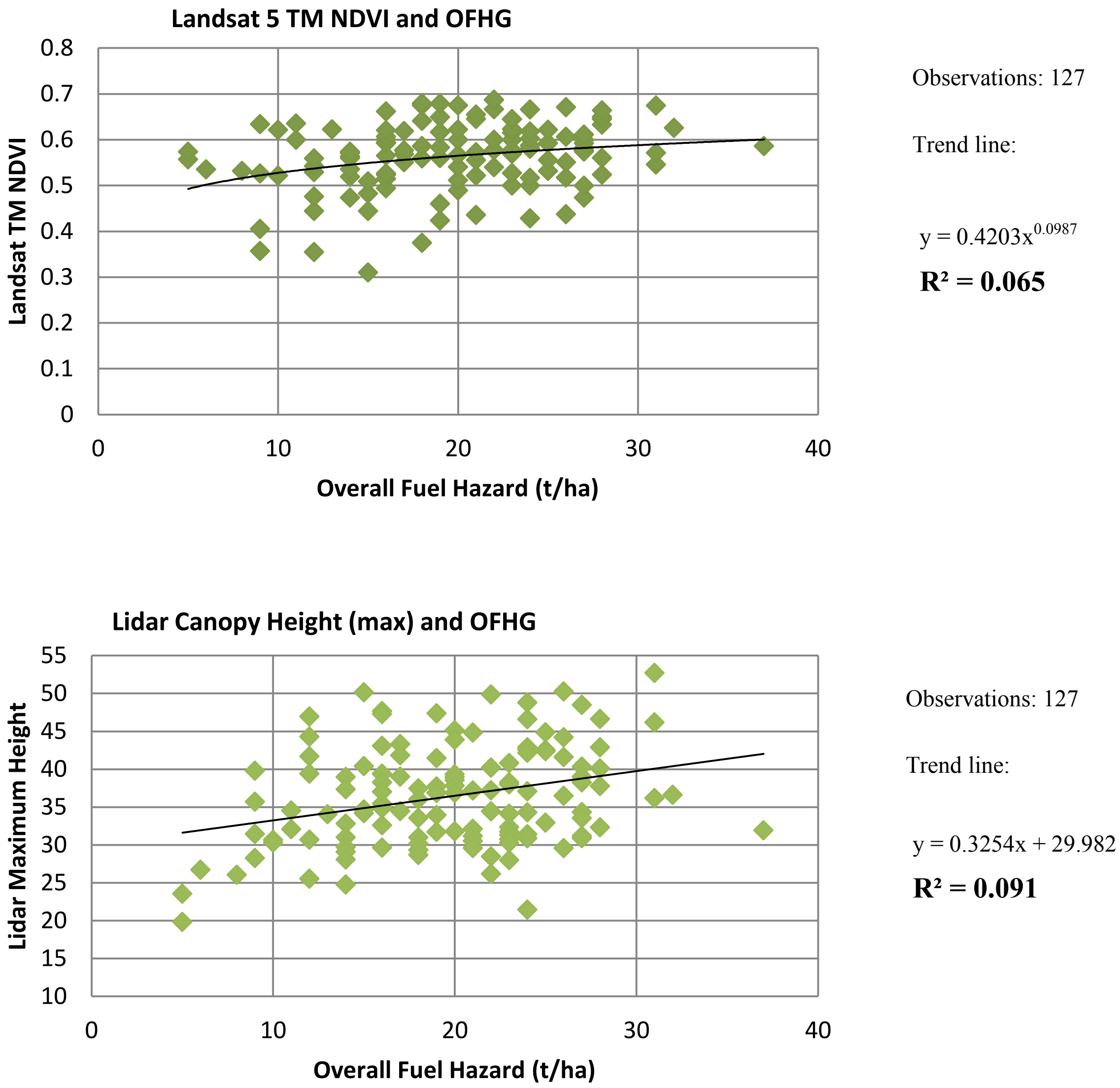

Figure 7.7 No significant relationship exists between OFHG and NDVI or OFHG and maximum height.

Results improved with the use of narrow band vegetation indices. The most successful index was the ARVI (Figure 7.8, right) has more dynamic range (distribution over greater spread of digital numbers) when a histogram of index values in compared is compared to NDVI (Figure 7.8, left). It is correspondingly sensitive to changes in vegetation structure in closed canopy forest.

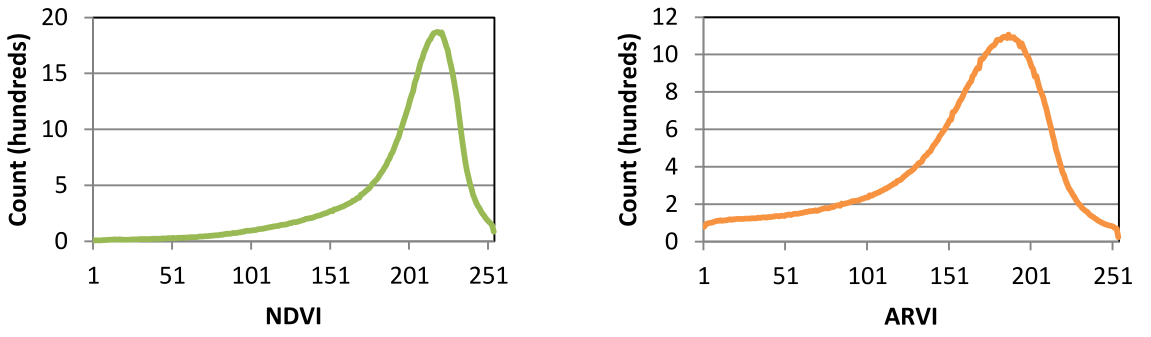

***Normalized Difference Vegetation Index* (NDVI) digital numbers**

***Atmospherically Resistant Vegetation Index* (ARVI) digital Numbers**

Figure 7.8 ARVI (right) has a higher dynamic range (the distribution is over greater spread of digital numbers) when compared to a histogram of NDVI (left). It is correspondingly sensitive to changes in vegetation structure in closed canopy forest.

ARVI is an enhancement of NDVI that is relatively resistant to atmospheric factors (for example, aerosol). It uses the reflectance in blue to correct the red reflectance for atmospheric scattering. The ARVI fuel load model is based on the ARVI. To create the model a non-linear relationship was developed between the field data and the vegetation index based on 33 sites sampled by the author (R^2 = 0.59). When a relationship was developed directly between the Rural Fire Service sampling and the ARVI the power regression had an R^2 value of 0.45 (see Figure 7.9).

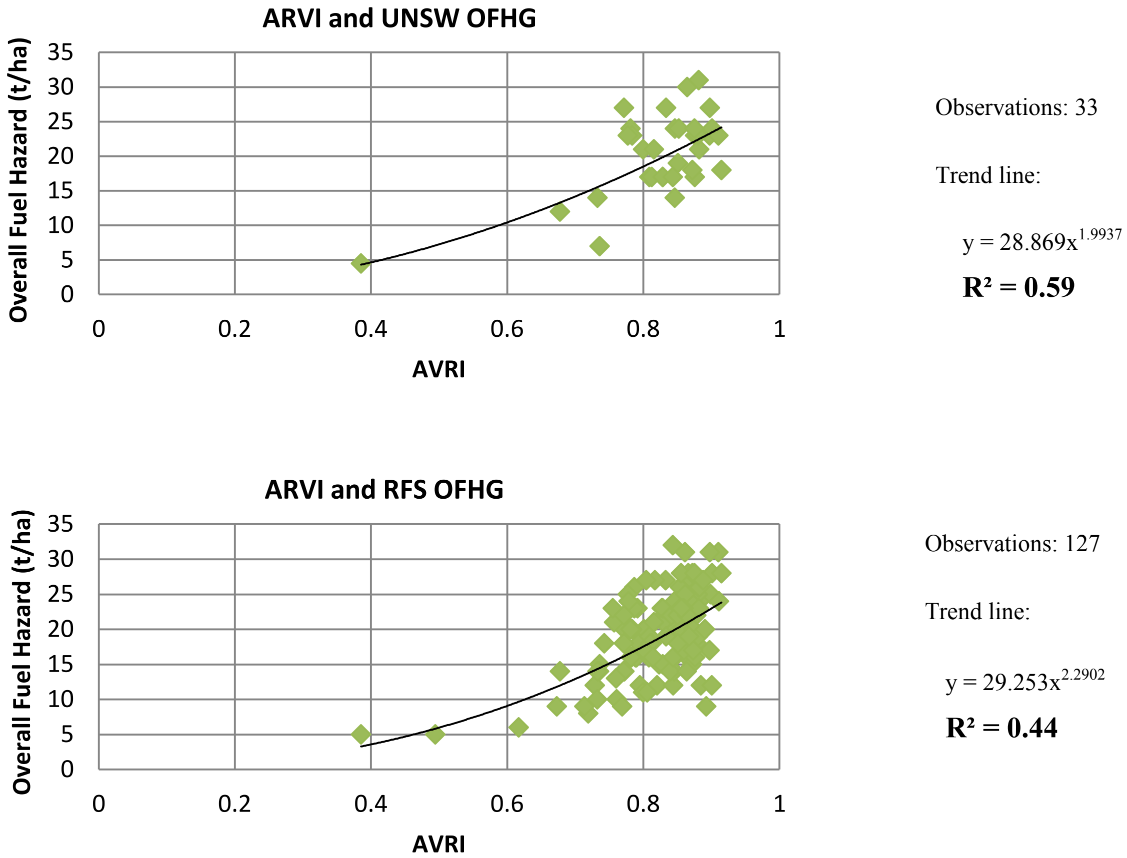

Figure 7.9 Narrow band ARVI in a non-linear regression (power) against the total fuel load measured in the field by the author (n = 33) (top) and the total fuel load measured in the field by the RFS (n = 127) (bottom).

The absolute error when comparing modelled predictions based on HyMap ARVI and OFHG (Figure 7.9) was less than 5 tonnes per hectare in 68% of cases (for 129 sampled plots). However, the dynamic range of the model is low and the majority of plots would be considered to have HIGH to VERY HIGH fuel loads (see Figure 7.10).

The study site has a highly diverse range of forest types driven primarily by aspect and elevation. The spatial dynamics of forest health, shade created from the sun angle and sensor geometry, and inconsistencies in fuel sampling methods all added variation to the remotely sensed data that may not have been sampled in the field. Accordingly, regression equations of all available plots (n=129) generally featured poor correlations or no correlation. Subsequently, a range of stratification methods were employed to find out where the modelling had been successful and where it was breaking down.

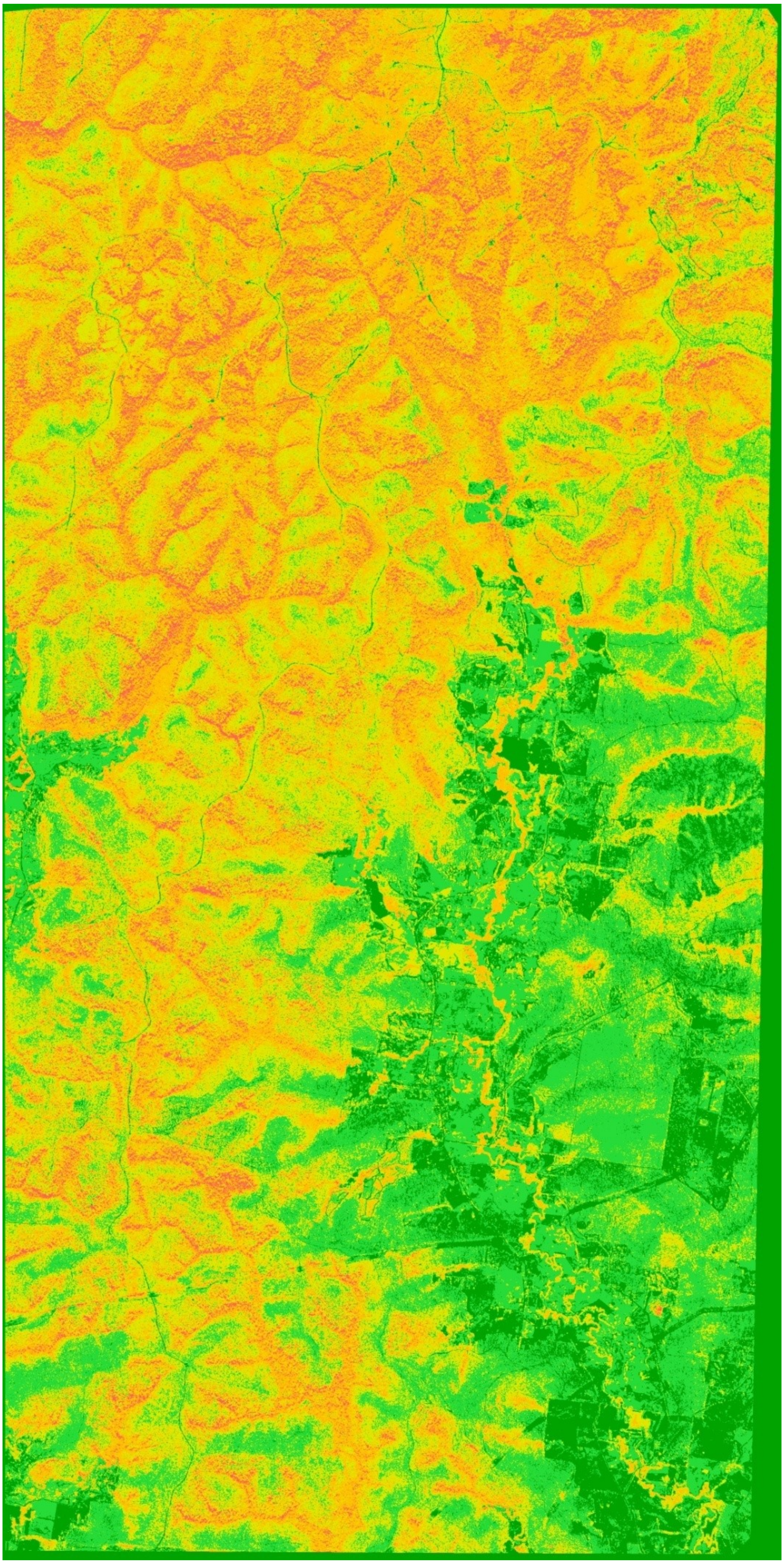

Figure 7.10 HyMap ARVI Fuel Load Model

The ARVI fuel load model is based on the Atmospherically Resistant Vegetation Index (ARVI).

A non-linear relationship was developed between the field data and the vegetation index based on 33 independently sampled sites.

$y = 28.869x1.9937$
$R^2 = 0.59$

The equation was applied to the Atmospherically Resistant Vegetation Index (ARVI) and the results divided into 5 broad classes.

The absolute error when comparing modelled and observed results was less than 5 tonnes per hectare in 68% of cases (for 129 sampled plots).

However, the dynamic range of the model is low and the majority of plots would be considered to have HIGH to VERY HIGH fuel loads.

I used the dominant tree species in each plot to stratify the samples for further analysis, based on the assumption that these species dominate a niche in an environmental gradient that should remain relatively consistent across the study area. The most immediate success was with dry open forest dominated by Grey Gum (*Eucalyptus punctata*), Spotted Gum (*Corymbia maculate*), and Blue Leaf Stringy Bark (*Eucalyptus agglomerata*). Stands of Spotted Gum in particular showed strong linear and non-linear relationships between variables measured in the field (Figure 7.11).

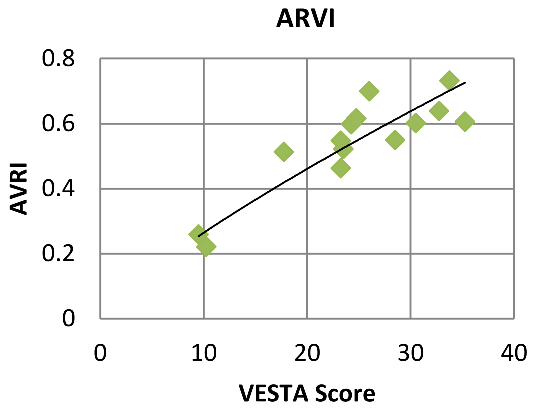

n = 15 $y = 0.0416x^{0.8029}$

R^2 = 0.86

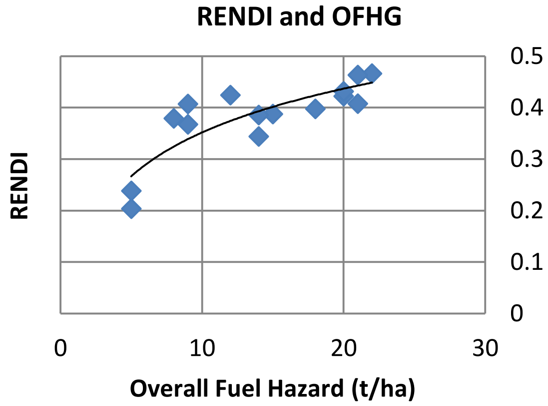

n = 15 $y = 0.1227\ln(x) + 0.0691$

R^2 = 0.72

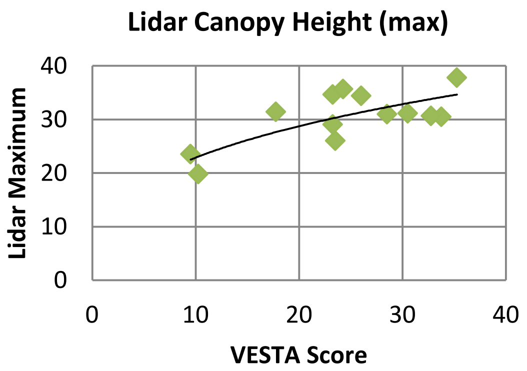

n = 15 $y = 10.712x^{0.3295}$

R^2 = 0.60

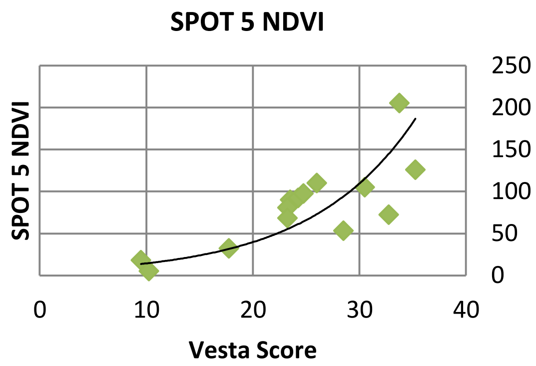

n = 15 $y = 5.1966e^{0.1016x}$

R^2 = 0.72

Figure 7.11 Narrow band and broad band vegetation indices and lidar variables all showed strong correlations with fuel attributes sampled in the field in dry open forest (Spotted Gum).

The RENDI differs from the NDVI by using bands along the red edge, instead of the main absorption and reflectance peaks. The NDVI 705 capitalises on the sensitivity of the vegetation red edge to small changes in canopy foliage content, gap fraction, and senescence, which are all properties readily attributable to fuel hazard. Narrow band vegetation indices, broad band vegetation indices and lidar variables all showed strong correlations with fuel attributes sampled in the field in dry and open forest (Spotted Gum). For the 15 plots sampled, the ARVI regression predicted fuel scores as measured in the field with an R^2 value of 0.86. Unfortunately, too few of these sites were sampled to make definitive conclusions. However, the results strongly suggest that fuel loads can be assessed spatially with remote sensing in dry open forests, as seen in previous research (Chafer et al., 2004, McCarthy, 2004).

7.5 Discussion

The difficulty with interpreting these data, and its relationship with field based fuel hazard scores, is that the all important under-storey is subject to occlusion. The complexity of the forest types in the Jilliby Catchment area have made mapping fuel loads based on remote sensing more difficult. However, the array of instruments at our disposal is helping to define significant relationships between what the sensors can "see" and what can be observed on the ground.

In addition, the Jilliby site suffers from dieback associated with *Manorina melanophrys* (bell miners) birds (Stone, 1996). The presence of the aggressive, colony-forming honeyeater, *Manorina melanophrys*, in the canopies of unhealthy eucalypts is thought to enable some phytophagous insect populations to rise to sustained, damaging levels. This has caused widespread tree deaths in moist gullies (Stone et al., 2008) and affects the structural composition of the forest.

McCarthy (2004) suggested a correlation between stand height and surface fine fuel load. However, the study excluded the upper and lower productivity extremes in the sites available. These were, for example, very low productivity sites of White Box (*Eucalyptus albens*) or Slender Cypress-pine (*Callitris preissii*) with stand heights of less than 10 m. Sites of very high productivity such as Alpine Ash (*Eucalyptus delegatensis*), Mountain Ash (*Eucalyptus regnans*) or Cut-tail (*Eucalyptus fastigata*) with stand heights of 40m and more were also excluded. McCarthy defended this decision by stating that neither extreme in the productivity range is usually prescribed burned for fuel hazard reduction purposes. Unfortunately, one third of all plots sampled at the Jilliby Catchment have trees taller than 40m, and more than half are over 35 metres (Figure 7.12).

Similarly, the method introduced by Chafer et al. (2004) relies on variation in multispectral satellite derived NDVI values. However, at the Jilliby Catchment site, there is very little variation in NDVI between the 129 plots assessed as they are primarily closed, tall forest (Figure 7.12). The high LAI and biomass of the moist forest means that the NDVI values become saturated and the result is low variation between sites. When this is coupled with the low dynamic range of the field data, the amount of information available to differentiate plots is small.

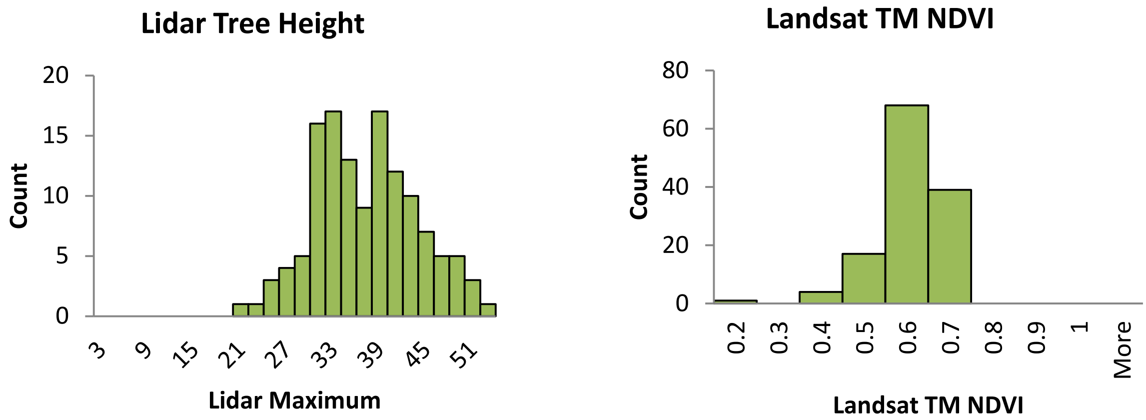

Figure 7.12 Histograms of the frequency of lidar returns from the top of canopy representing tree height (left) and the frequency of broad band Normalized Difference Vegetation Index (NDVI) values (right).

The relatively poor correlations achieved in this research from broad band sensors and tree heights (Figure 7.12) can be attributed to a number of factors. Table 7.8 demonstrated how poor canopy health and exotic species could confound the visual and destructive fuel loads. Disturbance was harder to quantify with evidence of recent logging at some of the sites and Bell Miner associated die back may have added to variation in spectral response that could not be associated with change in available fuel load.

Figure 7.11 illustrated that fuel loads could be successfully quantified even with coarse spectral resolution multi-spectral remote sensing instruments in open, dry forest. Narrow band vegetation indices outperformed broad band indices, largely because of extra information in the NIR that allowed the use of indices resistant to saturation. The AVRI (Kaufman and Tanre, 1992) was the best performing single index. Lidar was shown in parallel research (Turner, 2007) to be able to quantify elevated fuels in the under-storey at the Jilliby Catchment study site by calculating density of under-storey returns. However, as illustrated in Figure 7.5 more than two thirds of the overall fuel hazard came from the surface fuel component, which cannot be assessed using lidar.

The development of visual fuel scoring systems that better predict fire behaviour has been welcomed by the managers of native vegetation. However, while calibrating visual scoring systems with destructive sampling is a well accepted methodology, it has hampered the remote sensing of fuel hazard. Fuel scores are not directly linked to the weight of fuels, or the above ground biomass, but are tied to the arrangement of available fuels both horizontally and vertically. For example, there could be a thick under-storey of dead woody material, but anything over a 6mm maximum would not be considered to add to the available fuel. It would however, add substantially to the overall biomass and under-storey structure as assessed by remote sensing.

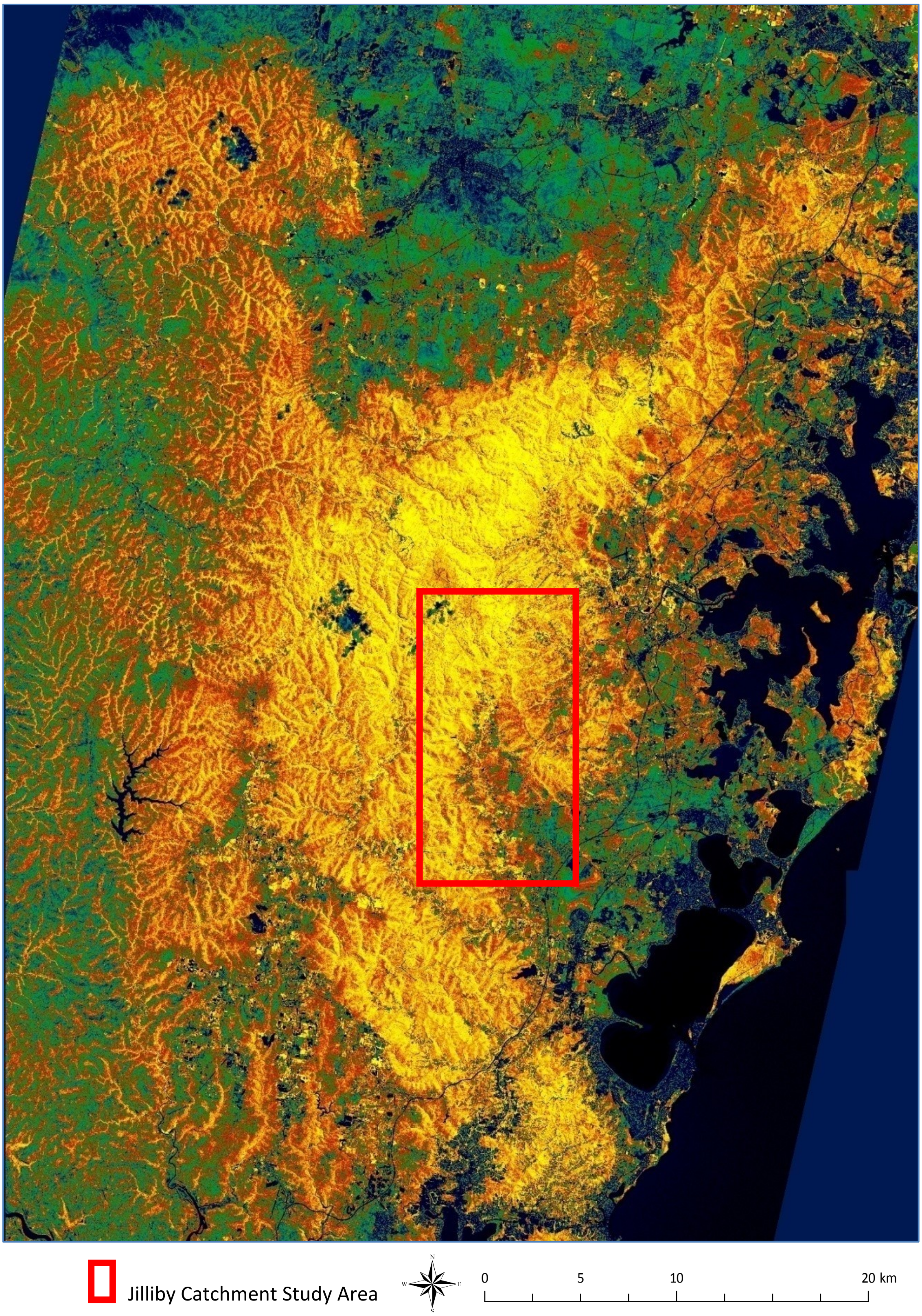

Figure 7.13 Broad band Normalized Difference Vegetation Index (NDVI) SPOT 5 for the region surrounding Jilliby.

Visual assessments of fuel hazard can be rapidly conducted individually but to expand this methodology to landscape scales would require extensive field sampling to establish robust correlations between remotely sensed variables and fuel loads. The methods trialled were successful in open, dry forest. However, the correlation between structural variables recorded in the field and remote sensing variables were weak in moist gullies and tall, closed forest.

7.6 Conclusions

The Jilliby Catchment study area posed significant obstacles to the mapping of fuel loads with remote sensing due to the tall, closed forest and complex topography. Unfortunately, the study site was not representative of the range of fuel loads encountered in the surrounding region. Canopy cover was found to vary independently of available fuel load at the Jilliby site, particularly in the tall, closed forest.

No significant relationship was found between broad band satellite data and tree height when the entire study site was included. When the site was stratified and only open, dry forest was included in the analysis, the sensors showed strong performance in the prediction of fuel hazard scores. Lidar was able to accurately measure the elevated fuels across the site, but this was only a small component of the overall fuel hazard as measured by visual assessment scores and destructive sampling.

A new index that summarises the Vesta fuel scoring attributes was introduced and found to be better correlated with remote sensing variables. The surface profile component of the Vesta scores proved to have a stronger relationship with the destructive sampling fuel weights than the surface measurements of the Overall Fuel Hazard Guide. Destructive sampling produced results that were only weakly correlated with visual assessment score totals and remote sensing variables. The OFHG (as applied at Jilliby) did not collect continuous variables for the surface fuel depth. This did not capture enough dynamic range in the surface fuel layer for effective modelling as it constituted the bulk of the accumulated fuel hazard.

Hyperspectral vegetation indices consistently outperformed broad band indices. The narrow bands in the near infrared allowed provided a greater variety of indices less sensitive to saturation in high canopy cover. The Atmospherically Resistant Vegetation Index was the best performing index when the whole site was considered. Remote sensing of forest fuel loads has an important role to play in the operational mapping of fire hazard and is particularly useful in open, dry forest.

Chapter 8

Assessing segmentation quality for multi-scale vegetation mapping

This chapter compares a variety of segmentation algorithms capable of delineating vegetation patterns based on SPOT-5 data and assesses how a multi-scale, object-based analysis performs in an operational setting. Segmentation algorithms require user input to be effective. The aim of this chapter was to seek optimal scale parameters of each algorithm for emulating API (Aerial Photo Interpretation). This allowed an opportunity to evaluate multiple segmentation algorithms for this application without bias, despite different algorithms being applied. It also offered the opportunity to test how image pre-processing affects segmentation quality. The results are used to produce a demonstration of multi-scale classification of vegetation.

Mapping vegetation is not an exact science, rather an applied science that imposes boundaries on a transition or continuum that is often temporal as well as spatial. The attempt is to capture unique map unit boundaries that are not always distinctly definable in nature: it is a form of generalisation. Map units can be defined as an assemblage of plant species which are discernible on an interpretive base (i.e. aerial photography, satellite imagery) and appear similar structurally and floristically and form repeatable units across the landscape (NT, 2009).

Segmentation algorithms function by grouping spectrally similar pixels into objects. Selecting an appropriate scale threshold for segmentation is problematic. The decision on how to merge adjacent pixels, and later objects, is based on threshold criteria of dissimilarity or homogeneity specific to each algorithm. Objects that are too small offer few benefits for reducing complexity of the raster imagery. Objects that are too large are poorly matched to the visually interpreted reference data.

The chapter begins by exploring empirical discrepancy methods to quantify segmentation quality. It tests whether optimising segmentation parameters can allow replication of manually digitised vegetation patterns. Based on these results, and applying segmentation at multiple scales, this chapter demonstrates how community scale objects may be classified based on homogenous crown size sub-objects in an operational environment.

8.1 Quantifying segmentation quality

In traditional maps, the term 'scale' is used to denote the ratio of a distance on the map to the corresponding distance on the ground. The area of the smallest unit in the map is dictated by its apparent size on a printed paper map. Reid (1988) suggests that a more or less circular polygon should not fall below about 5 mm diameter, while Gunn et al. (1988) suggest 10 mm diameter as a lower threshold (Emery et al., 2001). At a scale of 1:25 000 it is therefore possible to represent a minimum on-ground area of between 1.25 ha and 5 ha. At a scale of 1:100 000 it is possible to represent a minimum on ground area of between 20 ha and 80 ha.

As discussed in Chapter 2, the ideal level to map a patch of vegetation at has relatively homogenous parameter values. Such a patch will hardly ever be square, so pixels will are unlikely match a natural scale level. A solution can be found in irregularly shaped observation units, which are never present as such in remote sensing images, but which can be created using image segmentation (Addink et al., 2007). This is a procedure in which individual pixels are grouped into spatially continuous regions where the variance of a (group of) variable(s) (to be selected by the user) does not exceed a certain threshold (Haralick and Shapiro, 1985).

The segmentation algorithms applied here require a 'scale' parameter that defines how large image objects are allowed to grow, or the heterogeneity threshold. Each approach starts with an image element, such as a pixel or small cluster of pixels, which are combined with surrounding pixels. They essentially grow until certain criterion is reached (e.g., a merging cost or maximum heterogeneity). Though each algorithm functions differently, the success of each is dependent on the selection of an appropriate scale parameter.

Hierarchical segmentation produces regions of increasing average size which need to be linked to thematic levels. The quest for the appropriate segmentation level and thematic scale has led to several of empirical investigations and the development of numerous statistical methods (Hay et al., 2001).

Very little attention is paid to the selection of optimal segmentation parameters in the literature (Addink et al., 2007). However, the parameters are thought to affect the relationship between field observations of vegetation characteristics and spectral information (Marceau et al., 1994). Object definition by segmentation comprises both the choice of spectral bands to be considered and the setting of the heterogeneity threshold. With high correlations between adjacent bands, the variance that these bands represent easily gets too much weight.

Addink et al. (2007) studied the scale parameters for segmentation of leaf area index and biomass. They defined the optimal spatial definition as the level of segmentation that results in the lowest prediction error of the vegetation parameters. They segmented with ten different heterogeneities creating ten object sets. They compared field observations and spectral values and the optimised for the lowest prediction error, indicating the optimal heterogeneity for segmentation. Results showed that the scale of segmentation affected prediction accuracy and that aboveground biomass and LAI can be associated with different optimal object sizes. Different bands, or wavelengths, show different spatial variances (Atkinson and Aplin, 2004), which will also affect object definition.

The optimal scale of observation (i.e., object size with object-oriented image analysis) depends on the scale of the target, and on the spatial heterogeneity of the landscape. Therefore, multiple scales must be trialled to optimise for a solution. The superior approach will create image objects that are as large as possible (to reduce complexity and generalise patterns) and still maintain thematic homogeneity in each object. Ideally, each image object will delineate a patch of a single type or patch of vegetation, whether it is a riparian corridor surrounded by grassland or a patch of heath in a matrix of forest.

Visual methods have been the most widely-used method of assessing image segmentation quality (Zhan et al., 2005). That is, identifying parameters that produce high quality image segmentations by visually comparing multiple segmentations. However, a range of object validation techniques have been developed for assessing uncertainties in segmentation based object extraction (Hay et al., 2003, Möller et al., 2007, Shi et al., 2005). The majority of quantitative comparison studies of segmentation software are empirical discrepancy methods (Neubert et al., 2006). Empirical discrepancy methods calculate the difference between reference image objects drawn by hand and automatically delineated objects, with both topological and geometric measures (Zhan et al., 2005). The topological differences can be assessed by comparing the areas covered. Geometric object differences can be determined by the comparison of object positions or where their boundaries lie.

Möller et al. (2007) developed a comparison index for a relative comparison of segmentation results at different scales within Definiens Developer 7. They used the area and centre of gravity of segmented objects and reference polygons to guide their choice of scale threshold so that at a global scale they would reach a balance between over-segmentation and under-segmentation. Clinton et al. (2010) demonstrated a similar approach. Lucieer (2004) addressed over-segmentation by creating a ratio of the area of the reference polygon and the largest nested segmentation object.

Following Zhan et al. (2005) and Möller et al. (2007) this research initially focussed on quantitatively assessing the geometric and topological quality of a single class (woody vegetation). However, it was soon discovered that while an empirical evaluation of segmentation performance is relatively straight forward for isolated stands of trees or boundaries in modified landscapes, evaluating the success of boundary detection *between* contiguous vegetation communities is more difficult.

The Berkeley Segmentation Dataset and Benchmark (Martin et al., 2001) provides a way forward for comparing coarse scale segmentation and subjective reference polygons. It is a collection of 12,000 hand-labelled segmentations of 1,000 images from 30 human subjects. A range of developers have submitted segmentation algorithms to a public benchmark based on a training set of 200 images, and a test set of 100 images.

Performance on the simulated data available in the Berkeley dataset is not a suitable measure for segmentation on native forest. The noisy patterns in native vegetation are subjectively delineated by experienced interpreters based on field observations. Unfortunately, visual interpretation and delineation of vegetation patterns using one observer is already time consuming for operational map production. Using multiple air photo interpreters is impractical for map creation or even validation at a state-wide scale.

8.2 Methods

The first step in this analysis was to conduct a qualitative visual survey of segmentation results using the existing air photo interpretation layer and the fine spatial resolution panchromatic band as a reference. The scale was increased for each algorithm iteratively and any artefacts of the underlying algorithms were examined. This gave a subjective but informative indication of the strength and weaknesses of each of the algorithms.

All analysis was initially carried out on three 10m geometrically corrected digital number bands from SPOT-5 imagery. Pre-processing of SPOT 5 was observed (subjectively) to heighten between-class variations, and suppress within-class variation (see Figure 9.1). To quantify the improvements of pre-processing the analysis was performed a second time. The digital numbers representing woody vegetation were stretched to fill the entire range (histogram equalised), a Gaussian stretch was then performed on the saturation band in HSV space (saturation stretch), and Gram-Schmidt Spectral Sharpening (Laben and Brower, 2000) was used on the stretched multispectral bands (pan-sharpening) (see Figure 8.1).

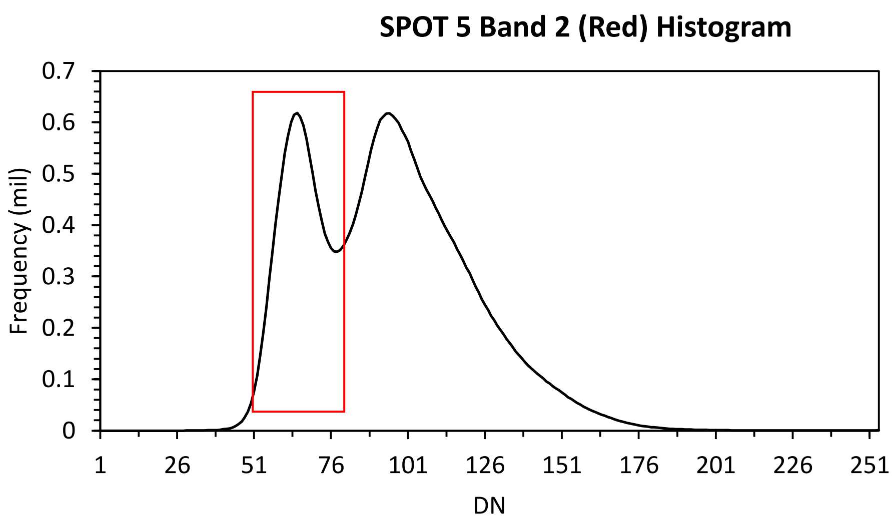

Figure 8.1 A histogram of raw SPOT 5 values highlighting the limited number of digital values that account for variation in reflectance of woody vegetation (highlighted in red).

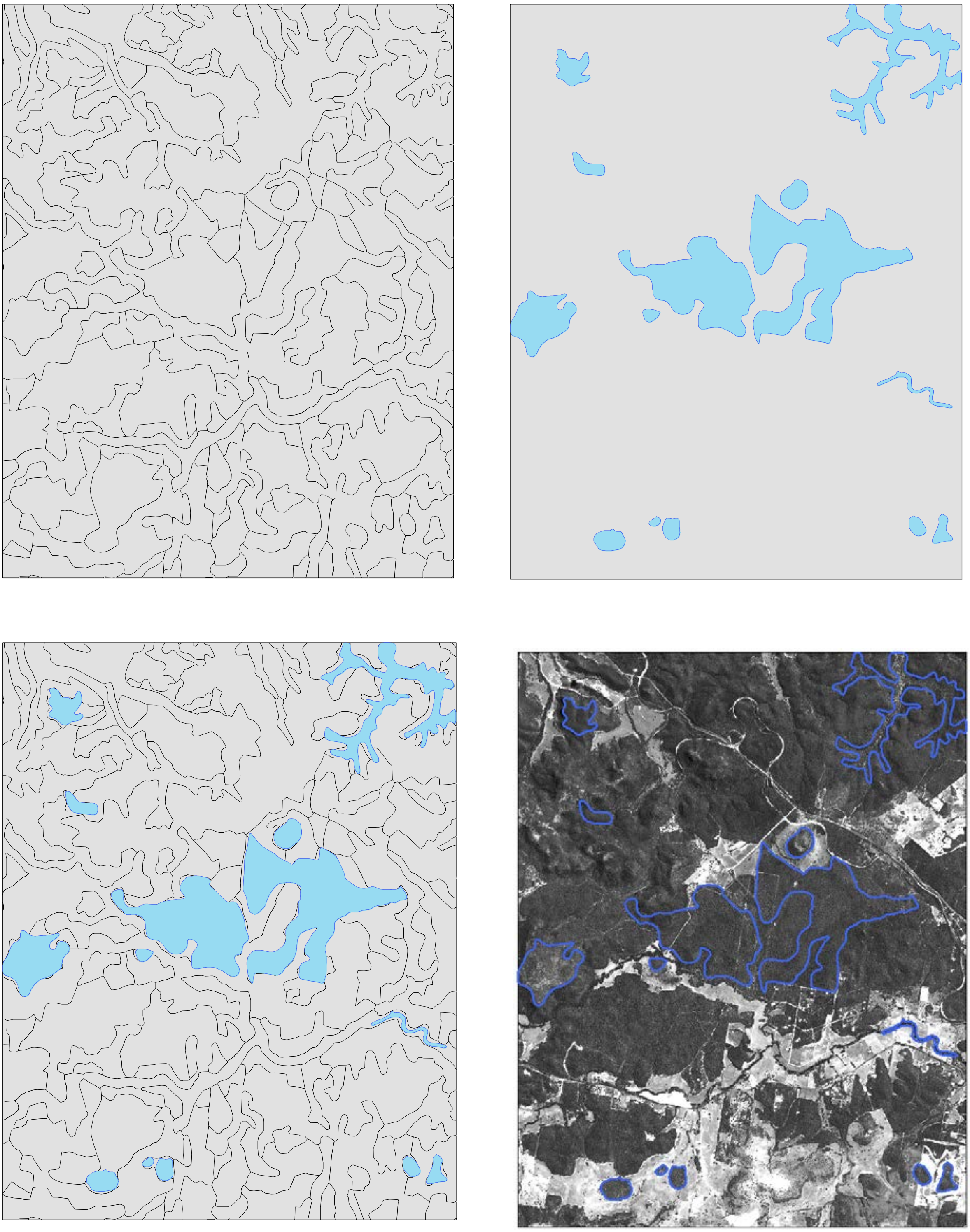

Figure 8.2 Reference polygons from the original aerial photo interpretation (API).

Segmentation quality was quantitatively compared using empirical discrepancy methods. For each automatically delineated object, both topological and geometric measures were assessed at each scale globally and locally. Global statistics were generated for the number of polygons in the image subset and their mean and maximum area. The topological differences were assessed by comparison with the reference area. The geometric object differences were determined by the comparison of object positions (where their boundaries lie) using the distance between the centroid of segmented objects and reference polygons.

The benchmark dataset for this research was manually delineated vegetation patterns derived from stereo aerial photography (Figure 8.2). The scale of the reference layer of vegetation delineated using aerial photography is 1: 100 000. The original aerial photo interpretation (API) data did not have sufficient geometric precision to use as training areas (top left) so several objects representative of a mix of shapes and sizes were selected (top right). The boundary between woody vegetation and non-woody vegetation were included, as well as objects with boundaries between classes of woody vegetation (bottom left). The panchromatic band was used as a reference when geo-registering API objects (bottom right).

Reference image objects were derived from the existing air photo interpretation and stratified by landscape position. The extents were geometrically registered using SPOT-5 panchromatic data (2.5m). From the 147 air photo polygons available, 14 were selected across 7 structural classes API relied on expert visual assessment of remote sensing data.

Each segmentation algorithm was run at multiple scales and parameters were adjusted systematically. For each automatically delineated object, both topological and geometric measures were assessed at each scale globally and locally. Global statistics were generated for the number of polygons in the image subset and their mean and maximum area. These were compared to global statistics of manually delineated vegetation patterns to seek an ideal segmentation threshold for each algorithm. Local statistics were generated for the number of polygons in each reference object and their mean and maximum area.

The topological differences were assessed by comparison with the reference area. The production of too many objects is characterised as over-segmentation and the production of too few objects, or objects larger than reference, is characterised as under-segmentation. The aim is to seek optimal scale parameters of each algorithm for emulating API. The geometric object differences were determined by the comparison of object positions (where their boundaries lie) using the distance between the centroid of segmented objects and reference polygons.

A modified Lucieer (2004)'Area-Fit-Index' was used to quantify over-segmentation by calculating the number of objects inside each reference polygon. The image is over-segmented if overlap is less than one hundred percent and under-segmented if overlap is more than one hundred percent. To quantify of the fit of each of the reference polygons with the largest segments overlapping these objects, the *Area Fit Index* (AFI) is used where A is the area.

$$AFI = A_{\text{reference polygon}} - A_{\text{largest object}} / A_{\text{reference polygon}} \qquad \text{Equation (10.2)}$$

For a perfect fit overlap is 100% and AFI equals 0.0. A reference polygon is over-segmented if overlap is less than 100% and AFI is greater than 0.0. A reference polygon is under-segmented if overlap is 100% and AFI less than 0.0. In some situations overlap can be less than 100% and AFI is less than 0.0, then the object is over-segmented but the largest segment is larger than the reference polygon.

Under-segmentation was quantified with a variation of Möller's ‘Comparison Index’(Möller et al., 2007). The centre of gravity of each reference polygon was used to select the central image object formed by each segmentation algorithm. The area of this central image object increased with the scale level and the area it overlaps the reference polygon is reported. As the scale increases the objects extend outside the reference areas and so their total area in proportion to the reference polygon is also reported. The distances between the gravity centre of each object were calculated following Zhan et al. (2005).

8.2.1 Multi-scale object-based classification

The results of segmentation were then used to produce a demonstration of multi-scale classification of vegetation. The multi-resolution segmentation algorithm (Baatz and Mimler, 2002, Baatz and Schäpe, 2000) in Definiens Developer 7 was selected based on its performance in topological and geometric measures. It is also novel because it includes the shape of the object in its measurement of heterogeneity. It allows the user to skew the segmentation in favour of regions with smooth edges and a more or less compact form (Figure 8.3).

300 floristic plots were available for the map sheet. Descriptions of the local distribution of vegetation had been recorded at each site by ecologists as well as cover and abundance. Fine scale image objects were labelled with a species code when their frequency was noted as clearly dominant (Figure 8.4). The object values were exported for each survey site and added to a database for processing. Logistic Model Trees (LMT) (Landwehr et al., 2005) in WEKA (Witten and Frank, 2005) was used to classify crown scale objects. These were used in turn to classify small patches or stands of trees. These classified patches were then aggregated to form classified vegetation community polygons.

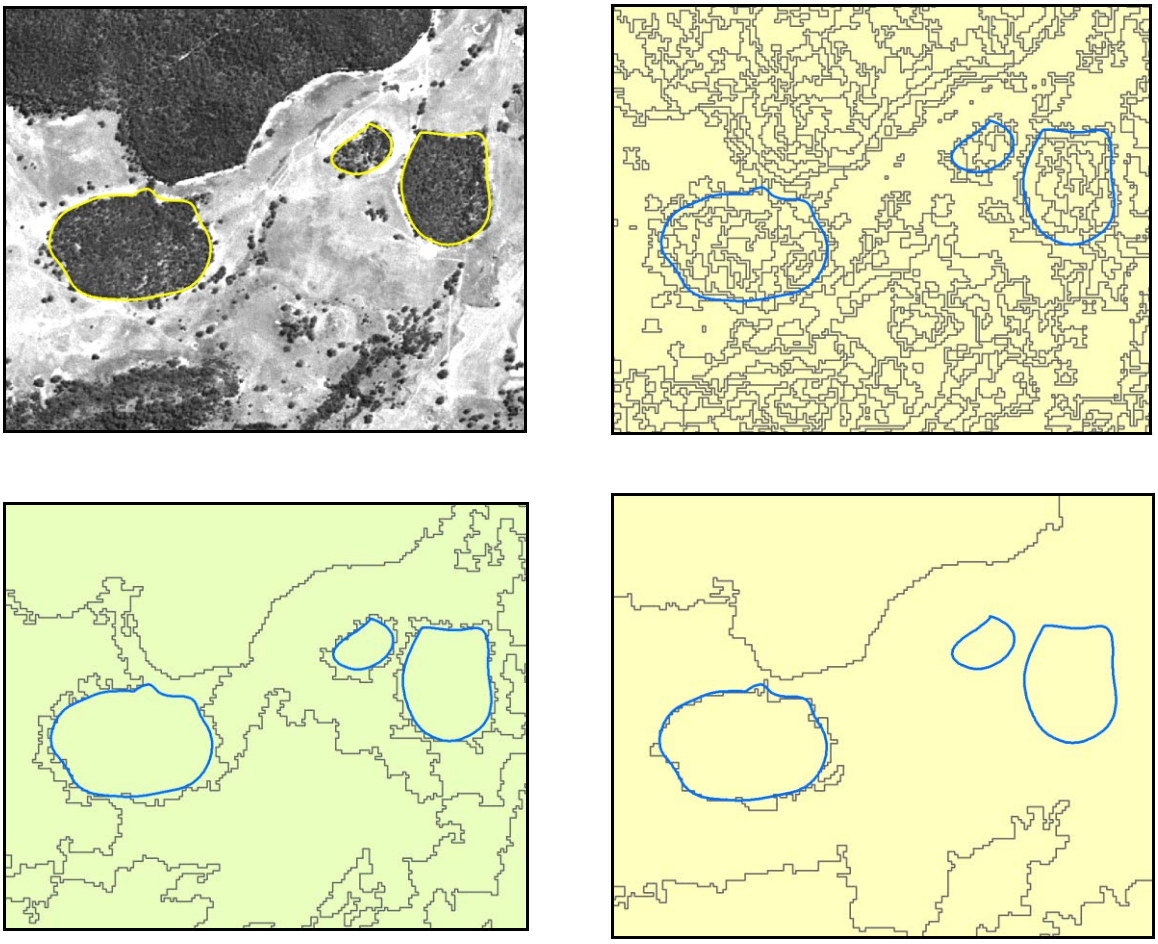

Figure 8.3 The effect of increasing the scale of multi-resolution segmentation.

The reference polygons are co-registered with panchromatic SPOT-5 data (top left) and segmentation of the image objects increases in scale from over-segmented (top right) to a scale that emulates API (bottom left) to an under-segmented scale (bottom right).

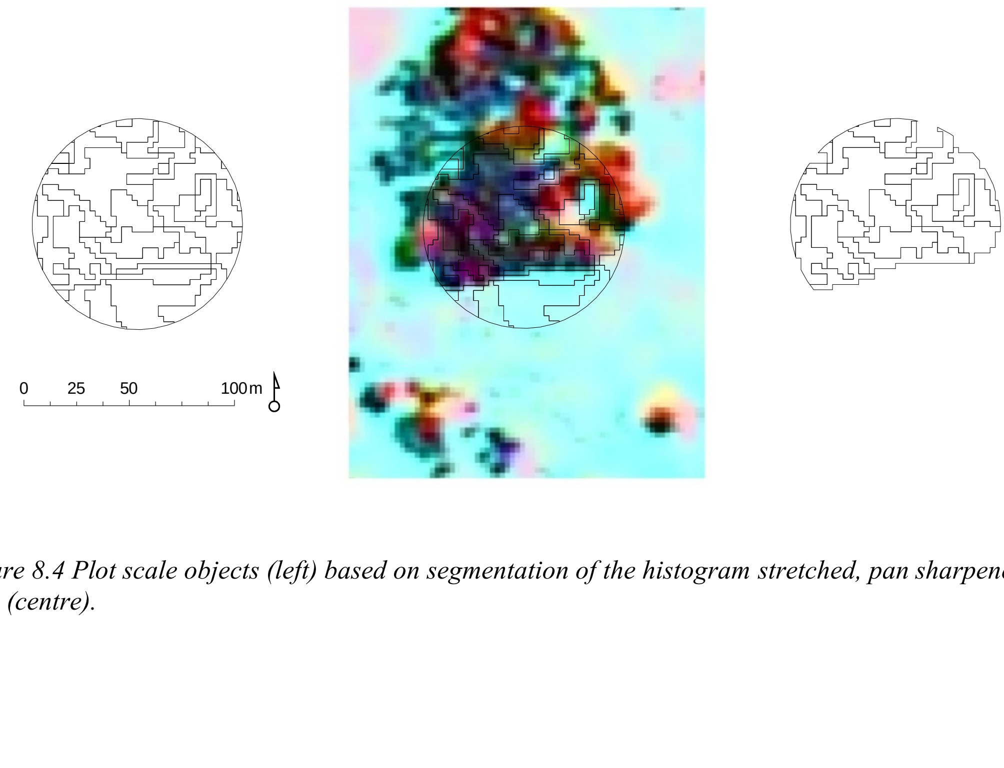

Figure 8.4 Plot scale objects (left) based on segmentation of the histogram stretched, pan sharpened SPOT 5 data (centre).

Chapter 5 described a spatial filter and a watershed algorithm used to delineate individual crowns from relatively coarse spatial resolution HyMap data. For a method to be used operationally it needs to be applicable to remote sensing data widely available at regional scales. A seamless coverage of SPOT 5 data (panchromatic and multi-spectral) is available for NSW but its use in vegetation mapping has been problematic (McCauley, 2006) not used in vegetation mapping. The coverage features three 10m multispectral bands and one 2.5m panchromatic band.

In this chapter the watershed function was replaced with the Full Lambda-Schedule algorithm (Robinson et al., 2002). The algorithm was originally designed to detect anomalies so the pre-processing steps were modified to turn each crown into an anomalous value. A 10m NDVI image was pan-sharpened with an inverted 2.5m histogram-equalised panchromatic image. This was subjected to a local maximum focal filter with a circular kernel size of 3 pixels radius. The result is that large crowns appear as circular objects and that isolated paddock trees are delineated. Figure 8.5 shows the results of pan-sharpening and spatial filtering on an NDVI image.

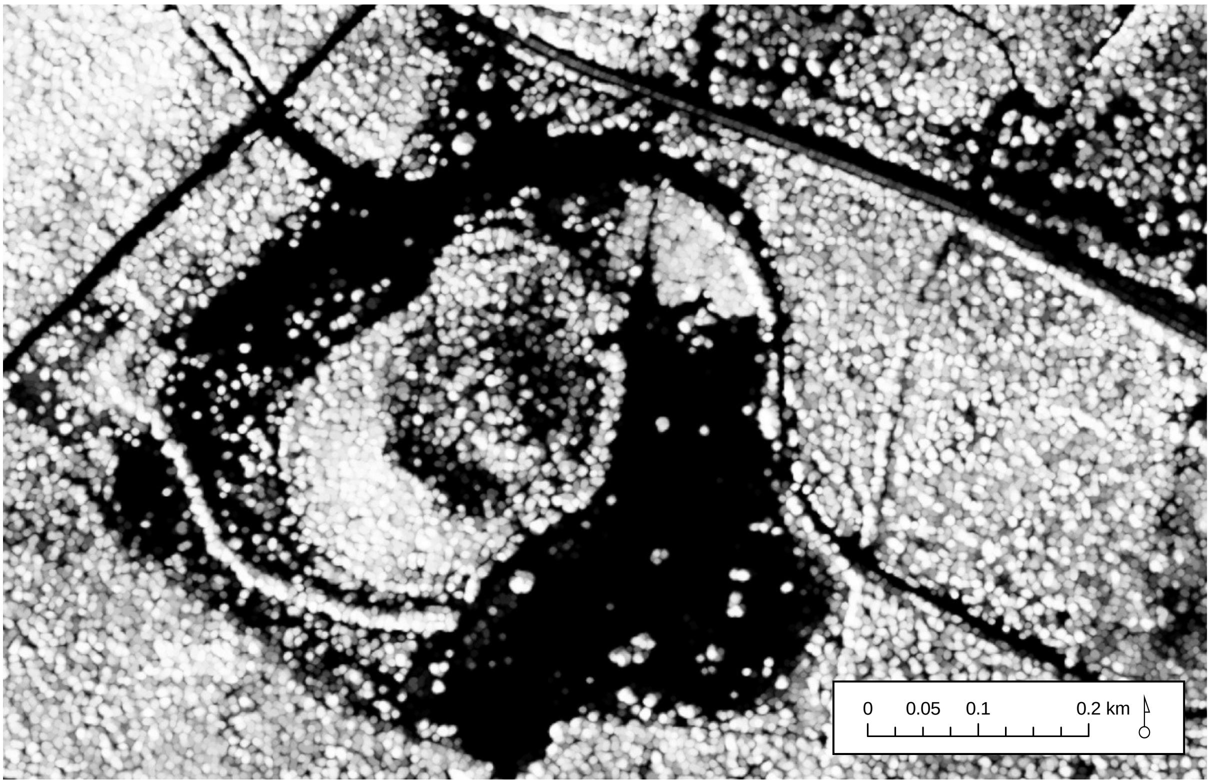

Figure 8.5 An inverted, histogram-equalised 2.5m spatial resolution panchromatic image was used to sharpen NDVI and delineate tree crowns.

8.3 Results

8.3.1 Topological accuracy for woody/non-woody boundaries

Analysis was first conducted on objects with simple linear boundaries between woody and non-woody vegetation. This reflects existing research (see Section 9.1) where empirical discrepancy methods have been used to assess segmentation quality of agricultural fields and other regular geometric shapes. As the scale parameters are labelled differently for each algorithm, the parameters have been standardised (Table 8.1). The segmentation approaches need to be able to delineate the broad variations in woody vegetation that are clearly visible on enhanced imagery without creating too many artefacts, effectively generalising the data. Each segmentation algorithm was tested using the raw digital numbers and the pre-processed equalisation-stretched imagery.

Table 8.1 Standardised measure of scale parameters between algorithms. Scale parameters in categories 1-5 were selected to match each other, not as an attempt to mirror the API scale.

Results	*Definiens Developer 7*	SCRM Minimum Area	ENVI FX (15% edge)
Scale 1	10	0.5	25
Scale 2	20	1	50
Scale 3	40	4	85
Scale 4	80	16	95
Scale 5	160	64	99

8.3.1.1 Quantifying under-segmentation of woody/non-woody areas

Under-segmentation was assessed by selecting the central image object within the reference polygon and comparing its area with the area of the reference area as the scale is increased. At fine scales only one very small object was selected so the 'area covered' score was low. All algorithms approached the ideal of 1.00 as the scale parameter reached 3 or 4 and the central objects increased in size (Figure 8.6).

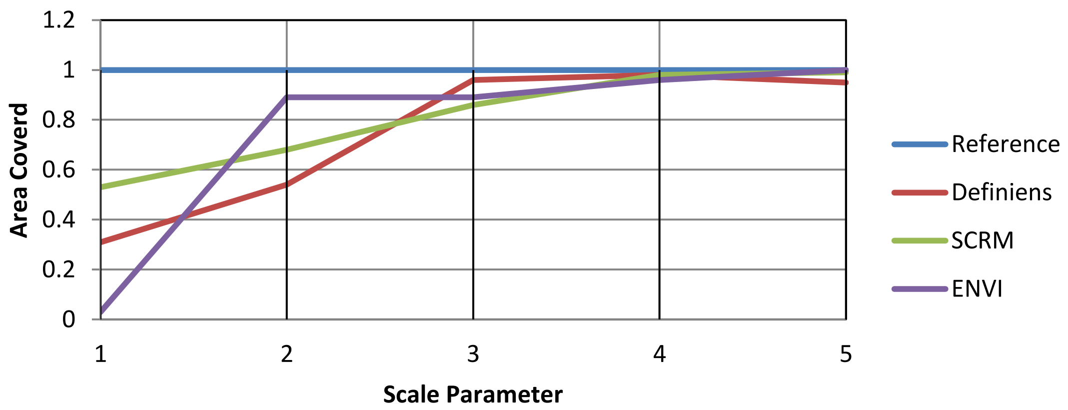

Figure 8.6 The central object increases in area with an increase in the segmentation scale parameter until it reaches 1.0.

The 'overlap' measure is a relative ratio of the area of the image object and the area of the reference polygon. Again, it started low with one small image-object selected but as the scale increased the area of the object eventually became larger than the reference polygon. The optimum scale of segmentation was scale 3 for Definiens and SCRM and scale 4 for ENVI (Figure 8.7).

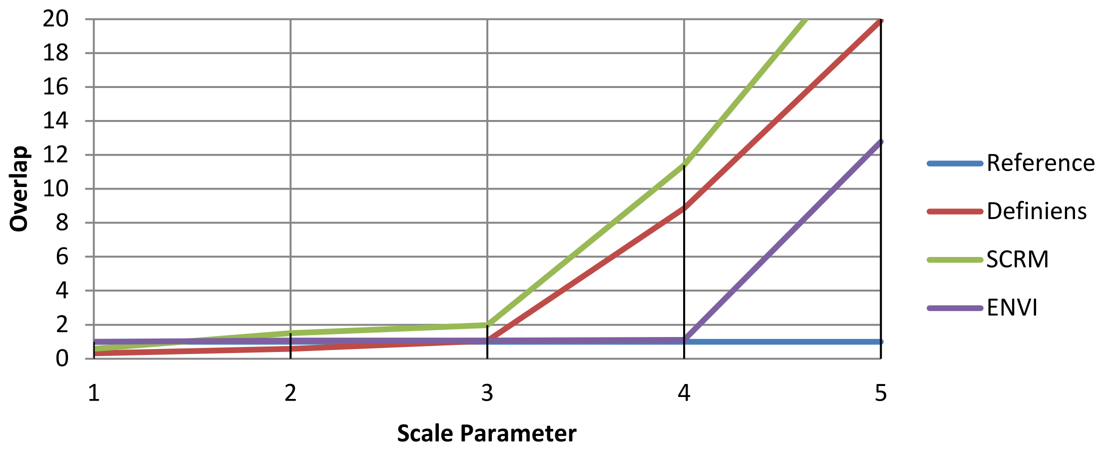

Figure 8.7 The central object increases in overlap with an increase in the segmentation scale parameter.

8.3.1.2 Quantifying over-segmentation of woody/non-woody areas

Over-segmentation was assessed by selecting all image objects with their centroid inside the reference polygon and comparing their area with the area of the reference polygons as the scale was increased. The polygon count started very high when over-segmentation was being assessed. As the scale increased it approached the ideal of 5.00 (the number of reference polygons) and then tend to 0.00 (if no objects have their centroid inside the reference polygon). Again, the optimum scale of segmentation the areas was Scale Parameter 3 for Definiens and SCRM and Scale Parameter 4 for ENVI (Figure 8.8).

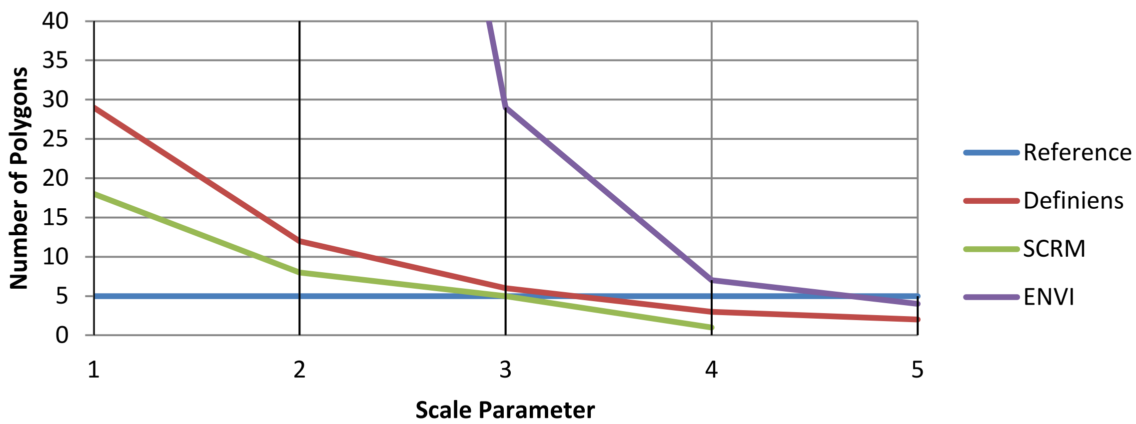

Figure 8.8 At a scale parameter of 1 there are many small objects. As the scale parameter increases the size of the objects begin to match the five reference polygons.

The 'overlap' measure is a relative ratio of the area of the image objects with their centroid inside the reference and the area of the reference polygon. The optimum scale parameter selected by the over-segmentation measure was near Scale Parameter 3 for Definiens and SCRM and before Scale

Parameter 4 for ENVI (Figure 8.9).

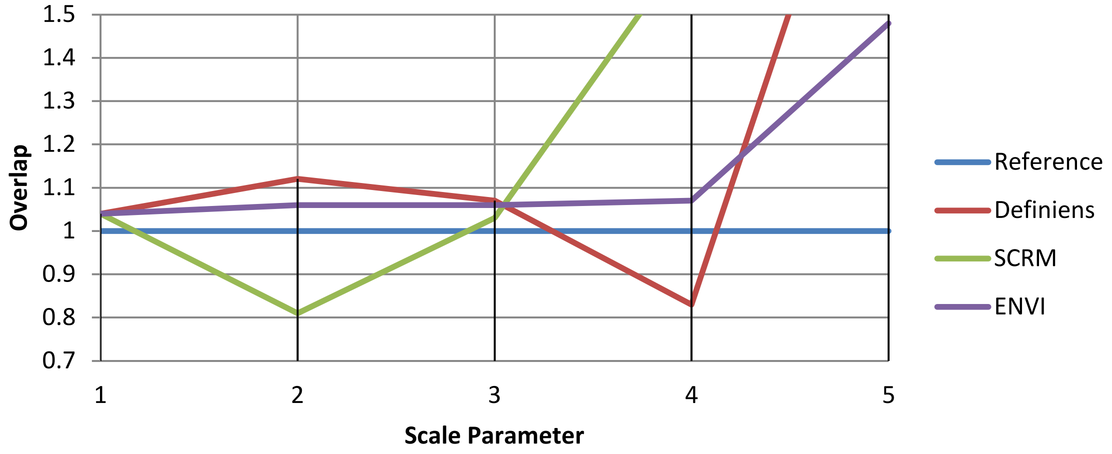

Figure 8.9 The area varies erratically as the scale increase because some of the polygons will fall out of the reference area according to their shape.

The results for the segmentation of woody/non-woody areas is as would be expected for all three algorithms. At fine scales they over-segmented the image reference polygons and the ratio of the area of overlap was accurate. At coarse scales the accuracy decreases and in some cases the image objects overlap the reference polygon area by as much as 30 times the area.

The optimum scale of segmentation for delineation of the binary woody vegetation reference objects was determined as the intersect of the reference result for all measures (Figure 8.10). All measures intersected close to Scale Parameter 3 allowing for the selection of standardised ideal segmentation scale parameter for each algorithm.

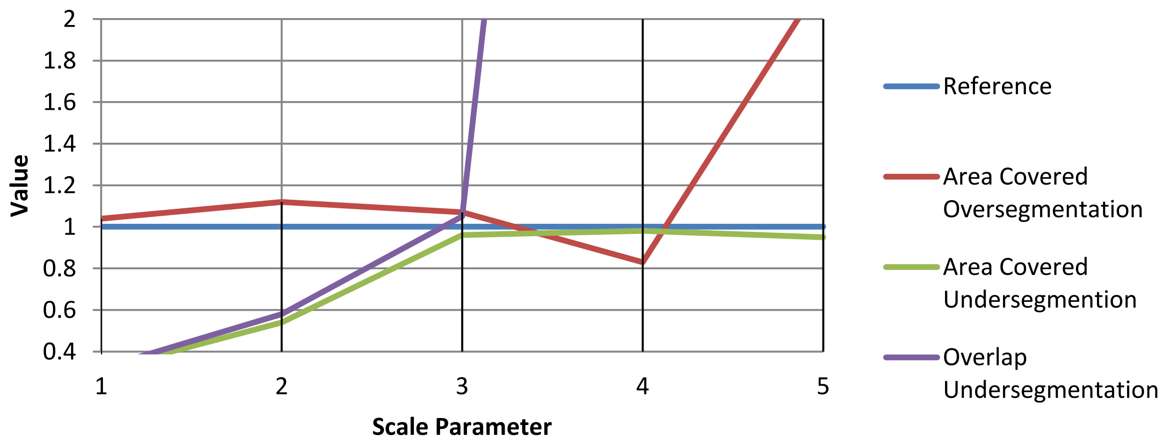

Figure 8.10 By plotting all of the measures (for Definiens in this case) the ideal scale parameter can be selected by based on the intersect with the reference polygon results.

8.3.2 Quantifying under-segmentation for all reference polygons

Under-segmentation was assessed by selecting the central image object within the reference polygon and comparing its area with the area of the reference area as the scale is increased. After analysis was conducted on woody/non-woody areas the reference set selection was widened to include API polygons (n=14) that were representative of internal vegetation type boundaries as well as binary woody boundaries.

Under-segmentation was assessed for all boundaries (including internal boundaries) for reference polygons by selecting the central image object within the reference polygon and comparing its area with the area of the reference area as the scale is increased. At fine scales only one very small object was selected and the 'Area Covered' score was low (Figure 8.11). When all reference polygons were used the area of the central image object only neared 1.00 as the Scale Parameter was increased to the maximum, higher than the woody, non-woody boundary results.

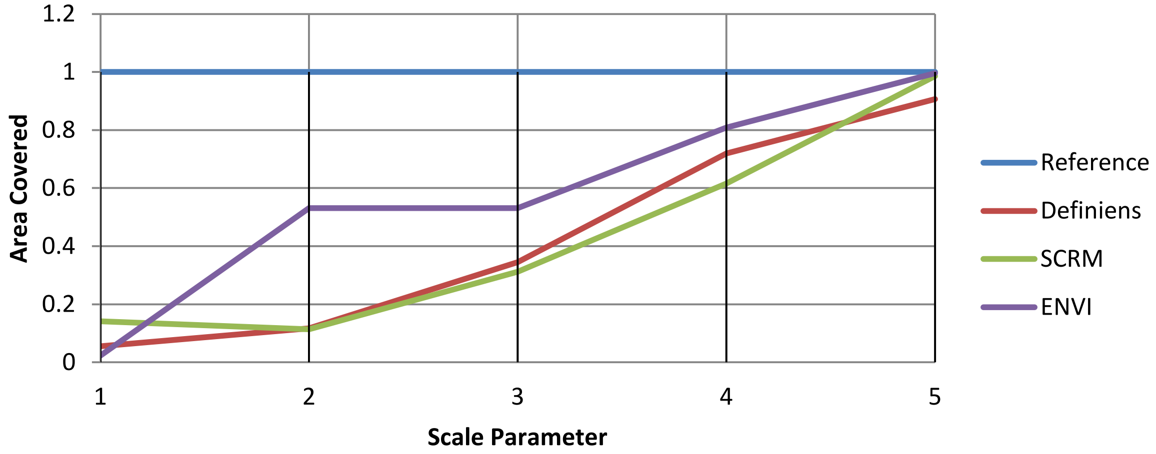

Figure 8.11 When all boundaries were assessed the central image object only neared 1.00 as the Scale Parameter was increased to the maximum.

The relative ratio of the area of the image object and the area of the reference polygon started low as only one image-object but all three algorithms reached an optimal scale, near Scale Parameter 3. However, they diverged significantly at higher scales (Figure 8.12). When these two measures are combined there is no optimum scale of segmentation that can offer the satisfactory combination of area covered and overlap. Without a clear unique optimum scale it is a trade of between over and under segmentation.

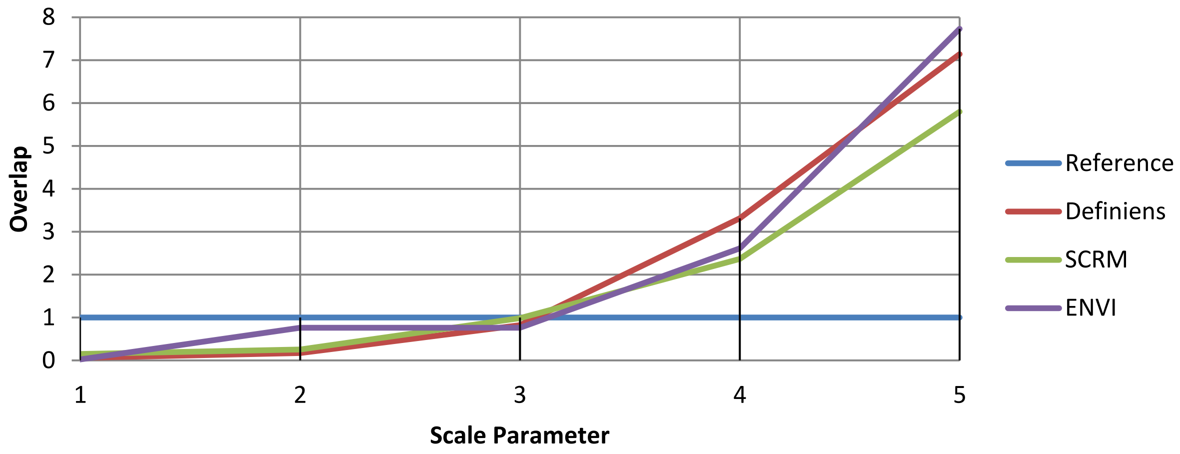

Figure 8.12 The overlap diverged at a similar place to the woody boundary but diverged to a greater degree at high scales.

8.3.3 Quantifying over-segmentation for all reference polygons

Over-segmentation was assessed by selecting all image objects with their centroid inside the reference polygon and comparing their area with the area of the reference polygons as the scale was increased. The polygon count started significantly higher when all reference polygons were used in the over-segmentation measures. At fine scales many objects were created inside the reference polygons and so the object count was very high (Figure 8.13). As the scale increased all three algorithms approached 1.00 (or 0.00 if no objects had their centroid inside the reference polygon). Similarly to the woody boundaries, the optimum scale parameter selected by the over-segmentation measure was near Scale Parameter 3 for Definiens and SCRM and before Scale Parameter 4 for ENVI.

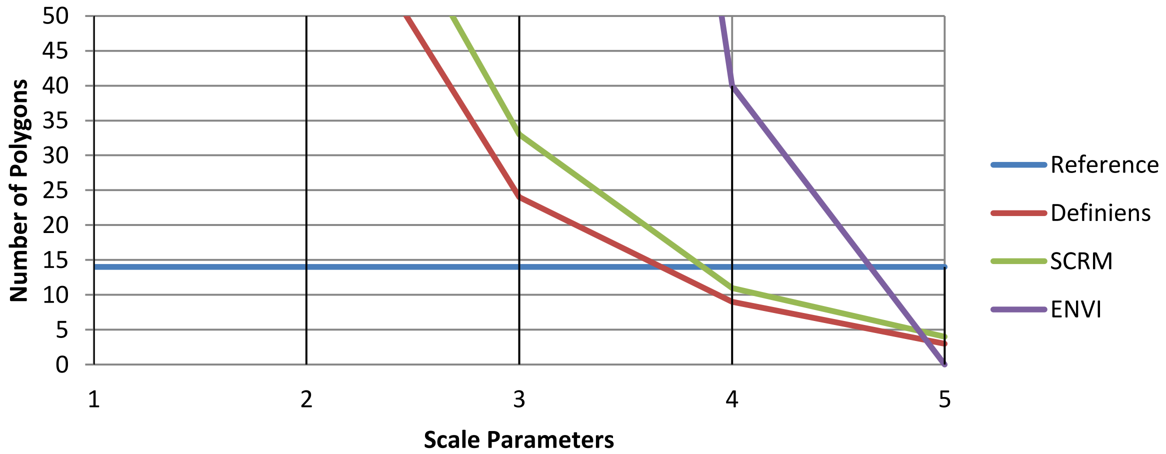

Figure 8.13 When all polygons were used the object count was very high at finer scales.

When all polygons were used, the optimum scale parameter selected by the global overlap measures was near Scale Parameter 3 for Definiens and SCRM and between Scale Parameter 3 and 4 for ENVI (Figure 8.14).

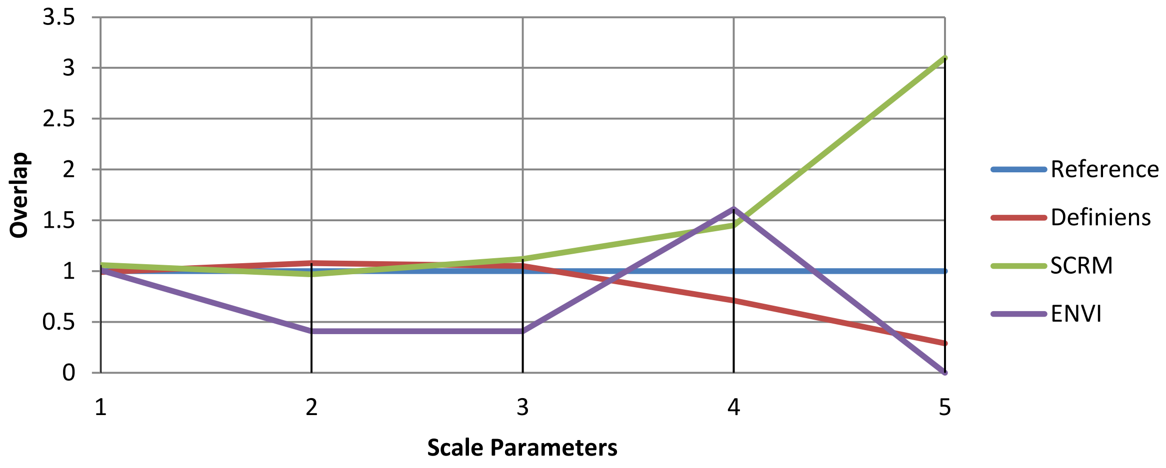

Figure 8.14 For this measure the smaller the polygons the better the fit. Their overlap begins to deviate significantly after Scale 3.

8.3.4 Global Statistics

As a global reference point the number of polygons and mean area per polygons were compared for the entire mapped area. The subset area is over 7000 hectares and featured 147 polygons with an average size of 49 hectares (Table 8.2). This is the benchmark for global statistics of each of the segmentation algorithms.

Table 8.2 Summary statistics of the reference air photo interpretation. Area is calculated in hectares.

Coonabararan Aerial Photo Interpretation	Map Sheet	Subset	Reference polygons
Count:	2906	147	19
Minimum:	0	0	2
Maximum:	11991	665	257
Sum:	264110	7236	738
Mean:	91	49	53
Standard Deviation:	404	88	77

From the global statistics for Definiens Developer 7 and SCRM we can infer that a Scale Parameter of 3 was ideal for replicating API (Figure 8.15). This is reinforced by a qualitative visual survey which indicates that these scales are visually the most similar to the reference layer.

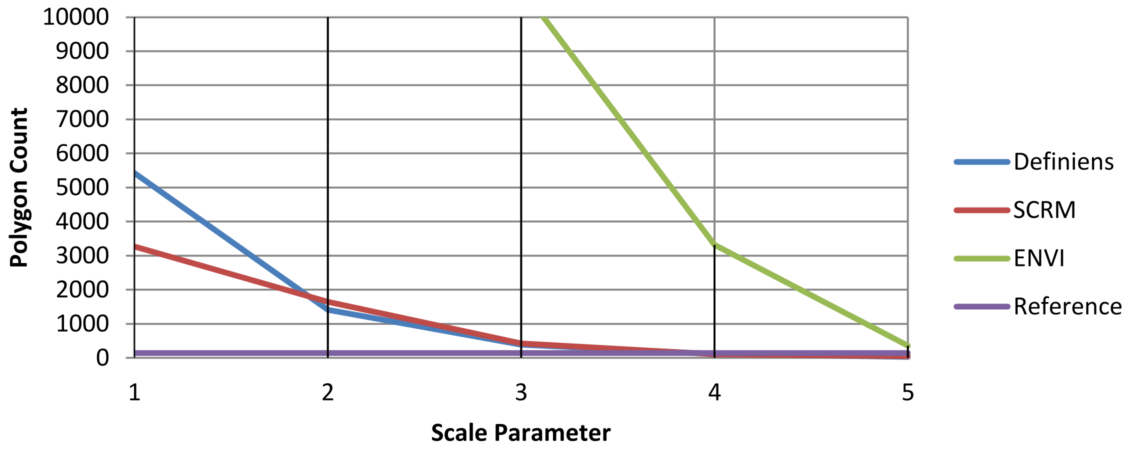

Figure 8.15 Global polygon count for reference and each segmentation approach.

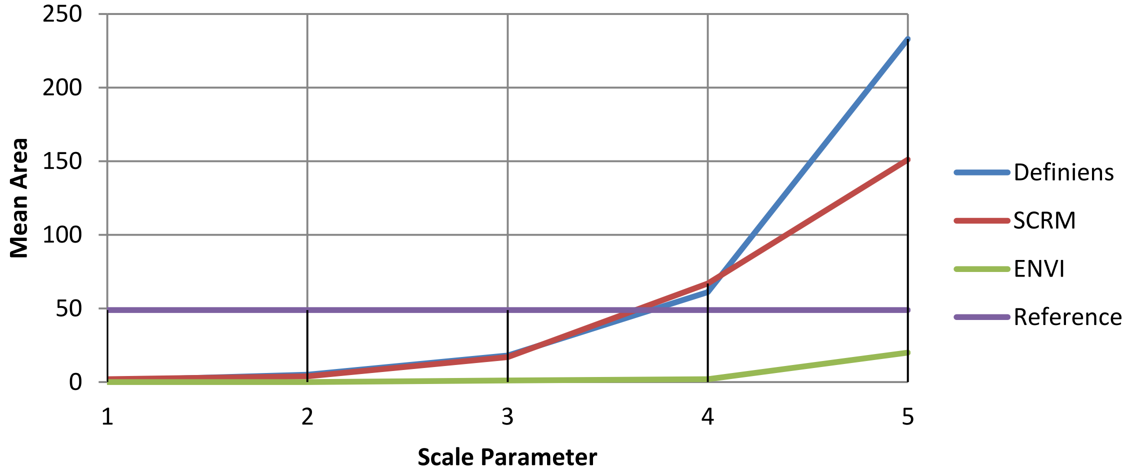

Figure 8.16 Global mean area for reference and each segmentation approach.

SCRM was the only algorithm to apply polygon smoothing by default and uses Douglas-Peucker simplification (Douglas and Peucker, 1973, Ramer, 1972) but this was discarded for parity with the other segmentation algorithms. The parameters applied are in Table 8.3. Global statistics inferred that a SCRM parameter scale of 4 was ideal for replicating API with 3 band digital number data.

Table 8.3 Segmentation scale parameters for Size Constrained Region Merging. Area is calculated in hectares.

SCRM	Scale 1	Scale 2	Scale 3	Scale 4	Scale 5
Minimum segment size	0.5	1	4	16	64
Desired Mean segment size	2	4	16	64	256
Maximum allowed merger size	4.5	9	36	144	576
Minimum Vertex Length	20 m	20 m	20 m	20 m	20 m

The ENVI FX algorithm was configured to detect edges at a fine scale (15%) and a range of region merging scales was executed (50%-99%). The number of objects detected by ENVI FX was larger than the other algorithms in the comparison because of its tendency to isolate anomalies such as small clearings and dams. This skews the global statistics making it difficult to compare with other methods. For this comparison the scales were chosen for their similarity with the other segmentation algorithms rather than best fit for the reference data. The best fit with reference data according to global statistics was 95% merging for digital number data and 99% merging for processed data, a better solution could be found by segmenting above Scale Parameter 5.

8.3.5 Geometric accuracy

Geometric accuracy was assessed at multiple scales, following Möller et al. (2007), by dissolving polygons with centroids inside the reference polygons. A matrix of the distance between points was calculated for the centre of gravity of dissolved image objects and the centre of gravity of reference polygons. A pictorial example is given with tables for Definiens Developer 7's multi-resolution segmentation of the three band digital number image. Despite all of the quantifiable topological measures recommending Scale Parameter 3 the results at this scale showed poor geometric accuracy (Table 8.4). The results indicate that over-segmentation (many small polygons) that are classified and then merged based on class will have superior geometric accuracy (Scale Parameter 1) (Figure 8.17).

Table 8.4 The geometric accuracy of Definiens Developer's multi-resolution segmentation of three band SPOT-5 digital number data (10m): a summary of the Euclidean distance (in metres) between centroids of dissolved image objects and reference polygons at multiple scales.

	Scale Parameter 1	Scale Parameter 2	Scale Parameter 3	Scale Parameter 4
Average distance between reference and image object centroids	130	350	443	1081

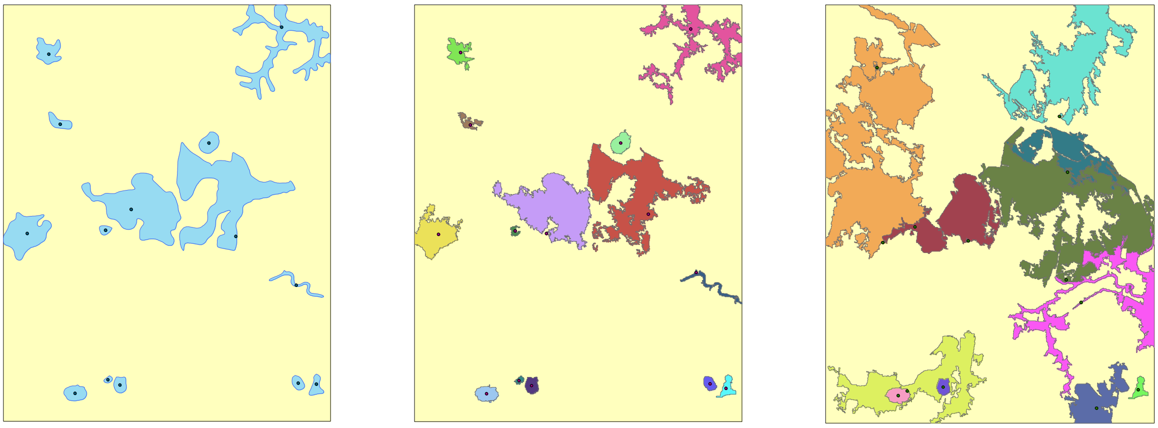

Figure 8.17 The larger objects show poor geometric fit as the shapes diverge from the reference.

The API used as a reference and the Definiens segmentation results have been overlayed on 2.5m panchromatic SPOT 5 imagery below to illustrate the differences (Figure 8.18 and Figure 8.19).

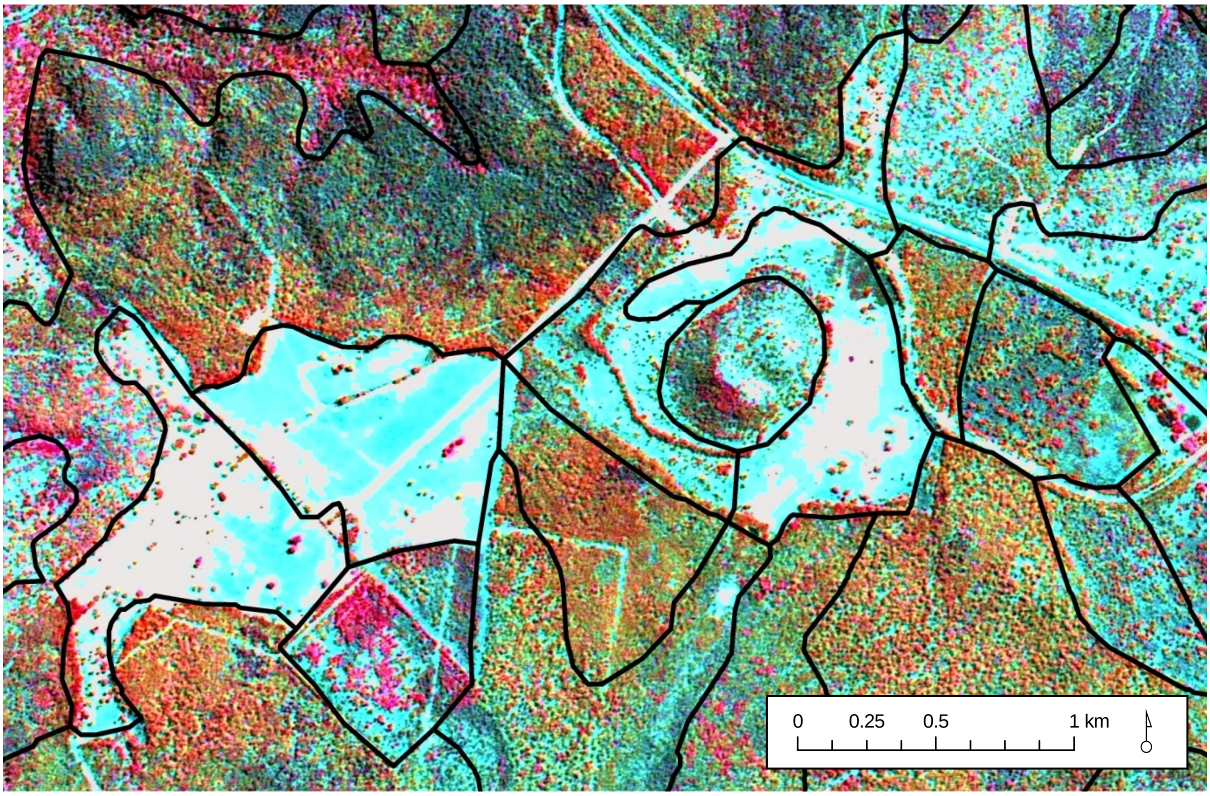

Figure 8.18 The manually delineated polygons based on air photo interpretation take into account colour, texture and landscape position. Detail is limited by effort.

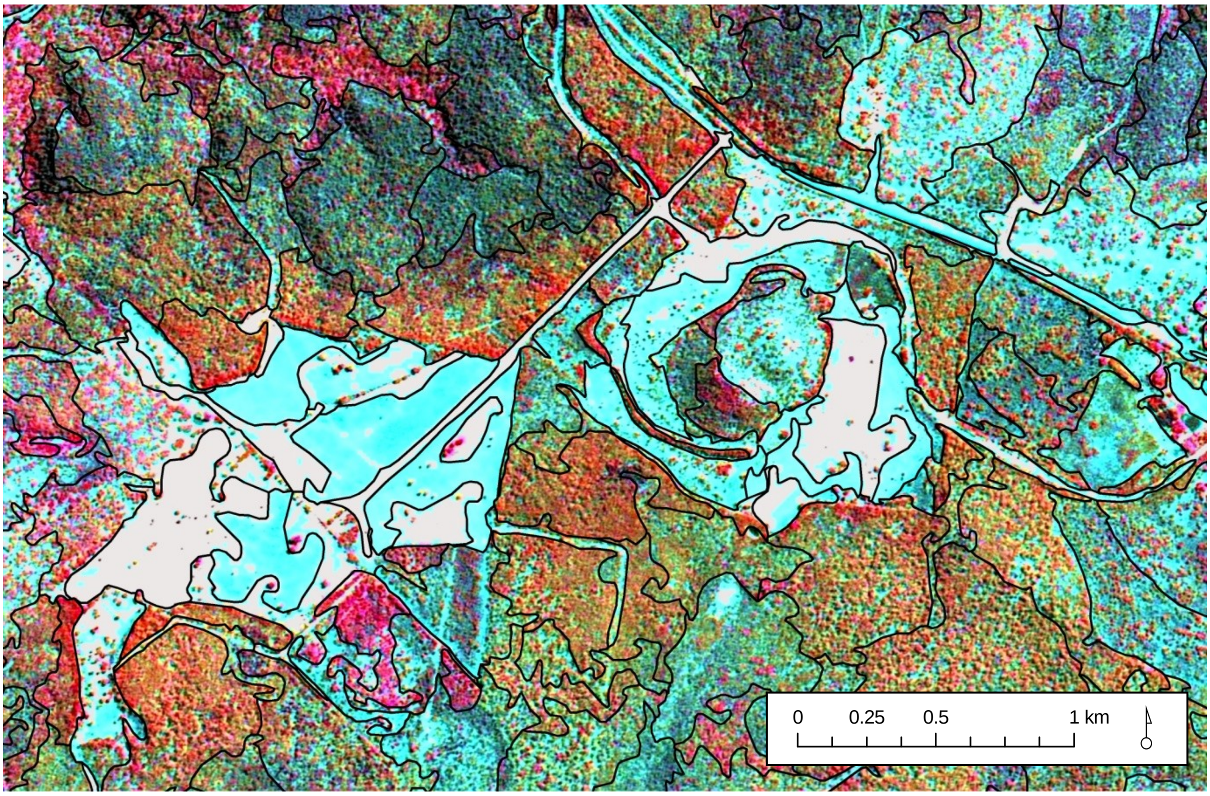

Figure 8.19 Definiens segmentation at the 'optimum' scale offered the best combination of polygon count and area matching but produce results with low geometric accuracy.

Manually delineated polygons based on air photo interpretation (Figure 8.18) effectively map variation in texture and shape but are limited by resolution and the effort applied. Automated segmentation (Figure 8.19) requires no more effort to produce finer scale results but eventually the usefulness of the generalisation that results decreases. Definiens performed well at scale 3. However, this choice of parameter produces results with low geometric accuracy (Figure 8.17). When the polygons were small (Scale 1) the smaller image objects had a much higher topological accuracy. The tested segmentation algorithms performed well on woody and non-woody vegetation boundaries. A standardised setting for SPOT-5 was derived (Scale 3 for Definiens and SCRM) using topological measures to assess performance. However, for segmentation of vegetation community boundaries (internal floristic boundaries in woody vegetation) geometric and topological accuracy was low.

8.3.6 SPOT 5 crown scale classification

I argued in Chapter 6 that the image object scale should match the thematic object scale for accurate classification. The combination of the HyMap Crown Delineation Algorithm pre-processing and ENVI FX allowed the imagery to be partitioned into image objects at the same scale as the target theme (crowns). When using SPOT data as an alternative to HyMap data the spatial and spectral resolution of SPOT-5 prevents the results providing accurate tree species inventory data. However, the image objects created are useful in multi-scale classification because they take account of the heterogeneity in natural landscapes (see Figure 8.20). Features such as shadow and clearing can be ignored in a multi-scale classification.

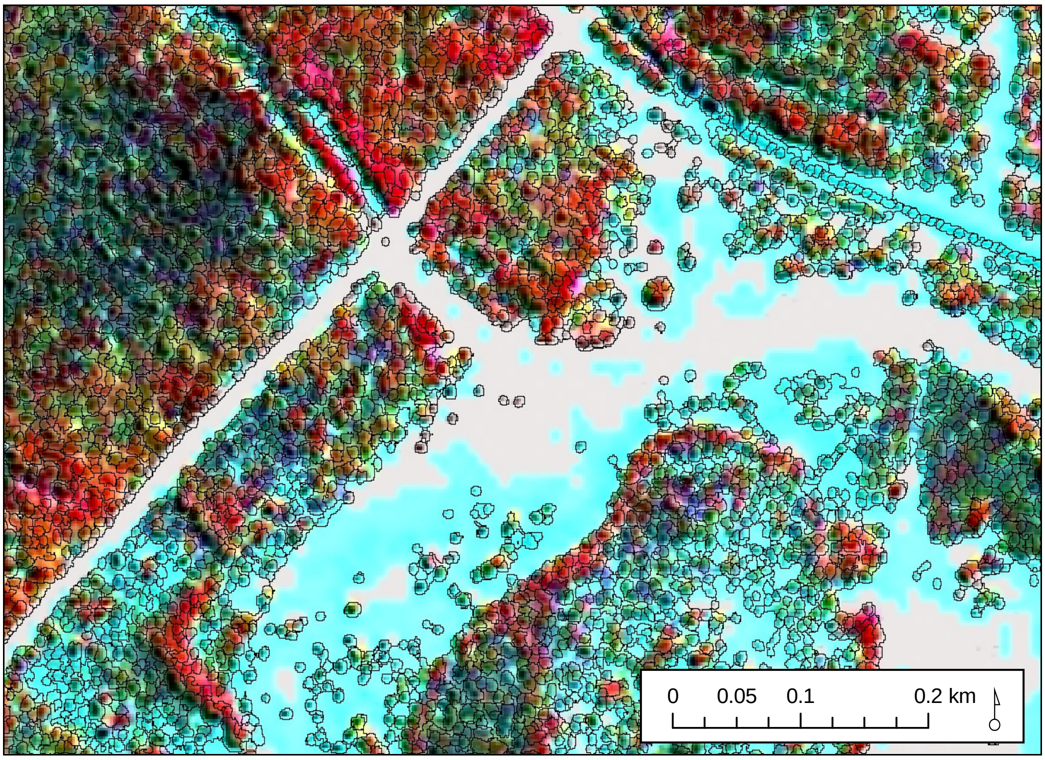

Figure 8.20 Image objects at a crown scale based on SPOT 5 data.

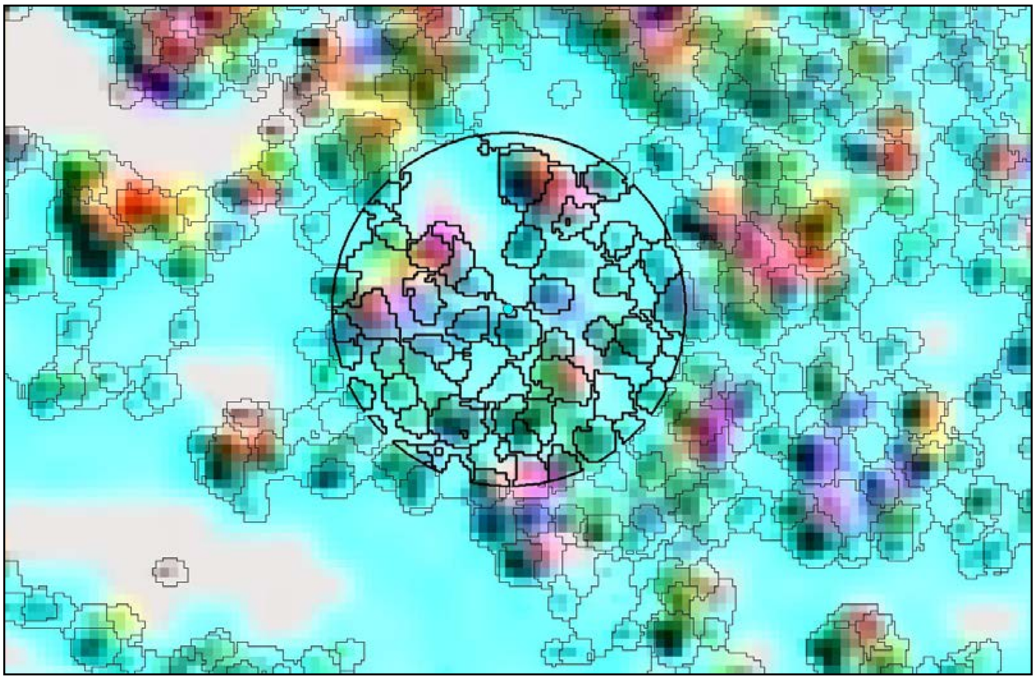

Figure 8.21 Example of a plot located in open woodlands.

Existing plot scale information (Ismay et al., 2004) has a GPS location but no spatial information about the distribution of species in the plot. As an example, site number COBB0125 is pictured (Figure 8.21). Tree crowns are scatted and isolated in Grassy White Box. The objects in bold are within a 50m radius of the plot centre.

The dominant species were listed in the field with comments about condition and structure. It was attributed with a floristic unit and the structure was described as shrubby tall open woodlands to open forests. This level of detail is too broad for precise crown scale classification so the species lists at each plot had to be examined.

The plot information described the surrounding area as 'Grassy White Box Woodland' with moderate community condition. The reflectance at this site is high because it is mostly grassland or exposed soil. This prevented crowns at this site being used as training areas even though White Box was clearly dominant over-storey species Table 8.5.

Table 8.5 Dominant species from the mid-storey and tallest strata were extracted from a full floristic list.

Site Number	Stratum	Lower height (m)	Upper height (m)	Percent cover (%)	Dominant species 1	Dominant species 2	Dominant species 3
COBB0125	Mid-storey	3	10	10	White Box	Acacia pennінervis	-
COBB0125	Tallest	16	16	25	White Box	-	-

Training and modelling were more successful in closed forest. From the dominant species recorded at each plot 275 training samples were selected with 25 different attributes. After classes with only one example were removed there were 20 classes, which include shadow and two grassland classes (Table 8.6). The WEKA results (Table 8.8) indicate that LMT showed moderate accuracy (kappa = 0.52) using image object means from 3 band of pan sharpened and histogram equalised SPOT-5 data. The crown scale classification accuracy was high for distinctive classes. The tall and spectrally distinctive Angophora floribunda and bright clearings performed particularly well. The dark and narrow crowned Callitris endlicheri, and Eucalyptus volcanica and Eucalyptus dealbata could be differentiated from other eucalypts. The confusion matrix (Table 8.1) shows that species with a mallee growth form (*Eucalyptus blakelyi*) or those in the mid-storey (Casuarina species) were rarely classified accurately. *Eucalyptus melliodora* and *Eucalyptus albens* were easily confused with each other.

Table 8.6 Species codes and scientific names of species used in crown and stand scale modelling.

Code	*Species Description*	Code	*Species Description*	Code	*Species Description*
YLB	*Eucalyptus melliodora*	NLI	*Eucalyptus crebra*	BLKY	*Eucalyptus Blakelyi*
WCP	*Callitris glauca*	MAC	*Eucalyptus macrorhyncha*	BCP	*Callitris endlicheri*
WBO	*Eucalyptus albens*	LFB	*Eucalyptus nortonii*	APLB	*Eucalyptus bridgesiana*
VOL	*Eucalyptus volcanica*	DEL	*Eucalyptus dealbata*	ANG	*Angophora floribunda*
UNKN	*Unknown*	COR	*Corymbia trachyphloia*	RED	*Eucalyptus camaldulensis*
SHD	*Shadow*	CLRA	*Clearing Aqua*	CAS	*Casuarina*
ROS	*Eucalyptus rossii*	CLRW	*Clearing White*		

Table 8.7 Modelling results in a confusion matrix. LMT was conducted on 252 samples.

Modelled as->				**a**	**b**	**c**	**d**	**e**	**f**	**g**	**h**	**i**	**J**	**k**	**l**	**m**	**n**	**o**	**p**	**q**	**r**	**s**	**t**
a	=	**YLB**		4	0	2	2	0	0	0	0	0	6	0	0	0	0	0	0	0	0	0	1
b	=	**WCP**		0	0	0	0	0	0	0	0	0	0	0	1	0	0	0	0	0	3	0	0
c	=	**WBO**		2	0	4	1	0	0	1	0	2	8	0	0	0	0	0	0	1	0	0	1
d	=	**VOL**		0	0	0	9	0	0	0	0	1	0	0	0	0	0	0	0	0	0	0	0
e	=	**UNKN**		0	0	0	0	8	0	0	0	0	0	0	0	0	0	0	0	1	0	0	0
f	=	**SHD**		0	0	0	2	0	0	0	0	1	0	0	1	0	0	0	0	0	0	0	0
g	=	**ROS**		0	0	1	0	0	0	3	0	9	0	0	1	0	0	0	0	0	0	0	0
h	=	**RED**		1	0	0	0	0	0	0	0	1	4	0	0	0	0	0	1	0	0	0	1
i	=	**NLI**		1	0	2	0	0	0	5	0	21	0	0	0	0	0	0	0	0	1	0	0
j	=	**MAC**		1	0	2	0	0	0	0	0	0	26	0	0	0	0	0	1	0	0	0	2
k	=	**LFB**		0	0	1	0	0	0	0	0	0	3	0	0	0	0	0	0	0	0	0	0
l	=	**DEL**		0	0	0	0	0	0	1	0	0	0	0	9	0	0	0	0	0	1	0	0
m	=	**COR**		0	0	0	0	0	0	0	0	1	0	0	0	0	0	0	0	0	3	0	0
n	=	**CLRA**		0	0	0	0	0	0	0	0	0	0	0	0	0	6	0	0	0	0	0	0
o	=	**CLRW**		0	0	0	0	0	0	0	0	0	0	0	0	0	0	5	0	0	0	0	0
p	=	**CAS**		5	0	0	0	1	0	0	0	1	1	0	0	0	0	0	1	0	0	1	0
q	=	**BLKY**		0	0	1	0	0	0	0	0	0	7	0	0	0	0	0	0	0	0	0	1

r	**=**	**BCP**		0	0	0	0	0	0	0	0	2	0	0	0	0	0	0	0	0	17	0	0
s	**=**	**APLB**		3	0	0	0	0	0	0	0	0	0	0	0	0	0	0	0	0	0	0	0
t	**=**	**ANG**		0	0	1	0	0	0	0	0	0	3	0	0	0	0	0	0	0	0	0	31

Table 8.8 Modelling results based on 252 'crown' objects with 20 attributes including shadow and two classes of grassland.

Description	Count
Correctly classified instances	144
Incorrectly classified instances	108
Total number of instances	252
Percent Correct	0.57
Kappa statistic	0.53

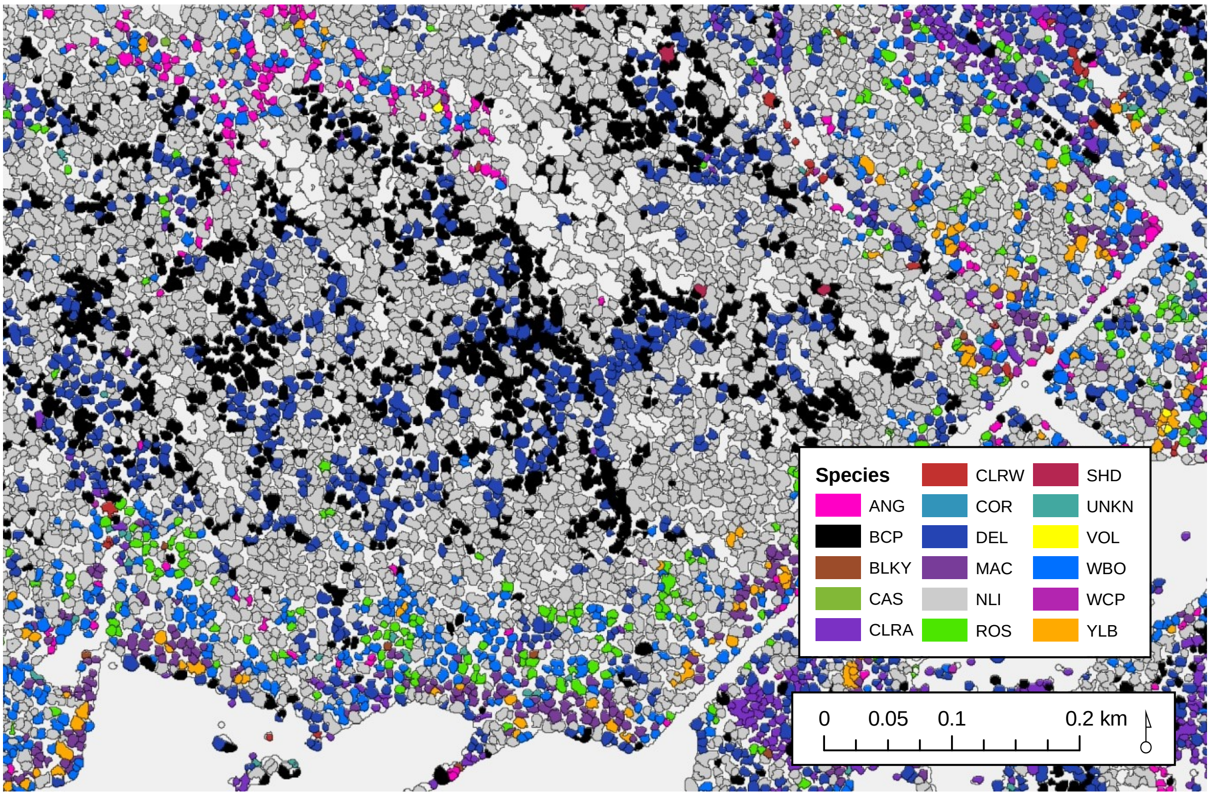

Figure 8.22 Tree crowns automatically delineated using the HyMap Crown Delineation Algorithm pre-processing and ENVI FX was classified using LMT.

8.3.6.1 SPOT 5 multi-scale classification results

The automated segmentation results are over-segmented. However, the added detail of variation of vegetation patterns is not limited by effort applied (Figure 8.24). Each image object has a relative number and area of classified tree crowns nested beneath it (Figure 8.24). Therefore objects can be classified based on cover and abundance of individual species (Figure 8.25).

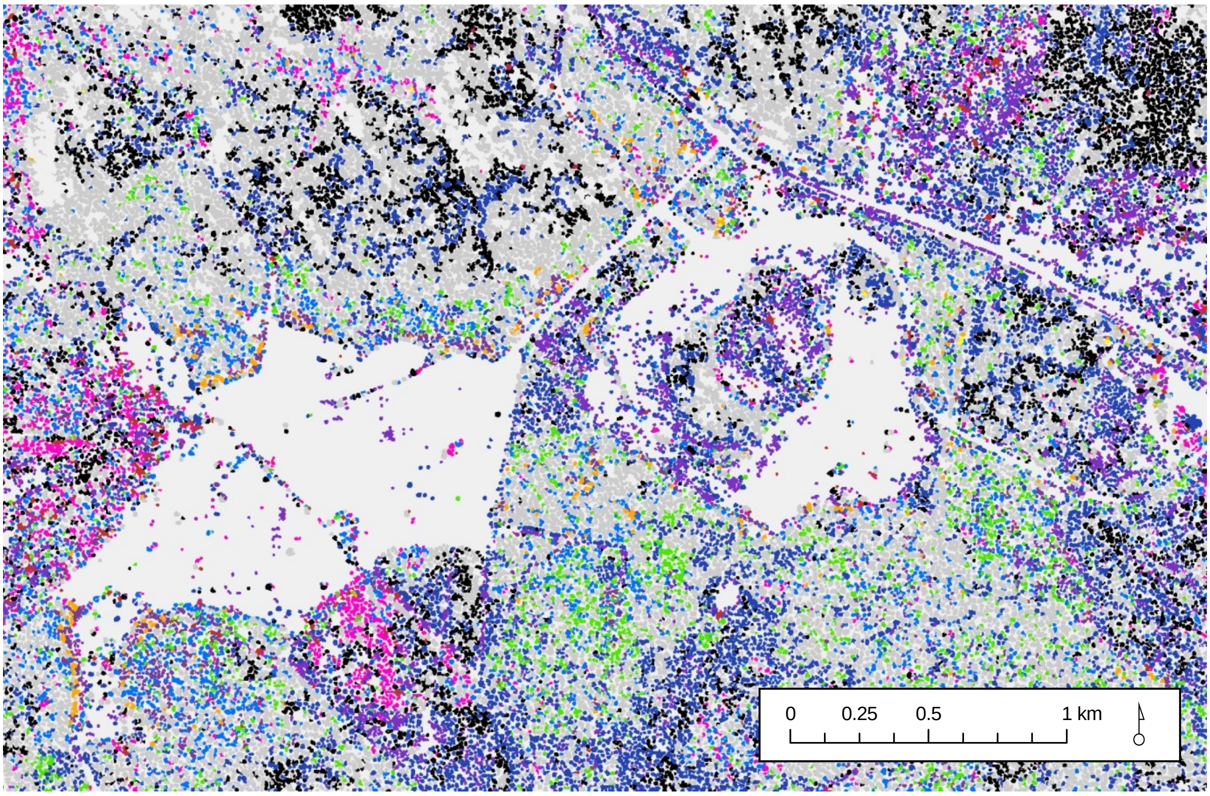

Figure 8.23 Tree crowns delineated from pan sharpened SPOT 5 imagery can be classified based on training samples.

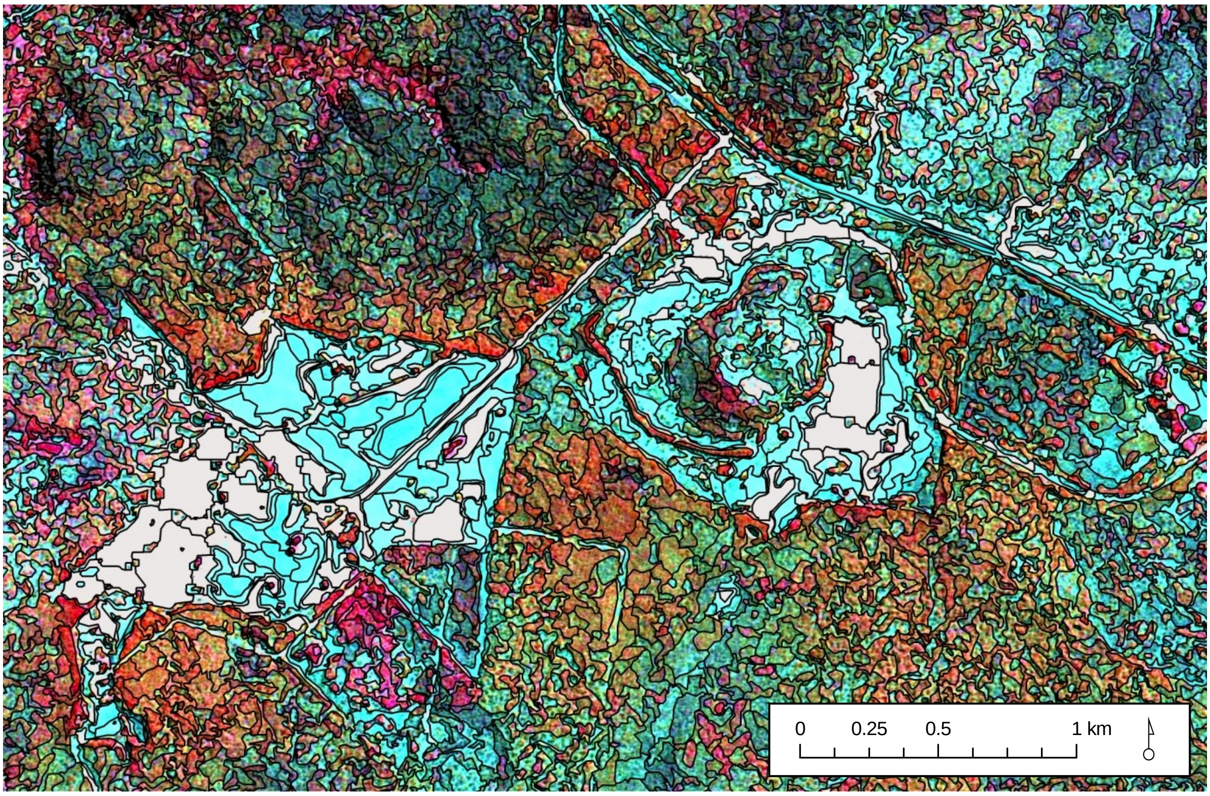

Figure 8.24 Over-segmentation allows for most variation in vegetation patterns at a patch scale to be recorded.

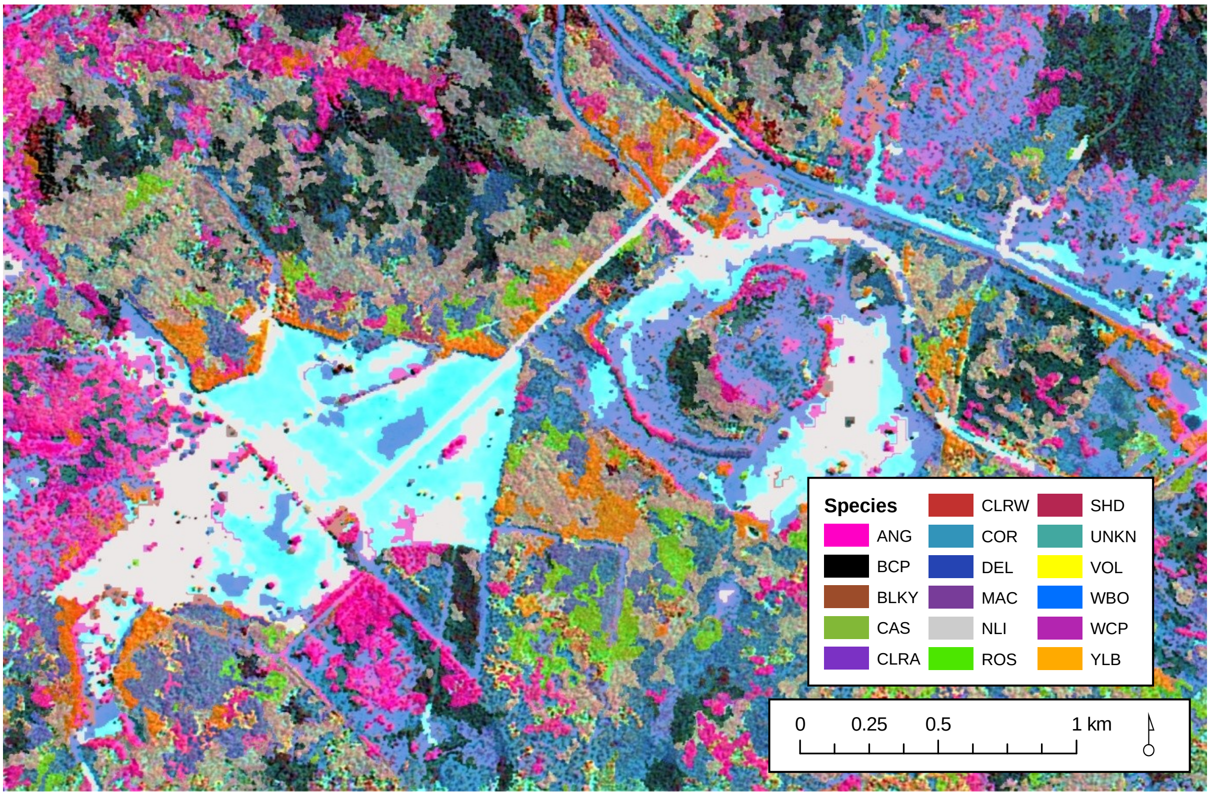

Figure 8.25 Patch scale image objects classified based on cover and abundance of crown scale sub-objects (crowns).

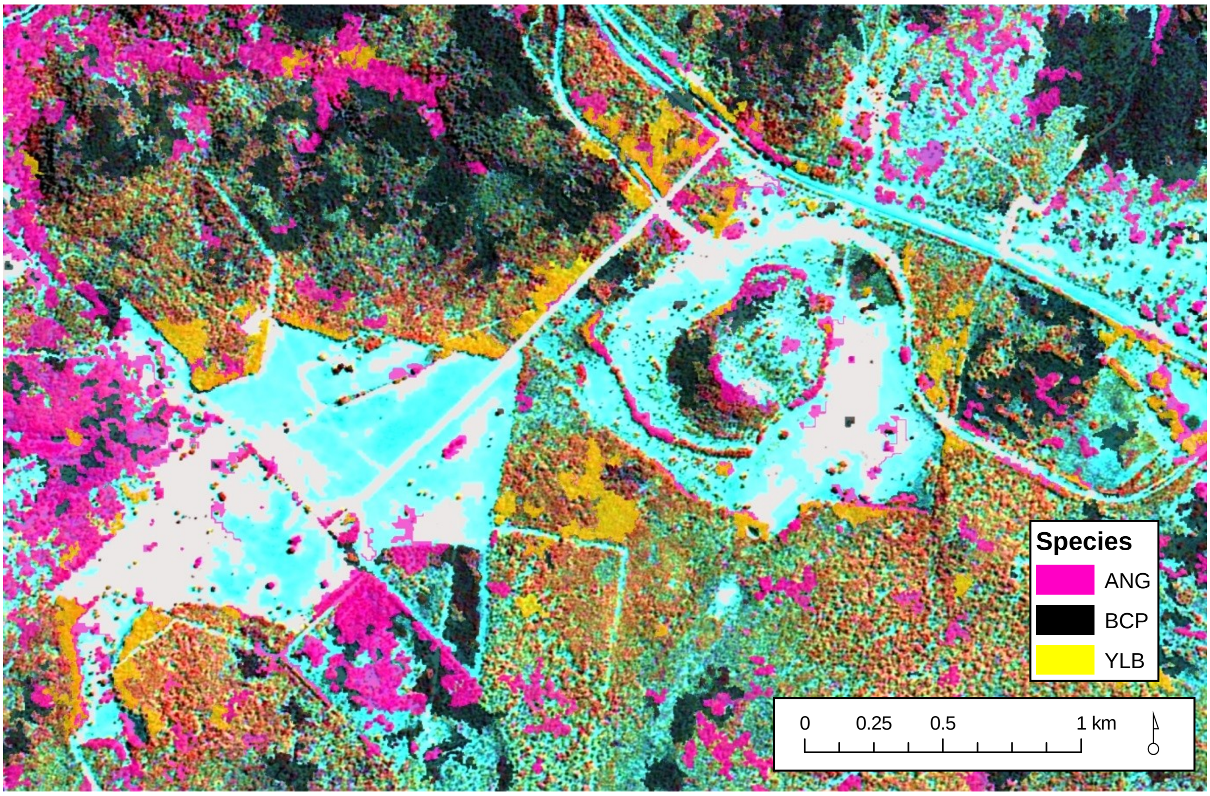

Figure 8.26 Patch scale image objects classified based on dominant crown species. This example shows objects with greater than 20% cover of Callitris endlicheri, Angophora floribunda or Eucalyptus melliodora.

Despite greater uncertainty in the modelling than seen at the Jilliby site, and the lack of data on the spatial distribution of species, the model was applied across the landscape as a proof of concept. The model could reliably differentiate between several broad groups of woody vegetation. The cypress pine species (*Callitris endlicheri* and *Callitris glauca*), and rough barked apple (*Angophora floribunda*) were easily differentiated from eucalypt species. *Eucalyptus crebra*, *Eucalyptus macrorhyncha,* and *Eucalyptus volcanic* could also be differentiated based on SPOT 5 spectral response. However, there were eight other eucalypt species sampled that were consistently confused with other species.

Figure 8.26 illustrates how image objects at a patch scale can be classified on the cover and abundance of individual species. *Callitris endlicheri* is easily identifiable by its dark photo pattern in SPOT 5 imagery. Despite a limited number of crown samples the mapping followed the expected distribution. *Callitris endlicheri* features a small narrow crown but was easily classified when all polygons with >20% were cover were selected. Tree counts are also possible though are less reliable. Similarly, *Angophora floribunda* patches were effectively classified despite them often occurring in shady gullies that would usually be problematic in a raster based classification. Shadow could be classified at a crown scale level and ignored for the patch scale. *Eucalyptus melliodora* is an example where the crowns were not particularly distinct but the model output follows the landscape position expected, i.e. large over mature tree crowns on the edge of cleared woodlands.

8.3.6.2 Smoothing of community polygon raster boundaries

The default polygon output from Definiens Developer is a polygon raster. The exported shape file describes the border of the image objects along a pixel raster which can lead to jagged and confusing edges and poor performance in boundary accuracy measures. Smoothed boundaries are easier to interpret as they remove the spatial noise associated with jagged edges.

Definiens Developer 7 has a variety of tools for smoothing region boundaries. However, these generated significant artefacts and distortion in the output regardless of scale. The Polynomial Approximation with Exponential Kernel (PAEK) smoothing (Bodansky et al., 2002) was found to provide good results. It calculates smoothed lines using a parametric continuous averaging technique, making the results easier to interpret for users accustomed to air photo interpretation (see Figure 8.27). Reference boundaries from higher resolution data (bottom left) are used to calculate boundary fit (bottom right) and the Area-Fit-Index.

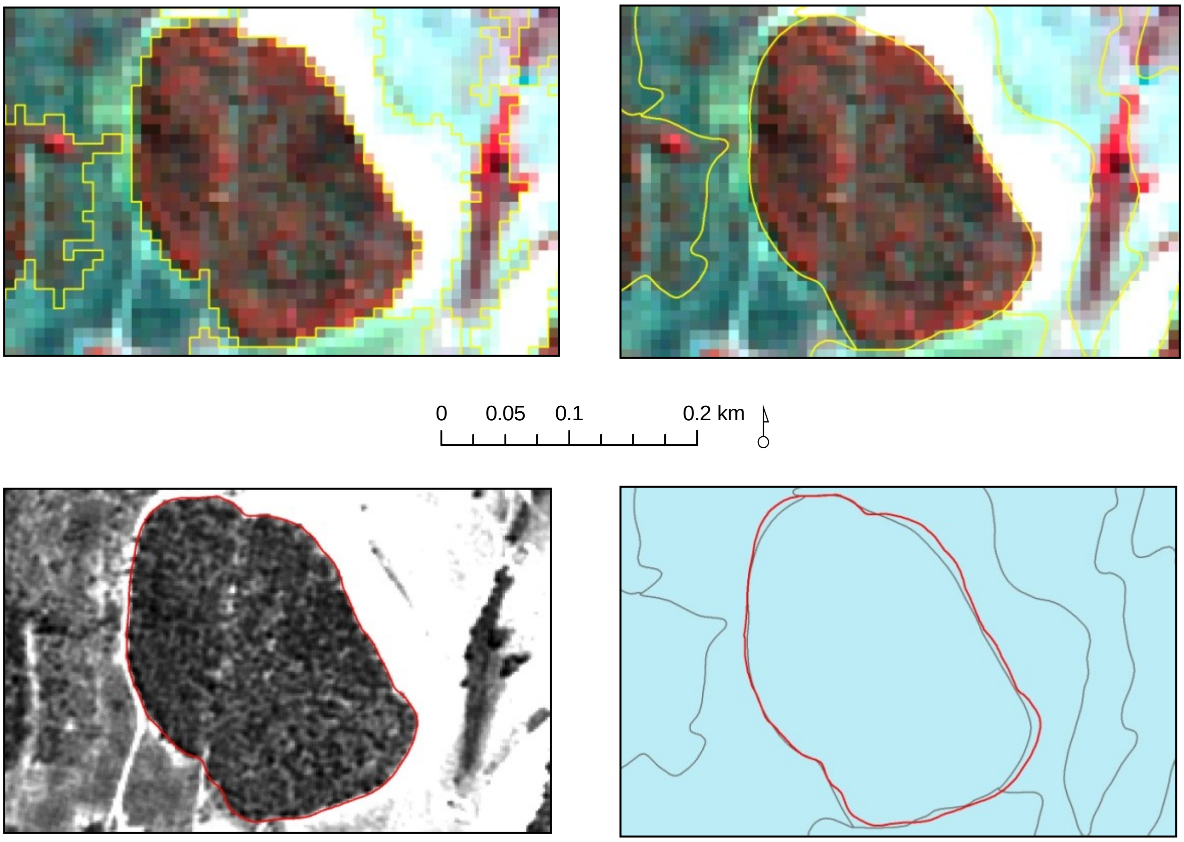

Figure 8.27 Segmentation results are a polygon raster by default (top left). The best performing smoothing solution was found to be the PAEK algorithm.

8.4 Discussion

The segmentation quality of three algorithms was evaluated at multiple scales using SPOT-5 data. The reference image objects were delineated manually. The measure of success for each algorithm included global statistics, area fitting, and a comparison of the distance between object centroids. The aim was to assess the operational feasibility of using segmentation on low spectral and spatial resolution data at regional scales.

The results show that pre-processing had the effect of making the equivalent scale finer, or producing more image objects than at the same scale using digital number data. Visually, this type of pre-processing increased between class variation and minimised illumination artefacts. Visual methods are widely-used for assessing image segmentation quality (Zhan et al., 2005).

Segmentation was performed at multiple scales, so that the optimal scale parameters could be selected based on reference polygons. The 'optimum' scale of segmentation was defined using topological and geometric metrics. For example, the optimum scale of segmentation for delineation of the binary woody vegetation reference objects for Definiens was Scale 3 for the topological measures tested (Figure 8.10).

However, when the internal boundaries of vegetation were included (Figure 8.11) the only way to produce segmented objects that were comparable with the size and shape of API was to use Scale 5, where all other measures performed poorly. Similarly, despite the good performance of Definiens at Scale 3, this choice of parameter produces results with low geometric accuracy when assessing vegetation community boundaries (Figure 8.17). The Euclidean distance between reference objects and segmented objects at Scale 3 was unsatisfactory (~500m) (Table 8.4).

So, Definiens, SCRM and ENVIFX performed poorly when trying to replicate the size and shape of community scale polygons based on API. However, a number of geometric and topological measures showed good performance at fine scales. Only the measures of global statistics and those used for quantifying over-segmentation detracted from the results.

The solution presented was to over-segment the imagery and rely on a classification of each small object to create meaningful landscape units following much the same schema as Chapter 6. Once tree crowns (or components of tree crowns) were classified (Figure 8.22) they were used to classify patch scale segmentation (Figure 8.24) by individual species occurrence (Figure 8.26) and cover/abundance. To create a community scale vegetation map these classes were merged (Figure 8.25).

Where sufficient field data are available, sub-object statistics at a crown scale can be used for classification at a community scale. The crown scale classification based on SPOT-5 allowed for the proportion of dominant species to be estimated. This approach produced meaningful arrangement of species at a formation level. Hilltop species were restricted to hilltops and woodland species were restricted to floodplains (Figure 8.25).

More field samples and better information about the spatial distribution of species within and around the plots would be needed for conclusive results. The approach dealt well with a heterogeneous landscape by allowing small patches of cleared land and shadows to be classified separately.

8.5 Conclusion

This study differs to previous research in a number of ways. The automated analysis at Coonabarabran is compared to vegetation boundaries determined manually by a human interpreter. More importantly, it assesses the performance of segmentation for detecting internal boundaries between vegetation types within closed forest.

Empirical evaluation of a segmentation algorithm's performance is relatively straight forward for isolated stands of trees and boundaries in modified landscapes. However, evaluating internal boundaries in closed forest is more challenging as their precise location is subjective.

Definiens Developer 7, the ENVI 4.5 Feature Extraction Module, and Size Constrained Region Merging all successfully segmented data at fine scales, but artefacts of their algorithms appear at broader scales. Vegetation mapping based on SPOT-5 data should take a multi-scale approach; classifying fine scale sub-objects based on field sampling and merging them based on class to create final map units.

Chapter 9

Discussion and Conclusions

The aim of this thesis was to develop tools for the delineation and classification of native vegetation. I argued that the main obstacle to successful spatial modelling of field data has been a lack of spatial and spectral resolution and an inability to make meaningful predictions through a change in scale. I suggested that heterogeneous vegetation needs to be analysed across multiple scales to be able to effectively categorise it as a vegetation community. Individual tree crown delineation and classification alone will not describe a community. Nor is it possible to delineate a patch of vegetation and decipher the component species based on the average spectral response.

A multi-scale, object-based, hierarchical approach was introduced to generalise floristic data collected at the plot scale to a vegetation community map using remote sensing. This framework used the cover and abundance of classified tree crown objects to inform the classification of larger patches of vegetation. Community scale image objects were then named using the same hierarchical framework used by ecologists in plant ecology.

I conclude in this chapter by describing what was novel in the context international studies. I look at the limitations of the research, and conclude by suggesting future avenues of research. I also cite some specific lessons relevant to vegetation mapping in Australia.

9.1 Hyperspectral remote sensing of vegetation type

There were a number of challenges in the use of airborne hyperspectral data but the solutions to these problems ended up enhancing its utility. The spatial precision of HyMap acquired at low altitude and over hilly terrain was poor. To improve the spatial precision, the HyMap data were co-registered with small footprint lidar. This took advantage of the additional spatial precision of lidar and the structural information implicit in an active canopy penetrating system.

An automated area-based ground control point selection algorithm selected 10, 000 GCPs were generated with an average RMSE of less than 3.0. This proved sufficient to co-register individual crowns in most cases. The key innovation here was to pre-process the optical data to offer a greyscale image that accentuated tree crowns so that they could be matched the canopy height model. Other studies that sought to co-register imagery and lidar have had mixed success. Mundt et al. (2006) successfully used GPS ground control based selection of GCPs but this was in flatter terrain. Koukoulas and Blackburn (2005) saw registration errors for small crowns (Koukoulas and Blackburn, 2005).

The practical limitations on field sampling presents a challenge for high spatial resolution hyperspectral remote sensing, including studies using image based training areas. There were hundreds of thousands of tree crowns that needed to be classified at the Jilliby site and only 130 plots were sampled (~800 tree crowns). However, this is a relatively high sampling density for the size of the study area when compared to other studies (Bunting and Lucas, 2006, Ismay et al., 2004).

Machine learning algorithms offer flexibility for classifying highly dimensional hyperspectral data. The results can reduce the number of bands needed in classification, further reducing co-linearity, and offer new insights into the structure of data. For example, the bands that contributed the most to differentiating crown species in the study area were in the SWIR and visible parts of the spectrum in sectors related to chlorophyll and leaf-moisture.

Logistic Model Trees (LMT) has rarely been used to classify vegetation. It combined the transparency of CART, the performance of MP and the inbuilt parameter (band) selection of LDA. It uses a step-wise fitting process to constructs the logistic regression models and can select relevant attributes (bands) in the data in a natural way. And it uses cross-validation to find a number of boosting iterations (Friedman et al., 2000) so that it doesn't overfit the training data. It also has the advantage of being computationally efficient and will scale well to larger datasets.

The HyMap Crown Delineation Algorithm (HCDA) introduced in Chapter 6 showed it was possible to use HyMap as the sole source of image data in the delineation of large tree crowns. The accuracy was assessed in terms of topological and geometric fit and classification accuracy. The imagery is coarser than those used in existing tree delineation studies (Bunting and Lucas, 2006, Culvenor, 2002, Leckie et al., 2005a). I would argue that the use of HyMap at a crown scale is defensible for large crowns but only if a secondary high spatial resolution data source is available selecting training areas and for validation.

The HCDA is based on existing principles of local maxima detection, top hat segmentation and watershed segmentation. It is computationally efficient and allows for extraction of spectral information from HyMap data for individual tree crowns. More samples are for a comprehensive quantitative evaluation. The study showed it performed well with large crowns, with some over-segmentation, but its performance was only moderate in open forest with exposed soils or in homogenous stands of small crowns.

Bands used for segmentation were selected by MLA, which has not featured in the literature, based on the premise that they would create objects that best differentiated species. SCRM created patch scale objects that were populated with species cover and abundance information for use in community scale classification. One of the advantages multi-scale, object-based classification framework presented here is that segmenting representative objects, whether at a branch scale or a small homogenous stand, can potentially allow for robust image objects for spectral extraction.

This approach was trialled on SPOT 5 data and produced meaningful arrangement of species at a formation level. Hilltop species were restricted to hilltops and woodland species were restricted to floodplains. The optimum scale of segmentation for delineation of vegetation communities was determined for three segmentation algorithms using quantitative metrics so the algorithms could be compared without bias. Air photo interpretation (API) was used as reference data and topological and geometric accuracy was assessed at multiple scales using un-processed and pre-processed imagery.

Again, more samples are required for an exhaustive quantitative comparison but the results were clear. Segmentation algorithms cannot produce 'API-like' polygons just by increasing the scale. Shadow and clearings dominate boundary detection and region-merging at course scales. The image-objects boundaries no longer intersect with thematic boundaries making the premise of classification tenuous. It is the same problem dealt with by Strahler et al. (1986) continuous scene model, where coarse resolution image elements are larger than the thematic attributes being mapped. The solution is a multi-scale, object-based classification framework where only small crown scale objects have relatively homogenous spectral and physical values are classified. The results can inform the classification of larger patches.

Australian natural resource management in require that vegetation be mapped and monitored but the limited resources available dictate that ecologists tasked with this responsibility have to rely on remote sensing data. Unfortunately, the existing operational survey methods for vegetation type are not ideal for use as training data for remote sensing.

Australian guidelines for vegetation survey methods do recommend that homogenous patches of vegetation should be sampled in the field (Hnatiuk et al., 2009, McCauley, 2006, Sivertsen and Metcalfe, 1995). However, native vegetation rarely occurs in homogenous stands. Instead it occurs in heterogeneous patches nested in a mosaic (Forman, 1995).

Hierarchy theory acknowledges the heterogeneity in natural systems and proposes that the classification of a landscape unit is dependent on the scale of observation. Ecologists conduct patch and crown scale analysis, and require remote sensing to answer questions at these regional scales. The sampling scale of operational satellites data is fixed at the sensor, but plot size is flexible.

To make the most of limited survey data I argued for a hierarchically nested series of plots. A 20m by 20m plot is considered a reasonable area for many vegetation types, the main exceptions being grassland (too large), and wet Eucalypt tall forests (too small) (Emery et al., 2001).

9.2 Fuel loads and remote sensing

Vegetation structure was assessed by quantifying forest fuel load using remote sensing. Hyperspectral vegetation indices outperformed broad-band indices for mapping the spatial distribution of forest fuels. The narrow bands provided a greater variety of indices less sensitive to saturation in high canopy cover.

Small footprint lidar successfully penetrated the canopy and offered quantitative information about the structure of the understorey. However, the total fuel load assessed in the field was dominated by leaf litter component in wet forest, which was problematic to quantify with remote sensing.

The Jilliby site was subject to rigorous field sampling of fuel structure and weight, which raised a number of important issues related to how fieldwork is conducted for remote sensing studies. We found the visual assessment of fuel hazard scores was not directly linked to the weight of fuels. In addition, the two rapid field assessment methods trialled gave different results for the same sites.

Existing research indicated that there is a relationship between tree height and fuel loads and between NDVI and fuel loads. However, no significant relationship was found between broad-band satellite data and tree height in the wet forest of the study site. Canopy cover was found to vary independently of available fuel load, particularly in tall, closed forest. Lidar was able to accurately measure the elevated fuels across the site, but this was only a small component of the overall fuel hazard as measured by visual assessment scores and destructive sampling.

A new index that summarises the Vesta fuel scoring attributes was introduced and found to be better correlated with remote sensing variables than the OFHG method. The surface profile component of the Vesta scores proved to have a stronger relationship with the destructive sampling fuel weights than the surface measurements of the OFHG. Destructive sampling produced results that were only weakly correlated with visual assessment score totals and remote sensing variables. This would likely change if larger areas were completely harvested, as seen in the successful quantification of total biomass by remote sensing (Turner, 2006). However, the relationship between total biomass and fuel load is uncertain.

Unfortunately, the OFHG did not collect continuous variables for the surface fuel depth. Thus, the method did not capture enough dynamic range in the surface fuel layer for effective modelling, as it constituted the bulk of the accumulated fuel hazard. I would recommend a more quantitative approach for the visual assessment of surface fuel sampling, as seen in the Vesta method.

9.3 Limitations of the research

Both study sites featured in this research were the subject of previous vegetation mapping (Bell and Driscoll, 2006, Ismay et al., 2004). The floristic groups mapped had been named on the basis of the dominant crown species and this research followed a similar approach.

Since optical remote sensing instruments detect changes in reflectance of material surfaces the study was limited this study to canopy species of woody vegetation. The use of this classification framework for nature conservation rests upon the assumption that they provide information about the distribution of many species, though this is rarely tested (Burgman et al., 1993). Predicting the distribution and composition of understorey species based on dominant overstorey species is problematic.

The crown species sampled at the Jilliby site were dominated by Blackbutt (*Eucalyptus pilularis*) as it has a characteristically large crown and was present in all strata. Independent species data was available for use in classification but further ground samples would be required to determine how robust the classification is in areas outside those described in the plots. Not all species in the study site were sampled in the field, and not all of the sampled species were included in the model. An additional source of error is that crown surveys record the location of crown stems, not the canopy centre. While visual adjustment of crown centres has precedent in the literature (Clark et al., 2005), it does introduce a source of bias.

The primary result of this thesis was a vegetation map classified on cover and abundance of dominant crown species. The multi-scale, object-based, hierarchical approach is used to generalise floristic data collected at the plot scale is novel. However, the approach is burdened by the need to survey tree crowns and can be confounded by highly diverse ecosystems. The assessment of vegetation type and fuel loads both have a temporal component; this was not assessed in the thesis.

9.4 Future research

Processing HyMap data with spatial co-registration, model-based atmospheric correction and cross-track illumination correction has the effect of changing the reflectance values of hyperspectral data. The effect pre-processing had on segmentation and classification at a crown object scale is unknown but would be a fruitful avenue for further research. For example, Behnia (2005) compared four frequently adopted image fusion algorithms (pan-sharpening) and concluded that the tested approaches improved the spatial resolution effectively but distorted the original spectral signatures.

Previous studies have shown that using an image-object based approach can improve classification accuracy over pixel-based approaches (Addink et al., 2007, Baatz and Schäpe, 2000, Benz et al., 2004). More research is required to determine if a multi-scale, object-based approach to vegetation types will provide gains over single scale results.

The scope of this work was restricted to spectral values and ignored textural and semantic information. Using expert knowledge to help constrain the distribution of vegetation types has shown to be successful in vegetation modelling (Keith and Bedward, 1999). Utilising this approach to create rules based on landscape position for patch scale polygons should further improve classification accuracy.

Airborne hyperspectral sensors are clearly disadvantaged by the limited spatial coverage they can provide. They are best used in concert with other data sources, which provide greater temporal and spatial coverage. They could be targeted towards high conservation or high risk areas or used to improve the analysis of broadband satellite data. For example, lidar and HyMap could be used as training areas to develop a relationship between structure and satellite based reflectance or for validation.

Fuel loads were predicted with higher accuracy in drier and more open forest. An object-based approach may also improve performance, as this has proven to be the case in other studies of structural attributes (Addink et al., 2007).

More work needs to be done on assessing segmentation quality. Finer scale air photo interpretation would be helpful as well as higher density field survey data. Varying the inputs to segmentation to include terrain and multiple sensor data is also promising.

9.5 Conclusions

Turning plot data into maps requires a transition between scales. The only tool capable of providing current information about landscape scale variables is remote sensing. Plot data needs to be used to train the classification of remote sensing data but a number of obstacles have been encountered.

Pixel-based classification of vegetation have underperformed in NSW (McCauley, 2006). They cannot transparently generalise local scale heterogeneity into broad map units as there is too much noise in natural images for them to be interpreted by managers of natural resources.

Hyperspectral remote sensing extra information, particularly in the SWIR, for differentiating eucalypt species. I presented a new multi-scale, object-based framework for classifying vegetation type using hyperspectral imagery. No assumptions were made about a relationship between scales of field information and remote sensing. An explicit link was formed by quantifying species diversity at a plot scale. This has enabled the multi-scale mapping of vegetation type that has potential uses at course scales in natural resource management and at fine scales for local decision making.

Forest fuel loads were found to vary independently of canopy cover in tall, wet forest. The relationship between the accumulation of fuels and remote sensing variables was clearer in the dry open forest that is more representative of the regional ecology. Lidar and optical sensors struggled to detect the leaf litter that drove overall fuel load.

I would encourage other remote sensing research to use the same language, and the same appreciation of scale, as ecologists. The reaction from government partners to chlorophyll content and sub-pixel abundance maps was not encouraging. However, my attempts to map the same variables they collect in the field were met with great enthusiasm.

Appendix

Source code for *HyMap Crown Delineation Algorithm in IDL (Chapter 4)*

Semi-automated crown delineation with HyMap: Watershed Workflow in IDL
To apply the watershed algorithm open the IDL Interactive Development Environment and follow the sample code below. Lines that are preceded with ";" are comments and do not have to be entered. Each line can be entered one at a time at the command prompt of the Interactive Development Environment, which will preview each step and create an output TIFF image.
IDL programming code for the watershed algorithm

```
;Radius of disc...
r = 2
;Create a disc of radius r
disc = SHIFT(DIST(2*r+1), r, r) LE r
 ;Read the image
a = READ_TIFF('USER_FILENAME.tif')
 ;Invert the image
b = MAX(a) - a
TVSCL, b, 0
 ;Remove holes of radii less than r
c = MORPH_CLOSE(b, disc, /GRAY)
TVSCL, c, 0
 ;Create watershed image
d = WATERSHED(c, CONNECTIVITY = 8, /LONG)
;Display it, showing the watershed regions
TVSCL, d, 0
;Merge original image with boundaries of watershed regions
e = a > (MAX(a) * (d EQ 0b))
TVSCL, e, 0
WRITE_TIFF, 'USER_FILENAME_D.tif', (d)
```

References

ACCAD, A. & NEIL, D. T. 2006. Modelling pre-clearing vegetation distribution using GIS-integrated statistical, ecological and data models: A case study from the wet tropics of Northeastern Australia. *Ecological Modelling,* 198**,** 85-100.

ADAMS, R. & SIMMONS, D. 1999. Ecological effects of fire fighting foams and retardants: a summary. *Australian Forestry,* 62**,** 307-314.

ADDINK, E. A., DE JONG, S. M. & PEBESMA, E. J. 2007. The importance of scale in object-based mapping of vegetation parameters with hyperspectral imagery. *Photogrammetric Engineering and Remote Sensing,* 73**,** 905-912.

ALLEN, T. F. H. & HOEKSTRA, T. W. 1992. *Toward a Unified Ecology,* New York, Columbia University Press.

ANDERSON, H. E. 1982. Aids to Determining Fuel Models for Estimating Fire Behavior. Ogden, Utah: United States Department of Agriculture, Forest Service.

ANDREW, M. E. & USTIN, S. L. 2006. Spectral and physiological uniqueness of perennial pepperweed (Lepidium latifolium). *Weed Science,* 54**,** 1051-1062.

ANDREW, M. E. & USTIN, S. L. 2008. The role of environmental context in mapping invasive plants with hyperspectral image data. *Remote Sensing of Environment,* 112**,** 4301-4317.

ANDREWS, P. L. & QUEEN, L. P. 2001a. Fire modeling and information system technology. *International Journal of Wildland Fire,* 10.

ANDREWS, P. L. & QUEEN, L. P. 2001b. Fire modeling and information system technology. *International Journal of Wildland Fire,* 10**,** 343-352.

ARROYO, L. A., PASCUAL, C. & MANZANERA, J. A. 2008. Fire models and methods to map fuel types: The role of remote sensing. *Forest Ecology and Management,* 256**,** 1239-1252.

ASNER, G. P. 1998. Biophysical and biochemical sources of variability in canopy reflectance. *Remote Sensing of Environment,* 64**,** 234-253.

ASNER, G. P., JONES, M. O., MARTIN, R. E., KNAPP, D. E. & HUGHES, R. F. 2008a. Remote sensing of native and invasive species in Hawaiian forests. *Remote Sensing of Environment,* 112**,** 1912-1926.

ASNER, G. P., KNAPP, D. E., KENNEDY-BOWDOIN, T., JONES, M. O., MARTIN, R. E., BOARDMAN, J. & HUGHES, R. F. 2008b. Invasive species detection in Hawaiian rainforests using airborne imaging spectroscopy and LiDAR. *Remote Sensing of Environment,* 112**,** 1942-1955.

ASNER, G. P., PALACE, M., KELLER, M., PEREIRA JR, R., SILVA, J. N. M. & ZWEEDE, J. C. 2002. Estimating canopy structure in an Amazon forest from laser range finder and IKONOS satellite observations. *Biotropica,* 34**,** 483-492.

ASNER, G. P. & WARNER, A. S. 2003. Canopy shadow in IKONOS satellite observations of tropical forests and savannas. *Remote Sensing of Environment,* 87**,** 521-533.

AUSTIN, M. 1987. Models for the analysis of species' response to environmental gradients. *Plant Ecology,* 69**,** 35-45.

AUSTIN, M. P. & BELBIN, L. 1982. A new approach to the species classification problem in floristic analysis. *Australian Journal of Ecology,* 7**,** 75-89.

BAATZ, M. & MIMLER, M. 2002. Bildobjekt-Primitive als Bausteine-Extraktion von Objekten of interest bzw. anthropogenen Objekten basierend auf der expliziten Kanteninformation von Bildobjekt-Primitiven. *GIS und Fernerkundung: Neue Sensoren–Innovative Methoden. Wichmann Verlag, Heidelberg***,** 179–188.

BAATZ, M. & SCHÄPE, A. 2000. Multiresolution Segmentation–an optimization approach for high quality multi-scale image segmentation. *Angewandte geographische informationsverarbeitung,* 12**,** 12-23.

BAI, Y., WALSWORTH, N., RODDAN, B., HILL, D. A., BROERSMA, K. & THOMPSON, D. 2005. Quantifying tree cover in the forest–grassland ecotone of British Columbia using crown delineation and pattern detection. *Forest Ecology and Management,* 212**,** 92-100.
BARRY, K. M., CORKREY, R., PHAM THI, H., RIDGE, S. & MOHAMMED, C. L. 2011. Spectral characterization of necrosis from reflectance of Eucalyptus globulus leaves with Mycosphaerella leaf disease or subjected to artificial lesions. *International Journal of Remote Sensing,* 32**,** 9243-9259.
BEADLE, N. C. W. & COSTIN, A. B. 1952. Ecological classification and nomenclature, with a note on pasture classification by C.W.E. Moore. *Proceedings of the Linnean Society NSW,* 77**,** 61-82.
BEERI, O., PHILLIPS, R., HENDRICKSON, J., FRANK, A. B. & KRONBERG, S. 2007. Estimating forage quantity and quality using aerial hyperspectral imagery for northern mixed-grass prairie. *Remote Sensing of Environment,* 110**,** 216-225.
BEHNIA, P. 2005. Comparison between four methods for data fusion of ETM+ multispectral and pan images. *Geo-Spatial Information Science,* 8**,** 98-103.
BELL, S. & DRISCOLL, C. 2006. Vegetation mapping of the Watagans National Park and Jilliby State Conservation Area. Sydney: Department of Environment and Conservation.
BENSON, J. 2008. New South Wales Vegetation Classification and Assessment Part 2: Plant communities of the NSW South-western Slopes Bioregion and update of NSW Western Plains plant communities. *Cunninghamia,* 10.
BENSON, J. S. 1994. Monaro grasslands. *Cunninghamia,* 3**,** 609–650.
BENSON, J. S. 2006. New South Wales vegetation classification and assessment: Introduction - The classification, database, assessment of protected areas and threat status of plant communities. *Cunninghamia,* 9**,** 331-382.
BENSON, J. S. & ASHBY, E. M. 2000. Natural vegetation of the Guyra (NSW) 1:100 000 map sheet. *Cunninghamia,* 6**,** 747–872.
BENZ, U. C., HOFMANN, P., WILLHAUCK, G., LINGENFELDER, I. & HEYNEN, M. 2004. Multi-resolution, object-oriented fuzzy analysis of remote sensing data for GIS-ready information. *ISPRS Journal of Photogrammetry and Remote Sensing,* 58**,** 239-258.
BINNS, D. L. 1997. Floristic and vegetation patterns of Coolah Tops, New South Wales. *Cunninghamia,* 5**,** 233–274.
BIRTH, G. & MCVEY, G. 1968. Measuring the Color of Growing Turf with a Reflectance Spectrophotometer. *Agronomy Journal,* 60**,** 640-643.
BLOSCHL, G. & SIVAPALAN, M. 1995. Scale Issues In Hydrological Modelling - A Review. *Hydrological Processes,* 9**,** 251-290.
BOARDMAN, J. W. Post-atrem polishing of AVIRIS apparent reflectance data using effort: A lesson in accuracy versus precision. JPL AVIRIS Earth Science Workshop, 1998. Pasadena, CA: JPL Publication Summaries, 53 – 57.
BODANSKY, E., GRIBOV, A. & PILOUK, M. Smoothing and Compression of Lines Obtained by Raster-to-Vector Conversion. Graphics Recognition Algorithms and Applications, 2002. Springer Verlag, 256-265.
BOM. 2008. *Climate statistics for Australian sites* [Online]. Canberra: Australian Bureau of Meteorology. Available: http://www.bom.gov.au/climate/averages/tables/ca_nsw_names.shtml.
BRADSTOCK, R. A., WILLIAMS, J. E. & GILL, A. M. 2002. *Flammable Australia: the fire regimes and biodiversity of a continent,* Cambridge, Cambridge University Press.
BRANDIS, K. & JACOBSON, C. 2003. Estimation of vegetative fuel loads using Landsat TM imagery in New South Wales, Australia. *International Journal of Wildland Fire,* 12**,** 185-194.
BRANDTBERG, T. & WALTER, F. 1998. Automated delineation of individual tree crowns in high spatial resolution aerial images by multiple-scale analysis. *Machine Vision and Applications,* 11**,** 64-73.
BRAUN-BLANQUET, J., FULLER, G. & CONARD, H. 1932. *Plant sociology. The study of plant communities,* New York, McGraw-Hill.
BRODLEY, C. E. & FRIEDL, M. A. 1997. Decision tree classification of land cover from remotely sensed data. *Remote Sensing of Environment,* 61**,** 399-409.

BUCKLEY, A. J. 1992. Fire behaviour and fuel reduction burning: Bemm River wildfire, October 1988. *Australian Forestry,* 55, 135-147.

BUNTING, P. & LUCAS, R. 2006. The delineation of tree crowns in Australian mixed species forests using hyperspectral Compact Airborne Spectrographic Imager (CASI) data. *Remote Sensing of Environment,* 101**,** 230-248.

BURGMAN, M. A., FERSON, S. & AKÇAKAYA, H. R. 1993. *Risk assessment in conservation biology,* Netherlands, Springer.

BURNETT, C. & BLASCHKE, T. 2003. A multi-scale segmentation/object relationship modelling methodology for landscape analysis. *Ecological modelling,* 168**,** 233-249.

BURROWS, N. D. 2001. Flame residence times and rates of weight loss of eucalypt forest fuel particles. *International Journal of Wildland Fire,* 10**,** 137-43.

BUSHFIRES, J. S. C. O. 2002. *Inquiry into 2001/2002 Bushfires* [Online]. Sydney, NSW: NSW Parliament. Available: http://www.parliament.nsw.gov.au/bushfires.

CALVA, T. & PALMEIRIM, J. M. 2004. Mapping Mediterranean scrub with satellite imagery: biomass estimation and spectral behaviour. *International Journal of Remote Sensing***,** 3113–3126.

CARNAHAN, J. A. 1981. Mapping at a continental level. *In:* GILLISON, A. N. & ANDERSON, D. J. (eds.) *Vegetation classification in Australia.* Canberra: CSIRO.

CASTILLA, G. 2004. *Object-oriented analysis of Remote Sensing images for land cover mapping: conceptual foundations and a segmentation method to derive a baseline partition for classification.* PhD, Polytechnic University of Madrid.

CASTILLA, G., HAY, G. J. & RUIZ-GALLARDO, J. R. 2008. Size-constrained region merging (SCRM): An automated delineation tool for assisted photointerpretation. *Photogrammetric Engineering and Remote Sensing,* 74**,** 409-419.

CATCHPOLE, W. R. & WHEELER, C. J. 1992. Estimating plant biomass - a review of techniques. *Australian Journal of Ecology,* 17**,** 121-131.

CHAFER, C. J., NOONAN, M. & MACNAUGHT, E. 2004. The post-fire measurement of fire severity and intensity in the Christmas 2001 Sydney wildfires. *International Journal of Wildland Fire,* 13**,** 227-240.

CHANDLER, C. C. 1983. *Fire in forestry,* New York, Wiley.

CHASTAIN JR, R. A., STRUCKHOFF, M. A., HE, H. S. & LARSEN, D. R. 2008. Mapping vegetation communities using statistical data fusion in the Ozark National Scenic Riverways, Missouri, USA. *Photogrammetric Engineering and Remote Sensing,* 74**,** 247-264.

CHEN, J. M., LIU, J., CIHLAR, J. & GOULDEN, M. L. 1999. Daily canopy photosynthesis model through temporal and spatial scaling for remote sensing applications. *Ecological Modelling,* 124**,** 9-119.

CHENEY, N. P. 1994. Bushfires - An Integral Part Of Australia's Environment. *In:* CASTLES, I. (ed.) *Year Book Australia.* Canberra: Australian Bureau Of Statistics.

CHENG, Y.-B., USTIN, S. L., RIANO, D. & VANDERBILT, V. C. 2008. Water content estimation from hyperspectral images and MODIS indexes in Southeastern Arizona. *Remote Sensing of Environment,* 112**,** 363-374.

CHENG, Y.-B., ZARCO-TEJADA, P. J., RIANO, D., RUEDA, C. A. & USTIN, S. L. 2006. Estimating vegetation water content with hyperspectral data for different canopy scenarios: Relationships between AVIRIS and MODIS indexes. *Remote Sensing of Environment,* 105**,** 354-366.

CHUVIECO, E. & CONGALTON, R. G. 1989. Application of remote-sensing and geographic information-systems to forest fire hazard mapping. *Remote Sensing of Environment,* 29**,** 147-159.

CHUVIECO, E. & SALAS, J. 1996. Mapping the spatial distribution of forest fire danger using GIS. *International Journal of Geographical Information Systems,* 10**,** 333-345.

CIHLAR, J., LATIFOVIC, R., BEAUBIEN, J., GUINDON, B. & PALMER, M. 2003. Thematic mapper (TM) based accuracy assessment of a land cover product for Canada derived from SPOT VEGETATION (VGT) data. *Canadian Journal of Remote Sensing,* 29**,** 154-170.

CLARK, M. L., CLARK, D. B. & ROBERTS, D. A. 2004. Small-footprint lidar estimation of sub-canopy elevation and tree height in a tropical rain forest landscape. *Remote Sensing of Environment,* 91**,** 68-89.

CLARK, M. L., ROBERTS, D. A. & CLARK, D. B. 2005. Hyperspectral discrimination of tropical rain forest tree species at leaf to crown scales. *Remote Sensing of Environment,* 96**,** 375-398.

CLINTON, N., HOLT, A., SCARBOROUGH, J. & PENG, G. 2010. Accuracy Assessment for Object-based Segmentation Goodness. *Photogrammetric Engineering and Remote Sensing,* 76**,** 289-299.

COCKS, T., JENSSEN, R., STEWART, A., WILSON, I. & SHIELDS, T. The HyMap Airborne Hyperspectral Sensor: The System, Calibration and Performance. *In:* SCHAEPMAN, M., SCHLÄPFER, D. & ITTEN, K. I., eds. 1st EARSeL Workshop on Imaging Spectroscopy, 1998 Zurich. Paris: EARSeL, 37- 43.

COOPS, N. C., HILKER, T., WULDER, M. A., ST-ONGE, B., NEWNHAM, G., SIGGINS, A. & TROFYMOW, J. A. T. 2007. Estimating canopy structure of Douglas-fir forest stands from discrete-return LiDAR. *Trees-Structure and Function,* 21**,** 295-310.

COOPS, N. C., STONE, C., CULVENOR, D. S. & CHISHOLM, L. 2004. Assessment of crown condition in eucalypt vegetation by remotely sensed optical indices. *Journal of Environmental Quality,* 33**,** 956-964.

CRACKNELL, A. P. 1998. Synergy in remote sensing - what's in a pixel. *International Journal of Remote Sensing,* 19**,** 2025-2047.

CRANE, R. B., MALILA, W. A. & RICHARDSON, W. 1972. Suitability of the normal density assumption for processing multispectral scanner data. *IEEE Transactions in Geoscience and Remote Sensing,* 10**,** 158–167.

CULVENOR, D. S. 2002. TIDA: an algorithm for the delineation of tree crowns in high spatial resolution remotely sensed imagery. *Computers & Geosciences,* 28**,** 33-44.

CUTLER, D. R., EDWARDS JR, T. C., BEARD, K. H., CUTLER, A., HESS, K. T., GIBSON, J. & LAWLER, J. J. 2007. Random forests for classification in ecology. *Ecology,* 88**,** 2783-2792.

DATT, B. 1999a. A new reflectance index for remote sensing of chlorophyll content in higher plants: Tests using Eucalyptus leaves. *Journal of plant physiology,* 154**,** 30-36.

DATT, B. 1999b. *Remote sensing of foliar biochemistry and biophysical properties in eucalyptus species : application of high spectral resolution reflectance measurements.* PhD, University of New South Wales.

DATT, B. 1999c. Visible/near infrared reflectance and chlorophyll content in Eucalyptus leaves. *International Journal of Remote Sensing,* 20**,** 2741-2759.

DE JONG, S. M., PEBESMA, E. J. & LACAZE, B. 2003. Above-ground biomass assessment of Mediterranean forests using airborne imaging spectrometry: The DAIS Peyne experiment. *International Journal of Remote Sensing,* 24**,** 1505-1520.

DE WULF, R. R., GOOSSENS, R. E., DEROOVER, B. P. & BORRY, F. C. 1990. Extraction of forest stand parameters from panchromatic and multispectral Spot-1 data. *nternational Journal of Remote Sensing,* 119**,** 1571– 1588.

DECC. 2008. *Warrumbungle National Park* [Online]. Hurstville, Sydney: Department of Environment and Climate Change. Available: http://www.environment.nsw.gov.au/NationalParks/parkNature.aspx?id=N0035.

DEFRIES, R., HANSEN, M. & TOWNSHEND, J. 1995. Global discrimination of land cover types from metrics derived from AVHRR pathfinder data. *Remote Sensing of Environment,* 54**,** 209-222.

DELVES, L. M., WILKINSON, R., OLIVER, C. J. & WHITE, R. G. 1992. Comparing the performance of SAR image segmentation algorithms. *International journal of remote sensing,* 13**,** 2121-2149.

DENNISON, P. E., CHAROENSIRI, K., ROBERTS, D. A., PETERSON, S. H. & GREEN, R. O. 2006. Wildfire temperature and land cover modeling using hyperspectral data. *Remote Sensing of Environment,* 100**,** 212–222.

DIRNBÖCK, T., DULLINGER, S., GOTTFRIED, M., GINZIER, C. & GRABHERR, G. 2003. Mapping alpine vegetation based on image analysis, topographic variables and Canonical Correspondence Analysis. *Applied Vegetation Science,* 6**,** 85-96.

DOBROWSKI, S. Z., SAFFORD, H. D., CHENG, Y. B. & USTIN, S. L. 2008. Mapping mountain vegetation using species distribution modeling, image-based texture analysis, and object-based classification. *Applied Vegetation Science,* 11**,** 499-508.

DOUGLAS, D. & PEUCKER, T. 1973. Algorithms for the reduction of the number of points required to represent a digitized line or its caricature. *The Canadian Cartographer,* 10**,** 112–122.

DUTHOIT, S., DEMAREZ, V., GASTELLU-ETCHEGORRY, J.-P., MARTIN, E. & ROUJEAN, J.-L. 2008. Assessing the effects of the clumping phenomenon on BRDF of a maize crop based on 3D numerical scenes using DART model. *Agricultural and Forest Meteorology,* 148**,** 1341-1352.

DYKSTERHUIS, E. J. 1949. Condition and management of range land based on quantitative ecology. *Journal of Range Management,* 2**,** 104-115.

ECOLOGICALAUSTRALIA 2008. Editing Mitchell Landscapes, Final Report. Sydney: Eco Logical Australia.

ELITH, J., H. GRAHAM, C., P. ANDERSON, R., DUDÍK, M., FERRIER, S., GUISAN, A., J. HIJMANS, R., HUETTMANN, F., R. LEATHWICK, J., LEHMANN, A., LI, J., G. LOHMANN, L., A. LOISELLE, B., MANION, G., MORITZ, C., NAKAMURA, M., NAKAZAWA, Y., MCC. M. OVERTON, J., TOWNSEND PETERSON, A., J. PHILLIPS, S., RICHARDSON, K., SCACHETTI-PEREIRA, R., E. SCHAPIRE, R., SOBERÓN, J., WILLIAMS, S., S. WISZ, M. & E. ZIMMERMANN, N. 2006. Novel methods improve prediction of species' distributions from occurrence data. *Ecography,* 29**,** 129-151.

ELITH, J., LEATHWICK, J. R. & HASTIE, T. 2008. A working guide to boosted regression trees. *Journal of Animal Ecology,* 77**,** 802-813.

ELMORE, A. J., MUSTARD, J. F., MANNING, S. J. & LOBELL, D. B. 2000. Quantifying vegetation change in semiarid environments: Precision and accuracy of spectral mixture analysis and the Normalized Difference Vegetation Index. *Remote Sensing of Environment,* 73**,** 87-102.

EMERY, K., PEASLEY, B., SHAIK, M., SIVERTSEN, D. & SMITH, P. 2001. Interpretation and Delineation of Patterns in Native Vegetation. *In:* SIVERTSEN, D. (ed.) *Guidelines for mapping native vegetation.* 2.1 ed. Sydney: New South Wales Department of Sustainable Natural Resources.

ERIKSON, M. 2004. Species classification of individually segmented tree crowns in high-resolution aerial images using radiometric and morphologic image measures. *Remote Sensing of Environment,* 91**,** 469-477.

EXELIS. 2008. *Cross-Track Illumination Correction* [Online]. Exelis Visual Information Solutions. Available: http://www.exelisvis.com/docs/routines-136.html.

FALKOWSKI, M. J., SMITH, A. M. S., HUDAK, A. T., GESSLER, P. E., VIERLING, L. A. & CROOKSTON, N. L. 2006. Automated estimation of individual conifer tree height and crown diameter via two-dimensional spatial wavelet analysis of lidar data. *Canadian Journal of Remote Sensing,* 32**,** 153-161.

FAZAKAS, Z., NILSSON, M. & OLSSON, H. 1999. Regional forest biomass and wood volume estimation using satellite data and ancillary data. *Agricultural and Forest Meteorology,* 98-99**,** 417–425.

FERNANDES, P. M. & BOTELHO, H. S. 2003. A review of prescribed burning effectiveness in fire hazard reduction. *International Journal of Wildland Fire,* 12**,** 117-128.

FERRIER, S. & GUISAN, A. 2006. Spatial modelling of biodiversity at the community level. *Journal of Applied Ecology,* 43**,** 393-404.

FERRIER, S., MANION, G., ELITH, J. & RICHARDSON, K. 2007. Using generalized dissimilarity modelling to analyse and predict patterns of beta diversity in regional biodiversity assessment. *Diversity and Distributions,* 13**,** 252-264.

FILIPPI, A. M. & JENSEN, J. R. 2006. Fuzzy learning vector quantization for hyperspectral coastal vegetation classification. *Remote Sensing of Environment,* 100**,** 512-530.

FISHER, P. 1997. The pixel: A snare and a delusion. *International Journal of Remote Sensing,* 18**,** 679-685.

FOGARTY, L. G., PEARCE, G., CATCHPOLE, W. R. & ALEXANDER, M. E. Adoption versus adoption: lessons learned from applying the Canadian Forest Fire Danger Rating System to

New Zeeland. *In:* VIEGAS, ed. 3rd International Conference Forest Fire Research, 1998 Coimbra, Portugal. 1011–1028.
FOODY, G. M. 2002. Status of land cover classification accuracy assessment. *Remote Sensing of Environment,* 80**,** 185-201.
FOODY, G. M. & ARORA, M. K. 1997. An evaluation of some factors affecting the accuracy of classification by an artificial neural network. *International Journal of Remote Sensing,* 18**,** 799-810.
FOODYA, G. M., BOYDB, D. S. & CUTLER, M. E. J. 2003. Predictive relations of tropical forest biomass from Landsat TM data and their transferability between regions. *Remote Sensing of Environment,* 85**,** 463–474.
FORMAN, R. T. T. 1995. *Land mosaics : the ecology of landscapes and regions,* New York, Cambridge University Press.
FRANCESETTI, A., CAMIA, A. & BOVIO, G. 2006. Fuel type mapping with Landsat TM images and ancillary data in the Prealpine region of Italy. *Forest Ecology and Management,* 234**,** 259.
FRANKLIN, J., ROGAN, J., PHINN, S. & WOODCOCK, C. 2003. Rationale and Conceptual Framework for Classification Approaches to Assess Forest Resources and Properties. *In:* WULDER, M. & FRANKLIN, S. (eds.) *Remote Sensing of Forest Environments.* Springer US.
FRIEDMAN, J., HASTIE, T. & TIBSHIRANI, R. 2000. Additive logistic regression: a statistical view of boosting. *Annals of Statistics,* 28**,** 337–407.
FUGRO. 2009. *Fugro Spatial Solutions* [Online]. Perth, Australia. Available: http://www.fugrospatial.com.au/.
GAHEGAN, M. 2003. Is inductive machine learning just another wild goose (or might it lay the golden egg)? *International Journal of Geographical Information Science,* 17**,** 69-92.
GAO, B. & GOETZ, A. F. H. 1990. Column atmospheric water vapor and vegetation liquid water retrievals from airborne imaging spectrometer data. *Journal of Geophysical Research,* 95**,** 3549 – 3564.
GAO, B. C., MONTES, M. J. & DAVIS, C. O. 2004. Refinement of wavelength calibrations of hyperspectral imaging data using a spectrum-matching technique. *Remote Sensing of Environment,* 90**,** 424-433.
GARCIA, M. & USTIN, S. L. 2001. Detection of interannual vegetation responses to climatic variability using AVIRIS data in a coastal savanna in California. *Ieee Transactions on Geoscience and Remote Sensing,* 39**,** 1480-1490.
GELLIE, N. J. H. 2005. Native Vegetation of the Southern Forests: South-east Highlands, Australian Alps, South-west Slopes, and SE Corner bioregions. *Cunninghamia,* 9**,** 219-253.
GIAKOUMAKIS, N. M., GITAS, I. Z. & SAN-MIGUEL, J. 2002. Object-oriented classification modelling for fuel type mapping in the Mediterranean, using LANDSAT TM and IKONOS imagery preliminary results. *In:* VIEGAS (ed.) *Forest Fires Research & Wildland Fire Safety.* Rotterdam: Millpress.
GIBBONS, P., AYERS, D., SEDDON, J., DOYLE, S. & BRIGGS, S. 2005. 'BioMetric Version 1.8. A Terrestrial Biodiversity Assessment Tool for the NSW Property Vegetation Plan Developer. Operational Manual'. New South Wales.
GIBBONS, P., ZERGER, A., JONES, S. & RYAN, P. 2006. Mapping vegetation condition in the context of biodiversity conservation. *Ecological Management & Restoration,* 7**,** S1-S2.
GITAS, I. Z., MITRI, G. H., KAZAKIS, G., GHOSN, D. & XANTHOPOULOS, G. 2006. Fuel type mapping in Anopolis, Crete by employing QuickBird imagery and object-based classification. *Ecological Management,* 234**,** 228.
GITELSON, A. & MERZLYAK, M. N. 1994. Spectral Reflectance Changes Associated with Autumn Senescence of Aesculus hippocastanum L. and Acer platanoides L. Leaves. Spectral Features and Relation to Chlorophyll Estimation. *Journal of Plant Physiology,* 143**,** 286-292.
GITELSON, A. A., KAUFMAN, Y. J. & MERZLYAK, M. N. 1996. Use of a green channel in remote sensing of global vegetation from EOS-MODIS. *Remote Sensing of Environment,* 58**,** 289-298.

GOODWIN, N., TURNER, R. & MERTON, R. 2005. Classifying Eucalyptus forests with high spatial and spectral resolution imagery: an investigation of individual species and vegetation communities. *Australian Journal of Botany,* 53**,** 337-345.
GOUGEON, F. A. 1995. A crown-following approach to the automatic delineation of individual tree crowns in high spatial resolution aerial images. *Canadian journal of remote sensing,* 21**,** 274-284.
GOUGEON, F. A. & LECKIE, D. G. 2003. Forest information extraction from high resolution images using an individual tree crown approach. *Information Report BC-X-396.* Victoria, BC: Natural Resources Canada, Canadian Forest Service.
GOULD, J. 2003. Fire Behaviour: Integrating science and management. *In:* LINDENMAYER, D., DOVERS, S. & CARY, G. J. (eds.) *Australia burning : fire ecology, policy and management issues.* Collingwood, Vic.: CSIRO Publishing.
GOULD, J. S., MCCAW, W. L., CHENEY, N. P., ELLIS, P. F., KNIGHT, I. K. & SULLIVAN, A. L. 2007. *Project vesta: fire in dry eucalypt forest: fuel structure, fuel dynamics and fire behaviour,* Perth, WA, Ensis-CSIRO, Canberra ACT and Department of Environment and Conservation.
GRACE, J., NICHOL, C., DISNEY, M., LEWIS, P., QUAIFE, T. & BOWYER, P. 2007. Can we measure terrestrial photosynthesis from space directly, using spectral reflectance and fluorescence? *Global Change Biology,* 13**,** 1484-1497.
GREAVES, B. L. & SPENCER, R. D. 1993. An evaluation of spectroradiometry and multispectral scanning for differentiating forest communities. *Australian Forestry,* 56**,** 68-79.
GUANG-XIONG, P., JING, L., YUN-HAO, C. & ABDUL-PATAH, N. 2007. A forest fire risk assessment using ASTER images in peninsular Malaysia. *Journal of China University of Mining and Technology,* 17**,** 232-237.
GUNN, R. H., BEATTIE, J. A., REID, R. E. & VAN DE GRAAFF, R. H. M. 1988. *Soil Survey Specifications. In: Australian Soil and Land Survey Handbook,* Melbourne, Inkata Press.
HAARA, A. & HAARALA, M. 2002. Tree species classification using semi-automatic delineation of trees on aerial images. *Scandinavian Journal of Forest Research,* 17**,** 556-565.
HANSEN, M., DUBAYAH, R. & DEFRIES, R. 1996. Classification trees: An alternative to traditional land cover classifiers. *International Journal of Remote Sensing,* 17**,** 1075-1081.
HARDEN, G. J. 1991. *Flora of New South Wales, Volume 2,* Kensington, Sydney, New South Wales University Press.
HASTIE, T., TIBSHIRANI, R. & FRIEDMAN, J. 2001. *The Elements of Statistical Learning: Data Mining,* Canada, Springer.
HAY, G. J., BLASCHKE, T., MARCEAU, D. J. & BOUCHARD, A. 2003. A comparison of three image-object methods for the multiscale analysis of landscape structure. *ISPRS Journal of Photogrammetry and Remote Sensing,* 57**,** 327-345.
HAY, G. J., CASTILLA, G., WULDER, M. A. & RUIZ, J. R. 2005. An automated object-based approach for the multiscale image segmentation of forest scenes. *International Journal of Applied Earth Observations and Geoinformation,* 7**,** 339-359.
HAY, G. J., DUBE, P., BOUCHARD, A. & MARCEAU, D. J. 2002. A scale-space primer for exploring and quantifying complex landscapes. *Ecological Modelling,* 153**,** 27–49.
HELMAN, C. E. 1983. *Inventory analysis of southern NSW rainforest vegetation.* MSc, University of New England, Armidale. .
HEURICH, M. 2008. Automatic recognition and measurement of single trees based on data from airborne laser scanning over the richly structured natural forests of the Bavarian Forest National Park. *Forest Ecology and Management,* 255**,** 2416-2433.
HIRSCHMUGL, M., OFNER, M., RAGGAM, J. & SCHARDT, M. 2007. Single tree detection in very high resolution remote sensing data. *Remote Sensing of Environment,* 110**,** 533-544.
HNATIUK, R., R., T. & J., W. 2009. Vegetation. *In:* NATIONAL COMMITTEE ON SOIL AND TERRAIN, C. (ed.) *Australian soil and land survey field handbook.* 3rd ed. Collingwood, Vic.: CSIRO Publishing.
HU, B. X., QIAN, S. E., HABOUDANE, D., MILLER, J. R., HOLLINGER, A. B., TREMBLAY, N. & PATTEY, E. 2004. Retrieval of crop chlorophyll content and leaf area index from

decompressed hyperspectral data: the effects of data compression. *Remote Sensing of Environment,* 92**,** 139-152.
HUANG, Z., TURNER, B. J., DURY, S. J., WALLIS, I. R. & FOLEY, W. J. 2004. Estimating foliage nitrogen concentration from HYMAP data using continuum removal analysis. *Remote Sensing of Environment,* 93**,** 18-29.
HUETE, A., DIDAN, K., MIURA, T., RODRIGUEZ, E. P., GAO, X. & FERREIRA, L. G. 2002. Overview of the radiometric and biophysical performance of the MODIS vegetation indices. *Remote Sensing of Environment,* 83**,** 195-213.
HUGHES, G. F. 1968. On the Mean Accuracy of Statistical Pattern Recognizers. *IEEE Transactions on Information Theory,* IT-14**,** 55-63.
HYVISTA. 2009. *HyVista Corporation Sensors* [Online]. Sydney, Australia. Available: http://www.hyvista.com/?page_id=275.
HYYPPÄ, J., HYYPPÄ, H., INKINEN, M., ENGDAHL, M., LINKO, S. & ZHU, Y. H. 2000. Accuracy comparison of various remote sensing data sources in the retrieval of forest stand attributes. *Forest Ecology and Management,* 128**,** 109-120.
HYYPPÄ, J., HYYPPÄ, H., LITKEY, P., YU, X., HAGGRÉN, H., RÖNNHOLM, P., PYYSALO, U., PITKÄNEN, J. & MALTAMO, M. 2004. Algorithms and Methods of Airborne Laser-Scanning for Forest Measurements. *International Archives of Photogrammetry, Remote Sensing and Spatial Information Sciences,* 36**,** 1682-1750.
IBRA. 2009. *Australia's bioregions (IBRA)* [Online]. Commonwealth of Australia. Available: http://www.environment.gov.au/land/nrs/science/ibra.
IM, J. & JENSEN, J. R. 2008. Hyperspectral remote sensing of vegetation. *Geography Compass,* 2**,** 1943-1961.
ISMAY, K., LEWER, S., DELUCA, S., MCKENZIE-GAY, M., POWRIE, S., BURNS, M., RYAN, C. & CHAFFEY, D. 2004. NSW Native vegetation report (1st Draft): Cobbora, Coolah, Coonabarabran, Mendooran, Tambar Springs 1: 100 000 map sheets. Dubbo, Australia: NSW Department of Infrastructure, Planning and Natural Resources.
JAKUBAUSKAS, M. E. 1996. Thematic Mapper characterization of lodgepole pine serals in Yellowstone National Park, USA. . *Remote Sensing of Environment,* 56**,** 118–132.
JENNINGS, S. B., BROWN, N. D. & SHEIL, D. 1999. Assessing forest canopies and understorey illumination: canopy closure, canopy cover and other measures. *Forestry,* 72**,** 59.
JENSEN, J. R. 2005. *Introductory digital image processing,* Upper Saddle River, NJ, Prentice-Hall.
JIA, G. J., BURKE, I. C., GOETZ, A. F. H., KAUFMANN, M. R. & KINDEL, B. C. 2006. Assessing spatial patterns of forest fuel using AVIRIS data. *Remote Sensing of Environment,* 102**,** 318-327.
JOHANSEN, K., COOPS, N. C., GERGEL, S. E. & STANGE, Y. 2007. Application of high spatial resolution satellite imagery for riparian and forest ecosystem classification. *Remote Sensing of Environment,* 110**,** 29-44.
JOHNSON, L. F., HLAVKA, C. A. & PETERSON, D. L. 1994. Multivariate-Analysis Of Aviris Data For Canopy Biochemical Estimation Along The Oregon Transect. *Remote Sensing of Environment,* 47**,** 216-230.
JOSEPH, G. 2005. *Fundamentals of Remote Sensing,* Hydrabad, University Press (India) Pvt. Ltd.
JOY, M. K. & DEATH, R. G. 2004. Predictive modelling and spatial mapping of freshwater fish and decapod assemblages using GIS and neural networks. *Freshwater Biology,* 49**,** 1036-1052.
JUNG, M., HENKEL, K., HEROLD, M. & CHURKINA, G. 2006. Exploiting synergies of global land cover products for carbon cycle modeling. *Remote Sensing of Environment,* 101**,** 534-553.
JURSKIS, V., SHIELDS, R. & BINNS, D. L. 1995. Flora survey, Queanbeyan/Badja Environmental Impact Statement Area, Southern Region, New South Wales. *Environmental Impact Statement for Queanbeyan & Badja Management Areas.* Beecroft: Research Division, State Forests of NSW.
KAUFMAN, Y. & TANRE, D. 1992. Atmospherically Resistant Vegetation Index (ARVI) for EOS-MODIS. *IEEE Transactions on Geoscience and Remote Sensing,* 30**,** 261-270.

KEANE, R. E., BURGAN, R. & VAN WAGTENDONK, J. 2001. Mapping wildland fuels for fire management across multiple scales: Integrating remote sensing, GIS, and biophysical modeling. *International Journal of Wildland Fire,* 10**,** 301-319.

KEITH, D. A. 1994. Floristics, structure and diversity of natural vegetation in the O'Hares Creek catchment, south of Sydney. *Cunninghamia,* 3**,** 543-594.

KEITH, D. A. & BEDWARD, M. 1999. Native vegetation of the South East Forests region, Eden, New South Wales. *Cunninghamia,* 6**,** 1-218.

KEITH, D. A. & BENSON, D. H. 1988. The natural vegetation of the Katoomba 1:100 000 map sheet. *Cunninghamia,* 2**,** 107–144.

KELLY, M., LIU, D., MCPHERSON, B., WOOD, D. & STANDIFORD, R. 2008. Spatial pattern dynamics of oak mortality and associated disease symptoms in a California hardwood forest affected by sudden oak death. *Journal of Forest Research,* 13**,** 312-319.

KENNEDY, R. E., COHEN, W. B. & TAKAO, G. 1997. Empirical methods to compensate for a view-angle-dependent brightness gradient in AVIRIS imagery. *Remote Sensing of Environment,* 62**,** 277-291.

KENT, M. & COKER, P. 1992. *Vegetation description and analysis : a practical approach,* London, Belhaven Press.

KERAMITSOGLOU, I., KONTOES, C., SYKIOTI, O., SIFAKIS, N. & XOFIS, P. 2008. Reliable, accurate and timely forest mapping for wildfire management using ASTER and Hyperion satellite imagery. *Forest Ecology and Management,* 255**,** 3556-3562.

KITCHENER, A. & HARRIS, S. 2005. *Forest to Fjaeldmark: Descriptions of Tasmania's Vegetation.,* Hobart, Tasmania, Department of Primary Industries, Parks, Water and Environment.

KNIPLING, E. B. 1970. Physical and physiological basis for the reflectance of visible and near-infrared radiation from vegetation. *Remote Sensing of Environment,* 1**,** 155-159.

KOKALY, R. F., DESPAIN, D. G., CLARK, R. N. & LIVO, K. E. 2003. Mapping vegetation in Yellowstone National Park using spectral feature analysis of AVIRIS data. *Remote Sensing of Environment,* 84**,** 437-456.

KOOP, H., RIJKSEN, H. D. & WIND, J. 1995. Tools to Diagnose Forest Integrity; An appraisal method substantiated by silvi-star assessment of diversity and forest structure. *In:* BOYLE, J. (ed.) *Measuring and Monitoring Biodiversity in Tropical and Temperate Forests.* Indonesia: Centre for International Forestry Research.

KOTZ, B., SCHAEPMAN, M., MORSDORF, F., BOWYER, P., ITTEN, K. & ALLGOWER, B. 2004. Radiative transfer modeling within a heterogeneous canopy for estimation of forest fire fuel properties. *Remote Sensing of Environment,* 92**,** 332-344.

KOUKOULAS, S. & BLACKBURN, G. A. 2005. Mapping individual tree location, height and species in broadleaved deciduous forest using airborne LIDAR and multi-spectral remotely sensed data. *International Journal of Remote Sensing,* 26**,** 431-455.

KRUSE, F. A., BOARDMAN, J. W., LEFKOFF, A. B., YOUNG, J. M., KIEREIN-YOUNG, K. S., COCKS, T. D., JENSSEN, R. & COCKS, P. A. AIG/HyVista 1999 USA HyMap Group Shoot: Overview and analysis examples. International Geoscience and Remote Sensing Symposium (IGARSS), 2000. 1373-1375.

LABEN, C. A. & BROWER, B. V. 2000. *Process for Enhancing the Spatial Resolution of Multispectral Imagery using PanSharpening*. U.S. 6,011,875 patent application.

LALIBERTE, A. S., FREDRICKSON, E. L. & RANGO, A. 2007. Combining decision trees with hierarchical object-oriented image analysis for mapping arid rangelands. *Photogrammetric Engineering and Remote Sensing,* 73**,** 197-207.

LALIBERTE, A. S., RANGO, A., HAVSTAD, K. M., PARIS, J. F., BECK, R. F., MCNEELY, R. & GONZALEZ, A. L. 2004. Object-oriented image analysis for mapping shrub encroachment from 1937 to 2003 in southern New Mexico. *Remote Sensing of Environment,* 93**,** 198-210.

LANDWEHR, N., HALL, M. & FRANK, E. 2005. Logistic model trees. *Machine Learning,* 59**,** 161-205.

LARSEN, M. & RUDEMO, M. 1998. Optimizing templates for finding trees in aerial photographs. *Pattern Recognition Letters,* 19**,** 1153-1162.

LASAPONARA, R. & LANORTE, A. 2007a. On the capability of satellite VHR QuickBird data for fuel type characterization in fragmented landscape. *Ecological Modelling,* 204**,** 79-84.
LASAPONARA, R. & LANORTE, A. 2007b. Remotely sensed characterization of forest fuel types by using satellite ASTER data. *International Journal of Applied Earth Observation and Geoinformation,* 9**,** 225-234.
LAWRENCE, R. L. & WRIGHT, A. 2001. Rule-Based Classification Systems Using Classification and Regression Tree (CART) Analysis. *Photogrammetric Engineering and Remote Sensing,* 67**,** 1137-1142.
LEATHWICK, J. R., ELITH, J. & HASTIE, T. 2006. Comparative performance of generalized additive models and multivariate adaptive regression splines for statistical modelling of species distributions. *Ecological Modelling,* 199**,** 188-196.
LEATHWICK, J. R., ROWE, D., RICHARDSON, J., ELITH, J. & HASTIE, T. 2005. Using multivariate adaptive regression splines to predict the distributions of New Zealand's freshwater diadromous fish. *Freshwater Biology,* 50**,** 2034-2052.
LECKIE, D., GOUGEON, F., HILL, D., QUINN, R., ARMSTRONG, L. & SHREENAN, R. 2003a. Combined high-density lidar and multispectral imagery for individual tree crown analysis. *Canadian Journal of Remote Sensing,* 29**,** 633-649.
LECKIE, D. G. 1990. Advances in remote sensing technologies for forest surveys and management. *Canadian Journal of Forest Research,* 20**,** 464-483.
LECKIE, D. G., GOUGEON, F. A., TIMS, S., NELSON, T., BURNETT, C. N. & PARADINE, D. 2005a. Automated tree recognition in old growth conifer stands with high resolution digital imagery. *Remote Sensing of Environment,* 94**,** 311-326.
LECKIE, D. G., GOUGEON, F. A., TINIS, S., NELSON, T., BURNETT, C. N. & PARADINE, D. 2005b. Automated tree recognition in old growth conifer stands with high resolution digital imagery. *Remote Sensing of Environment,* 94**,** 311-326.
LECKIE, D. G., GOUGEON, F. A., WALSWORTH, N. & PARADINE, D. 2003b. Stand delineation and composition estimation using semi-automated individual tree crown analysis. *Remote Sensing of Environment,* 85**,** 355-369.
LEES, B. G. & RITMAN, K. 1991. Decision Tree and Rule Induction Approach to Integration of Remotely Sensed and GIS Data in Mapping Vegetation in Disturbed or Hilly Environments. *Environmental Management,* 15**,** 823-31.
LEFSKY, M. A., COHEN, W. B., PARKER, G. G. & HARDING, D. J. 2002. Lidar remote sensing for ecosystem studies. *BioScience,* 52**,** 19-30.
LEICA. 2009. *Leica Geosystems* [Online]. Switzerland. Available: http://www.leica-geosystems.com/en/index.htm.
LEWIS, P. & DISNEY, M. 2007. Spectral invariants and scattering across multiple scales from within-leaf to canopy. *Remote Sensing of Environment,* 109**,** 196-206.
LIU, D., KELLY, M., GONG, P. & GUO, Q. 2007. Characterizing spatial-temporal tree mortality patterns associated with a new forest disease. *Forest Ecology and Management,* 253**,** 220-231.
LUCAS, R., BUNTING, P., PATERSON, M. & CHISHOLM, L. 2008. Classification of Australian forest communities using aerial photography, CASI and HyMap data. *Remote Sensing of Environment,* 112**,** 2088-2103.
LUCIEER, A. 2004. *Uncertainties in Segmentation and Their Visualisation.* PhD, Utrecht University.
LUDWIG, J. A., BASTIN, G. N., CHEWINGS, V. H., EAGER, R. W. & LIEDLOFF, A. C. 2007. Leakiness: A new index for monitoring the health of arid and semiarid landscapes using remotely sensed vegetation cover and elevation data. *Ecological Indicators,* 7**,** 442-454.
LUKE, R. H. & MCARTHUR, A. G. 1978. *Bushfires in Australia,* Canberra, Australian Government Publishing Service.
MACMILLAN, R. A., MOON, D. E. & COUPÉ, R. A. 2007. Automated predictive ecological mapping in a Forest Region of B.C., Canada, 2001–2005. *Geoderma,* 140**,** 353-373.
MAIER, H. R. & DANDY, G. C. 2000. Neural networks for the prediction and forecasting of water resources variables: A review of modelling issues and applications. *Environmental Modelling and Software,* 15**,** 101-124.

MALENOVSKY, Z., BARTHOLOMEUS, H. M., ACERBI-JUNIOR, F. W., SCHOPFER, J. T., PAINTER, T. H., EPEMA, G. F. & BREGT, A. K. 2007. Scaling dimensions in spectroscopy of soil and vegetation. *International Journal of Applied Earth Observation and Geoinformation,* 9**,** 137-164.
MALERBA, D., ESPOSITO, F., LANZA, A. & LISI, F. 2001. Machine learning for information extraction from topographic maps. *Geographic data mining and knowledge discovery***,** 291–314.
MARCEAU, D. J. & HAY, G. J. 1999. Remote Sensing Contributions to the Scale Issue (Review). *Canadian Journal of Remote Sensing,* 25.
MARGULES, C. R. & PRESSEY, R. L. 2000. Systematic conservation planning. *Nature,* 405**,** 243-253.
MARGULES, C. R., PRESSEY, R. L. & WILLIAMS, P. H. 2002. Representing biodiversity: Data and procedures for identifying priority areas for conservation. *Journal of Biosciences,,* 27**,** 309-326.
MARMION, M., PARVIAINEN, M., LUOTO, M., HEIKKINEN, R. K. & THUILLER, W. 2009. Evaluation of consensus methods in predictive species distribution modelling. *Diversity and Distributions,* 15**,** 59-69.
MARTIN, D., FOWLKES, C., TAL, D. & MALIK, J. Database of Human Segmented Natural Images and its Application to Evaluating Segmentation Algorithms and Measuring Ecological Statistics. 8th International Conference on Computer Vision, 2001. Institute of Electrical and Electronics Engineers, 416-423.
MARTIN, M. E., PLOURDE, L. C., OLLINGER, S. V., SMITH, M. L. & MCNEIL, B. E. 2008. A generalizable method for remote sensing of canopy nitrogen across a wide range of forest ecosystems. *Remote Sensing of Environment,* 112**,** 3511-3519.
MCARTHUR, A. G. 1967. Fire Behaviour in Eucalypt Forests. Canberra: Department of National Development Forestry and Timber Bureau.
MCCARTHY, G. J. 2004. Surface fine fuel hazard rating: forest fuels in East Gippsland. *Fire Management, no. 44.* Melbourne, Victoria: Department of Sustainability and Environment.
MCCARTHY, G. J., TOLHURST, K. & CHATTO, K. 1999. Overall Fuel Hazard Guide. *Research Report No. 47.* 3rd ed. Victoria: Fire Management Branch, Dept. of Natural Resources and Environment.
MCCAULEY, A. 2006. Vegetation Survey and Mapping of the Hunter, Central and Lower North Coast Region of NSW. A report prepared for the Hunter-Central Rivers Catchment Management Authority by the HCCREMS team. NSW: Environment Division of Hunter Councils Inc.
MCDONALD, R. C., R.F., I. & J.G., S. 2009. Land Surface. *In:* NATIONAL COMMITTEE ON SOIL AND TERRAIN, C. (ed.) *Australian soil and land survey field handbook.* 3rd ed. Collingwood, Vic.: CSIRO Publishing.
MCELHINNY, C. 2005. *Quantifying stand structural complexity in woodland and dry sclerophyll forest, South-Eastern Australia.* PhD thesis, The Australian National University.
MCKENZIE, N. J., GRUNDY, M. J., WEBSTER, R. & RINGROSE-VOASE, A. J. 2008. Guidelines for Surveying Soil and Land Resources (2nd Edition). CSIRO Publishing.
MCKENZIE, N. J. & RYAN, P. J. 1999. Spatial prediction of soil properties using environmental correlation. *Geoderma,* 89**,** 67-94.
MILLER, A. J. 1990. *Subset selection in regression,* New York, Chapman and Hall.
MILLER, J. R., WU, J., BOYER, M. G., BELANGER, M. & HARE, E. W. 1991. Seasonal patterns in leaf reflectance red-edge. *International Journal of Remote Sensing,* 12**,** 1509-1523.
MITCHELL, P. B. 2002. NSW ecosystems study: background and methodology. Hurstville: NSW National Parks and Wildlife Service.
MÖLLER, M., LYMBURNER, L. & VOLK, M. 2007. The comparison index: A tool for assessing the accuracy of image segmentation. *International Journal of Applied Earth Observation and Geoinformation,* 9**,** 311-321.
MORRISON, D. A. 2002. Effects of fire intensity on plant species composition of sandstone communities in the Sydney region. *Austral Ecology,* 27**,** 433-441.

MORSDORF, F., MEIER, E., KOTZ, B., ITTEN, K. I., DOBBERTIN, M. & ALLGOWER, B. 2004. LIDAR-based geometric reconstruction of boreal type forest stands at single tree level for forest and wildland fire management. *Remote Sensing of Environment,* 92**,** 353-362.
MUELLER-DOMBOIS, D. & ELLENBERG, H. 1974. *Aims and Methods of Vegetation Ecology,* New York, John Wiley & Sons.
MÜLLER, A., GEGE, P. & COCKS, T. The Airborne Imaging Spectrometers Used in DAISEX. *In:* M. WOODING & R.A. HARRIS, eds. The Digital Airborne Spectrometer Experiment (DAISEX), 2001. European Space Agency, 3.
MUMFORD, D. & SHAH, J. Boundary detection by minimizing functionals. Computer Society Conference on Computer Vision and Pattern Recognition, 1985 San Francisco. IEEE Computer Society Press, 22–26.
MUNDT, J. T., STREUTKER, D. R. & GLENN, N. F. 2006. Mapping sagebrush distribution using fusion of hyperspectral and lidar classifications. *Photogrammetric Engineering and Remote Sensing,* 72**,** 47-54.
MUTANGAO, O. & KUMAR, L. 2007. Estimating and mapping grass phosphorus concentration in an African savanna using hyperspectral image data. *International Journal of Remote Sensing,* 28**,** 4897-4911.
MUTLU, M., POPESCU, S. C., STRIPLING, C. & SPENCER, T. 2008. Mapping surface fuel models using lidar and multispectral data fusion for fire behavior. *Remote Sensing of Environment,* 112**,** 274-285.
NAGENDRA, H. 2001. Using remote sensing to assess biodiversity. *International Journal of Remote Sensing,* 22**,** 2377 - 2400.
NATIONAL COMMITTEE ON SOIL AND TERRAIN, C. 2009. *Australian soil and land survey field handbook,* Collingwood, Vic., CSIRO Publishing.
NELDNER, V. J., WILSON, B. A., THOMPSON, E. J. & DILLEWAARD, H. A. 2005. Methodology for Survey and Mapping of Regional Ecosystems and Vegetation Communities in Queensland. Brisbane: Queensland Herbarium, Environmental Protection Agency.
NEUBERT, M., HEROLD, H. & MEINEL, G. Evaluation of remote sensing image segmentation quality–further results and concepts. *In:* LANG, S., BLASCHKE, T. & SCHÖPFER, E., eds. 1 st International Conference on Object-Based Image Analysis, 2006 Salzburg University, Austria. International Society for Photogrammetry and Remote Sensing.
NEWSOME, A. E. & CATLING, P. C. 1979. Habitat preferences of mammals inhabiting heathlands of warm temperate coastal, montane and alpine regions of southeastern Australia. *In:* SPECHT, R. L. (ed.) *Ecosystems of the World. Vol. 9A. Heathlands and Related Shrublands of the World.* Amsterdam: Elsevier Publishing Co.
NIEMANN, K. O., ADAMS, S. & HAY, G. Automated tree crown identification using digital orthophoto mosaics. *In:* HILL, D. A. & LECKIE, D. G., eds. Proceedings of the International Forum on Automated Interpretation of High Spatial Resolution Digital Imagery for Forestry, 1998 Victoria, BC. Canadian Forest Service.
NIJLAND, W., ADDINK, E. A., DE JONG, S. M. & VAN DER MEER, F. D. 2009. Optimizing spatial image support for quantitative mapping of natural vegetation. *Remote Sensing of Environment,* 113**,** 771-780.
NOSS, R. F. 1999. Assessing and monitoring forest biodiversity: a suggested framework and indicators. *Forest Ecology and Management,* 115**,** 135-146.
NOUJDINA, N. V. & USTIN, S. L. 2008. Mapping downy brome (Bromus tectorum) using multidate AVIRIS data. *Weed Science,* 56**,** 173-179.
NPWS 2000. Vegetation survey, classification and mapping: Lower Hunter and Central Coast region. A project undertaken for the Lower Hunter and Central Coast Regional Environmental Management Strategy by CRA Unit. Sydney: NSW National Parks and Wildlife Service.
NPWS 2006. Jilliby State Conservation Area (North) Draft Fire Management Strategy. Sydney: National Parks and Wildlife Service.
NPWS 2010. Watagans National Park and Jilliby State Conservation Area Plan of Management. Sydney: Department of Environment, Climate Change and Water
NT. 2009. *Vegetation Survey and Mapping* [Online]. Northern Territory Government Land Resource Management. Available: http://www.lrm.nt.gov.au/natveg/vegmapping.

O'NEILL, R. V., HUNSAKER, C. T., TIMMINS, S. P., JACKSON, B. L., JONES, K. B., RIITTERS, K. H. & WICKHAM, J. D. 1996. Scale problems in reporting landscape pattern at the regional scale. *Landscape Ecology,* 11**,** 169-180.

OKIN, G. S., ROBERTS, D. A., MURRAY, B. & OKIN, W. J. 2001. Practical limits on hyperspectral vegetation discrimination in arid and semiarid environments. *Remote Sensing of Environment,* 77**,** 212-225.

OLIVER, I. & PARKES, D. 2003. A Prototype Toolkit for Scoring the Biodiversity Benefits of Land Use Change. Sydney: NSW Department of Infrastructure, Planning and Natural Resources.

OPENSHAW, S. 1984. The modifiable areal unit problem. *Concepts and Techniques in Modern Geography,* 38.

OVERTON, J. M., BARKER, G. M. & PRICE, R. 2009. Estimating and conserving patterns of invertebrate diversity: A test case of New Zealand land snails. *Diversity and Distributions,* 15**,** 731-741.

OZA, M. P., STRIVASTAVA, V. K. & DEVAIAH, P. K. 1996. Estimating tree volume in tropical dry deciduous forest from Landsat TM data. *Geocarto International***,** 33– 39.

PAL, M. & MATHER, P. M. 2003. An assessment of the effectiveness of decision tree methods for land cover classification. *Remote Sensing of Environment,* 86**,** 554-565.

PAPIÓ, C. & TRABAUD, L. 1991. Comparative study of the aerial structure of five shrubs of mediterranean shrublands. *Forest Science,* 37**,** 146-159.

PARKES, D., NEWELL, G. & CHEAL, D. 2003. Assessing the quality of native vegetation: The'habitat hectares' approach. *Ecological Management & Restoration,,* 4**,** 29-38.

PARUELO, J. & LAUENROTH, W. 1998. Interannual variability of NDVI and its relationship to climate for North American shrublands and grasslands. *Journal of Biogeography***,** 721–733.

PERKO, R. 2004. *Computer vision for large format digital aerial cameras.* PhD, Graz University of Technology.

PERRY, E. M. & DAVENPORT, J. R. 2007. Spectral and spatial differences in response of vegetation indices to nitrogen treatments on apple. *Computers and Electronics in Agriculture,* 59**,** 56-65.

PETERS, M., MADDEN, G. & DYKES, L. How image processing converted terabytes of data into one user-friendly base-map – The PANRIIE SPOT5 Imagery Project. 13th Australasian Remote Sensing and Photogrammetry Conference, 2006 Canberra. Spatial Sciences Institute.

POLLOCK, R. Individual tree recognition based on a synthetic tree crown image model. *In:* HILL, D. A. & LECKIE, D. G., eds. International Forum on Automated Interpretation of High Spatial Resolution Digital Imagery for Forestry, 1998 Victoria, BC. Canadian Forest Service.

POPESCU, S. C., WYNNE, R. H. & NELSON, R. F. 2003. Measuring individual tree crown diameter with lidar and assessing its influence on estimating forest volume and biomass. *Canadian Journal of Remote Sensing,* 29**,** 564-577.

PORTNERS, M. F., ASHBY, E. M. & BENSON, J. S. 1997. The natural vegetation of the Pooncarie 1:250 000 map. *Cunninghamia,* 5**,** 139–232.

POULIOT, D. A., KING, D. J., BELL, F. W. & PITT, D. G. 2002. Automated tree crown detection and delineation in high-resolution digital camera imagery of coniferous forest regeneration. *Remote Sensing of Environment,* 82**,** 322-334.

POULIOT, D. A., KING, D. J. & PITT, D. G. 2005. Development and evaluation of an automated tree detection-delineation algorithm for monitoring regenerating coniferous forests. *Canadian Journal of Forest Research/Revue Canadienne de Recherche Forestiere,* 35**,** 2332-2345.

POULOS, H. M., CAMP, A. E., GATEWOOD, R. G. & LOOMIS, L. 2007. A hierarchical approach for scaling forest inventory and fuels data from local to landscape scales in the Davis Mountains, Texas, USA. *Forest Ecology and Management,* 244**,** 1-15.

PRESSEY, R. L. & NICHOLLS, A. O. 1989. Efficiency in conservation evaluation: scoring versus iterative approaches. *Biological Conservation,* 50**,** 199-218.

PROBER, S. M., THIELE, K. R., PROBER, S. M. & THIELE, K. R. 1995. Conservation of the Grassy White Box Woodlands: Relative Contributions of Size and Disturbance to Floristic Composition and Diversity of Remnants. *Australian Journal of Botany,* 43**,** 349-366.

PU, R. 2009. Broadleaf species recognition with in situ hyperspectral data. *International Journal of Remote Sensing,* 30**,** 2759-2779.

RAISON, R. J., WOODS, P. V. & KHANNA, P. K. 1986. Decomposition and accumulation of litter after fire in sub-alpine eucalypt forests. *Australian Journal of Ecology,* 11**,** 9-19.

RAMER, U. 1972. An iterative procedure for the polygonal approximation of plane curves. *Computer Graphics and Image Processing,* 1**,** 244–256.

READ, J. M., CLARK, D. B., VENTICINQUE, E. M. & MOREIRA, M. P. 2003. Application of merged 1-m and 4-m resolution satellite data to research and management in tropical forests. *Journal of Applied Ecology,* 40**,** 592-600.

REDDING, N. J., CRISP, D. J., TANG, D. & NEWSAM, G. N. An efficient algorithm for Mumford-Shah segmentation and its application to SAR imagery. Conference on Digital Image Computing: Techniques and Applications, 1999 Perth. Defence Science and Technology Organisation.

REEVES, M. C., WINSLOW, J. C. & RUNNING, S. W. 2001. Mapping Weekly Rangeland Vegetation Productivity Using MODIS Algorithms. *Journal of Range Management,* 54**,** A90-A105.

REID, R. E. 1988. Guidelines for Survey. *In:* GUNN, R. H., BEATTIE, J. A., REID, R. E. & VAN DE GRAAFF, R. H. M. (eds.) *Soil Survey Specifications. In: Australian Soil and Land Survey Handbook.* Melbourne: Inkata Press.

RIAÑO, D., CHUVIECO, E., SALAS, F. J., PALACIOS-ORUETA, A. & BASTARRICA, A. 2002. Generation of fuel type maps from Landsat TM images and ancillary data in Mediterranean ecosystems. *Canadian Journal of Forest Research***,** 1301–1315.

RIANO, D., MEIER, E., ALLGOWER, B., CHUVIECO, E. & USTIN, S. L. 2003. Modeling airborne laser scanning data for the spatial generation of critical forest parameters in fire behavior modeling. *Remote Sensing of Environment,* 86**,** 177-186.

RICE, E. L. & KELTING, R. W. 1955. The Species-Area Curve. *Ecology,* 36**,** 7-11.

ROBERTS, D. A., DENNISON, P. E., GARDNER, M. E., HETZEL, Y., USTIN, S. L. & LEE, C. T. 2003. Evaluation of the potential of Hyperion for fire danger assessment by comparison to the Airborne Visible/Infrared Imaging Spectrometer. *Ieee Transactions on Geoscience and Remote Sensing,* 41**,** 1297-1310.

ROBERTS, D. A., GREEN, R. O. & ADAMS, J. B. 1997. Temporal and spatial patterns in vegetation and atmospheric properties from AVIRIS. *Remote Sensing of Environment,* 62**,** 223–240.

ROBERTS, D. A., USTIN, S. L., OGUNJEMIYO, S., GREENBERG, J., DOBROWSKI, S. Z., CHEN, J. & HINCKLEY, T. M. 2004. Spectral and Structural Measures of Northwest Forest Vegetation at Leaf to Landscape Scales. *Ecosystems,* 7**,** 545-562.

ROBINSON, D., REDDING, N. & CRISP, D. 2002. Implementation of a fast algorithm for segmenting SAR imagery. *Scientific and Technical Report.* Canberra, Australia: Defense Science and Technology Organization.

ROUSE, J., HAAS, R., SCHELL, J. & DEERING, D. Monitoring Vegetation Systems in the Great Plains with ERTS. Third ERTS Symposium, 1973. NASA, 309-317.

SAATCHI, S., HALLIGAN, K., DESPAIN, D. G. & CRABTREE, R. L. 2007. Estimation of forest fuel load from radar remote sensing. *Ieee Transactions on Geoscience and Remote Sensing,* 45**,** 1726-1740.

SANDERS, L., SCHOTT, J. & RAQUENO, R. 2001. A VNIR/SWIR atmospheric correction algorithm for hyperspectral imagery with adjacency effect. *Remote Sensing of Environment,* 78**,** 252-263.

SARKAR, S. & MARGULES, C. 2002. Operationalizing biodiversity for conservation planning. *Journal of biosciences,* 27**,** 299-308.

SCHAEPMAN, M. E., USTIN, S. L., PLAZA, A. J., PAINTER, T. H., VERRELST, J. & LIANG, S. 2009. Earth system science related imaging spectroscopy—An assessment. *Remote Sensing of Environment,* 113, Supplement 1**,** S123-S137.

SCHLERF, M., ATZBERGER, C. & HILL, J. 2005. Remote sensing of forest biophysical variables using HyMap imaging spectrometer data. *Remote Sensing of Environment,* 95**,** 177-194.

SCHMIDTLEIN, S. & SASSIN, J. 2004. Mapping of continuous floristic gradients in grasslands using hyperspectral imagery. *Remote Sensing of Environment,* 92**,** 126-138.

SCOTT, J. H., REINHARDT, E. D. & ELIZABETH, D. 2001. Assessing crown fire potential by linking models of surface and crown fire behavior. Fort Collins, Colorado: U.S. Department of Agriculture, Forest Service, Rocky Mountain Research Station.

SHI, W., EHLERS, M. & MOLENAAR, M. 2005. Uncertainties in integrated remote sensing and GIS. *International Journal of Remote Sensing,* 26**,** 2911–2915.

SIMS, D. A. & GAMON, J. A. 2002. Relationships between leaf pigment content and spectral reflectance across a wide range of species, leaf structures and developmental stages. *Remote Sensing of Environment,* 81**,** 337-354.

SIVERTSEN, D. 2009. Native Vegetation Interim Type Standard. Sydney: NSW Department of Environment, Climate Change and Water.

SIVERTSEN, D. P. & METCALFE, L. M. 1995. Natural Vegetation Remnants of the Southern Wheat-belt (Forbes and Cargelligo 1:250,000 map sheets). *Cunninghamia,* 4**,** 103-128.

SKOWRONSKI, N., CLARK, K., NELSON, R., HOM, J. & PATTERSON, M. 2007. Remotely sensed measurements of forest structure and fuel loads in the Pinelands of New Jersey. *Remote Sensing of Environment,* 108**,** 123-129.

SLUITER, R., JONG, S. D., KWAST, H. D. & WALSTRA, J. 2004. A Contextual Approach to Classify Mediterranean Heterogeneous Vegetation using the Spatial Reclassification Kernel (SPARK) and DAIS7915 Imagery. *In:* JONG, S. D. & MEER, F. V. D. (eds.) *Remote Sensing Image Analysis: Including The Spatial Domain.* Springer Netherlands.

SMITH, J. E., MOLINA, R., HUSO, M. M. P., LUOMA, D. L., MCKAY, D., CASTELLANO, M. A., LEBEL, T. & VALACHOVIC, Y. 2002a. Species richness, abundance, and composition of hypogeous and epigeous ectomycorrhizal fungal sporocarps in young, rotation-age, and old-growth stands of Douglas-fir(Pseudotsuga menziesii) in the Cascade Range of Oregon, U. S. A. *Canadian Journal of Botany,* 80**,** 186-204.

SMITH, M. A., GRANT, C. D., LONERAGAN, W. A. & KOCH, J. M. 2004. Fire management implications of fuel loads and vegetation structure in jarrah forest restoration on bauxite mines in Western Australia. *Forest Ecology and Management,* 187**,** 247-266.

SMITH, M. L., OLLINGER, S. V., MARTIN, M. E., ABER, J. D., HALLETT, R. A. & GOODALE, C. L. 2002b. Direct estimation of aboveground forest productivity through hyperspectral remote sensing of canopy nitrogen. *Ecological Applications,* 12**,** 1286-1302.

SOHN, Y. & REBELLO, N. S. 2002. Supervised and unsupervised spectral angle classifiers. *Photogrammetric Engineering and Remote Sensing,* 68**,** 1271-1280.

SOKAL, R. R. & ROHALF, F. J. 1962. The comparison of dendrograms by objective methods. *Taxon,* 11**,** 33-40.

SPANNER, M. A., PIERCE, L. L., PETERSON, D. L. & RUNNING, S. W. 1990. Remote sensing of temperate coniferous forest leaf area index—the influence of canopy closure, understory vegetation and background reflectance. *International Journal of Remote Sensing,* 111**,** 95–111.

SPECHT, R. L. 1970. Vegetation. *In:* LEEPER, G. W. (ed.) *Australian Environment.* 4th ed. Melbourne: Melbourne University Press.

STEININGER, M. 2000. Satellite estimation of tropical secondary forest above-ground biomass: Data from Brazil and Bolivia. *International Journal of Remote Sensing,* 21**,** 1139– 1157.

STONE, C. 1996. The role of psyllids (Hemiptera: Psyllidae) and bell miners (Manorina melanophrys) in canopy dieback of Sydney blue gum (Eucalyptus saligna Sm.). *Austral Ecology,* 21**,** 450-458.

STONE, C., KATHURIA, A., CARNEY, C. & HUNTER, J. 2008. Forest canopy health and stand structure associated with bell miners (Manorina melanophrys) on the central coast of New South Wale. *Australian Forestry,* 71**,** 294–302.

STONE, C., OLD, K., KILE, G. & COOPS, N. 2001. Forest Health Monitoring in Australia: National and Regional Commitments and Operational Realities. *Ecosystem Health,* 7**,** 48-58.

STRAHLER, A. H., WOODCOCK, C. E. & SMITH, J. A. 1986. On the nature of models in remote sensing. *Remote Sensing of Environment,* 20**,** 121-139.

TER BRAAK, C. J. F., PRENTICE, I. C., TER BRAAK, C. J. F. & PRENTICE, I. C. 2004. A Theory of Gradient Analysis. *Advances in Ecological Research,* 34**,** 235-282.

TETKO, I., LIVINGSTONE, D. & LUIK, A. 1995. Neural network studies. 1. Comparison of overfitting and overtraining. *Journal of chemical information and computer sciences,* 35**,** 826-833.
THACKWAY, R., LEE, A., DONOHUE, R., KEENAN, R. J. & WOOD, M. 2007. Vegetation information for improved natural resource management in Australia. *Landscape and Urban Planning,* 79**,** 127-136.
THENKABAIL, P. S., ENCLONA, E. A., ASHTON, M. S. & VAN DER MEER, B. 2004. Accuracy assessments of hyperspectral waveband performance for vegetation analysis applications. *Remote Sensing of Environment,* 91**,** 354-376.
TIESZEN, L., REED, B. & DEJONG, D. 1997. NDVI, C3 and C4 production, and distributions in the Great Plains grassland cover. *Ecological Applications,* 7**,** 59–78.
TODD, S. & HOFFER, R. 1998. Responses to spectral indicies to variations in vegetation cover and soil background. *Photogrammetry Engineering and Remote Sensing,* 64**,** 915-921.
TOLHURST, K. G., FLINN, D. W. & LOYN, R. H. 1992. Ecological Effects of Fuel Reduction Burning in a Dry Sclerophyll Forest: A Summary of Principal Research Findings and Their Management Implications. Melbourne: Department of Conservation and Environment.
TONGWAY, D. J. 1995. *Soil condition assessment of tropical grasslands,* Lyneham, A.C.T, CSIRO Division of Wildlife and Ecology.
TOU, J. T. & GONZALES, R. C. 1974. Pattern Recognition Principles. ISODATA Algorithm. *Pattern Classification By Distance Functions.* Reading, Massachusetts: Addison-Wesley.
TOWNSEND, P. A., FOSTER, J. R., CHASTAIN, R. A. & CURRIE, W. S. 2003. Application of imaging spectroscopy to mapping canopy nitrogen in the forests of the central Appalachian Mountains using Hyperion and AVIRIS. *Ieee Transactions on Geoscience and Remote Sensing,* 41**,** 1347-1354.
TOZER, M. 2003. The native vegetation of the Cumberland Plain, western Sydney: systematic classification and field identification of commuities. *Cunninghamia,* 8**,** 1-75.
TURNER, R. 2007. Assessment of Fuel Loads by Remote Sensing: Sub-report on Airborne Laser Scanner application in the Jilliby Catchment Area. Sydney: Forest Resources, Forests New South Wales.
TURNER, R. S. 2006. *An airborne Lidar canopy segmentation approach for estimating above-ground biomass in coastal eucalypt forests.* PhD, University of New South Wales.
UNDERWOOD, E., USTIN, S. & DIPIETRO, D. 2003. Mapping nonnative plants using hyperspectral imagery. *Remote Sensing of Environment,* 86**,** 150-161.
USTIN, S. & TRABUCCO, A. 2000. Using hyperspectral remote sensing to assess forest structure. *Journal of Forestry,* 98**,** 47-49.
VAN AARDT, J. A. N. & WYNNE, R. H. Combining High-Density Lidar Data with High Spatial Resolution Hyperspectral Imagery to Estimate Coniferous and Deciduous Forest Volume and Biomass by Species. Towards an Object-Oriented Approach, 2004 Blacksburg, Virginia. Virginia Tech.
VAN AARDT, J. A. N. & WYNNE, R. H. 2007. Examining pine spectral separability using hyperspectral data from an airborne sensor: An extension of field-based results. *International Journal of Remote Sensing,* 28**,** 431 - 436.
VAN DEN MEERSSCHAUT, D. & VANDEKERKHOVE, K. 1998. Development of a standscale forest biodiversity index based on the State Forest Inventory. *In:* HANSEN, M. & BURK, T. (eds.) *Integrated Tools for Natural Resources Inventories in the 21st Century.* Boise, Idaho: USDA.
VAN DER MAAREL, E. 2004. Vegetation Ecology - An Overview. *Vegetation Ecology.* Oxford: Blackwell Science.
VAN WAGNER, C. E. 1968. The Line Intersect Method in Forest Fuel Sampling. *Forest Science,* 14**,** 20-26(7).
VAN WAGTENDONK, J. W. & ROOT, R. R. 2003. The use of multi-temporal Landsat Normalized Difference Vegetation Index (NDVI) data for mapping fuel models in Yosemite National Park, USA. *International Journal of Remote Sensing,* 24**,** 1639-1651.
VAN ZYL, J. J. 2001. The Shuttle Radar Topography Mission (SRTM): a breakthrough in remote sensing of topography. *Acta Astronautica,* 48**,** 559-565.

VARGA, T. A. & ASNER, G. P. 2008. Hyperspectral and lidar remote sensing of fire fuels in Hawaii Volcanoes National Park. *Ecological Applications,* 18**,** 613-623.
VOGIATZAKIS, I. N. & GRIFFITHS, G. H. 2006. A GIS-based empirical model for vegetation prediction in Lefka Ori, Crete. *Plant Ecology,* 184**,** 311-323.
WALKER, J. 1981. Fuel dynamics in Australian vegetation. *In:* GILL, A. M., GROVES, R. H. & NOBLE, I. R. (eds.) *Fire and the Australian Biota.* Canberra: Australian Academy of Science.
WALSWORTH, N. & KING, D. J. Comparison of two tree apex delineation techniques. *In:* HILL, D. A. & LECKIE, D. G., eds. International Forum on Automated Interpretation of High Spatial Resolution Digital Imagery for Forestry, 1998 Victoria, BC.
WANG, L., GONG, P. & BIGING, G. S. 2004. Individual tree-crown delineation and treetop detection high-spatial-resolution aerial imagery. *Photogrammetric Engineering and Remote Sensing,* 70**,** 351-357.
WANG, L. & SOUSA, W. P. 2009. Distinguishing mangrove species with laboratory measurements of hyperspectral leaf reflectance. *International Journal of Remote Sensing,* 30**,** 1267-1281.
WATSON, J., FREUDENBERGER, D. & PAULL, D. 2001. An assessment of the focal-species approach for conserving birds in variegated landscapes in southeastern Australia. *Conservation Biology,* 15**,** 1364-1373.
WATT, A. S. 1947. Pattern and process in the plant community. *Journal of Ecology,* 35**,** 1-22.
WEBER, K. T. 2006. Challenges of integrating geospatial technologies into rangeland research and management. *Rangeland Ecology & Management,* 59**,** 38-43.
WENG, Q. & HU, X. 2008. Medium spatial resolution satellite imagery for estimating and mapping urban impervious surfaces using LSMA and ANN. *IEEE Transactions on Geoscience and Remote Sensing,* 46**,** 2397-2406.
WESSMAN, C. A. 1992. Spatial scales and global change - bridging the gap from plots to gcm grid cells. *Annual Review of Ecology and Systematics,* 23**,** 175-200.
WESTHOFF, V. & VAN DER MAAREL, E. 1978. The Braun-Blanquet approach. *In:* WHITTAKER, R. (ed.) *Classification of Plant Communities.* Springer Netherlands.
WILCOXON, F. 1945. Individual comparisons by ranking methods. *Biometrics Bulletin,* 1**,** 80–83.
WITTEN, I. H. & FRANK, E. 2005. *Data mining: Practical machine learning tools and techniques,* San Francisco, CA, Morgan Kaufmann.
WOODCOCK, C. & HARWARD, V. J. 1992. Nested-Hierarchical Scene Models And Image Segmentation. *International Journal of Remote Sensing,* 13**,** 3167-3187.
WU, C. Y., NIU, Z., TANG, Q. & HUANG, W. J. 2008. Estimating chlorophyll content from hyperspectral vegetation indices: Modeling and validation. *Agricultural and Forest Meteorology,* 148**,** 1230-1241.
WULDER, M., NIEMANN, K. O. & GOODENOUGH, D. G. 2000. Local maximum filtering for the extraction of tree locations and basal area from high spatial resolution imagery. *Remote sensing of environment,* 73**,** 103-114.
WULDER, M. A., HALL, R. J., COOPS, N. C. & FRANKLIN, S. E. 2004. High spatial resolution remotely sensed data for ecosystem characterization. *BioScience,* 54**,** 511-521.
XIE, Y. C., SHA, Z. Y. & YU, M. 2008. Remote sensing imagery in vegetation mapping: a review. *Journal of Plant Ecology,* 1**,** 9-23.
XU, B. & GONG, P. 2007. Land-use/land-cover classification with multispectral and hyperspectral EO-1 data. *Photogrammetric Engineering and Remote Sensing,* 73**,** 955-965.
XU, M., WATANACHATURAPORN, P., VARSHNEY, P. K. & ARORA, M. K. 2005. Decision tree regression for soft classification of remote sensing data. *Remote Sensing of Environment,* 97**,** 322-336.
YEE, T. W. & MITCHELL, N. D. 1991. Generalized Additive Models in Plant Ecology. *Journal of Vegetation Science,* 2**,** 587-602.
ZHAN, Q., MOLENAAR, M., TEMPFLI, K. & SHI, W. 2005. Quality assessment for geo-spatial objects derived from remotely sensed data. *International Journal of Remote Sensing,* 26**,** 2953–2974.